



UNIVERSIDADE D  
**COIMBRA**

Márcio Paulo Ferreira Gonçalves

**PERFORMANCE EVALUATION OF EXTERNAL  
VACUUM INSULATION FINISHING SYSTEM**

**PhD thesis in Civil Engineering, Constructions, supervised by  
Professor Nuno Albino Vieira Simões (University of Coimbra),  
Professor Inês dos Santos Flores Barbosa Colen (Instituto  
Superior Técnico) and Doctor Catarina Lopes Serra (Itecons), and  
submitted to the Department of Civil Engineering of the Faculty  
of Sciences and Technology of the University of Coimbra.**

December 2021



Faculty of Sciences and Technology of the University of Coimbra  
Department of Civil Engineering

# Performance Evaluation of External Vacuum Insulation Finishing System

Márcio Paulo Ferreira Gonçalves

PhD thesis in Civil Engineering, Constructions, supervised by Professor Nuno Albino Vieira Simões (University of Coimbra), Professor Inês dos Santos Flores Barbosa Colen (Instituto Superior Técnico) and Doctor Catarina Lopes Serra (Itecons), and submitted to the Department of Civil Engineering of the Faculty of Sciences and Technology of the University of Coimbra.

December 2021



UNIVERSIDADE D  
COIMBRA





*In memory of my mother*



## **Acknowledgements**

I would like to express my deepest gratitude to my supervisors, Professor Nuno Simões, Professor Inês Flores-Colen and Doctor Catarina Serra, for providing me continuous support, guidance, knowledge and motivation, and for allowing me to consume their precious time. Their contribution was undoubtedly essential to conducting this doctoral thesis.

I would like to thank Itecons - Institute for Research and Technological Development for Construction, Energy, Environment and Sustainability, and in particular to Professor António Tadeu for granting me the opportunity to carry out this research at the Institute.

I am grateful to all of my colleagues at Itecons that were indispensable to the fulfilment of this thesis, in particular to Ana Azevedo, António Nascimento, António Vieira, Aurélio Gonçalves, Beatriz Marques, Eliana Silva, Filipe Pedro, Inês Simões, Joana Prata, João Almeida, José Nascimento, Katya Coelho, Michael Brett, Rui Jerónimo, Sara Dias, Saúl Martins, and Tiago Jesus.

I would also like to express my thankfulness to the following researchers: Shahaboddin Resalati, Christoph Sprengard, Carolin Kokolsky, Kenny Rottenbacher and Flávia Almeida, for their contribution and productive transfer of knowledge regarding vacuum insulation technology.

I am also thankful to my family and closest friends for always encouraging me and supporting me, in particular to my father who is a constant source of inspiration.

Finally, I would like to dedicate this Doctoral Thesis to my lovely son Ivo and wife Diana, the main source of motivation for my life.

To all: thank you very much!



## **Financial and institutional support**

The research conducted in this thesis was supported by the Portuguese Foundation for Science and Technology (FCT), through the PhD grant PD/BD/135194/2017 under the Eco-Construction and Rehabilitation Programme.

The research works were carried out at Itecons - Institute for Research and Technological Development for Construction, Energy, Environment and Sustainability.

The investigation works were also supported by the:

- INNOVIP EU-Project “Innovative multi-functional Vacuum-Insulation-Panels (VIPs) for use in the building sector”, (Project number: 723441 - INNOVIP - H2020-EEB-2016-2017/H2020-EEB-2016) funding from the European Union’s Horizon 2020 research and innovation programme;
- OnThermalHP project “*Revestimentos delgados de elevado desempenho para aplicação sobre argamassas térmicas e soluções de isolamento térmico pelo exterior*”, (CENTRO-01-0247-FEDER-033390) co-financed by European Regional Development Fund (FEDER) through Centro 2020 Regional Operational Programme.

The following institutions were also involved in the research:

- Department of Civil Engineering of the University of Coimbra;
- Instituto Superior Técnico, Lisboa;
- FIW Munich - Research Institute for Thermal Insulation;
- Oxford Brookes University;
- Mostostal Warszawa;
- va-Q-tec AG;
- Secil Martigança, S.A;
- ARGACOL Tintas e Vernizes, S.A.



## **Abstract**

As building energy performance requirements continue to become stricter in order to fit in with nearly zero-energy buildings targets, there is an increasing demand for higher insulation levels. This has motivated the development of innovative solutions that incorporate super-insulating materials and products. Among these are solutions that incorporate vacuum technology. A vacuum insulation panel (VIP) is a top-of-the-line product characterized by having extremely low thermal conductivity, meaning it has potential to provide a great insulation level at a reduced thickness.

Since the External Thermal Insulation Composite System (ETICS) is one of the most popular construction technologies used for improving the energy efficiency of building walls, there is interest in combining the high thermal performance of VIPs with the known benefits of ETICS. However, in spite of showing strong potential in terms of thermal performance, the application of vacuum insulation panels in buildings presents several challenges that must be account for. Namely, those associated with design factors, handling and installation issues, as well as with the edge thermal bridging that occurs between panels, the doubts surrounding service life performance and, finally, the high investment costs of VIPs. Furthermore, there are several known anomalies that commonly occur in conventional ETICS and which could be exacerbated with VIPs. Hence, many aspects need to be carefully evaluated before VIP based ETICS become a viable solution for meeting energy targets.

The main goal of this research was to study the feasibility of incorporating a novel VIP solution into external thermal insulation composite systems. For this purpose, a comprehensive investigation into the solution was carried out. Laboratorial tests were performed to assess the effective behaviour of the solution in terms of physical, mechanical and hygrothermal performance. First, focus was put on the VIP product, in particular regarding the edge thermal bridging effect. Then, VIP based ETICS walls were evaluated in terms of the whole system hygrothermal performance and durability. Real onsite walls and laboratorial large-scale test specimens were assessed. New experimental procedures were defined to evaluate the durability of the solution and to enable the early identification of potential anomalies. Additionally, numerical models were used to simulate the steady and unsteady thermal behaviour of VIP products and their accuracy was evaluated against the experimental results. Finally, the cost-effectiveness of vacuum technology was also analysed by means of a whole-life cost assessment. Throughout the research, the evaluation of VIP based ETICS walls was often compared with other conventional solutions (used as a reference).

*Abstract*

**Keywords:** Vacuum insulation panels; ETICS; Hygrothermal behaviour; Experimental testing; Onsite monitoring; Numerical modelling; Whole-life cost assessment.



## Resumo

*O objetivo de se alcançarem edifícios com necessidades quase nulas de energia tem levado a um progressivo aumento dos requisitos de desempenho energético e, conseqüentemente, conduzido a uma crescente procura por níveis de isolamento térmico mais elevados. Este facto tem motivado o desenvolvimento de materiais e soluções inovadoras com propriedades excepcionais de isolamento térmico. De entre elas, destacam-se soluções que incorporam vácuo. Um painel de isolamento a vácuo (VIP) diferencia-se por ter uma condutibilidade térmica extremamente reduzida, o que significa que tem potencial para fornecer um ótimo nível de isolamento térmico associado a uma reduzida espessura.*

*Uma vez que os Sistemas Compósitos de Isolamento Térmico pelo Exterior (ETICS) são uma das tecnologias construtivas mais populares para a melhoria da eficiência energética das fachadas, surge o interesse em combinar o elevado desempenho térmico dos VIP com os benefícios dos ETICS. No entanto, apesar de apresentar um elevado potencial em termos de desempenho térmico, a aplicação de painéis de isolamento a vácuo em edifícios apresenta vários desafios que devem ser tidos em conta. Nomeadamente, constrangimentos de projeto e limitações associadas ao manuseamento e instalação, assim como associadas às pontes térmicas lineares nos seus bordos, às dúvidas relativas ao seu desempenho durante a vida útil e, por fim, ao seu elevado custo de investimento. Além disso, existem várias anomalias que ocorrem frequentemente em ETICS convencionais e que podem ser exacerbadas com a utilização dos VIPs. Portanto, antes dos sistemas ETICS com painéis de vácuo se tornarem uma opção viável, existem muitos aspetos que necessitam de ser cuidadosamente avaliados.*

*Este trabalho teve como principal objetivo o estudo da viabilidade duma nova solução de VIP em sistemas de isolamento térmico pelo exterior. Neste sentido, realizou-se uma extensa investigação à solução. Foram realizados ensaios laboratoriais para avaliar o desempenho efetivo da solução em termos físicos, mecânicos e higrotérmicos. Primeiro, focou-se na avaliação de desempenho do painel de vácuo, com particular destaque no efeito das pontes térmicas lineares causadas pelos seus bordos. De seguida, avaliou-se o desempenho higrotérmico e a durabilidade do sistema completo de ETICS com VIPs, onde se incluíram paredes e protótipos laboratoriais à escala real. Foram ainda definidos novos procedimentos experimentais para avaliar a durabilidade da solução e permitir a deteção precoce de potenciais anomalias. Adicionalmente, utilizaram-se modelos numéricos para simular o comportamento em regime permanente e variável da solução, bem como para avaliar a sua aplicabilidade através da comparação com resultados experimentais. Por último, foi também efetuado a análise custo-eficácia dos VIPs,*

## *Resumo*

*através da avaliação dos custos globais de ciclo de vida. Ao longo da investigação, a análise dos ETICS com VIPs foi frequentemente comparada com outras soluções convencionais (usadas como referência).*

***Palavras-chave:*** *Painéis de isolamento a vácuo; ETICS; Desempenho higrotérmico; Ensaios experimentais; Monitorização in situ; Modelação numérica; Avaliação do custo global do ciclo de vida.*

# Table of contents

<b>Acknowledgements</b> .....	<b>i</b>
<b>Financial and institutional support</b> .....	<b>iii</b>
<b>Abstract</b> .....	<b>v</b>
<b>Resumo</b> .....	<b>vii</b>
<b>Table of contents</b> .....	<b>ix</b>
<b>Index of figures</b> .....	<b>xv</b>
<b>Index of tables</b> .....	<b>xxi</b>
<b>1. Introduction</b> .....	<b>1</b>
1.1. Context and motivation .....	1
1.2. Research questions and objectives .....	3
1.3. Thesis structure .....	4
<b>2. Literature review: challenges posed by the use of vacuum insulation panels in ETICS</b> .....	<b>13</b>
2.1. Introduction .....	13
2.2. Vacuum insulation panels in ETICS applications .....	17
2.2.1. VIP products for external insulation of walls.....	18
2.2.2. Case studies .....	20
2.3. Challenges of VIP use in ETICS .....	24
2.3.1. Edge thermal bridging effect.....	25
2.3.2. Condensations .....	27
2.3.3. Service life.....	28
2.3.4. Design and installation .....	29
2.3.5. Economic viability .....	31
2.3.6. Environmental performance .....	32
2.4. Guidelines for experimental validation .....	33

## Table of contents

2.5. Conclusions .....	37
References .....	38
<b>3. Study of the edge thermal bridging effect in vacuum insulation panels.....</b>	<b>53</b>
3.1. Introduction .....	53
3.2. Materials and methods .....	55
3.2.1. VIP product .....	55
3.2.2. Experimental apparatus .....	57
3.2.3. Linear thermal transmittance calculation .....	59
3.2.4. Point thermal transmittance calculation .....	59
3.2.5. Specific heat capacity .....	60
3.2.6. Numerical modelling.....	61
3.3. Experimental results.....	66
3.3.1. Thermal conductivity at the centre of the panel .....	66
3.3.2. Linear thermal transmittance.....	67
3.3.3. Specific heat .....	68
3.4. Numerical results.....	69
3.4.1. Linear thermal transmittance.....	69
3.4.2. Point thermal transmittance of VIP based ETICS with plastic anchor.....	70
3.4.3. Dynamic numerical modelling validation .....	70
3.5. VIP design for building application: a sensitivity analysis .....	71
3.5.1. Edge material thermal conductivity .....	72
3.5.2. Size of air gap between panels .....	73
3.5.3. Materials thickness .....	73
3.5.4. Panel size and shape .....	75
3.5.5. Walls thermal performance and thermal delay.....	76
3.6. Discussion .....	78
3.7. Conclusions .....	80
References .....	81
<b>4. Onsite monitoring of VIP based ETICS in Warsaw: retrofitting of a real building ...</b>	<b>87</b>
4.1. Introduction .....	87

4.2.	Materials and methods .....	89
4.2.1.	Case study .....	90
4.2.2.	Weather data.....	93
4.2.3.	Measurement settings.....	93
4.2.4.	Hygrothermal parameters .....	95
4.2.5.	U-value estimation .....	96
4.2.6.	Infrared thermography.....	98
4.3.	Results and discussion.....	99
4.3.1.	Temperature analysis - cold season.....	99
4.3.2.	Temperature analysis - warm season.....	102
4.3.3.	Humidity analysis.....	104
4.3.4.	U-value estimation .....	105
4.3.5.	Infrared thermography inspection .....	108
4.4.	Conclusions .....	110
	References .....	112
<b>5.</b>	<b>Onsite monitoring of VIP based ETICS in Coimbra: comparison of different exposure conditions and insulation materials .....</b>	<b>119</b>
5.1.	Introduction .....	119
5.2.	Materials and methods .....	121
5.2.1.	Case study .....	121
5.2.2.	Weather data.....	123
5.2.3.	Measurement settings.....	124
5.2.4.	Infrared thermography inspection .....	125
5.2.5.	Surface condensation risk assessment.....	126
5.2.6.	Numerical modelling.....	127
5.3.	Results and discussion.....	127
5.3.1.	Temperature monitoring of VIP based ETICS .....	128
5.3.2.	Influence of ETICS walls orientation.....	130
5.3.3.	Infrared thermograms .....	131
5.3.4.	Surface condensation risk.....	132

*Table of contents*

5.3.5.	Numerical modelling results .....	136
5.4.	Conclusions .....	138
	References .....	140
<b>6.</b>	<b>Laboratory assessment of the hygrothermal performance of the VIP based ETICS</b>	<b>145</b>
6.1.	Introduction .....	145
6.2.	Materials and methods .....	148
6.2.1.	Test specimen and apparatus .....	148
6.2.2.	Test procedures .....	151
6.2.3.	Test specimen inspection .....	154
6.2.4.	Numerical modelling.....	155
6.3.	Results and discussion.....	156
6.3.1.	Stage 1: steady state condition results .....	156
6.3.2.	Stage 2: hygrothermal cycles results .....	159
6.3.3.	Stage 3: solar radiation cycles results.....	165
6.3.4.	Test specimen inspection .....	170
6.4.	Conclusions .....	178
	References .....	179
<b>7.</b>	<b>Whole-life cost assessment of VIP.....</b>	<b>185</b>
7.1.	Introduction .....	185
7.2.	Materials and methods .....	189
7.2.1.	Definition of the external wall.....	190
7.2.2.	Energy performance assessment .....	191
7.2.3.	Whole-life costing methodology .....	196
7.2.4.	Economic parameters .....	198
7.3.	Results .....	199
7.3.1.	Rental costs variation .....	200
7.3.2.	VIP price variation .....	202
7.3.3.	VIP panel size variation .....	203
7.3.4.	VIP service life analysis.....	203
7.3.5.	Payback period and internal rate of return .....	204

7.3.6. Influence of location.....	206
7.4. Discussion .....	207
7.5. Conclusions .....	209
References .....	211
<b>8. Conclusions and future works .....</b>	<b>219</b>
8.1. Overview and final statements .....	219
8.2. Future works.....	222





# Index of figures

Figure 1.1: Research thesis flowchart. ....	5
Figure 2.1: Thermal insulation products with the same thermal resistance: 170 mm thick EPS (on the left) and 20 mm thick VIP (on the right). ....	15
Figure 2.2: Vacuum insulation panel with cover layers scheme (adapted from [32] and [43]). .	17
Figure 2.3: Locations (blue dots) of the case studies of VIP based ETICS in the world. ....	20
Figure 2.4: Edge thermal bridge effect: a) simulated temperature distribution (temperatures in °C); b) edge thermal bridges onsite detection with infrared thermography (two VIPs).....	26
Figure 3.1: Vacuum insulation panels used in experimental measurements: a) overview of test specimens; b) identification of the sealing types; c) detail view of the barrier envelope side. ...	56
Figure 3.2: VIP based ETICS scheme.....	57
Figure 3.3: Guarded hot plate apparatus: a) photograph; b) measurement of the thermal conductivity at VIP CoP scheme ( $\lambda_{CoP}$ ); c) measurement of the thermal equivalent conductivity including edge effects ( $\lambda_{eq,ja}$ ). ....	58
Figure 3.4: Location of the temperature sensors on the panels: a) photograph; b) schematic position of the thermocouples: hot plate side, joint and cold plate side.....	58
Figure 3.5: GHP apparatus for specific heat determination using the indirect method: a) scheme with thermocouples positions (red dots); b) photography of the test apparatus with a test specimen. ....	60
Figure 3.6: Differential scanning calorimetry apparatus for specific heat capacity determination. ....	61
Figure 3.7: Representation of the 3D numerical model – VIP encapsulated in EPS. ....	64
Figure 3.8: Specific heat results by means of differential scanning calorimetry. ....	68
Figure 3.9: Linear thermal transmittance results comparison between numerical modelling and experimental measurements. ....	69
Figure 3.10: 3D numerical model isoflux diagram: a) without plastic anchor; b) with plastic anchor.....	70
Figure 3.11: Temperature measurements during experimental and numerical approaches – case study A. ....	71
Figure 3.12: Temperature measurements during experimental and numerical approaches – case study F.....	71
Figure 3.13: Linear thermal transmittance as function of the thermal conductivity of the edge material – case F.....	73
Figure 3.14: Linear thermal transmittance as function of the air joint thickness – case F. ....	73
Figure 3.15: Linear thermal transmittance as function of the panel thickness – case F: a) VIP thickness variation; b) cover layer thickness variation. ....	74

Figure 3.16: Linear thermal transmittance as function of the edge material width – case F: a) edge material width variation; b) edge and cover layer thickness variation. ....	74
Figure 3.17: Thermal delay determination for ETICS walls: a) ceramic brick wall with VIP based ETICS; b) ceramic brick wall with EPS based ETICS solution; c) stone wall with VIP based ETICS; d) stone wall with EPS based ETICS solution; e) wood wall with VIP based ETICS; f) wood wall with EPS based ETICS solution. ....	77
Figure 3.18: Thermal delay in hours of VIP based ETICS and EPS ETICS walls, for the different support walls. ....	78
Figure 4.1: Schematic drawing of the case study façades, including EPS reference wall and VIP layout pattern. ....	90
Figure 4.2: Photograph after renovation of the case study façades, including EPS and VIP based ETICS. ....	90
Figure 4.3: Encapsulated VIP solution: a) schematic cross-section; b) photography. ....	91
Figure 4.4: Representation of VIP ETICS wall layers. ....	91
Figure 4.5: Installation of VIP based ETICS: a) encapsulated panels with mechanical fixings at the corners; b) reinforced base coat mortar application. ....	92
Figure 4.6: Mean monthly weather data monitoring in 2019. ....	93
Figure 4.7: Schematic representation and photograph of the location of the sensors in the walls. ....	94
Figure 4.8: Schematic cross-section of the building walls and placement of temperature (T), temperature/humidity (TH) and heat flux (V) sensors: a) VIP wall; b) reference wall. ....	94
Figure 4.9: Temperatures during a representative week in the cold season: a) VIP wall with daily detail; b) reference wall with daily detail. ....	100
Figure 4.10: Temperature differences between layers during a cold season period: a) VIP wall; b) reference wall. ....	101
Figure 4.11: Temperature differences for VIP based ETICS wall in cold season period – CoP vs joint comparison. ....	102
Figure 4.12: Temperature curves during a warm season: a) VIP wall; b) EPS wall. ....	103
Figure 4.13: Temperature differences between layers during the warm season: a) VIP wall - CoP and joint area with daily detail; b) reference wall with daily detail. ....	104
Figure 4.14: Absolute humidity curves for VIP wall and reference wall: a) January 2019 week; b) December 2019 week. ....	105
Figure 4.15: Heat fluxes and ambient temperatures curves during a cold period. ....	106
Figure 4.16: Heat fluxes and ambient temperatures curves during a warm period. ....	106
Figure 4.17: U-value estimation at the VIP wall (centre of VIP panel) and reference wall after the renovation with ETICS and before the renovation. ....	108
Figure 4.18: Thermograms: a) reference external insulation wall; b) VIP external insulation wall application. ....	109

Figure 4.19: Thermograms taken of part of the VIP wall on several dates during winter period. .....	110
Figure 5.1: ETICS walls: a) different thermal insulation materials (EPS, TIM, ICB and VIP); b) different colour finishing coat (black and white). .....	122
Figure 5.2: Determination of finishing coat emissivity by means of TIR100-2.....	123
Figure 5.3: Mean monthly weather data monitored in 2019. ....	124
Figure 5.4: Schematic representation of the location of the thermocouples. ....	125
Figure 5.5: Temperature measurements in different VIP based ETICS layers during a week in winter: a) white wall (south); b) black wall (south). ....	128
Figure 5.6: Temperature and radiation registered during a week in winter. ....	129
Figure 5.7: Temperature measurements in different VIP based ETICS layers during a week in summer: a) white wall (south); b) black wall (south). ....	129
Figure 5.8: Temperature and radiation registered during a week in summer.....	129
Figure 5.9: Surface temperature and global radiation in the ICB ETICS white walls. ....	130
Figure 5.10: Surface temperature and global radiation in the ICB ETICS black walls. ....	130
Figure 5.11: Thermograms taken of part the VIP south-facing walls: a) black wall; b) white wall. .....	131
Figure 5.12: Thermograms of VIP black wall facing south on several dates.....	132
Figure 5.13: Temperature in ETICS white wall faced south: a) surface curves $T_s$ and dewpoint curve $T_{dp}$ ; b) positive temperature difference between dewpoint $T_{dp}$ and surface temperatures $T_s$ . .....	133
Figure 5.14: Temperature in ETICS black wall faced south: a) surface curves $T_s$ and dewpoint curve $T_{dp}$ ; b) positive temperature difference between dewpoint $T_{dp}$ and surface temperatures $T_s$ . .....	133
Figure 5.15: Surface condensation observed during the morning period in winter in the black walls: a) VIP centre of panel condensation; b) TIM without condensation. ....	135
Figure 5.16: Annual condensation risk analysis for different ETICS solutions: a) white wall; b) black wall. ....	135
Figure 5.17: Accumulated hours of surface condensation risk for different ETICS solutions: a) white wall; b) black wall. ....	136
Figure 5.18: Temperatures in a south-facing EPS wall, during winter: a) white colour; b) black colour.....	137
Figure 5.19: Temperatures in a south-facing VIP wall, during winter: a) white colour; b) black colour.....	138
Figure 6.1: Dark coloured ETICS façade with rendering anomalies. ....	147
Figure 6.2: Test specimen of VIP based ETICS wall: a) photograph of the test specimen at initial state; b) photograph of the test specimen after black painting areas. ....	149
Figure 6.3: Hygrothermal cycles apparatus: a) schematic drawing; b) photograph. ....	150
Figure 6.4: Sensor locations in the test specimen: a) cross-section; b) layout pattern. ....	150

## *Index of figures*

Figure 6.5: Experimental apparatus to simulate artificial solar radiation: a) white finishing coat; b) black finishing coat c) preliminary infrared thermogram. ....	154
Figure 6.6: Temperatures results along the wall with white finishing coat: a) CoP area (zone 3); b) joint area (zone 4). ....	157
Figure 6.7: Heat fluxes results in the wall with white finishing coat: a) CoP area (zone 3); b) VIP joint area (zone 4).....	158
Figure 6.8: Temperature monitoring during heat-rain cycles with white finishing coat: a) CoP area (zone 2); b) VIP joint area (zone 1).....	160
Figure 6.9: Temperature differences in VIP CoP area (zone 2) during heat-rain cycles with white finishing coat.....	161
Figure 6.10: Temperature monitoring in interface B, VIP joint area (zone 1) and VIP CoP area (zone 2) during heat-rain cycle: a) white finishing coat; b) black finishing coat.....	161
Figure 6.11: Temperature monitoring during freeze-thaw cycles with white finishing coat: a) VIP centre of panel (zone 2); b) VIP joint (zone 1).....	162
Figure 6.12: Temperature differences in VIP CoP (zone 2) during freeze-thaw cycles with white finishing coat.....	162
Figure 6.13: Temperature monitoring in layer B, VIP joint (zone 1) and VIP CoP (zone 2), during freeze-thaw cycles: a) white finishing coat; b) black finishing coat. ....	163
Figure 6.14: Heat flux monitoring: a) during hygrothermal cycles; b) during a freeze-thaw cycle. ....	163
Figure 6.15: Temperatures results at different VIP interfaces during hygrothermal cycles with white finishing coat: a) VIP CoP (zone 2); b) VIP joint (zone 1). ....	164
Figure 6.16: Appearance of the test specimen after hygrothermal cycles: a) overall view; b) close-up of the corner of the opening; c) close-up of the finishing coat.....	165
Figure 6.17: Temperature monitoring over insulation in VIP centre of panel area (zone 2 and 3) and in VIP joint area (zone 1 and 4) during solar radiation cycles: a) white finishing coat; b) black finishing coat.....	166
Figure 6.18: Heat flux monitoring in VIP centre of panel area (zone 2 and 3) and in VIP joint area (zone 1 and 4) during solar radiation cycles: a) white finishing coat; b) black finishing coat..	167
Figure 6.19: Temperature results during solar radiation cycles obtained at several VIP interfaces in a VIP CoP area (zone 3): a) white finishing coat; b) black finishing coat. ....	167
Figure 6.20: Visual inspection after solar radiation cycles: a) microcracking on the finishing coat layer; b) microcracking on the finishing coat layer at VIP joints; c) loss of flatness.....	168
Figure 6.21: Layout pattern scheme of VIPs and location of the microcracking (in red) on the finishing coat layer.....	169
Figure 6.22: Microscopic image of: a) cracking along joints between panels; b) cracking in the corner of an opening.....	169
Figure 6.23: Scanning electron microscope images: a) rendering system not exposed to solar radiation; b) rendering system exposed to solar radiation.....	170

Figure 6.24: Adhesive failure pattern after bond strength tests..... 174

Figure 7.1: Cross-section of external walls: a) VIP ETICS solution; b) EPS ETICS solution. 190

Figure 7.2: Detailed drawing of the 2-D model using a triangular mesh. .... 191

Figure 7.3: Heat flow through ETICS wall (with 40 mm encapsulated VIP) located in Berlin, expressed in kWh per square meter of façade: a) heat losses; b) heat gains. .... 195

Figure 7.4: Average difference between losses and gains through ETICS wall (40 mm encapsulated VIP) for three locations, expressed in kWh per square meter of façade..... 195

Figure 7.5: Stages of the whole-life cost assessment (adapted from [34])...... 196

Figure 7.6: Carbon price and energy price prediction for Berlin for both scenarios..... 199

Figure 7.7: Berlin cost-optimal curves for VIP and corresponding EPS equivalent thickness curve for financial perspective: a) primary energy on horizontal axis; b) corresponding U-values of wall on horizontal axis. .... 200

Figure 7.8: Rental cost analysis for Berlin for financial perspective: a) AC system; b) EH system. .... 201

Figure 7.9: Rental cost analysis for Berlin: a) financial perspective; b) macroeconomic perspective..... 201

Figure 7.10: VIP price analysis for Berlin for financial perspective: a) fixed rental cost of 150 €/m<sup>2</sup>.y; b) fixed rental cost of 250 €/m<sup>2</sup>.y; c) fixed rental cost of 350 €/m<sup>2</sup>.y)..... 202

Figure 7.11: Panel size analysis for Berlin for financial perspective: a) 440 mm x 440 mm; b) 640 mm x 640 mm; c) 1040 mm x 640 mm. .... 203

Figure 7.12: VIP service life analysis for Berlin for financial perspective: a) fixed rental cost of 150 €/m<sup>2</sup>.y; b) fixed rental cost of 250 €/m<sup>2</sup>.y; c) fixed rental cost of 350 €/m<sup>2</sup>.y)..... 204

Figure 7.13: Discounted payback period for Berlin results for financial perspective. – Rental costs analysis. .... 205

Figure 7.14: Discounted payback period for Berlin results for financial perspective – VIP price analysis. .... 205

Figure 7.15: Internal rate of return for Berlin results for financial perspective – rental price analysis. .... 205

Figure 7.16: Internal rate of return for Berlin results for financial perspective – VIP price analysis. .... 205

Figure 7.17: VIPs cost-optimal curves for different locations and corresponding EPS equivalent thickness curves for financial perspective (rental cost of 150 €/m<sup>2</sup>.y): a) Eurostat electricity prices prediction b) Electricity price with an increase of 2.8% per year..... 206

Figure 7.18: VIPs cost-optimal curves for different locations and energy prices prediction for financial perspective: a) with AC system; b) with EH system. .... 207



## Index of tables

Table 2.1: Commercial solutions for external insulation of walls.....	19
Table 2.2: Case studies of VIP based ETICS in new constructions based on literature review..	21
Table 2.3: Case studies of VIP based ETICS in retrofitting actions based on literature review.	23
Table 2.4: Risk of potential problems in VIP based ETICS, in relation with known ETICS anomalies.....	25
Table 2.5: Service life estimates in building applications.....	28
Table 2.6: Cost of vacuum insulation panels based on literature review. ....	31
Table 2.7: Summary of the assessment methods for validating a VIP based ETICS.....	34
Table 2.8: Summary of the assessment methods for validating each ETICS component. ....	35
Table 3.1: VIP joint assemblies (dimensions in mm). ....	56
Table 3.2: Numerical model properties – VIP encapsulated in EPS (case F). ....	63
Table 3.3: 3D numerical model properties – case F.....	64
Table 3.4: 2D dynamic numerical model properties. ....	65
Table 3.5: VIP thickness, apparent density and average thermal conductivity measured at centre of panel.....	66
Table 3.6: Equivalent thermal conductivity and linear thermal transmittance of VIP joint assemblies .....	67
Table 3.7: Apparent density, thermal conductivity and specific heat capacity results.....	68
Table 3.8: Summary of the parameters and respective range of variation assessed in section 3.5. ....	72
Table 3.9: Percentual increment of the equivalent thermal conductivity of VIPs due to the edge effect - case F. ....	75
Table 3.10: Effective U-value of the VIP based ETICS walls and EPS ETICS wall (in brackets), expressed in $W/(m^2 \cdot K)$ .....	76
Table 4.1: Thermophysical properties of each wall material. ....	92
Table 4.2: References and locations of the sensors.....	95
Table 4.3: U-values comparison between theoretical and experimental values.....	107
Table 4.4: U-values comparison between theoretical and numerical values.....	108
Table 5.1: Thermophysical properties of the materials used in the case-study walls. ....	123
Table 5.2: Percentage of time with condensation risk estimated for the south-facing walls in December 2018 and April 2019. ....	134
Table 5.3: Percentage of time with risk of condensation estimated for the south-facing walls in January 2019 and January 2020. ....	134
Table 6.1: Specimen components characteristics.....	149

## *Index of tables*

Table 6.2: Description of the equipment used in the hygrothermal cycles resistance test. ....	151
Table 6.3: Thermal transmittance estimation for several boundary conditions. ....	159
Table 6.4: Change in colour determined by numeric comparison of colorimetric parameters. ....	171
Table 6.5: VIP CoP thermal transmittance estimation for different ageing test periods. ....	172
Table 6.6: Test results of the bond strength tests between the base coat and the thermal insulation product. ....	173
Table 6.7: Hard body impact test results – 10 Joules. ....	175
Table 6.8: Hard body impact test results – 3 Joules. ....	176
Table 6.9: Summary of ageing tests results. ....	177
Table 7.1: Thermophysical properties of the materials. ....	190
Table 7.2: Thermal properties of an encapsulated VIP with 640 mm x 640 mm. ....	192
Table 7.3: Thermal properties of an encapsulated VIP with 440 mm x 440 mm. ....	193
Table 7.4: Thermal properties of an encapsulated VIP with 1040 mm x 640 mm. ....	193
Table 7.5: Economic parameters used in WLC for the different ETICS solutions. ....	198
Table 7.6: Economic parameters used in WLC analysis for different cities at starting year. ...	199
Table 7.7: Summary of WLC results and assumptions. ....	208







# **CHAPTER 1**

## **INTRODUCTION**



# 1. Introduction

## 1.1. Context and motivation

The building sector has been identified as being responsible for a great deal of the worldwide energy consumption and, consequently, indirect carbon emissions. In this context, the European Commission has set out ambitious goals to increase energy efficiency and boost renovation of the existing building stock, which is estimated to be largely inefficient. The EU 2030 Climate Target Plan is now aiming at reducing greenhouse emissions in at least 55% (from 1990 levels) and improving energy efficiency in at least 32.5%. In addition to concerns with climate change mitigation via decarbonization, improving energy efficiency in buildings can provide many benefits to owners and occupants, which include: lower energy costs, greater thermal comfort, higher property value, and increased safety and health. In pursuit of nearly zero-energy levels of performance, increasingly stricter thermal resistance requirements are being imposed on the building envelope, since it is responsible for a great amount of heat loss and, consequently, a large part of energy consumption in buildings. Such requirements have led to the need for increasingly thicker insulation layers, which can cause architectural constraints and can have a negative impact on the available floor area, especially in cold climates. In this context, one of the key actions of the European Commission defined in *“Towards an integrated strategic energy technology (SET) plan: Accelerating the European energy system transformation”* focuses on the development of (advanced) materials for cost-effective energy savings and on accelerating the large-scale market uptake of nearly zero-energy buildings. It should be noted that such materials should ensure a long-term high performance of buildings during their life cycle.

One of the most common solutions used to improve envelope thermal resistance is the External Thermal Insulation Composite System (ETICS). It consists in applying a thermal insulation material to an exterior wall using an adhesive product and/or mechanical fixing and protecting it with a reinforced rendering system. This solution is very popular for application in both new and existing buildings, mainly due to its outstanding thermal performance and relative low cost. Among the several advantages of this solution, the mitigation of thermal bridges and the benefit to the preservation of the thermal inertia of the building, which increase the occupant’s thermal

comfort and well-being, should be highlighted. Nonetheless, ETICS walls are often associated with the occurrence of anomalies that may affect their performance and durability (mechanical damage, cracks, water infiltration, biological growth, or even detachment). Such anomalies may be the result of design and application errors, material failure, or components incompatibility. Hence, there is growing interest in developing products using materials that are able to present a high thermal performance at a reduced thickness, known as super-insulating materials. Among them, are solutions that use vacuum insulation panels (VIPs).

Using vacuum technology in ETICS instead of conventional insulation materials could represent a significant step towards achieving the European Union's energy efficiency objectives. However, several challenges may be expected. Firstly, an issue associated with VIP use in buildings is the fact that, unlike most conventional insulation materials available in the market, VIPs cannot be cut or adapted on-site, leading to technical difficulties from the point of view of installation and performance. Also, VIP panels are very sensitive to mechanical damage and special care must be taken during all stages of the construction process to prevent loss of vacuum (which negatively affects VIPs performance). To go around this, when used in façades the panels must be provided with a covering layer to ensure mechanical protection and adequate capacity for adhesion. There is also concern regarding two other main aspects: the thermal bridging effect that occurs between panels (due to their metallized barrier envelope) and the issue of loss of performance during service life (due to loss of vacuum over time). Furthermore, it is necessary to determine if this solution may exacerbate the occurrence of the anomalies most frequently associated with ETICS, and to identify what measures could be taken to prevent and mitigate major issues. As this is a novel solution, there is currently a lack of standardized test methods for an adequate assessment of VIP based ETICS that take into account VIP specificities, such as the impossibility of being cut and the need to maintain their vacuum pressure during the service life. Finally, the high cost of VIPs is a major factor hindering the technology's penetration into the building market. However, the VIP high thermal performance coupled with its lower thickness may lead to economic benefits associated with space savings. For this reason, comprehensive research on VIP cost-effectiveness is warranted.

The research work presented in this thesis aimed at evaluating the feasibility of incorporating VIPs into ETICS, a novel solution henceforth referred to, in this study, as VIP based ETICS. First, in order to ensure a successful technical incorporation of VIPs into external finishing systems with rendering, the product was investigated regarding its hygrothermal behaviour and long-term performance. The main properties of an innovative VIP product designed for use in ETICS solutions were determined by means of a laboratory testing campaign, with particular attention to the edge thermal bridging effects.

Then, in order to assess the effective behaviour of the system, it was evaluated through onsite monitoring of real VIP based ETICS applications in different climates, looking to evaluate long-

term performance and detect early anomalies such as cracking, vacuum loss, blistering and biological growth (based on the evaluation of the surface condensation risk).

Furthermore, in this study, experimental test procedures were developed for evaluating the durability of the solution, and for enabling early identification of potential anomalies. In this context, a new test procedure that includes the influence of multiple dynamic boundary conditions, such as air temperature, relative humidity, rain and solar radiation simulation, was proposed and carried out on a large-scale test specimen.

Numerical models were also explored for VIP thermal performance evaluation, in particular to study the edge thermal bridging effects. The numerical approaches used were validated against the experimental measurements obtained in the study. Finally, in order to address the issue of cost, a whole-life cost assessment study was carried taking into account both energy and space savings.

During this research work, the VIP performance was often compared with a conventional thermal insulation material in order to evaluate the competitiveness of this innovative solution against the most commonly used ETICS solution.

## **1.2. Research questions and objectives**

This research work aims to evaluate the performance and feasibility of an external thermal insulation composite system that uses vacuum insulation panels instead of a conventional insulation material. Currently, there is a lack in knowledge regarding the successful use of this innovative solution in ETICS, however, it is expected that using VIPs in ETICS will entail a number of challenges associated with the specificities of VIPs, as well as with the anomalies known to be often found in ETICS solutions. For VIP based ETICS to be feasible, it is essential that they meet the relevant technical requirements during their service life. Consequently, in order to guarantee an adequate performance, there are issues that need to be studied.

To achieve this goal, the investigation was focused on the experimental performance evaluation of a VIP based ETICS solution, which include laboratorial testing and onsite measurements. Additionally, numerical modelling was used to simulate the thermal behaviour of VIP products.

Within this context, the following research questions were formulated:

- What are the main challenges associated with using VIPs in ETICS solutions?
- Can VIPs be successfully incorporated into external insulation finishing systems?

- What is the influence of the edge thermal bridging effect on the thermal performance of VIP based ETICS?
- What main potential anomalies can be expected in a VIP based ETICS during its service-life?
- What test methods and numerical models can be used to successfully evaluate and predict the effective behaviour of the solution?
- What conditions are needed for VIPs to be economically feasible?

In order to address these questions, the following specific objectives were set out:

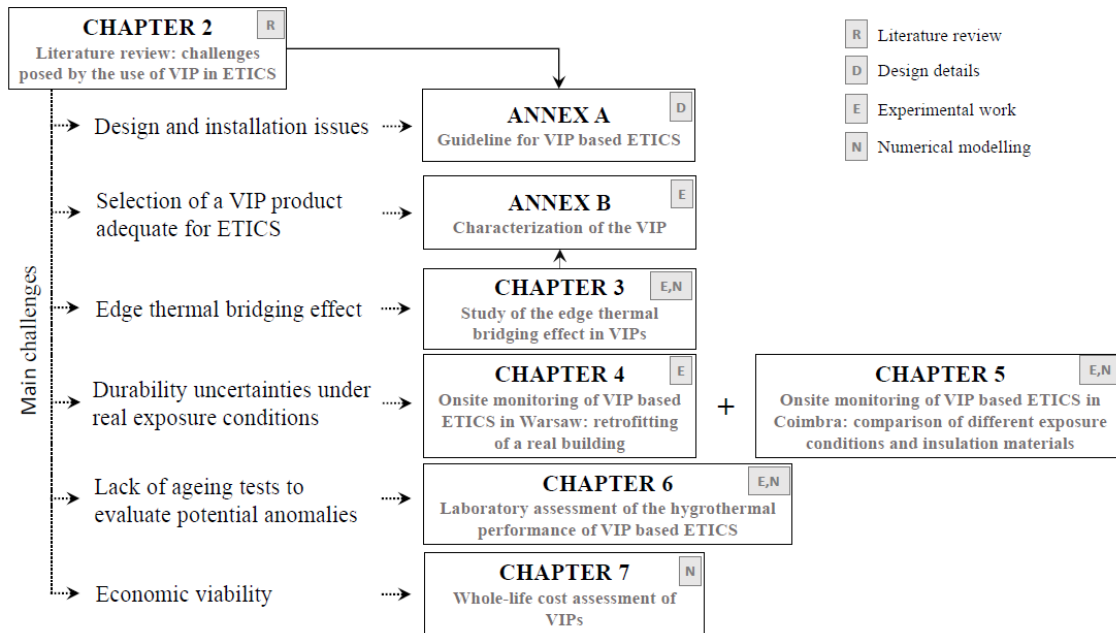
- To perform a literature review of VIP buildings applications, particularly in external walls insulation;
- To propose a guideline for VIP based ETICS installation;
- To characterize a VIP product, regarding their hygrothermal and mechanical behaviour, focusing on the specificities of vacuum technology, namely regarding the edge thermal bridging effect;
- To carry out the experimental onsite monitoring of real VIP based ETICS applications;
- To propose and implement experimental test methods aimed at evaluating hygrothermal performance, durability and potential anomalies;
- To validate the applicability of numerical models aimed at simulating the thermal behaviour of VIP under different exposure conditions;
- To assess the whole-life cost of VIP based ETICS.

Looking to address these research questions mentioned above, and meet these objectives, the thesis document has been structured into individual chapters. The thesis structure is detailed in the next section.

### **1.3. Thesis structure**

The thesis is divided into eight chapters which include the introduction, the conclusions, and the six main stages of the research work. Since each chapter contains its own introduction, materials and methods, results and discussion, conclusions and references, the chapters can be read individually. Figure 1.1 shows a flowchart that illustrates the structure of the research thesis.





**Figure 1.1:** Research thesis flowchart.

Chapter 2 of the thesis presents the literature review which supports the context and motivation of this thesis and focuses on identifying the main challenges posed by using VIPs in the external wall insulation of buildings. Looking to deepen the knowledge of VIP based ETICS, each section of this chapter addresses a specific challenge. Each chapter of the thesis seeks to study each of these main challenges, as illustrated in Figure 1.1. The VIP products available for the use in ETICS, as well as, the case studies found in the state-of-art are presented and the main findings are highlighted. The concerns regarding VIP based ETICS are discussed and guidelines for performing an adequate evaluation of this innovative solution are proposed. Based on the knowledge acquired, a design and installation guideline for VIP based ETICS is presented in Annex A.

Chapter 3 presents the novel VIP product used in this research work which was designed for use in ETICS solutions. This chapter focuses on the experimental characterization campaign carried out to determine the thermal performance of the VIP. Particular attention was given to the edge thermal bridging effects and its influence on the thermal performance of ETICS walls. For this purpose, experimental measurements were carried out using a guarded hot plate apparatus. Also, numerical modelling under steady and unsteady boundary conditions were carried out and compared against the experimental results. Looking to address the influence of VIP properties on the edge thermal bridging effect a sensitivity analysis was performed. Additionally, the contribution of the point thermal transmittance of mechanical fixing devices was numerically evaluated. Finally, transient thermal simulations are applied to VIP based ETICS in different support walls. Before the detailed thermal characterization, the mechanical and other hygrothermal properties of the VIP product were determined by means of a laboratory testing

campaign. These results, as well as detailed information about the selected VIP product used in this thesis are summarized in Annex B.

Looking to better understand the VIP based ETICS's hygrothermal behaviour, chapters 4 and 5 present results obtained under real environmental exposure, namely to identify potential anomalies in service conditions.

Chapter 4 presents the onsite monitoring of a VIP based ETICS application which took place in Warsaw, Poland, where a real retrofitted building wall was instrumented and monitored over a prolonged period. In this chapter, measurements of temperature, relative humidity and heat flux are discussed, and the edge thermal bridging effect is analysed. The experimental measurements are also compared with a conventional ETICS solution used as a reference. Furthermore, the thermal transmittance coefficient of the retrofitted wall was estimated based on temperature measurements.

In chapter 5, a surface condensation risk assessment study was carried out using results of an onsite monitoring of ETICS walls located in Coimbra, Portugal. This study compares the thermal behaviour of VIP based ETICS walls with conventional ETICS solutions and investigates the influence of the finishing coat colour and orientation on the surface condensation risk, and, consequently, on the risk of biological growth. Additionally, numerical simulations were carried out and compared against experimental measurements.

In chapter 6, aiming to provide an ageing test procedure to evaluate potential anomalies, a novel laboratory test campaign for assessing the hygrothermal performance of the VIP based ETICS solution is proposed and carried out using a large-scale specimen. The experimental procedure includes standard ageing cycles (heat/rain and freeze/thaw cycles), as well as a new approach which simulates solar radiation conditions. The introduction of solar radiation allowed for the assessing the influence of using different finishing coat colours in the ETICS rendering system. During the test campaign, the temperature and heat fluxes were recorded and analysed. Furthermore, in order to identify early signs of anomalies occurring at the level of the ETICS finishing coat layer, a complementary inspection by means of a crack microscope, a scanning electronic microscope, and a spectrophotometer were carried out. Also, mechanical tests after ageing, such as hard body impact resistance and bond strength, were performed. Experimental test results were also compared to numerical results based on 2D transient heat transfer numerical modelling.

Regarding the assessment of the economic viability of vacuum technology, chapter 7 presents a whole-life cost (WLC) analysis of the use of vacuum insulation panels in buildings façades. The proposed WLC methodology, based on the cost-optimal calculation approach proposed by European Union Commission, allowed for a comparison of the cost-effectiveness of VIPs against other conventional insulation material. Considering an office full-service leasing perspective, this investigation included the additional rental income expected due to the space savings resulting

from the lower thickness of the VIP installation. Energy calculations were performed based on transient heat transfer through the façade. This study takes into account varying parameters, such as location, cost of materials, insulation thickness, rental prices, amongst others. This chapter aims to demonstrate in which conditions the VIP based ETICS solution can be economically viable, identifying the range of VIP costs and rental prices that make their use in buildings cost-effective.

Finally, the last chapter presents an overview of the work and the main conclusions that can be drawn from it. Also, potential future research studies are suggested. These future investigations could be relevant to continue to deepen the knowledge regarding the use of super-insulating materials in buildings, both in terms of predicting the durability/service life performance, and in terms of defining new test methods that are able adequately assess these innovative solutions.

The research work conducted in this thesis has been published in international scientific journals and conference proceedings. A list of the papers and their relationship with each chapter are presented next:

- **Chapter 2:** M. Gonçalves, N. Simões, C. Serra, I. Flores-Colen, “A review of the challenges posed by the use of vacuum panels in external insulation finishing systems”, *Applied Energy*, vol. 257, 114028, 2020, <https://doi:10.1016/j.apenergy.2019.114028>;
- **Chapter 3:** M. Gonçalves, N. Simões, C. Serra, I. Flores-Colen, K., Rottenbacher, F. A. Almeida, “Study of the edge thermal bridging effect in vacuum insulation panels: steady and unsteady-state approaches using numerical and experimental methods”, *Energy and Buildings* vol. 258, 111821, 2022, <https://doi:10.1016/j.enbuild.2021.111821>.
- **Annex B:** M. Gonçalves, N. Simões, C. Serra, I. Flores-Colen, S. Martins, “Experimental characterization of a vacuum insulation panel product for ETICS”, in *CEES21 – International Conference Construction, Energy, Environment & Sustainability*, Coimbra, 12-15 October 2021;
- **Chapter 4:** M. Gonçalves, C. Serra, N. Simões, I. Flores-Colen, C. Kokolsky, C. Sprengard, “Onsite monitoring of a wall retrofitted with an external vacuum insulation composite system”, *Journal of Building Engineering*, vol. 44, 103301, 2021, <https://doi:10.1016/j.job.2021.103301>;
- **Chapter 5:** M. Gonçalves, N. Simões, C. Serra, J. Almeida, I. Flores-Colen, N. V. Castro, L. Duarte, “Onsite monitoring of ETICS comparing different exposure conditions and insulation materials”, *Journal of Building Engineering*, vol. 42, 103067, 2021, <https://doi:10.1016/j.job.2021.103067>;
- **Chapter 6:** M. Gonçalves, N. Simões, C. Serra, I. Flores-Colen, “Laboratory assessment of the hygrothermal performance of an external vacuum-insulation composite system”,

*Energy and Buildings* vol. 254, 111549, 2022,  
<https://doi.org/10.1016/j.enbuild.2021.111549>;

- **Chapter 7:** N. Simões, M. Gonçalves, C. Serra, S. Resalati, “Can vacuum insulation panels be cost-effective when applied in building façades?”, *Building and Environment* vol. 191, 107602, 2021, <https://doi.org/10.1016/j.buildenv.2021.107602>.





## **CHAPTER 2**

# **LITERATURE REVIEW: CHALLENGES POSED BY THE USE OF VACUUM INSULATION PANELS IN ETICS**





## **2. Literature review: challenges posed by the use of vacuum insulation panels in ETICS**

### **2.1. Introduction**

It is known that buildings account for a significant portion of global energy use and CO<sub>2</sub> emissions [1]. This has meant that energy efficiency in buildings needs to keep improving. A clear and cost-effective measure for reducing energy needs for heating and cooling buildings is to increase the level of insulation of their thermal envelope [2]. The Energy Performance of Buildings Directive (EPBD) - which was first published in 2002 [3] and is now on its third edition [4] - has imposed that all new buildings must have nearly zero or very low energy needs, which means that, in the pursuit for optimal energy performance, increasingly strict thermal resistance requirements must be met by the building envelope.

An insulation solution which has been steadily rising popularity is the External Thermal Insulation Composite System (ETICS) [5], also known as External Insulation Finishing System (EIFS). ETICS kits consist of a thermal insulation material that is applied to an exterior wall using an adhesive product and/or mechanical fixing. Then, a rendering system is then applied. This is a thin layer which usually consists of a base coat mortar with reinforcement mesh, a key coat (primer) and a finishing coat. Different types of thermal insulation materials such as expanded polystyrene (EPS), mineral wool (MW), expanded cork agglomerate – commercially known as insulation cork board (ICB), are among the products that can be used in ETICS solutions. In European countries, most ETICS applications use EPS (70%) or MW (26%), according to 2020 market data [6]. Currently, the thermal insulation thickness applied in Mediterranean climates ranges from 40 to 100 mm. However, in colder climates, as in central Europe for example, an insulation layer thickness of as much as 300 mm can be needed to satisfy energy performance requirements [7].

Implementing thermal insulation solutions in buildings can greatly help to reduce their environmental impact. It is known that energy savings made during the building's service life are more significant than the embodied energy of common insulation materials [8]. For example,

Luján *et al.* [9] concluded that ETICS walls were able to reduce energy loss by 57% and energy gains by 39%, compared with the original façade of a building located in Madrid. Zhang *et al.* [10] studied the effect of the insulation layer placement on the temperature and heat flow of the inner surface wall when air-conditioning was operating intermittently. Their results showed that the smallest variation of the inner surface temperature corresponded to the external wall insulation solution. This indicates that ETICS helps to lower thermal loads in buildings. Yuan *et al.* [11] also concluded that high insulation of external walls reduced the thermal loads of buildings in several regions in Japan.

Nowadays, this type of external thermal insulation is commonly used in all European countries. It is estimated that there are around 2 billion m<sup>2</sup> of ETICS applied in Europe up to 2017 [12]. Its popularity has grown due to its advantages over other thermal insulation techniques. In particular, it has relatively easy installation and low implementation costs, and it helps to mitigate thermal bridges and the risk of internal condensation. It also preserves the building's thermal inertia, increases the thermal comfort, protects the masonry and structural elements, and renovates the external appearance of the building by covering any existing defects [13]. However, the need for skilled labour (for proper installation), the low mechanical resistance of the system, and concerns with durability and aesthetic problems are the main issues associated with ETICS. Over time, such issues can lead to unsightly defects and can even adversely affect the system's performance [14].

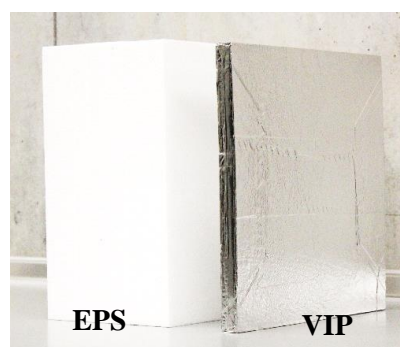
To ensure the system's adequate behaviour and durability, all the components need to be compatible. In 2000, EOTA (European Organisation for Technical Assessment) published the ETAG 004 – Guideline for European Technical Approval of External Thermal Insulation Composite Systems (ETICS) with rendering [15]. ETAG 004 was amended in 2011 and 2013 and converted in the European Assessment Document (EAD) 040083-00-0404 [16] in 2020. These documents established test procedures and essential performance requirements in accordance with the Construction Products Regulation (CPR) [17], including safety in use, energy economy and aspects of durability. While ETICS EAD assumes a service life of 25 years for ETICS solutions, several studies have suggested a longer service life of over 30 years [18]. However, such estimations strongly depend on the quality of maintenance actions [19], as well as the in-service conditions [20]. Nonetheless, to ensure the reliability of any maintenance strategy, consistent knowledge about the long-term performance of a solution is crucial [21].

When product selection or system installation is inadequate, anomalies in ETICS walls usually happen in the first 10 years of use [22]. The anomalies that most often occur in ETICS walls are [23]: lack of flatness, cracking, detachment and/or blistering of the plaster/final coating, partial or generalized detachment of the system, mechanical damage, water infiltration, and aesthetically unpleasant defects such as biological growth and soiling. Statistical surveys of inspections carried out on buildings with ETICS have confirmed the occurrence of these common anomalies [24]. For example, Amaro *et al.* inspected 146 façades with ETICS located in Mediterranean climate

[25] which allowed for a statistical analysis of their main weaknesses, detailed in [26]. These issues can cultivate a generally negative opinion of the technology in owners, designers and other players in the building sector, thereby decreasing its potential for success in the future. It cannot be overemphasized that the quality of the materials and their correct application are fundamental to the preservation of ETICS' performance and durability. In this context, and given the known benefits and still rising popularity of ETICS solutions, more attention must be given to achieving a deeper understanding of the behaviour and durability of new solutions for the external insulation of buildings, such as systems incorporating vacuum insulation panels (VIPs).

As the worldwide demand for energy savings calls for improvements in thermal performance requirements, stricter standards such as the Passive House and zero-energy concepts, are making super-insulating materials more and more appealing. A brief comparison between the collected data on thermal transmittance (U-values) requirements published by EURIMA [27] in 2007 and current requirements [28], confirm the need for increasingly thicker insulation layers in European buildings. To reach the U-value requirements with traditional insulation materials, such as MW or EPS, buildings are required to have walls up to 500 mm thick, or even more [29]. Such a thick envelope may not be desirable for a number of reasons, including architectural/design limitations and reduction of available floor area.

To achieve higher thermal resistance with lower thicknesses, a new generation of super-insulating materials such as those using vacuum technology [30] is entering the market. VIPs provide one of the lowest thermal conductivity values available in the insulation market. The thermal conductivity of a vacuum panel in its initial state is approximately 2 to 4.5 mW/(m·K), depending on the core material ([31],[32]), whereas other conventional insulation materials such as EPS or MW have thermal conductivity of around 35 to 40 mW/(m·K) [33]. Lower thermal conductivity allows planners to achieve higher insulation and to benefit from more usable space, thus avoiding some architectural integration issues. For example, a wall would require a layer of conventional insulation 170 mm thick to provide a thermal transmittance of 0.21 W/(m<sup>2</sup>·K). With vacuum insulation panels, the same thermal transmittance could be achieved by a thickness of 20 mm. An illustration of this advantage is showed Figure 2.1. To sustain this level of performance, the panels must be handled carefully, as loss of vacuum severely impairs the product's performance.



**Figure 2.1:** Thermal insulation products with the same thermal resistance: 170 mm thick EPS (on the left) and 20 mm thick VIP (on the right).

Thanks to their thermal insulation potential, VIPs are slowly being introduced into buildings, notably through incorporation into roofs, ceilings, floors and walls, but also in the form of specific elements, such as façade panels [34], glass panels [35] and masonry blocks [36]. Unlike most existing external VIP application case studies, which have been carried out using a rigid finishing layer (such as wooden material board [37]) to protect the VIPs and ensure watertightness, ETICS characteristically use a thin rendering layer around 5 mm thick (normally composed of a base coat, primer and finishing coat). Most studies found on ETICS have been published recently (in the last 12 years). A quick search using ScienceDirect shows that more than 80% of the ETICS studies in this database still focus on using EPS and/or MW. A small number of the studies found (around 5%) mentioned VIPs ETICS applications, which further demonstrates the novelty of this technology. The rest include the use of other types of insulation materials, such as ICB.

The use of VIPs in external walls will contribute to improving the energy efficiency of buildings via a significant upgrade of the thermal performance of the envelope. This innovative technology will help to promote a more sustainable building sector towards nearly zero-energy buildings and to reach the climate change mitigation goals. Their fairly recent introduction to the market (and lack of penetration), together with the specificity of the solution, provide the grounds for a review work that compiles information and addresses the most important challenges posed by the solution.

To guarantee good system performance, adequate service life and prevent façade anomalies, the incorporation of VIPs into ETICS in this way needs to be carefully investigated. In this chapter an overview of vacuum panels used in external insulation systems is given. The goal is to gather detailed information on the many challenges posed when incorporating VIPs into external thermal insulation composite systems. First, a briefly description of the VIP technology is presented. This includes market research of products that are available for use on external walls. Afterwards, the state-of-the-art of case studies that have employed this technology is established. The main limitations that arise from using VIP in buildings, such as edge thermal bridging, inner and superficial condensations, durability and potential anomalies concerns, installation issues, high investment costs and environmental performance, are discussed. Then, looking to address the lack of knowledge around the long-term performance of ETICS that incorporate VIPs, specific assessment methods are proposed. Looking to contribute to addressing with the main challenges presented in this chapter, and in line with the goals set out for this thesis, a guideline for VIP based ETICS installation is proposed in Annex A. This document provides information about the design, installation, maintenance works and disassembly of VIP based ETICS, aiming to ensure the successful performance of this innovative solution.

## 2.2. Vacuum insulation panels in ETICS applications

ETICS using vacuum insulation panels is a solution in which the traditional insulation layer is replaced by a VIP product with covering layers (*e.g.* thin EPS). The development of VIPs started in the first half of the twentieth century. The first patent for this technology dates back to as early as 1930. However, only in 1999 did the first applications for buildings appear [38]. VIP thermal insulation products for roofs have been the most popular applications in buildings. For example in Switzerland, the flat roof application covers more than 95% of the market share of VIPs used in buildings [39].

A VIP consists of an evacuated open core material surrounded by thin laminates, composed of a barrier envelope (multi-film layer), used to maintain the vacuum. The main components are the inner core, barrier envelope, getters, desiccants and opacifiers. There are many possible ways to combine alternative envelopes and cores in different VIP solutions [40]. Because of its reduced thermal conductivity, fumed silica is generally used as the core material [41]. To maintain the inner vacuum, getters and desiccants are often part of the components used to produce VIPs. Getters are inserted inside the VIP core to adsorb gases, while desiccants are inserted to adsorb water vapour, which might penetrate into the VIP through the envelope barrier [32]. The opacifiers are added to make the core opaque to infrared radiation, thereby reducing the radiative conductivity to a low level. A common opacifier for fumed silica cores is silicon carbide powder [42].

VIPs are being adapted to the needs of building applications. To provide protection against mechanical damage and enable them to be applied to walls (ensuring flatness and bonding adhesion), VIP products for buildings benefit from an additional protective covering layer, such as expanded polystyrene or polyurethane foam. This is known as an encapsulated VIP, which is represented in Figure 2.2.

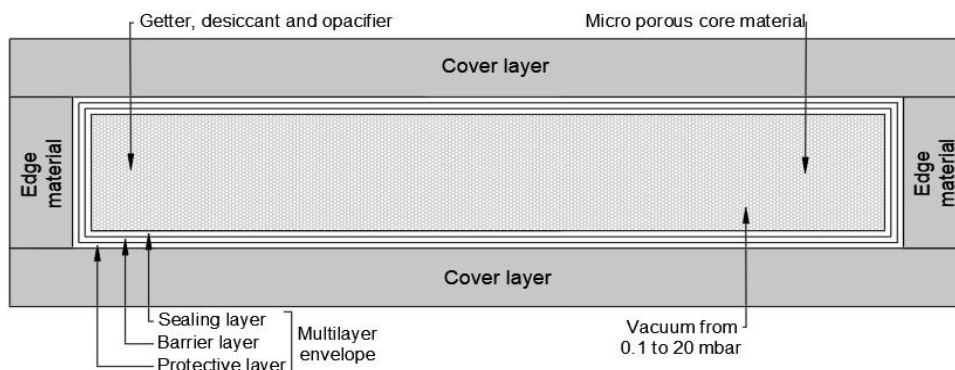


Figure 2.2: Vacuum insulation panel with cover layers scheme (adapted from [32] and [43]).

Typical values of VIP thermal conductivity (centre of the panel) at 1 mbar pressure can be less than  $5 \text{ mW}/(\text{m}\cdot\text{K})$  [44]. The literature review shows VIP thermal conductivity values between 2






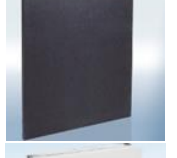


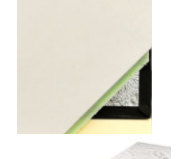
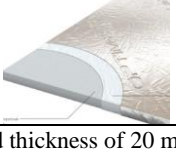
and 4.5 mW/(m·K) in initial state, and 7 to 8 mW/(m·K) after 25 years [30]. When the panel is punctured, the thermal conductivity values rise to around 22 mW/(m·K), in case of fumed silica core. This is still lower than that of conventional thermal insulation materials such as EPS or MW, which usually have conductivity values around or above 35 mW/(m·K), respectively. It has also been reported that the thermal conductivity changes with temperature, moisture and ageing, especially under severe boundary conditions [45]. In particular, the main ageing mechanisms that affect thermal performance are increased inner pressure and moisture inside the panels.

Regarding the assessment of products to be introduced to the market, specification documents have recently been made available. Specifically, the European Assessment Document – EAD 0040011-00-1201 [46] for VIPs with factory applied protection layers was published in December 2017, while the VIP product specification standard EN 17140 [47] was recently approved in 2020. EN 17140 defines characteristics for factory made VIPs used for the thermal insulation of buildings. However, this standard does not apply to VIPs that use getters because there is little experience with the ageing of these panels. These recent publications attest to the innovative character of VIP products and confirm the interest of their use in building systems, such as the ETICS solutions.

### **2.2.1. VIP products for external insulation of walls**

Recently, as VIP production has become more industrialized [48], a number of VIP products have been developed with cover layers. Table 2.1 shows commercial VIP products that can be externally applied on walls as insulation. Regarding the panel's core material, most VIP manufacturers use fumed silica because of its low thermal conductivity. Nevertheless, looking to reduce costs, other core solutions are being developed such as ones using expanded cork [49], glass fibre [50], expanded perlite [51], aerogel [52] and polyurethane powder [53]. While most manufacturers assume that their external wall insulation products will be applied behind a rigid finishing layer, a few solutions are clearly meant for ETICS solutions with thin rendering (composed by a reinforced base coat and a finishing coat layer).

**Table 2.1:** Commercial solutions for external insulation of walls.

Ref.	Manufacturer (Product)	Illustration	Core	Protective layer	Thickness [mm]	Thermal conductivity [mW/(m·K)]	Apparent density [kg/m <sup>3</sup> ]
[54]	Vaku-isotherm (SP-2)		Fumed silica	EPS	10 - 50	8 <sup>(1)</sup>	--
[55]	Vaku-isotherm (SP-2/E)		Fumed silica	EPS	1 - 50	8 <sup>(1)</sup>	--
[56]	Vaku-isotherm (BAUPLATTE)		Fumed silica	Plastic recycling panel and EPS	10 - 50	8 <sup>(1)</sup>	--
[57]	Porextherm (Vacupor PS-B2-S)		Fumed silica	EPS	10 - 50	7 <sup>(2)</sup>	170 – 210
[58]	Weber Saint-Gobain (Weber.therm. LockPlate)		Fumed silica	EPS	10 - 50	7	190
[59]	va-Q-tec (va-Q-vip B)		Fumed silica	Black glass fibre textile	10 - 50	4.3 <sup>(3)</sup> 7 – 8 <sup>(4)</sup>	180 – 210
[60]	va-Q-tec (va-Q-vip F-EPS)		Fumed silica	EPS	10 - 50	4.3 <sup>(3)</sup> 7 – 8 <sup>(4)</sup>	180 – 210
[61]	va-Q-tec (va-Q-vip F-GGM)		Fumed silica	Rubber granulate lamination	10 - 40	4.3 <sup>(3)</sup> 7 – 8 <sup>(4)</sup>	180 – 210
[62]	Variotec (VT-A-HYDRO)		Pyrogenic silica	Extruded polystyrene	20 - 50	7	190 – 220
[63]	Kingspan (OPTIM-R)		Microporous material	Without protective layer	20 - 60	7	--

<sup>(1)</sup> Value after 30 years and thickness of 20 mm;

<sup>(2)</sup> Value measured at the centre of the panel;

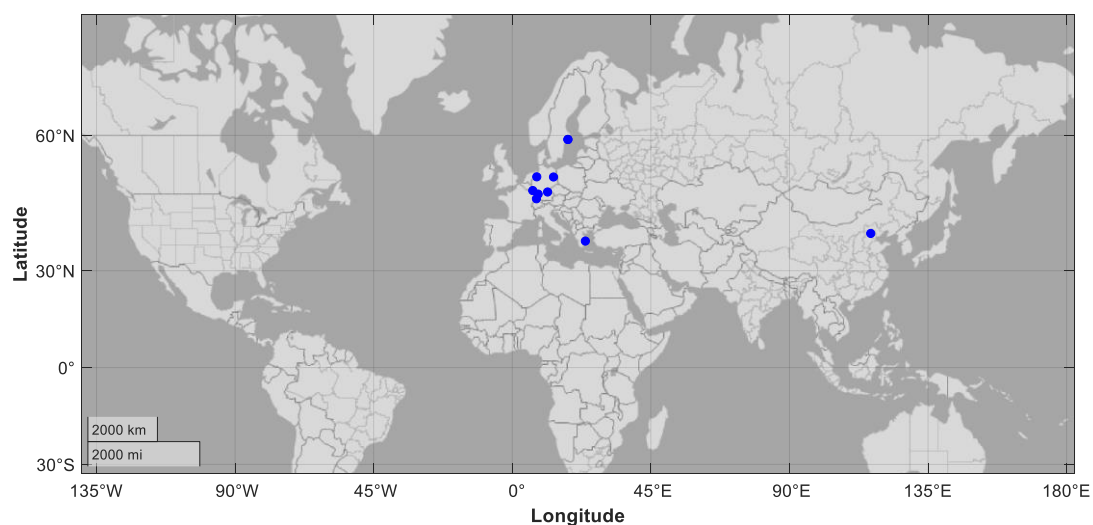
<sup>(3)</sup> Initial value, measured at the centre of the panel;

<sup>(4)</sup> Including ageing and edge losses.

## 2.2.2. Case studies

Several studies and academic works have been published with the goal of understanding the performance and durability of VIP applications in buildings, for example, those by Tenpierik [64] and Karami [65]. However, few studies focus on external thermal insulation composite systems with rendering. As mentioned, most VIP applications for external walls include a rigid board [37] or other special elements, such as ventilated vacuum insulated façades. For example, Johansson *et al.* [66] evaluated the performance of VIPs in a retrofitted building façade where VIPs were applied on the external wall behind a wooden cover board. In a detached house in Switzerland, VIPs applied to the façades were covered with a hard plate [67].

In 2005, a number of international studies on VIPs were gathered in the IEA/ECBCS Annex 39 High Performance Thermal Insulation (HiPTI) ([48], [68]). This research was divided into two subtasks, where the first part concerned VIP properties and durability, while the second part described various demo cases. In total, 20 constructions were built or retrofitted, and the outcomes regarding energy use, thermal bridges and moisture performance were analysed. A few applications used ETICS with a thin rendering (common ETICS rendering solution), but mostly using a rail mounting system and a polystyrene cover layer. In ETICS with a rail mounting system, there is very little danger of damage to the VIPs, and the rails were found to cause small thermal bridges. The research team concluded that vacuum technology has become a feasible and important means for designing more energy efficient buildings. Nevertheless, they note that there are challenges to overcome, particularly in terms of high cost and issues with the long-term performance of VIPs in buildings. In the next subsections, these studies are divided into new and existing buildings and their main takeaways are highlighted. As can be observed in Figure 2.3, most of these applications took place in Central Europe, where VIP technology is more established.



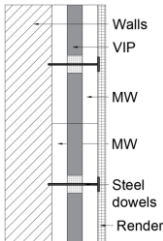
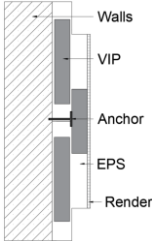
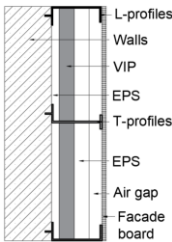
**Figure 2.3:** Locations (blue dots) of the case studies of VIP based ETICS in the world.



### 2.2.2.1. New construction

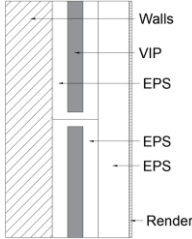
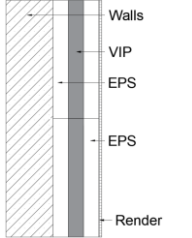
Table 2.2 shows several case studies of VIP applications in ETICS. These include both onsite applications in real buildings and test specimens. These studies differ by type of solution, cover layer, fixation, and thickness of the insulation layer. The design and installation of the solution affects not only the safety of the system, but the wall's thermal performance, too. Kim *et al.* [69] concluded that in ETICS solutions the effective thermal transmittance of VIPs with cover layers decreased by 26%, compared with VIPs without cover layers. This is because VIPs with EPS cover layers reduce the thermal bridging caused by the VIP barrier envelope. Nevertheless, this effect cannot be completely prevented, as the cover layer material is still significantly more conductive than the VIP panel. VIP size also has great influence on overall heat loss [70]. Small panels have lower thermal resistance due the edge thermal bridging effect being more predominant.

**Table 2.2:** Case studies of VIP based ETICS in new constructions based on literature review.

Location / Reference	Illustration	Goals	Construction solution	Fixation	Main results / conclusions
Athens, Greece [44]		Comparative assessment (experimental and numerical) of conventional and VIP based ETICS in a mock-up two-storey building.	Lightweight steel-frame mock-up with gypsum boards (internally) and cement boards (externally) with drywall systems, using 20 mm VIP covered by 20 mm of mineral wool on both sides.	Adhesive mortar with two steel dowels for each board (VIP with two built-in holes).	Marked difference between predicted and achieved performance.
Munich, Germany [71]		Demonstration of a new VIP system for ETICS that was applied in a residential building.	Wall <sup>(1)</sup> with 20 mm VIP covered by EPS with overlapping plate.	Adhesive with fasteners.	The two insulation layers reduce the edge thermal bridges. If this system were to be replaced by thick insulation, a difference in room area of 6.5% is estimated.
Stockholm, Sweden [72]		Illustration of a new VIP mounting system in a laboratory specimen.	Aerated concrete with 20 mm thick VIP embedded between 20 and 10 mm thick EPS plus a façade board (with air space).	Adhesive and stainless-steel profiles (L and T-profiles).	VIPs will not lead to high relative humidity in the wall or at the joint. Attention must be given to leakage at joints and penetrating rain.

<sup>(1)</sup>Support wall information not provided by the authors.

**Table 2.2 (continued):** Case studies of VIP based ETICS in new constructions based on literature review.

Location / Reference	Illustration	Goals	Construction solution	Fixation	Main results / conclusions
Bersenbrück, Germany [73]		Application of VIPs in a detached house.	Wall <sup>(1)</sup> with 20 mm VIP encapsulated on all sides within 20 mm EPS and additional layer of 80 mm EPS.	Information not provided.	The main disadvantage with encapsulation of the VIP is the thermal bridges at the connections of the panels, which cannot be prevented.
Trier, Germany [73]		Application of VIPs in 12 terraced houses.	Wall <sup>(1)</sup> with 20 mm VIPs, with 20 mm EPS on both sides.	Information not provided.	Not available.

<sup>(1)</sup> Support wall information not provided by the authors.

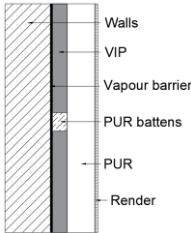
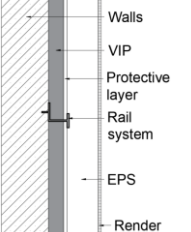
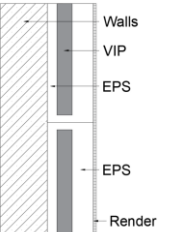
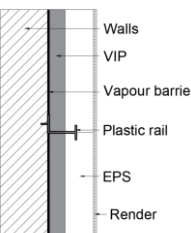
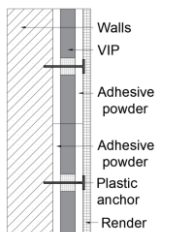
Mandilaras *et al.* [44] presented a comparative assessment of a conventional ETICS solution with EPS and a VIP based solution consisting of a vacuum panel covered with MW on both sides. The two layers of MW serve to protect the panel from mechanical damage and from the alkaline nature of the bonding mortar. This special VIP panel has two holes that allow mechanical fixation with steel dowels, without affecting the sealing membrane. The holes are filled with EPS to reduce thermal bridges, and to protect the VIP panel. In terms of thermal behaviour of the solution, the authors concluded that standardized techniques failed to accurately predict the effective behaviour of VIP insulated walls. Experimental thermal resistance values for the VIP wall were around 21%, 25%, 22% and 39% lower than for a theoretical R-value wall, considering ISO 9869 [74] (dynamic analysis method), ISO 9869 with stud effect, CFD simulation and field measurements, respectively. For super-insulating materials, the high sensitivity of the calculated values for linear and punctual thermal bridges increase the risk of erroneous design values. More detailed simulation could be used to overcome these limitations and to handle some of the issues related to convection and radiation phenomena, as well as with the mechanical fixing.

Simmler and Brunner [75] investigated the service life of an ETICS solution that consists of 20 mm VIP covered by a 10 mm layer of polystyrene on both sides. The theoretical results showed that a reasonable service life can be expected for this kind of application. However, it should be noted that conventional ETICS solutions use a finishing rendering (base coat + primer + finish layer) that is around 5 mm thick, which is considerably less than the 30 mm which was used in this study. Consequently, higher surface temperatures can be expected along with accelerated ageing. Moreover, in this study, the authors only considered the ageing mechanisms of temperature and humidity. Other stresses like those of mechanical and/or chemical origin, were not considered.

## 2.2.2.2. Retrofitting

Table 2.3 lists case studies involving retrofitting buildings with VIP applications in ETICS. As with new construction case studies, these applications differ by type of construction solution, cover layer, fixation and thickness of the insulation material.

**Table 2.3:** Case studies of VIP based ETICS in retrofitting actions based on literature review.

Location / Reference	Illustration	Goals	Construction solution	Fixation	Main results / conclusions
Munich, Germany [73]		Retrofitting of an apartment and office block.	Concrete wall with vapour barrier plus rigid polyurethane foam (PUR) battens and 20 mm VIP covered with 80 mm PUR layer.	VIP was attached between compressed PUR battens.	Not available.
Karlsruhe, Germany [37]		To explore the performance of VIP in the retrofitting of multi-family building.	Brick wall / Timber wall with 40 mm VIP covered by 4 mm protective cover and 50 mm EPS.	Rail system.	Deviation between the measured and simulated relative humidity in the wall was explained by vertical air leakage paths in the wall.
Central Europe [76]		Evaluation of the deterioration of VIPs applied in a building façade.	Wall <sup>(1)</sup> with VIPs encapsulated in EPS with 30 mm at the bottom and 10 mm on all other sides.	Information not provided.	The façade had blisters on 17 out of 88 VIPs. This was found to be caused by a systematic failure in the metallization of the VIP envelope.
Nuremberg, Germany [73]		Retrofitting an old building.	Wall <sup>(1)</sup> with exterior vapour barrier plus 20 mm VIPs covered by 35 mm EPS.	Plastic rail fixation.	The U-value of the wall was improved from 0.70 to 0.19 W/(m <sup>2</sup> ·K). After 8 years, infrared thermography analysis showed punctured panels.
Freiburg, Germany [73]	---	Retrofitting of Fraunhofer ISE building.	Information not provided.	Adhesive directly applied to VIP.	Punctured VIP was found on a façade with infrared thermography.
China [77]		Practical applications of VIP in commercial and residential buildings.	Existing walls <sup>(1)</sup> with VIP with adhesive powder on both sides.	Adhesive mortar with one plastic anchor for each board (VIPs with one spacer hole).	VIP with spacer hole shows bond strength increase of about 50%. Nonetheless, energy lost due to thermal bridge effect was rather high.

<sup>(1)</sup> Support wall information not provided by the authors.

ETICS solutions with encapsulated VIPs using EPS covers were applied to a façade in an urban area in Central Europe [76]. After some time, a number of panels had deteriorated, as blisters appeared on the façade. This anomaly indicated that the inner pressure of the VIPs must have risen dramatically. The reason for this defect was attributed to a systematic failure in the metallization process (VIP production). In Germany in 2004, the Fraunhofer ISE building was retrofitted using VIPs that had been coated with an organically based plaster [73]. Several damaged VIP were removed and replaced in 2004. However, by 2005 more VIPs were found to have been punctured.

These case studies with VIPs applied in ETICS had a number of performance and service life problems. Such issues call for the development and implementation of dedicated laboratory testing methods that enable the evaluation of the durability of this innovative solution. In the next section, based on the current state-of-the-art, the main challenges of VIP based ETICS solutions are identified and discussed in detail.

### **2.3. Challenges of VIP use in ETICS**

Research studies have established the strong potential of VIP applications in buildings regarding energy savings [78]. However, these studies have also identified a number of limitations and issues that need to be carefully investigated. The use of VIPs in buildings, and in particular in external thermal insulation composite systems, presents many challenges. On the one hand, there are the issues associated with the specific nature of VIP products, and on the other, there are the problems often reported about the ETICS solution's durability. The thermal bridging effect at the edges of the panels, the loss of performance during service life, and the high material costs are often highlighted as the main challenges of VIP based ETICS solutions.

Vacuum panels cannot be adapted or cut to size onsite, unlike most conventional insulation materials available on the market. Therefore, panels must be pre-designed for the specific dimensions of the building in question and detailed construction drawings must be prepared. The edges of the product need to be adjustable, allowing some cutting of cover layer material in order to accommodate to slight size adjustments during onsite work. Also, since the panels are very sensitive to mechanical damage, puncture and loss of vacuum, special care must be taken during all stages of the construction process, including transport, handling and application of the system. An aspect that must not be neglected for a successful application of this solution is the need for specifically qualified labour.

Furthermore, the use of VIPs in external insulation finishing system may potentiate some of the anomalies often found in ETICS buildings façades. Due the higher thermal resistance of the novel insulation panel, it is expected that the thin rendering layer will be subjected to more extreme external solicitations. The relationship between known conventional ETICS anomalies, their causes, and the potential risks associated with this innovative solution are summarized in Table 2.4.

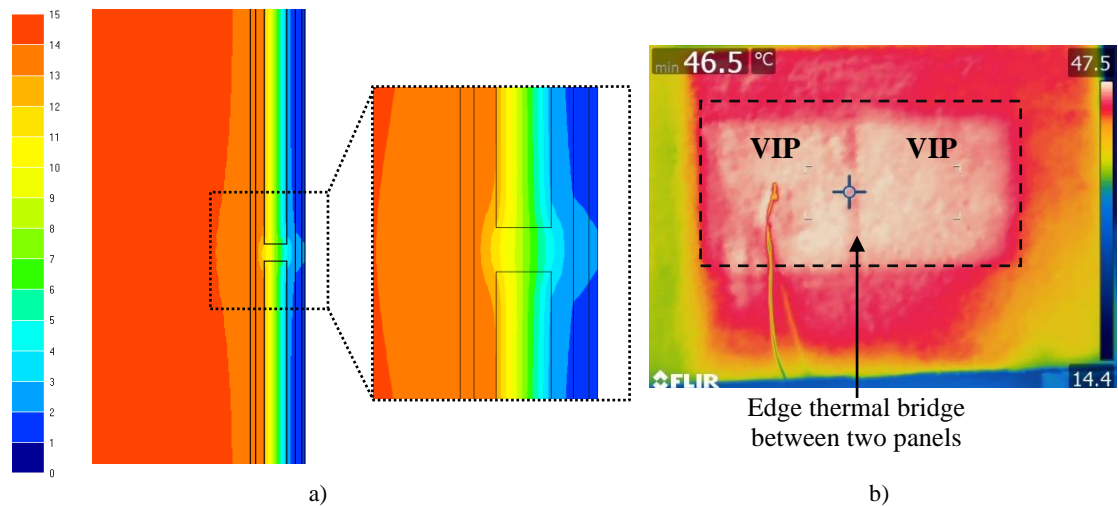
**Table 2.4:** Risk of potential problems in VIP based ETICS, in relation with known ETICS anomalies.

ETICS anomalies	Main cause	VIP based ETICS risks
Cracking	High temperature gradient	By increasing the thermal resistance of the wall, higher surface temperatures are to be expected.
Blistering	Materials with different behaviour	Water absorption, water vapour transmission and air leaks through joints between panels could be a weakness in the solution; Issues with the inner pressure of the VIP.
Biological growth and soiling	Surface condensation	Night-time surface temperatures are expected to be lower with VIPs, when compared with conventional insulation materials.
Lack of flatness	Dimensional variation	Exposure to high temperatures could change the dimensional stability of the VIPs; Variation of surface temperature due the edge thermal bridging may promote lack of flatness.
Detachment	Inappropriate bonding or mechanical fixing	VIP panels cannot be perforated; Mechanical fixing should be carefully evaluated.
Mechanical damage	Accidental impacts and vandalism	Due the fragility of the panel and the thin rendering system, impacts may cause the perforation of the panel, resulting in loss of system performance.

The next few sections, provide an overview of the main issues concerning VIP based ETICS solutions. In particular, the issues related to thermal bridging, condensation, service life, design/installation, economic and environmental viability are explored.

### **2.3.1. Edge thermal bridging effect**

The ratio between heat loss due to the thermal bridging effect and overall thermal loss is greater in highly insulated buildings, when compared with buildings that have low or medium insulation levels [79]. In fact, one of the most critical issues affecting VIP technology, and which is difficult to be avoided, is the thermal bridging effect that occurs at the edges of the panels [44]. Thermal bridges in vacuum panels occur because the barrier envelope used to maintain the vacuum establishes a link from the cold to the warm side, due the different thermal conductivity of the edge material, and due to a gap space that may be formed between adjacent panels. The influence of thermal bridges in the overall thermal performance of ETICS with VIPs is considerable [72]. This phenomenon is illustrated in Figure 2.4.



**Figure 2.4:** Edge thermal bridge effect: a) simulated temperature distribution (temperatures in °C); b) edge thermal bridges onsite detection with infrared thermography (two VIPs).

A number of studies have focused on the influence of edge thermal bridging in VIP applications [78]. Thermal bridges have been calculated numerically [70], analytically [42] and experimentally [80]. The results showed a big influence on the total overall thermal performance due the laminated aluminium foils and gaps between panels. Lorenzati *et al.* [81] showed how the joint technologies affect the thermal performance of VIPs assemblies. This experimental investigation demonstrated that thermal behaviour strictly depended on physical and geometrical properties, where the joint air gap had greater influence. Also, thickness of panel and film influenced the thermal bridge, as did the thermal conductivity of the surrounding materials [48]. In 2016, Lorenzati *et al.* [80] reported that the thermal performance of buildings using VIP panels can mainly be improved by adopting suitable materials to create the joints and fixtures of the VIP panels and by using large square VIP panels, since the effective thermal conductivity has quite a strong linear dependence on the panels' form factor (perimeter/area). Nussbaumer *et al.* [82] studied, numerically and experimentally, the thermal performance of VIP (encapsulated in EPS) application similar to a conventional ETICS. In this study, the most challenging task of the numerical analysis was to develop a simplified model able to simulate the abrupt changes in size and thermal conductivity of this kind of ETICS application (*i.e.* aluminium layers). The results showed that increasing EPS thickness reduced the edge effect of the VIPs caused by the aluminium layers within the barrier envelope. The staggering of double layers of VIPs to minimize thermal bridging was investigated by Wakili *et al.* [83] whose work aimed to determine the effective thermal conductivity by means of a minimum number of required tests and the simplest numerical model. This strategy has also been adopted in commercial solutions [71].

The state-of-the-art shows that thermal bridging in VIPs is not negligible and needs to be considered when assessing building energy performance. One of the most effective ways to reduce the influence of edge thermal bridges consists in reducing the thermal conductivity of the VIP cover layers and of the bonding materials [84]. Gaps between panels should be avoided.

Staggering two layers of VIPs is also a good solution, covering the thermal bridges of the first layer by a second layer of VIP. However, this is a more expensive option and increases wall thickness, leading to a reduction in the space savings benefits of using VIPs.

### **2.3.2. Condensations**

The water vapor permeability of a VIP is practically zero because the high barrier film of the envelope is vapor tight. This may cause problems on the edge's panels if the connection between them allows for air and vapor diffusion through the layer [73]. Information about condensation issues in VIP insulated building are available in the literature [48]. Any condensation on the external side of the vacuum insulation panels has the potential to result in deterioration of the barrier envelope, leading to possible mechanical damage, and consequently loss of thermal performance [85]. To mitigate this, an insulation material (protective cover layer) is placed over the VIP to raise the external VIP surface temperature and minimize the amount of moisture that is in contact with the VIP. In some cases, sealing tape on panel's edges has been used to increase the airtightness of the connections [73]. Another option is the use of a vapor retarder to ensure a vapor tight layer. Numerical simulations indicate that the VIPs in an ETICS solution do not pose a moisture problem to the construction [72]. However, this numerical model did not take into account the water leakage of rainwater through the joints of the panels. Protecting the entire wall against moisture, along with its effective thermal resistance, should take the airtightness of the solution into account.

In ETICS solutions, internal walls surface condensations are minimized. However, it is important to avoid condensations on the VIPs surface (risk of damage) and external surface condensations (risk of biological growth). Biological growth is one of the most frequent anomalies in conventional ETICS. This phenomenon happens due to high surface moisture content, which results from a combination of effects: external surface condensation, wind-driven rain, drying process and rendering properties [86]. The high surface moisture on ETICS façades can be attributed to better thermal insulation and lower thermal capacitance of external walls, leading to frequent condensation of outdoor air caused by the exchange of long wave radiation between the façade and the atmosphere, leading to low surface temperatures, in particular during the night periods [87]. Johansson *et al.* [88] monitored the temperature and relative humidity surfaces in different Swedish house façades (including ETICS) over 20 months. The results showed that thin rendering (3 to 5 mm) on thermal insulation layer has higher surface moisture when compared to traditional façades with higher thermal inertia, resulting in a higher potential for mould growth. Since external condensation is most likely to occur on well insulated walls when the external

layers have a low thermal inertia [87] and reduced thickness of the rendering system, as happens with ETICS solutions, the application of a super-insulating product may worsen this issue. Thus, it will be a challenge to avoid or minimize biological growth in VIP based ETICS.

### 2.3.3. Service life

In buildings, the service life of the used construction materials is a key issue. Service life can be defined by the period of time after installation during which the product keeps its performance in economic feasibility and under normal maintenance actions [89]. Although there is huge potential for the use of VIPs in buildings, the ageing of the thermal insulation layer cannot not be neglected, due to the need to ensure the high thermal resistance. Buildings have a large lifespan, typically between 80 and 100 years [73]. For insulation materials, a service life of over 30 years is expected [35]. The service life of VIPs for buildings applications was evaluated within the IEA/ECBCS Annex 39 project [68]. Based on these studies, 30 to 50 years can be expected for this solution. However, the prediction of the long-term performance of VIPs remains a challenge [90]. Table 2.5 summarizes the predicted service life values of VIPs in buildings as reported in the literature. The different estimations of service life are yielded by several methods and have allowed for varying factors, such as weather conditions, application/orientation [91], introduction of getters and desiccants, core material and barrier envelope, panel thickness, dimensions [64], and other aspects, resulting in a wide range of values.

**Table 2.5:** Service life estimates in building applications.

Reference	Product	Estimated service life
[42]	VIP with fumed silica core (single-layer metallized film)	10 years
[42]	VIP with fumed silica core (three-layer metallized film)	18 to 40 years
[75]	VIP with fumed silica core (three-layer metallized polymer envelope)	32 years
[52]	VIP with aerogel core	> 50 years
[60]	VIP with pressed powder made of silicic acid	up to 60 years <sup>(1)</sup>
[64]	VIP with fumed silica core (three-layer metallized film)	40 to 50 years <sup>(2)</sup>
[64]	VIP with fumed silica core (aluminium foil laminate)	45 to 50 years <sup>(2)</sup>
[92]	VIP with glass fibre core	5 to 20 years
[93]	VIP with fumed silica core (two-layer metallized envelope)	16 to 38 years
[94]	VIP with fumed silica and expanded perlite composite core	30 years
[94]	VIP with expanded perlite core	20 years
[95]	VIP with chopped strand core	> 15 years

<sup>(1)</sup> Depending on application.

<sup>(2)</sup> Estimated values for a 500 mm x 500 mm panel, 20 mm thick.



The conservation of the initial low pressure and low humidity inside a VIP are essential to maintain the long-term thermal performance [96]. Kim *et al.* [97] found significant differences between manufacturer-provided data and measurements of thermal conductivity and internal pressure of VIPs after ageing. These uncertainties around expected lifetime is a crucial factor for scepticism concerning VIPs [29]. Fantucci *et al.* [45] evaluated experimentally the variation in the thermal conductivity of VIPs with the average temperature, considering roof applications at various ageing stages. They proved the importance of considering the variation in the thermal conductivity of a VIP according to the temperature, especially when severe boundary conditions occur. This conclusion could be particularly relevant in the case of VIPs used in ETICS, since the external boundary conditions are more severe.

Yrieix *et al.* [98] showed through analytical models that the ageing of VIPs in buildings also depends on the application technology. For example, ETICS applications have higher calculated acceleration factors for ageing (based on the operating conditions and severity criteria) than internal walls VIP application. The authors highlighted four essential components to estimate the service life of VIP in buildings applications: the characteristics of the core material and of the barrier envelope, the service conditions and the thickness of the panels. For Tenpierik *et al.* [34] the main properties influencing the service life are the properties of the barrier envelope and the size, aspect ratio and thickness of the panels. Some research studies based on experimental data, have introduced numerical models of VIPs lifetime predictions based on Arrhenius law [75]. They have concluded that VIPs service life could reach several decades, but the proper installation technique must be considered [77]. Data of real long-term performance is needed in order to define adequate laboratory tests conditions and a better understand of its performance and potential anomalies.

### **2.3.4. Design and installation**

Another set of important issues that must be dealt with when using VIPs are related with the need to introduce adequate covering layers to ensure flatness of the surface, to define an adequate fixation system and to allow connection with other building elements (technical and architectural compatibility). To prevent damage of VIPs during their transport, handling and application, VIPs products for buildings generally involve the use of protective cover layers [82]. Nevertheless, as mentioned previously, ETICS solutions with VIPs should be assembled by workers with specialized training in handling this kind of products. Also, adequate tools and construction details must be made available to them. To ensure proper handling, VIPs should also be labelled in a way so as to warn the workers to be extra careful with the products [48].

Designers and builders have to be aware of the special requirements of VIPs early on in the design process [73]. Since VIPs cannot be adapted onsite, planners must supply detailed drawings of the solution. The size and position of the panels should be labelled to facilitate the work and avoid mistakes and delays. Special attention must be given to the joints between the panels. Suitable materials must be specified for adapting the edge joints. The joints and edges are usually sealed with a special adhesive aluminium tape which assures tightness [48]. The airtightness of walls with VIPs in ETICS should be ensured since it can greatly affect energy efficiency. In fact, the energy consumption in buildings can differ significantly from the theoretical values if airtightness is ignored [99]. This can be minimized by preparing construction details [100]. All accessories need to be carefully designed since anchors, brackets, profiles, window accessories and other components may damage the VIP. In conventional construction works, often times when the insulation panels do not fit perfectly together, mortar (from the base coat) is used to fill in the gaps between panels [101]. This must be avoided as it creates thermal bridges, moisture risks and surface cracking.

In ETICS systems, the mechanical fixation system also leads to point thermal bridges, with effects on the building energy consumption [102]. These can be reduced through reasonable selection and optimal design of anchors application [103]. The use of thermal breaks can reduce these effects. Architects and builders are advised to use stainless steel or plastic anchors instead of the widely used aluminium anchors. A reasonable way to reduce thermal bridging is to cover up the fasteners with a second layer of insulation [70]. Park *et al.* [104] investigated numerically the thermal performance of mechanically and adhesively fixed external insulation solutions using VIPs. Regarding mechanical fixation, they studied dowels installed at the joints of the insulation units (to avoid damage the VIP) and several steel fasteners. Each alternative was evaluated in terms of the thermal performance, construction costs and ease of installation. The authors highlighted the solution covered with three-layer insulation unit (EPS + VIP + EPS) without EPS on the edges as most effective one.

Regarding the thin rendering layer, the state-of-the-art demonstrates lack of information about finishing layers to fulfil the ETICS requirements with VIPs. However, hygrothermal simulations have been performed [104], and shown a significant impact of the finishing coats on the hygrothermal behaviour of the whole ETICS solution. Since a great deal of the anomalies in ETICS are found in the rendering system, a careful selection of the materials must be done. Moreover, the application of super-insulating products implies that there will be an increase in the temperature difference across the several different layers, and particularly in the finishing coat, which may promote the occurrence of some anomalies such as cracking, blistering, loss of flatness and biological growth.

In summary, the VIP based ETICS imposes additional cares regarding design and installation of vacuum panels. Aiming to help the designers and installers to carry out an adequate implementation of VIP based ETICS façades, a guideline for VIP based ETICS was proposed in

Annex A of this thesis. In this document, information regarding all stages of the construction is provided, such as design and planning, installation, maintenance, disassembly and waste disposal. Furthermore, several recommendations and detailed drawings were proposed.

### 2.3.5. Economic viability

The wide-scale commercialization of VIP products for buildings has not achieved its full potential, mainly due to their high cost when compared with the traditional thermal insulation materials [105]. In 2014, only 10% of VIPs production was intended for insulating buildings [38]. The high cost for current VIPs building products results not only from high prices for the panel's core and envelope materials, but also from the issues related with designing and executing construction works with non-adjustable and fragile panels. Since investment profitability in buildings depends largely on the cost of insulation material [106], a great challenge that vacuum industries and researchers face is the development of high performance products with lower costs. Looking to improve and increase the economic competitiveness of VIP solutions, over the last few years a number of studies have been published focusing on changing the composite getter [99] or the material core by using expanded cork with fumed silica [49], diatomaceous earth, glass bubbles [50], nanofoams, aerogel composites [107], glass fibres or expanded perlite [108]. Based on the literature review, Table 2.6 presents the range of VIPs prices for buildings applications. This table only includes the price of the insulation product, and therefore other ETICS components and installation costs were not considered.

**Table 2.6:** Cost of vacuum insulation panels based on literature review.

Reference	Product	Thickness [mm]	Cost [€/m <sup>2</sup> ]	Thermal conductivity [mW/(m·K)]	Cost per thermal resistance [€/R <sup>(1)</sup> ]
[30]	VIP - fumed silica	60	200.0	6.2	20.7
[32]	VIP - fumed silica	10; 25 - 60	80.0; 91.4	4.0	32.0; 6.1
[109]	VIP - fumed silica	20; 30	49.4; 74.5	4.5	11.1; 11.2
[110]	VIP - nano silica aerogel	50	52.9	3.0	3.2
	VIP - fumed silica	25	67.6	4.3	11.6
	VIP - fumed silica & expanded perlite	25	61.5	7.6	18.7
[94]	VIP - expanded perlite	25	51.7	13.0	26.9
	VIP - polyurethane	25	57.2	9.0	20.6
	VIP - glass fibre	25	41.8	2.8	4.7
[111]	VIP - fumed silica <sup>(2)</sup>	20	193.8	4.0	38.8

<sup>(1)</sup> Thermal resistance of insulation material expressed in (m<sup>2</sup>·K)/W.

<sup>(2)</sup> Price includes purchase, transport and installation (internal wall insulation).

The price depends on: size of panels, introduction of opacifiers and getters, type of envelope material, and other variables (information not provided by most authors). Also, the level of industrialization of vacuum technology could change the initial VIP costs. If we analyse the cost per thermal resistance value (R), it can be said that vacuum technology could be competitive against conventional thermal insulation materials, since a range of traditional insulation costs about 6 to 30 €/R [112].

The investment on thermal insulation has a significant impact on the environment since insulation materials contribute directly for reducing energy consumption during the service life [113]. Therefore, a whole-life cost (WLC) or life-cycle cost (LCC) analysis [114] can be important tools to support the investment decision making process and risk assessment. In the case of the VIPs, the savings of building floor area can represent an economic benefit that may contribute to balance out the higher initial investment costs. Therefore, in order to evaluate the economic feasibility of VIP solutions, new cost models for estimating life cycle costs are needed [64].

An economic study [115] performed in Sweden stated that VIP is not an economical alternative, when compared with EPS, and that the price of 20 mm thick VIP (approx. 200 €/m<sup>2</sup>) should decrease for it to become viable. However, the VIP investment may be considered more profitable if the floor area savings are taken into account, especially where the available space for the construction is limited, as Alam *et al.* demonstrated [94]. Giuseppe *et al.* [111] proposed a probabilistic LCC methodology where super-insulating materials for thermal insulation were included. They concluded that super-insulating materials allowed the reduction of indirect costs due to the lower loss of floor area. Nevertheless, this advantage did not pay off in terms of the global costs, which were strongly affected by the higher initial investments. The key for a widely use of VIPs as external insulation will be to provide panels at competitive prices, while also taking into account the benefit of the space savings and low energy consumptions.

### **2.3.6. Environmental performance**

Regarding the life cycle assessment (LCA) of VIP applications in buildings, only a reduced number of studies are found. An extensive literature review of 223 values about the embodied energy and carbon emissions of building insulation materials was performed by Grazieschi *et al.* [116], among which only 5 values were reported for VIP products. Also, there are few Environmental Products Declarations (EPDs) issued according to ISO 14025 [117] publicly available [31]. Lolli and Hestnes [118] presented the results of energy use and life cycle carbon emissions calculations for MW, aerogel and VIP in the retrofitting of an apartment building in

Norway. Based on equivalent U-value, super-insulating materials are reported to have higher embodied emissions per unit of mass than those of MW. However, the results do not give a clear answer to which alternatives could be considered, since the results are strongly influenced by electricity-to-emissions conversion factors. In Sweden, Karami *et al.* [119] carried out a comparative LCA study of the environmental impact of the construction and operation of three hypothetical buildings: a standard residential building; a regular well-insulated (MW and EPS) building; and a building insulated with VIPs. The study shows a comparatively lower operational energy for the VIP insulated building and a relatively lower total greenhouse gas emission, as well as the possibility to save significant living space. However, including the production stage, VIPs revealed greater environmental impact than conventional insulation in all categories except for ozone depletion potential. The results also showed that the core material of the VIPs has considerable impact on the results. For this reason, Resalati *et al.* [120] carried out a comparative analysis of the environmental impact of several alternative core materials based on a cradle-to-gate assessment. The fumed silica, the most common core material, had the highest environmental impact out of the core materials considered (glass fibre, expanded polystyrene, aerogel and a silica/sawdust hybrid), suggesting that the recycling of the core material alongside the deployment of eco-friendlier manufacturing techniques should be considered.

## **2.4. Guidelines for experimental validation**

As noted above, efforts have been made to model the behaviour of VIP building products and predict their service life, but results have been varied and sometimes inconclusive. Furthermore, since external VIP applications on walls are still few, not standardized, and fairly recent, there is little information available about their actual long-term performance and anomalies. Further experimental work is required to obtain more reliable data. Given the pressing need to properly validate this innovative solution, this section is designed to contribute to providing a framework for the experimental characterization of VIP based ETICS solutions.

Table 2.7 provides a list of assessment methods that can be employed to evaluate relevant VIP based ETICS characteristics and verify the relevant essential requirements of the CPR [17].

**Table 2.7:** Summary of the assessment methods for validating a VIP based ETICS.

Basic works requirements	Product characteristic	Assessment method
Hygiene, health and environment	Water absorption (capillarity test)	ETICS EAD [16]
	Watertightness: hygrothermal behaviour	ETICS EAD [16]
	Watertightness: freeze-thaw behaviour	ETICS EAD [16]
	Impact resistance	ETICS EAD [16] / ISO 7892 [121]
Safety in use	Resistance to perforation	ETAG 004:2011 [122]
	Bond strength <sup>(1)</sup>	ETICS EAD [16]
Safety in case of fire	Dynamic wind uplift test	ETICS EAD [16]
	Reaction to fire	ETICS EAD – Annex B [16]
Energy economy and heat retention	Thermal resistance	EN ISO 8990 [123]
	Linear thermal transmittance	ISO 10211 [124]
	Thermal performance under dynamic conditions	Numerical simulation or experimental procedures
Aspects of durability and serviceability	Resistance to driving rain under pulsating air pressure	EN 12865 [125]
	Condensation risk assessment	Dynamic numerical simulation EN ISO 13788 [126]
	Bond strength after ageing	ETICS EAD [16]
	Solar radiation behaviour	Experimental procedures
	Biological growth risk assessment	Numerical simulation
	Detection of anomalies ( <i>e.g.</i> cracks, delamination and loss of vacuum)	Thermographic testing EN 16714 [127]
Economic viability	Global costs	WLC/LCC assessment ISO 15686-5 [114] or CDR 244/2012 ([128],[129])
Sustainable use of natural resources	Environmental performance	Life Cycle Assessment ISO 14040 [130] and ISO 14044 [131]

<sup>(1)</sup> Test carried out before and after ageing.

This list excludes onsite testing, however it is essential to carry out laboratory durability tests on real-scale test specimens, such as hygrothermal and freeze-thaw cycles. During the accelerated ageing tests, non-destructive techniques, such as infrared thermography can be used to detect and locate anomalies [132] such as cracking, delamination or loss of vacuum. Mechanical tests after ageing, such as bond strength resistance and impact with a hard body, are also important. Evaluation of the resistance to perforation could be particularly relevant, since VIP perforation causes a major loss of thermal performance. The majority of these assessment methods are included in ETAG 004 [15], recently converted in ETICS EAD [16]. However, to ensure good service life performance and prevent frequent anomalies, certain other characteristics should be examined. In particular, since aesthetic degradation is one of the more prevalent anomalies found in ETICS [26], risk of surface condensation and biological growth should be carefully assessed. Another issue that is usually not evaluated in ETICS systems is the long-term effects that exposure

to solar radiation has on the performance of the rendering layer. In particular, this could be even more significant when using super-insulating material, since high surface temperatures should be expected. Regarding the economic viability challenge of using VIPs in buildings, an LCC assessment should be done to satisfy an economically reasonable working life. Additionally, the environmental impact of the solution must be evaluated, especially in the solution development phase.

Besides evaluating the whole system, it is necessary to know the characteristics of each ETICS component. Table 2.8 presents the essential characteristics that should be verified for ETICS components. For example, estimating thermal conductivities (including after ageing and considering the edge thermal bridging effect) is essential to evaluate the energy economy of the system during its service life. The contribution of the mechanical fixing device to the overall thermal transmittance should also be evaluated.

**Table 2.8:** Summary of the assessment methods for validating each ETICS component.

Component	Essential characteristics	Assessment method
Vacuum insulation panel (including VIP with protective layers)	Thermal resistance and thermal conductivity <sup>(1)</sup>	EN 12667 [133]
	Specific heat	Experimental procedures
	Water vapour permeability	EN 12086 [134]
	Length and width	EN 822 [135]
	Thickness	EN 823 [136]
	Squareness	EN 824 [137]
	Flatness	EN 825 [138]
	Density	EN 1602 [139]
	Mass per square meter	EAD 040011-00-1201 [46]
	Oxygen permeability of the multilayer high barrier foil of VIP	DIN 53380-3 [140] or ASTM D 3985 [140]
	Compressive strength at 10%	EN 826 [141]
	Dimensional stability under specified temperature and humidity	EN 1604 [142]
	Deformation under specified compressive load and temperature conditions	EN 1605 [143]
	Tensile strength (perpendicular to the face)	EN 1607 [144]
	Tensile strength of the multilayer high barrier foil of VIP <sup>(2)</sup>	EN ISO 527-3 [145]
Inner pressure	EN 17140 (Annex G) [47]	
Shear strength and shear modulus of elasticity	EN 12090 [146]	
Behaviour under point load	EN 12430 [147]	
Compressive creep	EN 1606 [148]	
Bending	EN 12089 [149]	
Water absorption	EN 12087 [150] / EN 1609 [151]	
Anchors	Thermal transmittance	EOTA TR 025 [152]
	Pull-out strength of anchors	EAD 330196-00-0604 [153]
	Pull-through resistance of fixings from profiles	ETICS EAD [16]

<sup>(1)</sup> Including ageing and edge effect. The thermal conductivity of the punctured VIP must also be ascertained.

<sup>(2)</sup> Test carried out before and after ageing.

**Table 2.8 (continued):** Summary of the assessment methods for validating each ETICS component.

Component	Essential characteristics	Assessment method
Reinforced mesh	Render strip tensile test	ETICS EAD [16]
	Tensile strength and elongation <sup>(2)</sup>	ETICS EAD [16]
Rendering products <sup>(3)</sup>	Water vapour permeability	EN ISO 7783 [154]
	Young modulus	EN 13412 [155]
	Emissivity	---
	Mould growth	ASTM D 3273-16 [156]

<sup>(2)</sup> Test carried out before and after ageing.

<sup>(3)</sup> Including base coat mortar, primer and finishing/decorative layers.

Assessing the specific heat of VIPs could be important for performing numerical simulation under dynamic boundary conditions. However, there are no standard testing methods for non-homogeneous insulation materials such as vacuum insulation products. There are test procedures for plastics [157], ceramics [158], phase change materials [158], for thermal insulating materials that are homogeneous and composed of matter in the solid state [159], and tabulated values ([160], [161]). Other methods using a calorimeter [162] or heat flow meter [158] could thus be studied and adapted for this novel solution.

To prevent cracking and lack of flatness of the surface wall, it is very important to test flatness, dimensional stability under different temperature and humidity conditions, and the dimension tolerances of panels. Furthermore, cracking of the reinforced base coat should also be evaluated and mechanical tests are needed to ensure safety in use. These include tensile strength, shear strength and behaviour under point load. Since the ETICS rendering layer is subjected to aggressive hygrothermal conditions that might be worsened by the use of a super-insulating material, its properties are also essential for the overall system behaviour. For example, choosing mortars with reduced modulus of elasticity will help to mitigate cracking and detachment issues. Regarding surface biological growth issues, it would be useful to assess the potential for mould growth in the finishing layers' products, as well as their optical properties. Numerical simulations could play a part in assessing the condensation risk [163]. Several authors used WUFI software [164] to analyse the hygrothermal behaviour of a façade and the risk of surface condensation. For example, Zirkelbach *et al.* used it to predict the hygrothermal behaviour of ETICS with a mineral wool insulation layer. Barreira and Freitas [86] also used this tool to evaluate the risk of surface condensation on ETICS. Other numerical approaches can be used to perform a detailed analysis of the dynamic behaviour of solutions, such as models based on the boundary element method to simulate the coupled heat, air and moisture flow through multi-layered porous solids [165] or the VTT model, that is often used to predict the risk of condensation and mould growth in the building envelope [166].

Furthermore, it is particularly important to evaluate the water vapour of the rendering and VIP in the joints between panels, since this directly influences the condensation phenomena and other anomalies. It should be noted that all ETICS components (adhesive, base coat mortar, finishing



layer products, reinforcement mesh and mechanical fixing devices) must have CE marking and must meet the EAD 040083-00-0404 requirements. Other tests such as the protection against noise should also be performed (not included in previous tables).

Although there are several challenges and there is still a need for test methods and evaluation procedures to prove the suitability of VIPs for use in the building sector [44], the growing energy efficiency requirements and the insulating potential of VIP products means that these are still considered to be an interesting alternative to conventional building insulation, especially those used in ETICS solutions.

## **2.5. Conclusions**

This chapter presented an overview of the state-of-the-art concerning the use of vacuum technology in external insulation systems with finishing rendering. Combining the known advantages of ETICS with the super-insulating qualities of VIPs would create the potential for a competitive, innovative, thermal insulation solution, both for new buildings and for retrofitting work. Additionally, looking to promote a successful implementation of VIP in ETICS façades, guidelines for VIP based ETICS solutions were presented in the Annex A of this thesis.

This literature review, first identified several commercial products that could be used in ETICS, along with a number of case studies. It was found that different configurations have been attempted and published in various studies, considering different forms of mechanical fastening, type of panels, cover layers and finishing products. It was noted that the use of VIPs in ETICS presents several challenges regarding design and installation, performance and durability, and economic viability, which need to be carefully investigated. From the reported studies, it can be concluded that the greatest problems lie in dealing with minimizing the edge thermal bridging effect and the risk of surface condensation, tackling the perforation vulnerability of the panel, and predicting and ensuring service life performance. Thus, although some applications of VIPs in ETICS can already be found, if the use of vacuum insulation is to become widespread the following three major factors must be overcome: the high cost and high embodied energy; the lack of confidence in VIP technology and its long-term performance in external walls; and the missing product approvals for VIP based ETICS. Removing uncertainties around VIPs is an important factor for the broader commercialization of this solution. Preferably, further improvements should be achieved in the panels to reduce the technology costs, extend/assure its long-term performance and recycling the core material.

To increase reliability, it is important to address the main issues and potential anomalies set out in this chapter. The experimental validation of this type of solution is therefore considered essential. Since there are as yet no test procedures suited to VIPs' use in ETICS, this study proposes a set of methods to assess the behaviour of ETICS with vacuum technology in the context of the main identified challenges. Knowledge about the overall behaviour of the system, including potential anomalies in the rendering such as biological growth or cracking caused by solar radiation need to be furthered.

The literature review shows that the use of VIPs in ETICS has potential to be successfully applied on a larger scale, especially in cold climates. Since real onsite applications are still few and recent, at this stage it is important to use the knowledge generated by manufacturers and laboratories developing and applying VIPs technology in ETICS solutions. The experimentally validated test results and case studies under realistic climatic conditions will increase the confidence of the builders, architects and owners. The wide-spread use of VIPs could be an extremely useful solution to significantly improve the energy performance of buildings towards nearly zero-energy buildings.

## References

- [1] European Commission, "Mapping and analyses of the current and future (2020 - 2030) - heating/cooling fuel deployment (fossil/renewables)", Final report, 2016.
- [2] L. Aditya, T. M. I. Mahlia, B. Rismanchi, H. M. Ng, M. H. Hasan, H. S. C. Metselaar, O. Muraza, H. B. Aditya. "A review on insulation materials for energy conservation in buildings". *Renew. Sustain. Energy. Rev.* vol. 73, pp. 1352–65, 2017, doi:10.1016/j.rser.2017.02.034.
- [3] European Parliament, "Directive 2002/65/EC of the European Parliament and of the Council of 16 December 2002 on the energy performance of buildings", *Off. J. Eur. Communities*. pp. 65–71, 2002, doi:10.5040/9781782258674.0021.
- [4] European Parliament, "Directive (EU) 2018/844 of the European Parliament and of the Council of 30 May 2018 amending Directive 2010/31/EU on the energy performance of buildings and Directive 2012/27/EU on energy efficiency", *Off. J. Eur. Union*. pp. 75–91, 2018
- [5] R. Norvaišienė, V. Buhagiar, A. Burlingis, K. Miškinis, "Investigation of mechanical resistance of external thermal insulation composite systems (ETICS)", *J. Build. Eng.* vol. 32, 101682, 2020, doi:10.1016/j.job.2020.101682.
- [6] R. Pasker, "The European ETICS market - Facts & figures", in *European ETICS Forum*, 2015.

- [7] M. Mihai, V. Tanasiev, C. Dinca, A. Badea, R. Vidu, “Passive house analysis in terms of energy performance”. *Energy Build.* vol. 144, pp. 74–86, 2017, doi:10.1016/j.enbuild.2017.03.025.
- [8] C. Spirinckx, L. Peeters, W. Debacker, B. Vandeveldel, G. Theo, A. Durand, G. Thomas, L. Caroline, L. Arnoud, “Exploratory study with regard to Ecodesign of thermal insulation in buildings (Lot 36): MEerP tasks 0, 1 and 7 (partly)”, Final report, VITO, 2014.
- [9] S. Varela, C. Viñas, A. Rodríguez, P. Aguilera, M. González, “Experimental comparative study of the thermal performance of the façade of a building refurbished using ETICS, and quantification of improvements”. *Sustain. Cities Soc.* Vol. 51, 101713, 2019, doi:10.1016/j.scs.2019.101713.
- [10] L. Zhang, T. Luo, X. Meng, Y. Wang, C. Hou, E. Long, “Effect of the thermal insulation layer location on wall dynamic thermal response rate under the air-conditioning intermittent operation”, *Case Stud. Therm. Eng.* vol. 10, pp. 79–85, 2017, doi:10.1016/j.csite.2017.04.001.
- [11] J. Yuan, C. Farnham, K. Emura, M. A. Alam, “Proposal for optimum combination of reflectivity and insulation thickness of building exterior walls for annual thermal load in Japan”. *Build. Environ.* vol. 103, pp. 228–37, 2016, doi:10.1016/j.buildenv.2016.04.019.
- [12] R. Pasker, “The European ETICS market - Do ETICS sufficiently contribute to meet political objectives?” in: *4<sup>th</sup> European ETICS Forum*, 2017.
- [13] C. Fernandes, J. de Brito, C. O. Cruz, “Architectural integration of ETICS in building rehabilitation”. *J. Build. Eng.* vol. 5, pp.178–84, 2016, doi:10.1016/j.job.2015.12.005.
- [14] E. Barreira, V. P. de Freitas, “External thermal insulation composite systems: critical parameters for surface hygrothermal behaviour”. *Adv. Mater. Sci. Eng.* vol. 2014, 2014. doi:10.1155/2014/650752.
- [15] *Guideline for European Technical Approval of External Thermal Insulation Composite Systems (ETICS) with Rendering*, ETAG 004, European Organisation for Technical Approvals, Edition 2000, amended 2013.
- [16] *European Assessment Document: External Thermal Insulation Composite Systems with rendering*, EAD 040083-00-0404, European Organisation for Technical Approvals, 2019.
- [17] European Commission, “Regulation (EU) No 305/2011 of the European Parliament and of the Council of 9 March 2011 laying down harmonised conditions for the marketing of construction products and repealing Council Directive 89/106/EEC”, *Off. J. Eur. Union*, pp 43–88, 2011.
- [18] J. A. L. Carvalho, “ITE 24 – Classification and general of coverings for masonry walls or concrete” (in portuguese), LNEC, Lisbon, 1990.
- [19] J. A. R. M. Silva, J. Falorca, “A model plan for buildings maintenance with application in the performance analysis of a composite facade cover”, *Constr. Build. Mater.* vol. 23, pp. 3248–3257, 2009, doi:10.1016/j.conbuildmat.2009.05.008.
- [20] S. Madureira, I. Flores-Colen, J. de Brito, C. Pereira, “Maintenance planning of facades in current buildings”, *Constr. Build. Mater.* vol. 147, pp. 790–802, 2017, doi:10.1016/j.conbuildmat.2017.04.195.
- [21] L. Silva, I. Flores-Colen, N. Vieira, A. B. Timmons, P. Sequeira, “Durability of ETICS and premixed one-coat renders in natural exposure conditions”, in *New Approaches to Building*

- Pathology and Durability*, Springer, vol. 6, pp. 131–158, 2016,. doi:10.1007/978-981-10-0648-7.
- [22] E. Edis, N. Türkeri, “Durability of external thermal insulation composite systems in Istanbul Turkey”, in *Journal of Faculty of Architecture*, Istanbul Technical University Faculty of Architecture, vol. 9, pp.134–48, 2012.
- [23] E. Barreira. “Biological defacement of façades covered with external thermal insulation systems due to hygrothermal behaviour” (in portuguese), PhD thesis. Faculty of Engineering of University of Porto, 2010.
- [24] V. Sulakatko, I. Lill, E. Liisma, “Analysis of on-site construction processes for effective external thermal insulation composite system (ETICS) installation”, *Procedia Econ. Financ.* vol. 21 pp. 297–305, 2015. doi:10.1016/S2212-5671(15)00180-X.
- [25] B. Amaro, D. Saraiva, J. de Brito, I. Flores-Colen, “Inspection and diagnosis system of ETICS on walls”. *Constr. Build. Mater.* vol. 47, pp. 1257–1267, 2013. doi:10.1016/j.conbuildmat.2013.06.024.
- [26] B. Amaro, D. Saraiva, J. de Brito, I. Flores-Colen, “Statistical survey of the pathology, diagnosis and rehabilitation of ETICS in walls”. *J. Civ. Eng. Manag.* vol. 20, pp. 511–526, 2014, doi:10.3846/13923730.2013.801923.
- [27] ECOFYS, “U-Values - For a Better Energy Performance Of Buildings”, EURIMA, 2007.
- [28] ZEBRA 2020, ”Nearly zero-energy building strategy 2020 - D 4.2: Overview of buildings-related policies”, 2016.
- [29] S. E. Kalnæs, B. P. Jelle, “Vacuum insulation panel products: a state-of-the-art review and future research pathways”. *Appl. Energy*, vol. 116, pp. 355–375, 2014, doi:10.1016/j.apenergy.2013.11.032.
- [30] B. P. Jelle, “Traditional, state-of-the-art and future thermal building insulation materials and solutions – Properties, requirements and possibilities”. *Energy Build.* vol. 43, pp. 2549–2563, 2011, doi:10.1016/j.enbuild.2011.05.015.
- [31] International Energy Agency, “Long-Term Performance of Super-Insulating Materials in Building Components and Systems”, Report of Subtask I: State of the art and case studies, EBC Annex 65, U. Heinemann, ed., 2020.
- [32] S. Schiavoni, F. D’Alessandro, F. Bianchi, F. Asdrubali, “Insulation materials for the building sector: a review and comparative analysis”. *Renew. Sustain. Energy. Rev.* vol. 62, pp. 988–1011, 2016, doi:10.1016/j.rser.2016.05.045.
- [33] M. Tenpierik, A. Van Timmen, W. Van der Spoel, H. Cauberg, “Vacuum insulation panels and architecture: cradle-to-cradle façade systems”, in *3<sup>rd</sup> Int. Conf. Smart Sustain. Built Environ.*, 2009.
- [34] F. Gubbels, D. D. Santi, V. Baily, “Durability of vacuum insulation panels in the cavity of an insulating glass unit”. *J. Build. Phys.* vol. 38, pp. 485–99, 2015, doi:10.1177/1744259114522118.
- [35] J. Zach, V. Novák, “Study of the use of vacuum insulation as integrated thermal insulation in ceramic masonry blocks”, *Procedia Eng.* vol. 151, pp. 206–213, 2016, doi:10.1016/j.proeng.2016.07.391.
- [36] P. Johansson, C. E. Hagentoft, A. S. Kalagasidis, “Retrofitting of a listed brick and wood

- building using vacuum insulation panels on the exterior of the facade: measurements and simulations”. *Energy Build.* vol. 73, pp. 92–104, 2014, doi:10.1016/j.enbuild.2014.01.019.
- [37] S. Brunner, K. Wakili, T. Stahl, B. Binder, “Vacuum insulation panels for building applications - Continuous challenges and developments”. *Energy Build.* vol. 85, pp.592–606, 2014, doi:10.1016/j.enbuild.2014.09.016.
- [38] S. Brunner, “Superinsulating materials present applications”.in *Int. Symp. Superinsulating Mater.*, Brussels, 2012.
- [39] J. M. Cremers, “Typology of applications for opaque and translucent VIP in the building envelope and their potential for temporary thermal insulation”, pp. 1–8, 2005.
- [40] R. Baetens, B. P. Jelle, A. Gustavsen, “Aerogel insulation for building applications: a state-of-the-art review”. *Energy Build.* vol. 43, pp. 761–769, 2011, doi:10.1016/j.enbuild.2010.12.012.
- [41] M. Alam, H. Singh, M. C. Limbachiya, “Vacuum insulation panels (VIPs) for building construction industry - a review of the contemporary developments and future directions”. *Appl. Energy*, vol. 88, pp.3592–3602, 2011, doi:10.1016/j.apenergy.2011.04.040.
- [42] R. Baetens, B. P. Jelle, J. V. Thue, M. J. Tenpierik, S. Grynning, S. Uvsløkk, A. Gustavsen, “Vacuum insulation panels for building applications: a review and beyond”. *Energy Build.* vol.42 pp.147–172, 2010, doi:10.1016/j.enbuild.2009.09.005.
- [43] M. Zimmermann, H. Bertschinger, “High performance thermal insulation systems vacuum insulated products (VIP)”, in *Proc. Int. Conf. Work. EMPA*, Dübend, 2001.
- [44] I. Mandilaras, I. Atsonios, G. Zannis, M. Founti, “Thermal performance of a building envelope incorporating ETICS with vacuum insulation panels and EPS”. *Energy Build.* vol.85, pp.654–665, 2014, doi:10.1016/j.enbuild.2014.06.053.
- [45] S. Fantucci, A. Lorenzati, A. Capozzoli, M. Perino, “Analysis of the temperature dependence of the thermal conductivity in vacuum insulation panels”, *Energy Build.* vol. pp.64–74, 2019, doi:10.1016/j.enbuild.2018.10.002.
- [46] *European Assessment Document: Vacuum Insulation Panels (VIP) with factory applied protection layers*, EAD 040011-00-1201, European Organisation for Technical Approvals, 2017.
- [47] *Thermal insulation products for buildings - Factory-made vacuum insulation panels (VIP) - Specification*, EN 17140, European Committee for Standardization, 2020.
- [48] A. Binz, A. Moosmann, G. Steinke, U. Schonhardt, F. Fregnan, H. Simmler, S. Brunner, K. G. Wakili, R. Bundi UH, “Vacuum Insulation in the Building Sector – Systems and Applications”, Final Report of Subtask B, IEA/ECBCS Annex 39, 2005.
- [49] J. Zhuang, S. H. Ghaffar, M. Fan, J. Corker, “Restructure of expanded cork with fumed silica as novel core materials for vacuum insulation panels” *Composites Part B Eng.* vol. 127, pp.215–221, 2017, doi:10.1016/j.compositesb.2017.06.019.
- [50] B. Chang, L. Zhong, M. Akinc, “Low cost composites for vacuum insulation core material”, *Vacuum*, vol. 131, pp. 120–126, 2016. doi:10.1016/j.vacuum.2016.05.027.
- [51] M. Alam, H. Singh, S. Brunner, C. Naziris, “Experimental characterisation and evaluation of the thermo-physical properties of expanded perlite — Fumed silica composite for effective vacuum insulation panel (VIP) core. *Energy Build.* vol. 69, pp. 442–450, 2014,

doi:10.1016/j.enbuild.2013.11.027.

- [52] Y. Liang, H. Wu, G. Huang, J. Yang, H. Wang, “Thermal performance and service life of vacuum insulation panels with aerogel composite cores”. *Energy Build.* vol. 154, pp. 606–617, 2017, doi:10.1016/j.enbuild.2017.08.085.
- [53] T. Thorsell, “Advances in thermal insulation - Vacuum insulation panels and thermal efficiency to reduce energy usage in buildings”. PhD thesis. KTH Royal Institute of Technology School of Architecture and the Built Environment Department of Civil and Architectural Engineering, Stockholm, 2012.
- [54] Vaku-Isotherm, “Vaku-Isotherm: SP-1 & 2”, <https://www.vaku-isotherm.de/en/industries/building-applications#sp-1-sp-2> (accessed May 8, 2018).
- [55] Vaku-Isotherm, “Vaku-Isotherm: SP-2/E”, <https://www.vaku-isotherm.de/en/industries/building-applications#sp-2-e> (accessed May 8, 2018).
- [56] Vaku-Isotherm, “Vaku-isotherm: bauplatte”, <https://www.vaku-isotherm.de/en/industries/building-applications#bauplatte> (accessed May 8, 2018).
- [57] Porextherm, “Vacupor PS-B2-S”, <http://www.porextherm.com/en/products/vacupor/vacupor-ps-b2-s.html> (accessed May 9, 2018).
- [58] Weber Saint-Gobain, “LockPlate System - ETICS with integrated VIP”, [http://www.cesb.cz/cesb10/partners/GEN\\_Weber/WeberLockPlate A4.pdf](http://www.cesb.cz/cesb10/partners/GEN_Weber/WeberLockPlate A4.pdf) (accessed May 9, 2018).
- [59] va-Q-tec, “va-Q-vip B”, <https://www.va-q-tec.com/en/products/vacuum-insulation-panel-vip/va-q-vip-b.html> (accessed May 9, 2018).
- [60] va-Q-tec, “va-Q-vip EPS”, <https://www.va-q-tec.com/en/products-industries/construction/products/va-q-vip-eps.html> (accessed May 9, 2018).
- [61] va-Q-tec, “va-Q-vip F-GGM”, <https://www.va-q-tec.com/en/produkte/va-q-vip-f-ggm/> (accessed February 5, 2019).
- [62] Variotec, “VT-A-HYDRO 2”, [http://www.variotec.de/en/home/products/vip\\_qasa\\_vacuum-insulation/external-insulation/facade-insulation/vt-a-hydro/](http://www.variotec.de/en/home/products/vip_qasa_vacuum-insulation/external-insulation/facade-insulation/vt-a-hydro/) (accessed February 5, 2018).
- [63] Kingspan Insulation Ltd., “OPTIM-R External Wall System”, <https://www.kingspan.com/gb/en-gb/products/insulation/insulation-boards/optim-r/optim-r-external-wall-system> (accessed August 16, 2019).
- [64] M. Tenpierik, “VIP A B C - Vacuum Insulation Panels Applied in Buildings Constructions”, PhD thesis, Technische Universiteit Delft, 2009.
- [65] P. Karami, “Robust and Durable Vacuum Insulation Technology for Buildings”, PhD thesis, KTH Royal Institute of Technology, 2015.
- [66] P. Johansson, B. Adl-Zarrabi, A. S. Kalagasidis, “Evaluation of 5 years’ performance of VIPs in a retrofitted building façade”, *Energy Build.* vol. 130, pp. 488–94, 2016, doi:10.1016/j.enbuild.2016.08.073.
- [67] S. Brunner, C. Tanner, K. G. Wakili, “Vakuumdämmung in verputzten Fassaden” (in german), Final report, EMPA, Swiss Federal Laboratories for Materials Science and Technology, Bern, 2011.

- [68] H. Simmler, S. Brunner, U. Heinemann, H. Schwab, K. Kumaran, P. Mukhopadhyaya, D. Quénard, H. Sallée, K. Noller, E. Küçükpinar-Niarchos, C. Stramm, M. Tenpierik, J. Cauberg, M. Erb, “Vacuum Insulation Panels - Study on VIP - components and Panels for Service Life Prediction of VIP in Building Applications”, Final Report of Subtask A, IEA/ECBCS Annex 39, 2005.
- [69] J. H. Kim, S. M. Kim, J. T. Kim, “Simulation performance of building wall with vacuum insulation panel”, *Procedia Eng.* vol. 180, pp. 1247–55, 2017, doi:10.1016/j.proeng.2017.04.286.
- [70] C. Sprengard, A. H. Holm, “Numerical examination of thermal bridging effects at the edges of vacuum-insulation-panels (VIP) in various constructions”, *Energy Build.* vol. 85, pp.638–643, 2014, doi:10.1016/j.enbuild.2014.03.027.
- [71] L. Kubina, “ETICS with integrated vacuum insulation”, in *Proc. Int. Conf. Cent. Eur. Towar. Sustain. Build.*, Prague, 2010, pp. 2–5.
- [72] P. Karami, K. Gudmundsson, F. Björk, L. Heymans, “ETICS with vacuum insulation panels for retrofitting buildings from the great Swedish housing program ‘Miljonprogrammet’”, in *12<sup>th</sup> International Vacuum Insulation Symposium*, Yokohama 2015, pp.1–6.
- [73] P. Johansson, “Vacuum insulation panels in buildings. Literature review”, Report in Building Physics. Department of Civil and Environmental Engineering, Chalmers University of Technology, Göteborg, Sweden 2012.
- [74] *Energy performance of buildings - Energy needs for heating and cooling, internal temperatures and sensible and latent heat loads*, ISO 52016-1, International Organization for Standardization, 2017.
- [75] H. Simmler, S. Brunner, “Vacuum insulation panels for building application: basic properties, aging mechanisms and service life”, *Energy Build.* vol. 37, pp.1122–1131, 2005, doi:10.1016/j.enbuild.2005.06.015.
- [76] S. Brunner, T. Stahl, K. G. Wakili, “An example of deteriorated vacuum insulation panels in a building façade”, *Energy Build.* vol. 54, pp. 278–282, 2012, doi:10.1016/j.enbuild.2012.07.027.
- [77] F. E. Boafu, Z. Chen, C. Li, B. Li, T. Xu, “Structure of vacuum insulation panel in building system”, *Energy Build.* vol. 85, pp. 644–653, 2014, doi:10.1016/j.enbuild.2014.06.055.
- [78] P. Johansson, “Building Retrofit using Vacuum Insulation Panels: Hygrothermal Performance and Durability”, PhD thesis, Chalmers University of Technology, 2014.
- [79] M. Citterio, M. Cocco, H. Erhorn-Kluttig, “Thermal bridges in the EPBD context: overview on MS approaches in regulations”. EPBD Building Platform, 2008.
- [80] A. Lorenzati, S. Fantucci, A. Capozzoli, M. Perino, “Experimental and numerical investigation of thermal bridging effects of jointed vacuum insulation panels”, *Energy Build.* vol. 111, pp. 164–175, 2016, doi:10.1016/j.enbuild.2015.11.026.
- [81] A. Lorenzati, S. Fantucci, A. Capozzoli, M. Perino, “The effect of different materials joint in vacuum insulation panels”, *Energy Procedia*, vol.62, pp. 374–381, 2014, doi:10.1016/j.egypro.2014.12.399.
- [82] T. Nussbaumer, K. G. Wakili, C. Tanner, “Experimental and numerical investigation of the thermal performance of a protected vacuum-insulation system applied to a concrete wall”,

- Appl. Energy*, vol. 83, pp. 841–855, 2006, doi:10.1016/j.apenergy.2005.08.004.
- [83] K. G. Wakili, T. Stahl, S. Brunner, “Effective thermal conductivity of a staggered double layer of vacuum insulation panels”, *Energy Build.* vol. 43, pp. 1241–1246, 2011, doi:10.1016/j.enbuild.2011.01.004.
- [84] F. Isaia, S. Fantucci, A. Capozzoli, M. Perino, “Vacuum insulation panels: thermal bridging effects and energy performance in real building applications”, *Energy Procedia*, vol. 83, pp. 269–278, 2015, doi:10.1016/j.egypro.2015.12.181.
- [85] P. Mukhopadhyaya, D. MacLean, J. Korn, D. Van Reenen, S. Molleti, “Building application and thermal performance of vacuum insulation panels (VIPs) in Canadian subarctic climate”. *Energy Build.* vol. 85, pp. 672–680, 2014, doi:10.1016/j.enbuild.2014.08.038.
- [86] E. Barreira, V. P. de Freitas, “Experimental study of the hygrothermal behaviour of External Thermal Insulation Composite Systems (ETICS)”, *Build. Environ.* vol. 63, pp. 31–39, 2013, doi:10.1016/j.buildenv.2013.02.001.
- [87] H. M. Künzle, “Factors determining surface moisture on external walls”, in *Build. X.*, 2007.
- [88] S. Johansson, L. Wadsö, K. Sandin, “Estimation of mould growth levels on rendered façades based on surface relative humidity and surface temperature measurements”, *Build. Environ.* vol. 45, pp.1153–1160, 2010, doi:10.1016/j.buildenv.2009.10.022.
- [89] *Buildings and constructed assets -- Service life planning -- Part 1: General principles and framework*, ISO 15686-1, International Organization for Standardization, 2011.
- [90] E. Pons, B. Yrieix, S. Brunner, “Evaluation of VIPs after mild artificial aging during 10 years: focus on the core behavior”, *Energy Build.* vol. 162, pp. 198–207, 2018, doi:10.1016/j.enbuild.2017.12.016.
- [91] A. Batard, T. Duforestel, L. Flandin, B. Yrieix, “Prediction method of the long-term thermal performance of vacuum insulation panels installed in building thermal insulation applications”, *Energy Build.* vol. 178, pp. 1–10, 2018, doi:10.1016/j.enbuild.2018.08.006.
- [92] X. Di, Y. Gao, C. Bao, S. Ma, “Thermal insulation property and service life of vacuum insulation panels with glass fiber chopped strand as core materials”. *Energy Build.* vol. 73, pp. 176–83, 2014, doi:10.1016/j.enbuild.2014.01.010.
- [93] H. Schwab, U. Heinemann, A. Beck, H. Ebert, “Prediction of useful life time for vacuum insulation panels with fumed silica kernel and foil cover”., *J. Build. Phys.* vol. 28, pp. 357–374, 2005, doi:https://doi.org/10.1177/1097196305051894.
- [94] M. Alam, H. Singh, S. Suresh, D. A. G. Redpath, “Energy and economic analysis of vacuum insulation panels (VIPs) used in non-domestic buildings”. *Appl. Energy*, vol. 188, pp. 1–8, 2017, doi:10.1016/j.apenergy.2016.11.115.
- [95] X. Di, Y. Gao, C. Bao, Y. Hu, “Optimization of glass fiber based core materials for vacuum insulation panels with laminated aluminum foils as envelopes”. *Vacuum*, vol. 97, pp. 55–59, 2013, doi:10.1016/j.vacuum.2013.04.005.
- [96] M. Bouquerel, T. Duforestel, D. Baillis, G. Rusaouen, “Mass transfer modeling in gas barrier envelopes for vacuum insulation panels: a review”, *Energy Build.* vol. 55, pp. 903–920, 2012, doi:10.1016/j.enbuild.2012.09.004.
- [97] J. H. Kim, F. E. Boafu, S. M. Kim, J. T. Kim, “Aging performance evaluation of vacuum



- insulation panel (VIP)", *Case Stud. Constr. Mater.* vol. 7, pp. 329–335, 2017, doi:10.1016/j.cscm.2017.09.003.
- [98] B. Yrieix, B. Morel, E. Pons, "VIP service life assessment: interactions between barrier laminates and core material, and significance of silica core ageing", *Energy Build.* vol. 85, pp. 617–630, 2014, doi:10.1016/j.enbuild.2014.07.035.
- [99] J. Wang, Y. Zhan, W. Wei, S. Chen, R. Wang, "A new cost effective composite getter for application in high-vacuum-multilayer-insulation tank", *Vacuum*, vol. 131, pp. 44–50, 2016, doi:10.1016/j.vacuum.2016.05.025.
- [100] J. Šadauskiene, L. Šeduikyte, V. Paukštys, K. Banionis, A. Gailius, "The role of air tightness in assessment of building energy performance: case study of Lithuania", *Energy Sustain. Dev.* Vol. 32, pp. 31–39, 2016, doi:10.1016/j.esd.2016.02.006.
- [101] B. Daniotti, R. Paolini, F. Cecconi, "Effects of ageing and moisture on thermal performance of ETICS cladding", in *Durability of Buildings Materials and Components*, Springer, 2014, doi:10.1007/978-3-642-37475-3\_6.
- [102] A. Nowos, B. Orlik-Koźdoń, A. Nowoświat, P. Krause, T. Ponikiewski, "A numerical and experimental investigation of temperature field in place of anchors in ETICS system", *Constr. Build. Mater.* vol. 167, pp. 553–565, 2018, doi:10.1016/j.conbuildmat.2018.02.039.
- [103] R. Ji, Z. Zhang, Y. He, J. Liu, S. Qu, "Simulating the effects of anchors on the thermal performance of building insulation systems". *Energy Build.* vol. 140, 501–507, 2017, doi:10.1016/j.enbuild.2016.12.036.
- [104] S. Park, B. H. Choi, J. H. Lim, S. Y. Song, "Evaluation of mechanically and adhesively fixed external insulation systems using vacuum insulation panels for high-rise apartment buildings", *Energies*, vol. 7, pp. 5764–5786, 2014, doi:10.3390/en7095764.
- [105] S. S. Alotaibi, S. Riffat, "Vacuum insulation panels for sustainable buildings: a review of research and applications". *Int. J. Energy Res.* vol. 31, pp.135–147, 2013, doi:10.1002/er.
- [106] O. Kaynakli, "A review of the economical and optimum thermal insulation thickness for building applications". *Renew. Sustain. Energy Rev.*, vol. 16, pp. 415–425, 2012, doi:10.1016/j.rser.2011.08.006.
- [107] E. Kucukpinar, O. Miesbauer, Y. Carmi, M. Fricke, L. Gullberg, C. Erkey, R. Caps, M. Rochefort, A. G. Moreno, C. Delgado, M. Koehl, P. Holdsworth, K. Noller, "Development of transparent and opaque vacuum insulation panels for energy efficient buildings". *Energy Procedia*, vol. 78, pp. 412–417, 2015, doi:10.1016/j.egypro.2015.11.685.
- [108] M. Alam, "Development of Vacuum Insulation Panel With Low Cost Core Material", PhD thesis, Department of Mechanical, Aerospace and Civil Engineering, College of Engineering, Design and Physical Science, Brunel University London, 2015.
- [109] K. Cho, Y. Hong, J. Seo, "Assessment of the economic performance of vacuum insulation panels for housing projects". *Energy Build.* vol. 70, pp. 45–51, 2014, doi:10.1016/j.enbuild.2013.11.073.
- [110] A. M. Mujeebu, N. Ashraf, A. Alsuwayigh, "Energy performance and economic viability of nano aerogel glazing and nano vacuum insulation panel in multi-story office building", *Energy*, vol. 113, pp. 949–956, 2016, doi:10.1016/j.energy.2016.07.136.
- [111] E. Di Giuseppe, M. Iannaccone, M. Telloni, M. D'Orazio, C. Di Perna, "Probabilistic life

- cycle costing of existing buildings retrofit interventions towards nZE target: Methodology and application example”. *Energy Build.* vol. 144, pp. 416–432, 2017, doi:10.1016/j.enbuild.2017.03.055.
- [112] S. Tadeu, A. Tadeu, N. Simões, M. Gonçalves, R. Prado, “A sensitivity analysis of a cost optimality study on the energy retrofit of a single-family reference building in Portugal”, *Energy Effic.* pp. 1–22, 2018, doi:10.1007/s12053-018-9645-5.
- [113] J. Adamczyk, R. Dylewski, “The impact of thermal insulation investments on sustainability in the construction sector”, *Renew. Sustain. Energy Rev.* vol. 80, pp. 421–429, 2017, doi:10.1016/j.rser.2017.05.173.
- [114] *Buildings and constructed assets - Service life planning - Part 5: Life-cycle costing*, ISO 5686-5, International Organization for Standardization, 2017.
- [115] E. Pramsten, M. Hedlund, “Economical analysis of vacuum insulation panels in outer walls” (in swedish), PhD thesis. KTH Byggetenskap Samhällsbyggnad, Stockholm 2009.
- [116] G. Grazieschi, F. Asdrubali, G. Thomas, “Embodied energy and carbon of building insulating materials: a critical review”, *Clean. Environ. Syst.* vol. 2, 100032, 2021, doi:10.1016/j.cesys.2021.100032.
- [117] *Environmental labels and declarations - Type III environmental declarations - Principles and procedures*, ISO 14025, International Organization for Standardization, 2006.
- [118] N. Lolli, A. G. Hestnes, “The influence of different electricity-to-emissions conversion factors on the choice of insulation materials”, *Energy Build.* vol. 85, pp. 362–373, 2014, doi:10.1016/j.enbuild.2014.09.042.
- [119] P. Karami, N. Al-Ayish, K. Gudmundsson, “A comparative study of the environmental impact of Swedish residential buildings with vacuum insulation panels”, *Energy Build.* vol. 109, pp. 183–194, 2015. doi:10.1016/j.enbuild.2015.10.031.
- [120] S. Resalati, T. Okoroafor, P. Henshall, N. Simões, M. Gonçalves, M. Alam, “Comparative life cycle assessment of different vacuum insulation panel core materials using a cradle to gate approach”, *Build. Environ.* vol. 188, 107501, 2021, doi:10.1016/j.buildenv.2020.107501.
- [121] *Vertical building elements - Impact resistance tests - Impact bodies and general test procedures*, ISO 7892, International Organization for Standardization, 1988.
- [122] *Guideline for European Technical Approval of External Thermal Insulation Composite Systems (ETICS) with Rendering*, ETAG 004, European Organisation for Technical Approvals, Edition 2011.
- [123] International Organization for Standardization. EN ISO 8990: Thermal insulation - Determination of steady-state thermal transmission properties - Calibrated and guarded hot box 1996.
- [124] *Thermal bridges in building construction - Heat flows and surface temperatures - Detailed calculations*, ISO 10211, International Organization for Standardization, 2017.
- [125] *Hygrothermal performance of building components and building elements - Determination of the resistance of external wall systems to driving rain under pulsating air pressure*, EN 12865, European Committee of Standardization, 2001.
- [126] *Hygrothermal performance of building components and building elements - Internal*

- surface temperature to avoid critical surface humidity and interstitial condensation - Calculation methods*, EN ISO 13788, International Organization for Standardization, 2012.
- [127] *Non-destructive testing - Thermographic testing*, EN 16714, European Committee for Standardization, 2016.
- [128] European Commission, “Commission Delegated Regulation (EU) No 244/2012 of 16 January 2012 supplementing Directive 2010/31/EU of the European Parliament and of the Council on the energy performance of buildings by establishing a comparative methodology framework for calculating”, *Off. J. Eur. Union*. vol. pp. 1-38, 2012, doi:10.3000/1977091X.C\_2012.115.eng.
- [129] European Commission, “Guidelines accompanying Commission Delegated Regulation (EU) No 244/2012 of the European Parliament and of the Council on the energy performance of buildings by establishing a comparative methodology framework for calculating cost-optimal levels of minimum energy performance requirements for buildings and building elements”, *Off. J. Eur. Union*. pp. 1–28, 2012.
- [130] *Environmental management - Life cycle assessment - Principles and framework*, ISO 14040, International Organization for Standardization, 2006.
- [131] *Environmental management - Life cycle assessment - Requirements and guidelines*, ISO 14044, International Organization for Standardization, 2006.
- [132] C. Serra, A. Tadeu, N. Simões, “Heat transfer modeling using analytical solutions for infrared thermography applications in multilayered buildings systems”, *Int. J. Heat Mass Transf.* vol. 115 , pp. 471–478, 2017, doi:10.1016/j.ijheatmasstransfer.2017.08.042.
- [133] *Thermal performance of building materials and products - Determination of thermal resistance by means of guarded hot plate and heat flow meter methods - Products of high and medium thermal resistance*, EN 12667, European Committee for Standardization, 2001.
- [134] *Thermal insulating products for building applications - Determination of water vapour transmission properties*, EN 12086, European Committee for Standardization, 2013.
- [135] *Thermal insulating products for building applications - Determination of length and width*, EN 822, European Committee for Standardization, 2013.
- [136] *Thermal insulating products for building applications - Determination of thickness* EN 823 European Committee for Standardization, 2013.
- [137] *Thermal insulating products for building applications - Determination of squareness*, EN 824, European Committee for Standardization, 2013.
- [138] *Thermal insulating products for building applications - Determination of flatness*, EN 825, European Committee for Standardization, 2013.
- [139] *Thermal insulating products for building applications - Determination of the apparent density*, EN 1602, European Committee for Standardization, 2013.
- [140] *Testing of plastics - Determination of gas transmission rate - Part 3: Oxygen-specific carrier gas method for testing of plastic films and plastics mouldings*, DIN 53380-3, German Institute for Standardization, 1998.
- [141] *Thermal insulating products for building applications - Determination of compression behaviour*, EN 826, European Committee for Standardization, 2013.

- [142] *Thermal insulating products for building applications - Determination of dimensional stability under specified temperature and humidity conditions*, EN 1604, European Committee for Standardization, 2013.
- [143] *Thermal insulating products for building applications - Determination of deformation under specified compressive load and temperature conditions*, EN 1605, European Committee for Standardization, 2013.
- [144] *Thermal insulating products for building applications - Determination of tensile strength perpendicular to faces*, EN 1607, European Committee for Standardization, 2013.
- [145] *Plastics - Determination of tensile properties - Part 3: Test conditions for films and sheets*, EN ISO 527-3, European Committee for Standardization. 2018.
- [146] *Thermal insulating products for building applications - Determination of shear behaviour*, EN 12090, European Committee for Standardization, 2013.
- [147] *Thermal insulating products for building applications - Determination of behaviour under point load*, EN 12430, European Committee for Standardization, 2013.
- [148] *Thermal insulating products for building applications - Determination of compressive creep*, EN 1606, European Committee for Standardization, 2013.
- [149] *Thermal insulating products for building applications - Determination of bending behaviour*, EN 12089, European Committee for Standardization, 2013.
- [150] *Thermal insulating products for building applications - Determination of long term water absorption by immersion*, EN 12087, European Committee for Standardization, 2013.
- [151] *Thermal insulating products for building applications - Determination of short term water absorption by partial immersion*, EN 1609, European Committee for Standardization, 2013.
- [152] *Point thermal transmittance of plastic anchors for ETICS*, TR 025, European Organisation for Technical Approvals, 2016.
- [153] *European Assessment Document: Plastic Anchors Made of Virgin or Non-Virgin Material for Fixing of External Thermal Insulation Composite Systems With Rendering*, EAD 330196-00-0604, European Organisation for Technical Approvals. 2016.
- [154] *Paints and varnishes - Determination of water-vapour transmission properties - Cup method*, ISO 7783, International Organization for Standardization, 2018.
- [155] *Products and systems for the protection and repair of concrete structures - Test methods - Determination of modulus of elasticity in compression*, EN 13412, European Committee for Standardization, 2006.
- [156] *Standard Test Method for Resistance to Growth of Mold on the Surface of Interior Coatings in an Environmental Chamber*, D 3273-16, ASTM International, 2016.
- [157] *Plastics - Differential scanning calorimetry (DSC) - Part 4: Determination of specific heat capacity*, ISO 11357-4, International Organization for Standardization, 2014.
- [158] *Advanced technical ceramics. Monolithic ceramics. Thermo-physical properties. Determination of specific heat capacity*, EN 821-3, European Committee for Standardization, 2005.
- [159] *Standard Test Method for Mean Specific Heat of Thermal Insulation*, C351-92b, ASTM International, 1999.

- [160] *Masonry and masonry products - Methods for determining thermal properties*, EN 1745, European Committee for Standardization, 2012.
- [161] *Building materials and products - Hygrothermal properties - Tabulated design values and procedures for determining declared and design thermal values*, ISO 10456, International Organization for Standardization, 2007.
- [162] *Standard Test Method for Determining Specific Heat Capacity by Differential Scanning Calorimetry*, E1216-11, ASTM International, (2018).
- [163] N. Simões, F. Branco, A. Tadeu, “Definition of two-dimensional condensation via BEM, using the Glaser method approach”. *Eng. Anal. Bound. Elem.* vol. 26, pp. 527–536, 2002, doi:10.1016/S0955-7997(02)00011-5.
- [164] H. M. Künzle, “Simultaneous Heat and Moisture Transport in Building Components One- and two-dimensional calculation using simple parameters”, Fraunhofer Institute of Building Physics, 1995. ISBN v.3-8167-4103-7.
- [165] L. Škerget, A. Tadeu, C. A. Brebbia, “Transient simulation of coupled heat and moisture flow through a multi-layer porous solid exposed to solar heat flux”. *Int. J. Heat Mass Transf.* vol. 117, pp. 273–279, 2018, doi:10.1016/j.ijheatmasstransfer.2017.10.010.
- [166] M. Ibrahim, H. Sayegh, L. Bianco, E. Wurtz, “Hygrothermal performance of novel internal and external super-insulating systems: in-situ experimental study and 1D/2D numerical modeling”. *Appl. Therm. Eng.* vol. 150, pp. 1306–1327, 2019, doi:10.1016/j.applthermaleng.2019.01.054.



## **CHAPTER 3**

# **STUDY OF THE EDGE THERMAL BRIDGING EFFECT IN VACUUM INSULATION PANELS**





## **3. Study of the edge thermal bridging effect in vacuum insulation panels**

### **3.1. Introduction**

A vacuum insulation panel (VIP) consists of an evacuated micro-porous core structure which is surrounded by a barrier envelope used to keep the vacuum. Typical values of VIP thermal conductivity (measured at the centre of panel) can range from 2 to 4.5 mW/(m·K) after production [1], to 6 to 8 mW/(m·K) after 25 years of ageing and including edge effects [2].

Even though there is a high energy-savings potential associated with these innovative insulation products, their application in buildings raises some challenges, as stated in previous chapter. In particular, one of the most critical issues regarding vacuum insulation technology is the thermal bridging effect that occurs along the edges of the panels [3]. VIPs thermal bridges can occur due to the high barrier envelope linking the cold and warm sides; due to the use of cover layers to encapsulate VIP panels and edge materials; and due to the difficulty in completely eliminating small air gaps at the joints between adjacent panels and due to building irregularities. Initially, barrier envelope materials mostly consisted of aluminium foils or laminated polymer films. Gradually, these developed into laminated metallized polymer films with low water vapour and gas permeability [4], reducing the edge thermal bridging effect of the foils [5]. Also, different VIP-based solutions have been designed for buildings applications, namely adopting additional protective cover layers and edge materials in order to enable them to be easier applied to the walls and to provide protection against mechanical damage. Several VIP solutions (with different VIP edge/joint assemblies) suited to be used in ETICS were identified in previously in chapter 2.

VIP thermal bridges have been investigated by several researchers through numerical calculations and experimental tests ([6], [7]), showing the effect of the laminated aluminium foils and the air gaps between panels on the linear thermal transmittance. In order to evaluate the effective thermal conductivity of VIP products, Tenpierik and Cauberg [4] investigated the influence of the VIP characteristics and barrier envelope properties. These authors studied the effect of varying laminate thickness, laminate thermal conductivity, core material thermal conductivity and panel

thickness on the linear thermal transmittance. Other researchers ([8], [9]) have investigated thermal bridges resulting from the edge material, looking to reduce thermal bridging effects. Lorenzati *et al.* [10] showed how using different joint technologies affects the thermal performance of VIP assemblies. This experimental investigation demonstrated that the thermal behaviour of VIP assemblies depends on physical and geometrical properties. Staggering double layers of VIPs in order to minimize the thermal bridges effect has also been studied [11]. Nussbaumer *et al.* [12] studied the thermal performance of VIPs encapsulated in expanded polystyrene numerically and experimentally. The authors considered that the most challenging task of the numerical analysis was to develop an adequate simplified model to simulate the abrupt changes in size and thermal conductivity of the materials. In fact, simulating the VIP edge thermal bridging effects is a complex task that requires skilled and experienced simulators [13].

From the literature, it can be concluded that linear thermal bridging in vacuum panels is far from negligible and needs to be considered when assessing overall building energy performance [14]. Nonetheless, most researchers have focused on studying the performance of single panels. Most studies investigating thermal bridging focus on steady state simulations and the determination of equivalent thermal conductivities for VIP elements. However, steady state thermal transmittance of façades fails to encompass the dynamic behaviour resulting from time-varying outdoor conditions and building usage [15]. In fact, it is not usual to find steady-state conditions during the seasonal and daily climatic conditions [16]. Since, in reality, buildings are subjected to unsteady conditions, a more accurate assessment of the thermal performance of building elements requires calculations using dynamic models based on the time dependent behaviour of the solutions [17]. Thus, the edge thermal bridging effects should be evaluated under dynamic conditions. Particularly in ETICS, the thermal delay of façades with VIP as an external thermal insulation layer is of interest. Additionally, the point thermal transmittance of panels joints and the point thermal transmittance due to the mechanical fixing devices should also be evaluated in order to estimate overall thermal transmittance of building façades for design purposes [18].

For an adequate assessment of the transient behaviour of façades, it is essential to determine the materials density and thermal conductivity, as well as specific heat capacity. Specific heat means the quantity of heat required to change the temperature of a unit mass of panel one degree, measured as the quantity over the temperature range specified [19]. Although there are no standard test procedures set for determining the specific heat of composite materials, such as VIPs encapsulated in expanded polystyrene, test methods using a calorimeter [20], heat flow meter [21] or guarded hot plate [22] could be explored.

Prior to studying the VIP panels edge thermal bridging effect, the mechanical and hygrothermal properties of the vacuum insulation product used in this thesis were determined by means of a laboratory testing campaign. The test procedures used and the results obtained are summarized in Annex B. The VIP solution was shown to be suitable for use in ETICS.

The work presented in this chapter aimed at performing an experimental and numerical investigation of the edge thermal bridging effects considering different VIP assemblies. In particular, focused was made on solutions suitable for use in ETICS. Firstly, experimental measurements were carried out using a guarded hot plate apparatus in order to assess the linear thermal transmittance between panel joints. The experimental measurements have included the determination of specific heat capacity using an indirect test method. Then, a numerical modelling validation was performed for steady-state and transient boundary conditions. A sensitivity analysis regarding the use of different VIP based products, joint assemblies, edge materials and panel dimensions was also carried out. Also, the contribution of the point thermal transmittance of the mechanical fixing devices was numerically evaluated. Finally, transient thermal simulations were conducted considering VIP based ETICS applied in different support walls, namely ceramic brick, granite stone and wood. The thermal performance of ETICS walls, including the thermal delay analysis, were presented and compared to other conventional ETICS solution.

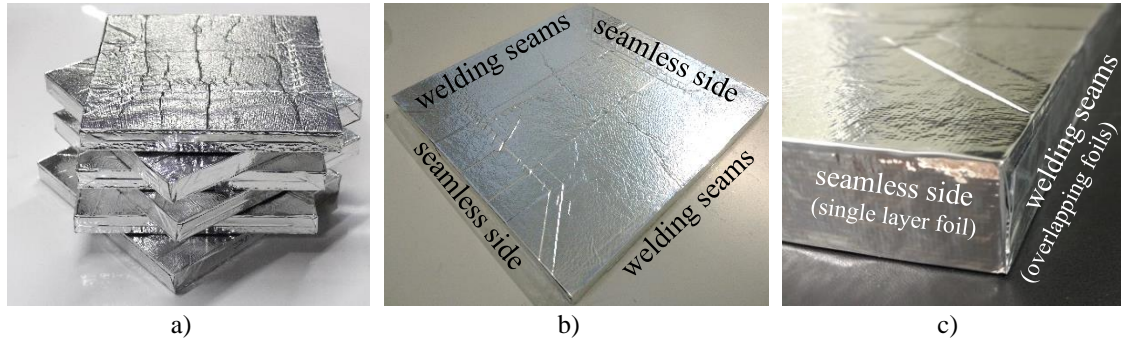
## **3.2. Materials and methods**

In this section, first, the VIP product being studied is presented. Then, information about the methods used to determine the linear thermal transmittance, the point thermal transmittance and specific heat capacity are presented, including both experimental and numerical approaches. Finally, in order to allow for the evaluation of the overall thermal performance under 2D transient numerical simulations, the properties of a VIP based ETICS wall are identified.

### **3.2.1. VIP product**

The VIP product considered in this investigation is a 20 mm fumed silica panel with a tri-metallized multilayer polymer film as packaging. According to information provided by the manufacturers [23], the VIP product has a density of 180 to 210 kg/m<sup>3</sup> and a thermal conductivity at centre of panel (CoP)  $\leq 4.3$  mW/(m·K). The panels used in the experimental measurements are 300 mm x 300 mm in size. After production, the internal gas pressure is 0.50 to 0.68 mbar. The

panel edges have two sides with welding seams (also called as overlapping foils edge design) and two seamless side (single layer edge design). Figure 3.1 shows the VIP used in the experimental measurements. Further details of the VIP product are given in Annex B.



**Figure 3.1:** Vacuum insulation panels used in experimental measurements: a) overview of test specimens; b) identification of the sealing types; c) detail view of the barrier envelope side.

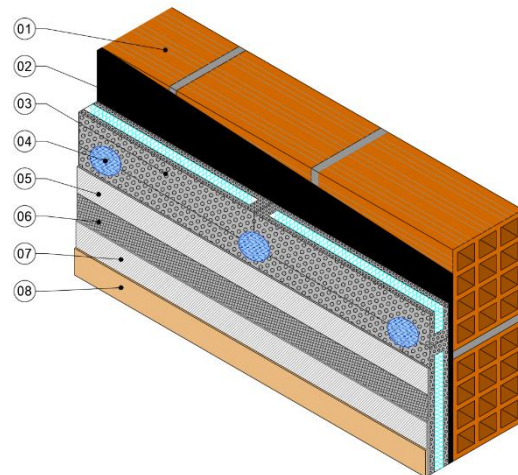
Table 3.1 summarizes the several joint assembly case studies analysed in this chapter, which include, overlapping, single foils and protected edges. Also, solutions with expanded polystyrene (EPS) edge cover layers (case E and F) are included, since these are the VIP products suited for ETICS applications.

**Table 3.1:** VIP joint assemblies (dimensions in mm).

Case	Description	Figure layout
A	VIPs with single layer joints (seamless side)	
B	VIPs with mixed joints (welding seams with seamless side)	
C	VIPs with overlapping foils joints (welding seams)	
D	VIPs with EPS edge material (seamless side)	
E	VIPs with EPS protective cover layer (seamless side)	
F	Encapsulated VIPs in EPS (seamless side)	

Cases studies A to C consist in the VIP joints with different types of panels sealings, namely a seamless side against a seamless side joint (case A), seamless side against a welding seams side joint (case B) and welding seams joints in both panels (case C). The VIP thickness is 20 mm for all cases. In case D, two pieces of EPS with 10 mm width is introduced in the VIP joints (considering seamless side in both panels). In case E, the VIPs are covered with a protective layer of EPS with a thickness of 10 mm. This cover layer material is intended to protect the VIP from mechanical damages. The case F – called in this thesis as encapsulated VIP - was selected for the VIP based ETICS further investigations, considering the determination of the point thermal transmittance and the building application sensitivity analysis. This product consists in a VIP covered with a protective layer made of EPS with a thickness of 10 mm on each side and 10 mm along the edges (combination of case D and E). This solution allows the use of mechanical fixation between panels without perforating the VIP panel, as can be observed in Figure 3.2, which is crucial to maintain vacuum and thermal performance of the panels.

1. Support wall
2. Adhesive
3. Encapsulated VIP
4. Plastic anchor
5. Base coat (first layer)
6. Reinforcement (glass fibre mesh)
7. Base coat (second layer)
8. Finishing coat (primer and decorative coating)



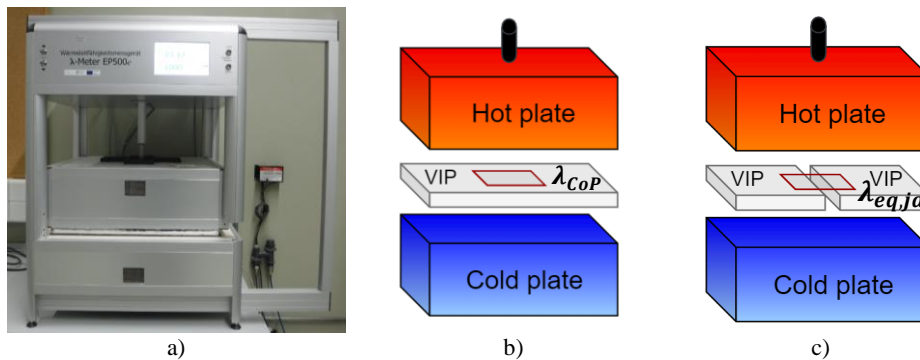
**Figure 3.2:** VIP based ETICS scheme.

### **3.2.2. Experimental apparatus**

Thermal transmittance measurements were performed on a guarded hot plate apparatus (GHP),  $\lambda$ -Meter EP500e (Figure 3.3a), following ISO 8302 [24] and EN 12667 [25]. In these tests, the heat flow rate is obtained from the measurement of the power input to the heating unit in the metering area (150 mm x 150 mm). The tests were carried out in a controlled laboratory environment with  $(23 \pm 2)^{\circ}\text{C}$  air temperature and  $(50 \pm 5)\%$  air relative humidity. Before any test, the specimens were conditioned in the controlled chamber with for at least 24h prior to the test, ensuring similar initial conditions for all the specimens. Since the panel's dimensions were lower

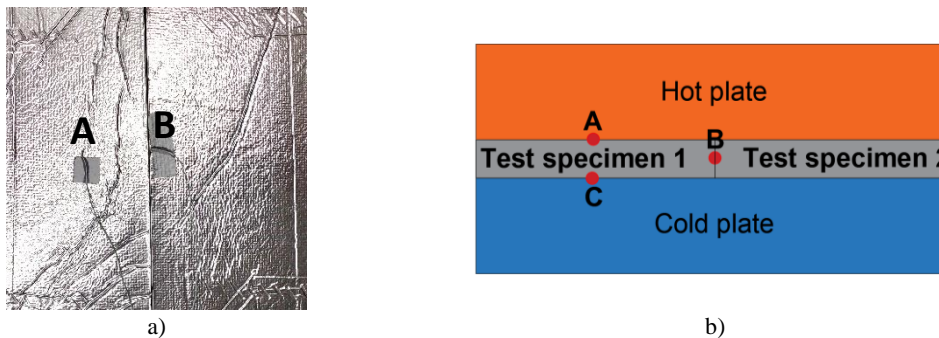
than the 500 mm x 500 mm (required for the GHP measurements), an insulation frame made of polyester fibres was used to fulfil the remaining area, in order to minimize the disturbance of the heat fluxes between plates.

First, the thermal conductivity at the centre of panel ( $\lambda_{CoP}$ ) was determined for each specimen (Figure 3.3b). Then, the linear thermal transmittance between panel joints was measured. For this purpose, two panels were assembled within the GHP apparatus so that their joint was within the measuring area (Figure 3.3c). All tests were performed with a compression of the plates over the specimen of 1000 Pa. The measurements were carried out for three average temperatures: 10°C, 25°C and 40°C. The temperatures of the cold plate were, respectively: 2.5°C; 17.5°C; and 32.5°C, while the temperatures of the hot plate were 17.5°C; 32.5°C; and 47.5°C.



**Figure 3.3:** Guarded hot plate apparatus: a) photograph; b) measurement of the thermal conductivity at VIP CoP scheme ( $\lambda_{CoP}$ ); c) measurement of the thermal equivalent conductivity including edge effects ( $\lambda_{eq,ja}$ ).

Temperature measurements were used to validate the numerical model, presented in section 3.2.6.3. Figure 3.4 gives the location of the temperature sensors (thermocouples type T), namely: thermocouple A is at the centre of panel on the hot plate side; thermocouple B is at the centre of measuring area (VIP joint) and at 10 mm depth; and thermocouple C is at the centre of panel on the cold plate side.



**Figure 3.4:** Location of the temperature sensors on the panels: a) photograph; b) schematic position of the thermocouples: hot plate side, joint and cold plate side.

### 3.2.3. Linear thermal transmittance calculation

According to EN 17140 [13], the linear thermal transmittance,  $\psi$ , is determined by measuring the thermal conductivity in the centre of a panel,  $\lambda_{CoP}$ , and of the joint assembly on panels with similar thickness, using equation 3.1:

$$\psi_m = \frac{A_m}{d \cdot l_\psi} \cdot (\lambda_{eq,ja} - \lambda_{CoP}) \quad [\text{mW}/(\text{m} \cdot \text{K})] \quad (3.1)$$

where,  $\psi_m$  is the linear thermal transmittance for the joints in the measuring area,  $A_m$ ,  $d$  is the thickness of panels,  $l_\psi$  is the length of the joints within the measuring area,  $\lambda_{CoP}$  is the thermal conductivity for the centre of panel and  $\lambda_{eq,ja}$  is the equivalent thermal conductivity including edge effects for a specific joint assembly. The surface resistance can be omitted from this calculation since the heating and cooling plates are in perfect thermal contact with the test specimens. Next, in order to calculate the equivalent thermal conductivity of a panel  $\lambda_{eq}$  equation 3.2 is applied:

$$\lambda_{eq} = \lambda_{CoP} + \frac{\psi_m}{2} \cdot d_N \left( \frac{P_N}{S} \right) \quad [\text{mW}/(\text{m} \cdot \text{K})] \quad (3.2)$$

where the linear thermal transmittance value for a joint,  $\psi_m$ , is the value obtained in equation 3.1,  $S$  is the surface area (length x width) of the panel,  $P_N$  is the nominal perimeter of the panel and  $d_N$  nominal thickness.

### 3.2.4. Point thermal transmittance calculation

Besides the edge thermal bridging effects, the point thermal transmittances generated by mechanical fixation also need to be included in the effective thermal transmittance. Following the methods described in EOTA TR025 [26] and ISO 10211 [27], the point thermal transmittance,  $\chi$ , is numerically calculated according the equation 3.3:

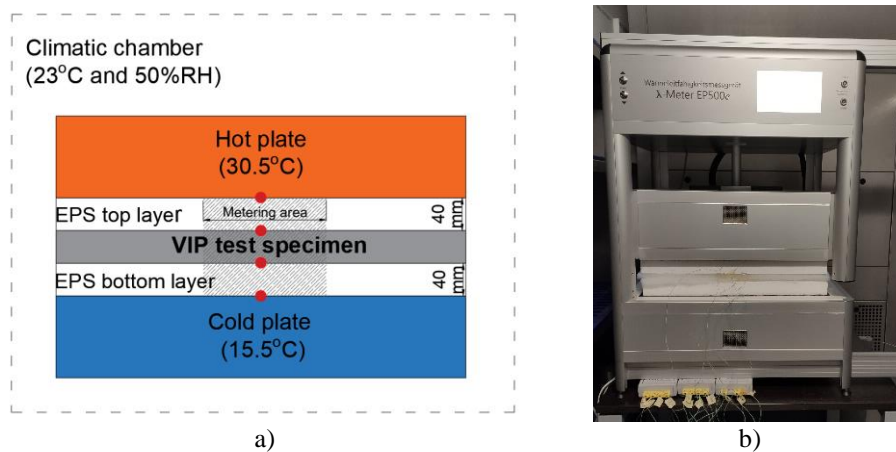
$$\chi = L_{3D} - \sum_{p=1}^{N_p} U_{CoP} \cdot A_p - \sum_{j=1}^{N_j} \psi \cdot l_j \quad [\text{mW}/\text{K}] \quad (3.3)$$

where,  $L_{3D}$  is the thermal coupling coefficient obtained from 3D calculation of the component separating the two environments being considered;  $U_{CoP}$  is the thermal transmittance of the centre of the panel;  $A_p$  is the area over which the value  $U_{CoP}$  applies;  $l_j$  is the length over which the

value  $\Psi$  applies;  $\Psi$  is the linear thermal transmittance;  $N_p$  is the number of 1D components, *i.e.* the number of panels;  $N_j$  is the number of 2D components, *i.e.* the number of joints; To calculate the  $L_{3D}$  a numerical model was defined as detailed in section 3.2.6.2.

### 3.2.5. Specific heat capacity

The dynamic thermal properties of the VIP products were evaluate using an indirect test method based on the methodology proposed by Simões *et al.* [17] and explored in non-homogeneous materials by Marques *et al.* ([22],[28]). This method combines experimental data with results given by a one-dimensional analytical transient heat transfer model. For this purpose, the test specimen was instrumented with thermocouples and subjected to heat transfer by using the guarded hot plate apparatus located inside a climatic chamber at  $(23 \pm 2)^\circ\text{C}$  temperature and  $(50 \pm 5)\%$  relative humidity. Figure 3.5 shows a scheme of the experimental apparatus and includes the location of the thermocouples. Two thermocouples were placed at each interface layer. The temperature sensors were connected to a data logger programmed to record every minute. Two layers of a known and homogeneous thermal insulation material (expanded polystyrene) were introduced at the top and the bottom of the test specimen.



**Figure 3.5:** GHP apparatus for specific heat determination using the indirect method: a) scheme with thermocouples positions (red dots); b) photography of the test apparatus with a test specimen.

The guarded hot plate was set at a mean temperature of  $23^\circ\text{C}$ . A difference of  $15^\circ\text{C}$  was thus established between the hot and the cold plates, at  $30.5^\circ\text{C}$  and  $15.5^\circ\text{C}$ , respectively. The energy input was maintained until a permanent heat flow rate was maintained for 300 min. Then, the GHP apparatus was turned off and the temperature monitoring kept going until the initial climatic chamber conditions ( $23^\circ\text{C}$ ) were reached. The total thickness and the thermal conductivity of the multilayer system were recorded and used as input in the analytical model. The average



temperature variation at each interface layer and the thermo-physical properties (thickness, apparent density, thermal conductivity and specific heat) of the different layers were also used in the analytical model. Then, the specific heat capacity of VIP was determined by aligning the experimental temperature measurements with the analytical model results, using an iterative approach. The specific heat value corresponds to the smallest mean squared error between the temperature results [22]. The specific heat determination of VIP panels was carried out on three similar test specimens (same size and production batch) with 400 mm x 400 mm. In order to evaluate the repeatability of the method, two tests were carried out for each specimen.

Additionally, in order to validate the indirect test method, the specific heat capacity of the fumed silica and EPS material was also determined by means of a differential scanning calorimetry, model DSC 200 F3 by Netzsch, according to ASTM E1269-11 [29] test procedure. For this purpose, a synthetic sapphire disk ( $\text{Al}_2\text{O}_3$ ) was used for calibration. Figure 3.6 illustrates the equipment used.



**Figure 3.6:** Differential scanning calorimetry apparatus for specific heat capacity determination.

### **3.2.6. Numerical modelling**

Over the following paragraphs, the numerical models used in the study are described. Numerical modelling simulations were carried out to determine: the linear thermal transmittance for several VIP joint assemblies with steady state boundary conditions (2D models); the VIP based ETICS point thermal transmittance with steady state conditions (3D model); and the VIP based ETICS walls thermal performance, including thermal delay assessment, under unsteady conditions (2D model). For the point thermal transmittance modelling and the assessment of the ETICS walls thermal performance under dynamic conditions, real nominal dimensions of the encapsulated VIP (commercially available size) of 440 mm x 440 mm and 640 mm x 640 mm were considered.

### 3.2.6.1. Linear thermal transmittance

Besides experimental measurements, EN 17140 [13] allows the determination of the linear thermal transmittance by numerical simulations according to ISO 10211 [27]. For this purpose, numerical modelling simulations were carried out with BISCO software [30] version 11.0w by Physibel. This software allows 2D steady state numerical simulations based on finite element methods (FEM). Additional conformity check of the simulation program was first carried out by using the validation examples in ISO 10211 [27] and EN ISO 10077-2 [31] and the results were found to be in very close agreement. For the case studies, a preliminary analysis was performed in order to define a grid (number of nodes) and to check the accuracy of the model. For example, regarding the modelling of case F, a triangular mesh with 114300 nodes was defined, since increasing the number of nodes resulted in differences lower than 2%.

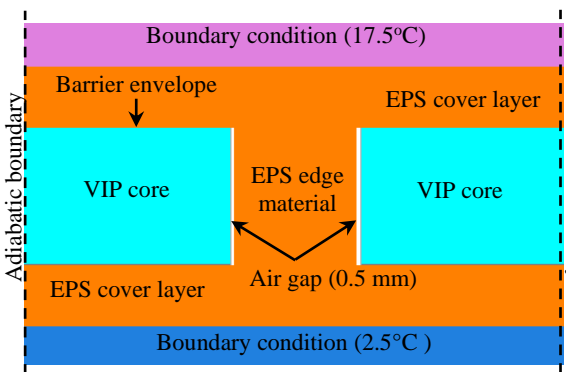
The linear thermal transmittance,  $\psi$ , has been calculated using the equation 3.4:

$$\psi = \frac{Q}{T_h - T_c} - U_{CoP1} \cdot l_1 - U_{CoP2} \cdot l_2 \quad [\text{mW}/(\text{m} \cdot \text{K})] \quad (3.4)$$

where,  $Q$  is the total heat transfer;  $T_h$  and  $T_c$  are the temperature boundary conditions, for the hotter side and colder side, respectively;  $U_{CoP}$  is the thermal transmittance of each panel;  $l$  is the length of each panel.

A detailed schematic representation of the model used in the numerical modelling (example for case F) is presented in Table 3.2. The properties of the materials were determined in a laboratory, except for the thickness and the thermal conductivity of the VIP barrier envelope which were provided by the manufacturer. Following the recommendations of the VIP standard [13], which indicates that small air gaps between panels should be taken into account, an air gap with 0.5 mm width between VIP joints was considered in the models. This value was based on experimental measurements of VIP joints by means of a feeler gauge. Surface thermal resistances were not considered.

**Table 3.2:** Numerical model properties – VIP encapsulated in EPS (case F).

Schematic representation	Material	Thickness [mm]	Thermal conductivity <sup>(1)</sup> [mW/(m·K)]	Source
	VIP barrier envelope	0.097	900	[23]
	VIP CoP	20	4.2	(3)
	EPS cover layer	10	36	(3)
	EPS edge material	20	36	(3)
	Air gap	0.5	67 <sup>(2)</sup>	[30]

<sup>(1)</sup> Thermal conductivity measured at 10°C.

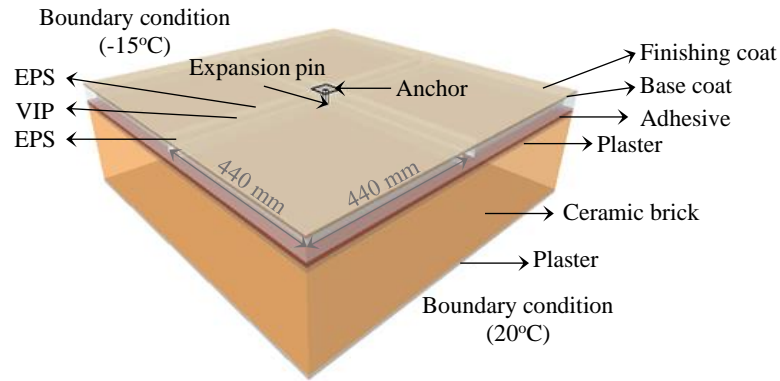
<sup>(2)</sup> Equivalent thermal conductivity automatically calculated by BISCO, in accordance with EN ISO 10077-2 [31].

<sup>(3)</sup> Experimental measurement.

### 3.2.6.2. Point thermal transmittance

In order to determine the point thermal transmittance and, in particular, to calculate  $L_{3D}$ , TRISCO software version v14.0w by Physibel [32] was used. TRISCO allows 3D steady state numerical simulations based on FEM. For this purpose, a representative VIP based ETICS (encapsulated VIP) applied over a ceramic brick wall with 440 mm x 440 mm encapsulated panels was modelled. To avoid increasing the complexity of the model, the ceramic brick wall was modelled using an equivalent thermal conductivity of a ceramic hollow brick wall. Since the wall is thermally insulated externally, the detail of the thermal bridging between bricks is considered to be negligible.

Calculations were done with (and without) plastic anchors centrally placed between four VIP panels (worst case scenario), as can be observed in Figure 3.7. The thickness and thermal conductivity of the materials are presented in Table 3.3. The thermal properties considered for the ETICS components were based on information gathered from technical datasheets provided by manufactures, as well as from the TRISCO database provided by Physibel. The plastic anchor has nominal diameter of 9 mm, a drill hole depth of 65 mm and a plate with 26.4 cm<sup>2</sup>. Since TRISCO only allows rectangular shapes, a simplification of the model was carried out for the shape of the plate, considering a square with an equivalent area of a conventional circular plastic anchor.



**Figure 3.7:** Representation of the 3D numerical model – VIP encapsulated in EPS.

**Table 3.3:** 3D numerical model properties – case F.

Constructive layer component	Thickness [mm]	Thermal conductivity [mW/(m·K)]	Source
Finishing coat	2	400	[33]
Base coat	5	450	[34]
Anchor (polypropylene)	3	220	[32]
Expansion pin (reinforced polyamide)	--	300	[32]
EPS cover layer	10	36	<sup>(1)</sup>
VIP	20	4.2	<sup>(1)</sup>
EPS cover layer	10	36	<sup>(1)</sup>
Adhesive	10	450	[34]
Plaster	10	1 300	[35]
Ceramic brick	220	520	[36]
Plaster	10	1 300	[35]

<sup>(1)</sup> Experimental measurement.

Calculations were performed with  $-15^{\circ}\text{C}$  and  $20^{\circ}\text{C}$  for internal and external environments, respectively, in accordance with EOTA TR025 [26]. Also, internal and external surface thermal resistances of  $0.04 \text{ (m}^2\cdot\text{K)/W}$  and  $0.13 \text{ (m}^2\cdot\text{K)/W}$ , respectively, were considered.

### 3.2.6.3. Thermal performance of ETICS walls under dynamic conditions

The calculations under unsteady boundary conditions were performed by using the dynamic thermal simulation software, BISTRA version v4.0w by Physibel [37]. BISTRA is a thermal

analysis software based on FEM used for calculating transient heat transfer in 2D free-form objects. A timestep of 60 seconds was defined. For this purpose, three different support walls were considered, namely a ceramic brick wall, a granite stone wall and lightweight wall of wood medium density fibreboard (MDF). For the ceramic brick wall, a simplification of the model was followed. Namely, a solid ceramic wall with thermal properties equivalent to those of a hollow brick wall was modelled. Regarding the wood support, a simplification was made and the wood studs were not considered in the model. Table 3.4 presents the detailed thermal characteristics of the walls and the VIP based ETICS components. The properties of the support walls were based on technical data. The thermal conductivity values of the ETICS components were obtained using a guarded hot plate apparatus ( $\lambda$ -Meter EP500e) for an average temperature of 10°C, as recommended by the EN 12667 [25] and EN 12664 [38].

In the case of VIP based ETICS walls performance, determination of thermal conductivity should include 25 years ageing. For this purpose, an accelerated ageing test according to Annex C of EN 17140 [13] was carried out. This was done by storing the panel at 50°C and 70% relative humidity over a period of 180 days. An increase in average VIP thermal conductivity of 1.28 mW/(m·K) (600 mm x 600 mm panels) and 2.36 mW/(m·K) (400 mm x 400 mm panels) was obtained by means of GHP measurements at 10°C in accordance with EN 12667 [25]. Further information about the thermal conductivity tests after ageing is given in Annex B. Specific heat of VIP and EPS material was determined according the indirect method explained in section 3.2.5. The remaining properties are based on technical datasheets.

**Table 3.4:** 2D dynamic numerical model properties.

Layer	Constructive layer	Thickness [mm]	Thermal conductivity [mW/(m·K)]	Emissivity [-]	Apparent density [kg/m <sup>3</sup> ]	Specific heat [J/(kg·K)]	Source
<b>Support</b>	Ceramic brick	220	520	0.90	850	840	[32], [36]
	Granite stone	220	3000	0.90	2600	840	[17]
	Wood (MDF)	18	180	0.90	800	1700	[32]
	Plaster	10	1300	0.90	1650	840	[35], [39]
	Adhesive	0	450	0.90	1350	40	[34], [39]
<b>VIP based ETICS (considering case study F)</b>	EPS	10	36	0.90	20	1775	<sup>(3)</sup>
	VIP	20	5.5 <sup>(1)</sup> - 6.6 <sup>(2)</sup>	0.10	200	1019	<sup>(3)</sup>
	Base coat	5	450	0.90	1350	840	[34], [39]
	Finishing coat	2	400	0.91	1650	1000	[33], [39]

<sup>(1)</sup> Thermal conductivity measured at CoP of VIP with 600 mm x 600 mm after ageing.

<sup>(2)</sup> Thermal conductivity measured at CoP of VIP with 400 mm x 400 mm after ageing.

<sup>(3)</sup> Experimental measurements.

Previously to performing the unsteady-state simulations on VIP based ETICS walls, the numerical modelling software was validated by comparing the temperature behaviour of VIP panels recorded during the experimental measurements with those obtained numerically. Section 3.4.3 presents these results.

Dynamic numerical modelling allowed the estimation of the thermal delay and the thermal damping for both VIP CoP areas and VIP joint areas for different support walls. The thermal delay was evaluated by subjecting the external surface of the model wall to a sinusoidal temperature variation with 40°C amplitude, ranging between 0°C and 40°C in a 24h period, and by recording the internal surface temperature variation. Then, the thermal delay is defined as the time difference between when the thermal variation is recorded on the external surface and when it appears on the internal surface.

### 3.3. Experimental results

This section presents the experimental results of the laboratory testing by means of a GHP apparatus, namely regarding the determination of thermal conductivity at centre of panel (CoP), the linear thermal transmittance for different VIP joint assemblies and the specific heat capacity.

#### 3.3.1. Thermal conductivity at the centre of the panel

Table 3.5 shows the average VIP thermal conductivity measured at the centre of each panel, under different boundary conditions, as well as the thickness and apparent density of the test specimens. These values result from five tests being performed per specimen. The average VIP thermal conductivity measured at 10°C at the centre of panels is 4.20 mW/(m·K). While, the average thermal conductivity measured at 25°C and 40°C, increased 4.40 mW/(m·K) and 4.67 mW/(m·K), respectively. A maximum standard deviation of 0.021 mW/(m·K) was found for test specimen 2 (based on 5 measurements).

**Table 3.5:** VIP thickness, apparent density and average thermal conductivity measured at centre of panel.

VIP	Thickness [mm]	Apparent density [kg/m <sup>3</sup> ]	$\lambda_{CoP}$ [mW/(m·K)] (standard deviation)		
			$\lambda_{10}$	$\lambda_{25}$	$\lambda_{40}$
Test specimen 1	20.6	204.7	4.23 (0.012)	4.44 (0.017)	4.72 (0.004)
Test specimen 2	20.4	193.8	4.16 (0.021)	4.35 (0.016)	4.62 (0.007)
<b>Mean values</b>	<b>20.5</b>	<b>199.3</b>	<b>4.20</b>	<b>4.40</b>	<b>4.67</b>

Additional measurements were performed on intentionally perforated panels (loss of vacuum), resulting in a thermal conductivity of 21.6 mW/(m·K), which was still lower than that of some conventional insulation materials.

### 3.3.2. Linear thermal transmittance

To measure the linear thermal transmittance at the VIP joints, two VIPs were assembled within the GHP apparatus so that their joint was within the measuring area. Table 3.6 shows the GHP results (equivalent thermal conductivity including the edge effect) and the linear thermal transmittance values calculated according to equation 3.1 for different temperature boundary conditions.

**Table 3.6:** Equivalent thermal conductivity and linear thermal transmittance of VIP joint assemblies

Joint assembly	$\lambda_{eq,ja}^{(1)}$ [mW/(m·K)]			$\psi_m^{(2)}$ [mW/(m·K)]		
	$\lambda_{10}$	$\lambda_{25}$	$\lambda_{40}$	$\psi_{10}$	$\psi_{25}$	$\psi_{40}$
A - VIPs with single layer joints	5.63	5.86	6.19	10.15	10.44	10.88
B - VIPs with mixed joints	6.29	6.59	6.92	15.17	16.01	16.35
C - VIPs with overlapping foils joints	6.55	6.86	7.20	16.60	17.42	17.91
D – VIPs with EPS edge material	9.54	10.06	10.62	38.13	40.50	42.54
E- VIPs with EPS protective cover layer	9.10	9.56	10.08	6.57	6.87	6.94
F - Encapsulated VIPs	12.55	13.24	14.08	19.77	20.95	22.25

<sup>(1)</sup> Equivalent thermal conductivity including edge effects.

<sup>(2)</sup> Linear thermal transmittance.

The results highlight the edge thermal bridging effect of the VIP barrier envelope (A-C). The overlapping foils result in higher linear thermal bridges, as expected. The inclusion of a protective cover layer (case E) reduces the linear thermal bridge effect. However, the use of EPS edge material (cases D and F) results in higher linear thermal bridges, due to the higher thermal conductivity of EPS material when compared with VIP core material. The linear thermal transmittance of case study F is around 2 times higher than case A.

### 3.3.3. Specific heat

Table 3.7 summarizes the specific heat capacity test results, which resulted in an average specific heat of 1019 J/(kg·K) for the vacuum insulation panel. This value was used in the numerical simulations with unsteady-state boundary conditions.

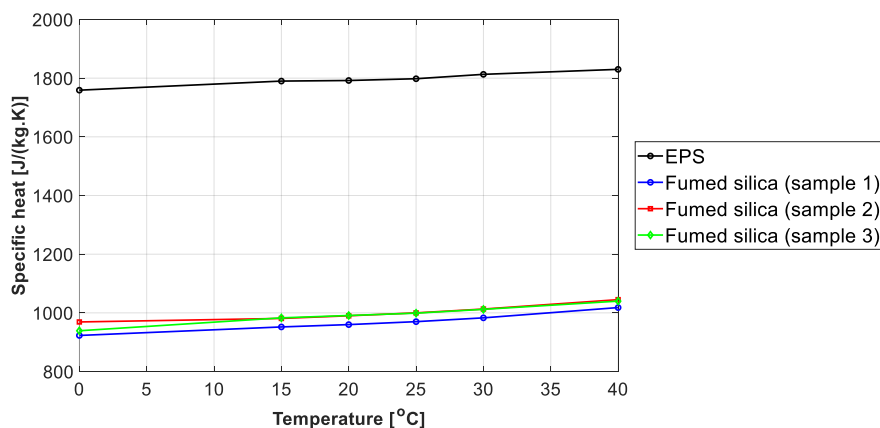
**Table 3.7:** Apparent density, thermal conductivity and specific heat capacity results.

Test specimen	Apparent density [kg/m <sup>3</sup> ]	Thermal conductivity <sup>(1)</sup> [mW/(m·K)]	Test no.	Specific heat [J/(kg·K)]	Average specific heat [J/(kg·K)]
VIP 1	195.8	4.51	Test 1	940	<b>1019</b> (± 57)
			Test 2	987	
VIP 2	203.9	4.99	Test 3	1030	
			Test 4	1058	
VIP 3	189.9	4.76	Test 5	1058	
			Test 6	1041	

<sup>(1)</sup> Thermal conductivity measured at centre of panel at a mean temperature of 23°C .

The specific heat capacity determination by means of the indirect method in GHP apparatus showed acceptable repeatability and reproducibility, resulting in an uncertainty of  $\pm 57$  J/(kg·K). The uncertainty was calculated according to JCGM 106:2012 [40]. The evaluation (type A) was made from a series of repeated measurements, where the standard deviation of the repeatability and reproducibility measurements were taken into account. The number of degrees of freedom was equal to the number of measurements minus one.

For validation of the indirect test method, the specific heat capacity of fumed silica core and EPS material was also determined by means of a differential scanning calorimetry. The results are presented in Figure 3.8, showing an average specific heat capacity at 20°C of 980 J/(kg·K) for fumed silica and 1775 J/(kg·K) for EPS material. As expected, the results of fumed silica are very close to the vacuum panels confirming the reliability of the indirect test method.



**Figure 3.8:** Specific heat results by means of differential scanning calorimetry.



### 3.4. Numerical results

The numerical modelling results are presented in this section, including the linear thermal transmittance for the VIP joint assemblies under study, the point thermal transmittance caused by panels joints and by plastic anchors, as well as the unsteady state simulation validation. The linear thermal transmittance numerical results are compared with those obtained experimentally. Also, the dynamic numerical modelling is compared against experimental measurements in the GHP apparatus.

#### 3.4.1. Linear thermal transmittance

Figure 3.9 compares the linear thermal transmittance obtained experimentally (presented in Table 3.6) and numerically, considering an average test temperature of 10°C.

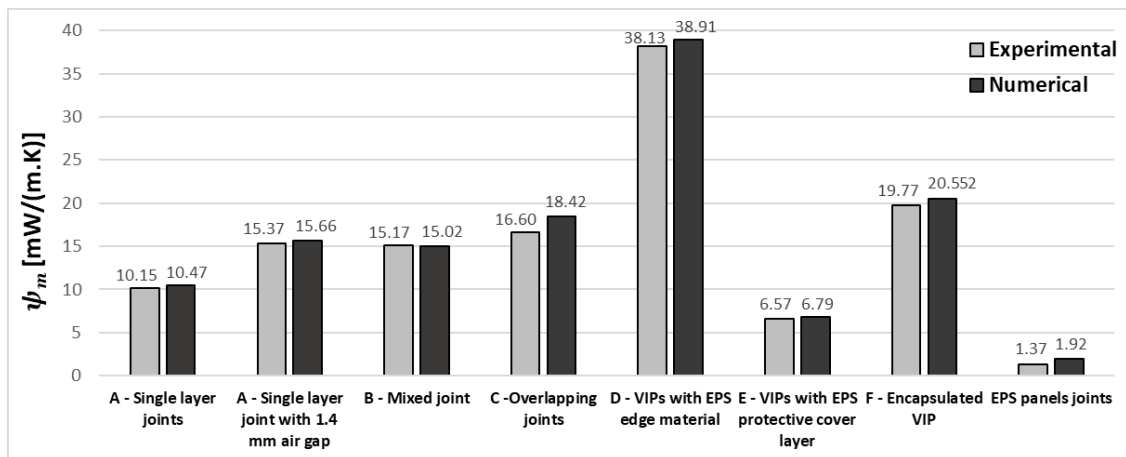
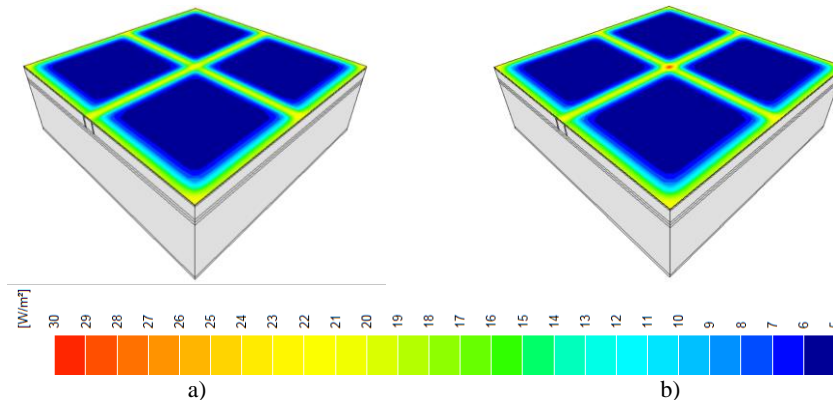


Figure 3.9: Linear thermal transmittance results comparison between numerical modelling and experimental measurements.

Numerical results showed good agreement with the experimental measurements. A maximum absolute difference of 1.8 mW/(m·K) was reached for case C, which could be related with a difficulty in simulating the welding seams in the simplified model. Additionally, the results for expanded polystyrene panels joints showed a reduced linear thermal transmittance value, as expected. Since the numerical results revealed a good accuracy, a numerical modelling approach was used for the sensitivity analysis presented in section 3.5.

### 3.4.2. Point thermal transmittance of VIP based ETICS with plastic anchor

For determination of the point thermal transmittance in a VIP based ETICS solution, the encapsulated VIP assembly was selected. Figure 3.10 shows the 3D numerical model results by presenting the isoflux diagram of the 4 panels model, with and without mechanical fixing.



**Figure 3.10:** 3D numerical model isoflux diagram: a) without plastic anchor; b) with plastic anchor.

The isoflux diagram clearly highlights the edge thermal bridging effect of VIP panels installed over a support wall. In the model without mechanical fixing (Figure 3.10a), a point thermal transmittance of 4.63 mW/K was obtained. When the plastic anchor was included (Figure 3.10 b), the point thermal transmittance increased to 4.94 mW/K.

According to EOTA TR025 [26], the thermal bridge effect of the anchor can be neglected in the U-value calculation if the  $\chi$  is smaller than 0.5 mW/K, which is the case (0.31 mW/K). However, the point thermal bridging effect of the VIP edges is relevant and should be considered in the design values. Thus, the calculation of the U-value taking into account the total amount of anchors per  $m^2$  should be used.

### 3.4.3. Dynamic numerical modelling validation

In order to validate the numerical modelling under unsteady boundary conditions, the case studies were simulated and compared with the temperature behaviour of VIP panels during the experimental measurements. The dynamic numerical modelling validation is aimed at ensuring the accuracy of the software before carrying out the modelling of the ETICS walls thermal performance (which will be presented in section 3.5.5). For this purpose, Figure 3.11 and Figure

3.12 show the comparison between experimental measurements and numerical results, regarding the simpler case (case A) and a the more complex case (case F) respectively.

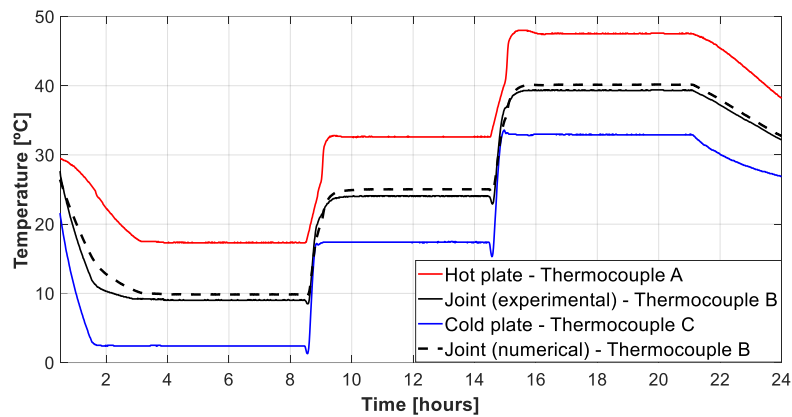


Figure 3.11: Temperature measurements during experimental and numerical approaches – case study A.

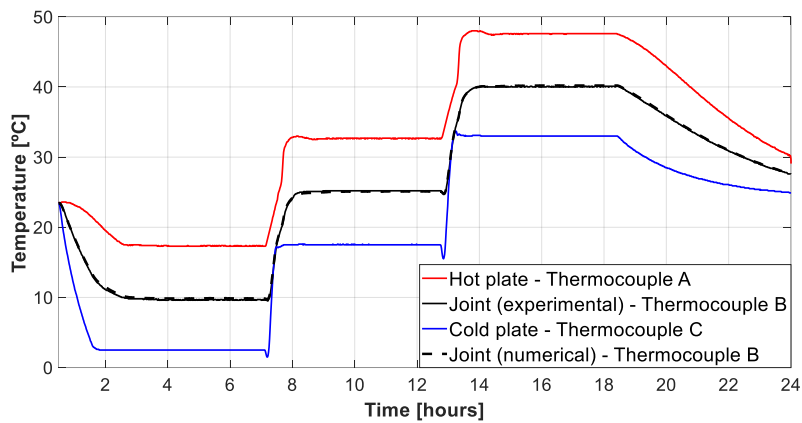


Figure 3.12: Temperature measurements during experimental and numerical approaches – case study F.

Numerical results for the central middle point (thermocouple B) of VIP joint shows there is a good agreement with the experimental measurements. As expected, the measurement at the joint sensor stabilizes at the levels corresponding to the average test temperature, namely 10°C, 25°C and 40°C. Thus, it can be concluded that the numerical models are reliable in terms of simulating the temperature behaviour in different ETICS walls (study presented in section 3.5.5).

### 3.5. VIP design for building application: a sensitivity analysis

In the previous sections it was demonstrated that the numerical modelling results showed very good agreement with the experimental measurements, both for steady-state and unsteady-state

conditions. For example, the comparison between the experimental measurement and the numerical calculation of the linear thermal transmittance of case F resulted in a maximum deviation of 4%. Hence, this section presents the results of a sensitivity analysis carried out (based on numerical simulations). This analysis included the variation of several properties of a VIP product designed for use in ETICS (case F), such as the thermal conductivity of the edge/cover material, the panel thickness, the air gap thickness between panels, as well as the VIP size. The reference values obtained in the numerical simulations are highlighted in each figure (triangular mark). Table 3.8 summarizes the parameters and the respective range of values analysed in the following subsections. Also, the thermal performance of ETICS walls with different support materials was assessed, which included the calculation of the U-value and the thermal delay of the walls. For this purpose, the linear and point thermal transmittance values were taken into account, as well as the thermal conductivity measured after ageing.

**Table 3.8:** Summary of the parameters and respective range of variation assessed in section 3.5.

Parameter	Range of values
Edge material thermal conductivity	20 to 40 mW/(m·K))
Air gap thickness between panels	0 to 2 mm
VIP thickness	10 to 60 mm
EPS Cover layer thickness	10 to 30 mm
EPS edge material width	5 to 25 mm
Panel size	200 x 200 mm to 1200 x 1200 mm

### 3.5.1. Edge material thermal conductivity

Figure 3.13 shows the influence of the thermal conductivity of the edge material on the linear thermal transmittance of the VIP joints. In encapsulated VIPs, which are used in ETICS applications (case F), the edge thermal bridging can be minimized by selecting a low conductivity edge material for use in the VIPs joints. For example, considering rigid polyurethane ( $\lambda = 25$  mW/(m·K)) instead of EPS ( $\lambda = 36$  mW/(m·K)) the thermal bridging could be decreased by around 30%.

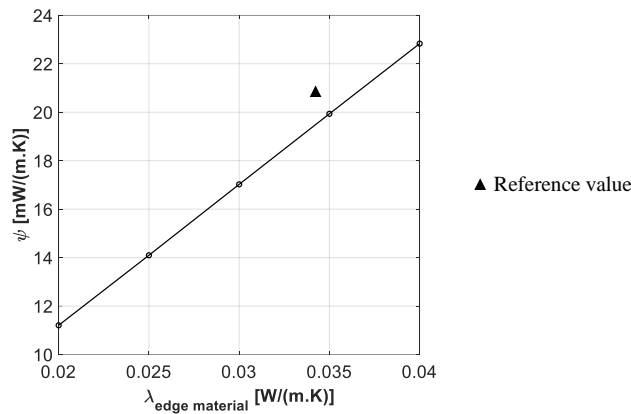


Figure 3.13: Linear thermal transmittance as function of the thermal conductivity of the edge material – case F.

### 3.5.2. Size of air gap between panels

An adequate installation is crucial for a good thermal performance of VIP. The existence of air gaps between panels will contribute to increasing the linear thermal transmittance, as shown in Figure 3.14, and consequently, negatively affecting the overall thermal performance of the VIP walls.

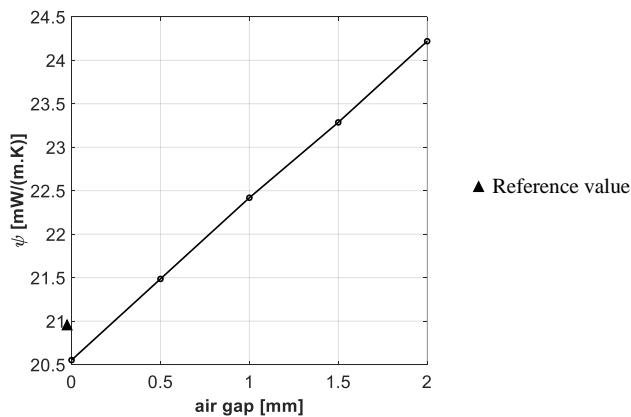
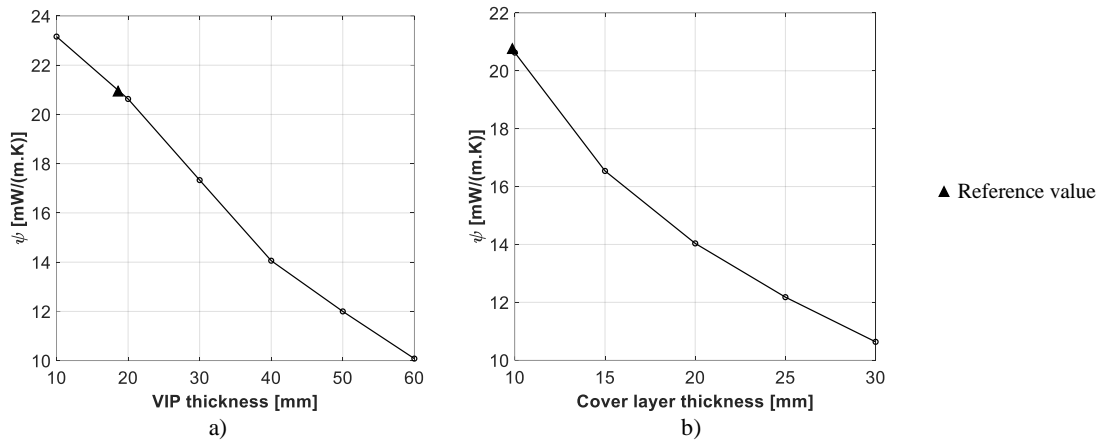


Figure 3.14: Linear thermal transmittance as function of the air joint thickness – case F.

### 3.5.3. Materials thickness

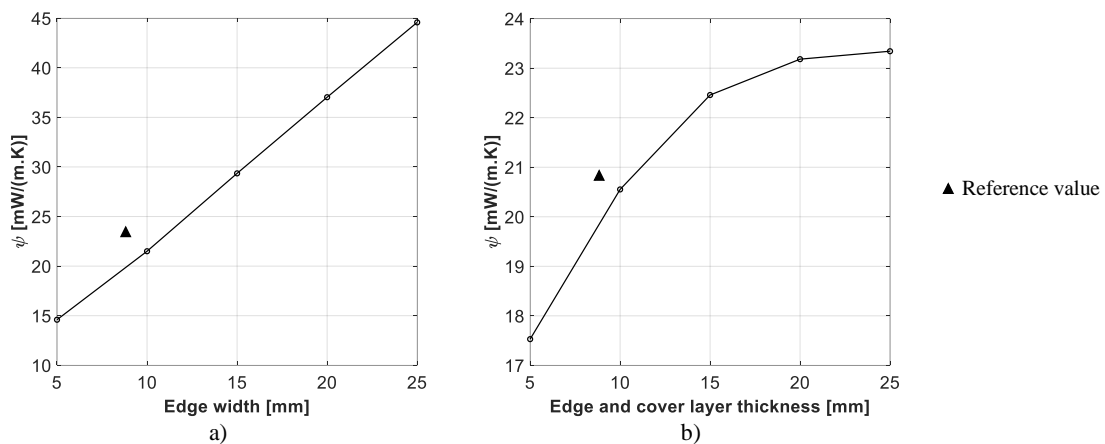
Figure 3.15 presents an analysis of the linear thermal transmittance variation with the VIP thickness (Figure 3.15a) and cover layer thickness (Figure 3.15b). In Figure 3.15a, a fixed cover

layer of 10 mm was selected, while in Figure 3.15b, a fixed VIP panel thickness of 20 mm was defined. Increasing VIP thickness leads to reduction of the edge thermal bridging effect. Also, increasing the thickness of the EPS cover layers reduces the linear thermal transmittance. This behaviour is explained due to the increase in edge material thermal resistance. However, excessive thickness of material could not be technical and economical feasible for VIP use in buildings.



**Figure 3.15:** Linear thermal transmittance as function of the panel thickness – case F: a) VIP thickness variation; b) cover layer thickness variation.

Figure 3.16 shows the influence of the edge material width on the linear transmittance of VIP panels, considering the VIP case F. In Figure 3.16a, a top and bottom cover layer is fixed with 10 mm and the edge material width is varied, while Figure 3.16b includes simultaneously both variation of edge width and cover layer thickness.



**Figure 3.16:** Linear thermal transmittance as function of the edge material width – case F: a) edge material width variation; b) edge and cover layer thickness variation.

Reducing the width of the edge material minimizes the impact of the linear thermal transmittance. However, small edges will not allow the installation of mechanical fixings. Furthermore, the edge material can be used to carry out small adjustments regarding panel size. As stated in Figure 3.15b, higher cover layer thickness leads to reduction of the edge thermal bridging effect. Combining this effect with the negative effect of the increase of edge width results in the curve

shown in Figure 3.16b. In this case, reducing the edge material width prevails over the effect of increasing the cover layer thickness.

### 3.5.4. Panel size and shape

The increment of the equivalent thermal conductivity of the VIPs due to the inclusion of edge thermal bridging effects is presented in Table 3.9 (as a function of the size of the panel). These values are based on the assumption that the vertical rims of the panels have seamless joints ( $\psi_{10} = 9.89 \text{ mW}/(\text{m}\cdot\text{K})$ ), while the horizontal rims are assembled with overlapping foils ( $\psi_{10} = 11.20 \text{ W}/(\text{m}\cdot\text{K})$ ).

**Table 3.9:** Percentual increment of the equivalent thermal conductivity of VIPs due to the edge effect - case F.

		<b>Horizontal rims (overlapping foils)</b>						
		<b>200</b>	<b>300</b>	<b>400</b>	<b>600</b>	<b>800</b>	<b>1000</b>	<b>1200</b>
<b>Vertical rims (seamless joints)</b>	<b>200</b>	114%	96%	87%	78%	74%	71%	69%
	<b>300</b>	94%	76%	67%	58%	54%	51%	49%
	<b>400</b>	84%	66%	<b>57%</b>	48%	44%	41%	39%
	<b>600</b>	74%	56%	47%	<b>38%</b>	33%	31%	29%
	<b>800</b>	68%	51%	42%	33%	28%	26%	24%
	<b>1000</b>	65%	48%	39%	30%	25%	23%	21%
	<b>1200</b>	63%	46%	37%	28%	23%	21%	19%

For the smallest sized panel (200 mm x 200 mm), the equivalent thermal conductivity increases 114% compared to the conductivity measured at the centre of the panel. As expected, using larger panels will reduce the influence of the edge thermal bridging. Also, the shape of the panels is relevant as the ratio between CoP area and VIP joints length may change. For example, considering the same panel area, a square shape of 400 mm x 400 mm has a lower equivalent thermal conductivity than a rectangular panel of 800 mm x 200 mm, since its ratio between CoP area and VIP joints length is higher.

### 3.5.5. Walls thermal performance and thermal delay

Table 3.10 shows the U-values of the walls with encapsulated VIP for panel dimensions 440 mm x 440 mm and 640 mm x 640 mm (real panel dimensions available – EPS edge with 20 mm width) considering the thermal conductivity of VIP at CoP (including 25 years ageing),  $U_{CoP_a}$ , and the edge thermal bridging effects,  $U_{\psi}$ . The effective U-value,  $U_{wall}$ , includes the linear and point thermal transmittance. The point thermal transmittance influence was calculated considering a number of mechanical fixings for each panel of 5 per square meter for smaller panels and 3 per square meter for larger panels. Additionally, the values considering a conventional insulation material (EPS) with 4 cm thickness (same as VIP solution) instead the VIP solution are presented in brackets for use as reference. Internal and external surface thermal resistances of 0.13 (m<sup>2</sup>·K)/W and 0.04 (m<sup>2</sup>·K)/W were considered.

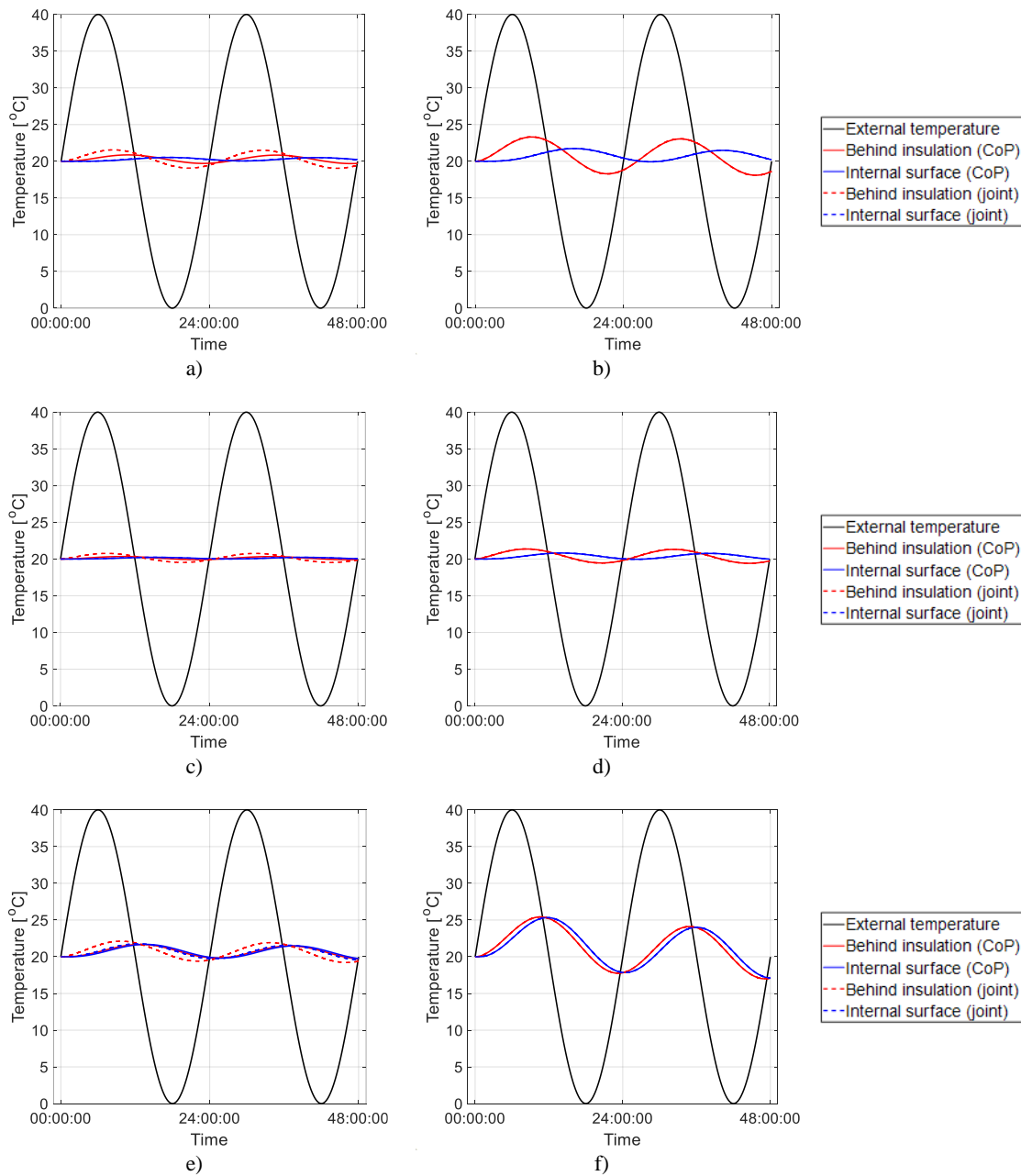
**Table 3.10:** Effective U-value of the VIP based ETICS walls and EPS ETICS wall (in brackets), expressed in W/(m<sup>2</sup>·K).

	Ceramic brick wall		Granite stone wall		Wood wall	
Panel size	440 mm x 440 mm	640 mm x 640 mm	440 mm x 440 mm	640 mm x 640 mm	440 mm x 440 mm	640 mm x 640 mm
$U_{CoP_a}$	0.235 (0.568)	0.206 (0.568)	0.256 (0.709)	0.222 (0.709)	0.254 (0.695)	0.221 (0.695)
$U_{\psi}$	0.286 (0.574)	0.244 (0.572)	0.304 (0.715)	0.258 (0.711)	0.302 (0.701)	0.257 (0.701)
$U_{wall}$	<b>0.311</b> (0.576)	<b>0.259</b> (0.573)	<b>0.328</b> (0.717)	<b>0.273</b> (0.714)	<b>0.327</b> (0.703)	<b>0.272</b> (0.700)

It can be seen that the edge thermal bridging effects highly increase the effective U-value of the wall. As expected, in smaller panels (440 mm x 440 mm) the thermal performance is strongly affected by linear thermal transmittance due to the lower ratio between CoP area and VIP joints (edge thermal bridging effect) length. The thermal bridging that occurs where several panel edges meet (point thermal transmittance) or as a result of mechanical fixations account for lower heat losses when compared with the thermal bridging between linear panels joints. Compared with  $U_{CoP_a}$ , the effective U-value of the VIP based ETICS walls (including linear and point thermal bridges) is 32.3% higher for smaller panels and 25.8% higher for larger panels, for the ceramic brick wall case.

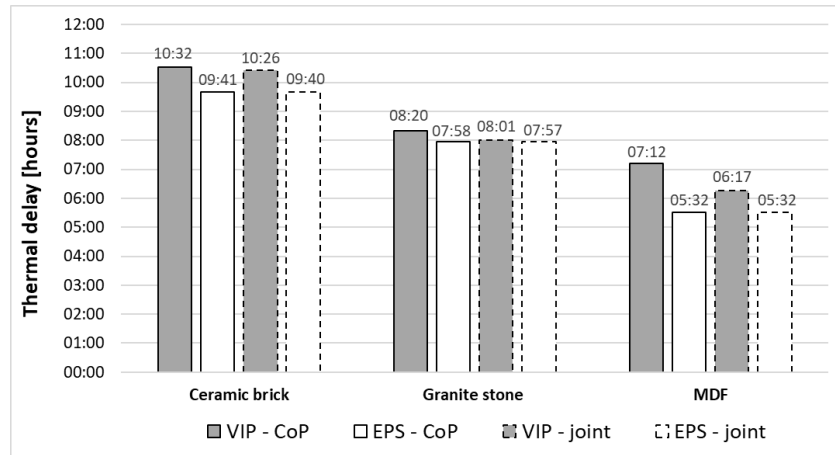
The thermal delay of ETICS walls was determined based on the graphs of Figure 3.17 which shows the temperature results of the numerical simulations (considering VIP size of 640 mm x 640 mm), including the external temperature condition and the temperature simulated behind insulation layer and at the internal surface of the wall, for both CoP and VIP joints areas. The thermal delay is given by the time difference between peaks in temperature. For comparison, the results for an EPS based ETICS wall are also presented.





**Figure 3.17:** Thermal delay determination for ETICS walls: a) ceramic brick wall with VIP based ETICS; b) ceramic brick wall with EPS based ETICS solution; c) stone wall with VIP based ETICS; d) stone wall with EPS based ETICS solution; e) wood wall with VIP based ETICS; f) wood wall with EPS based ETICS solution.

Figure 3.18 summarizes the thermal delay results for different support walls, including the results of the VIP based ETICS solution and a conventional EPS based ETICS solution.



**Figure 3.18:** Thermal delay in hours of VIP based ETICS and EPS ETICS walls, for the different support walls.

As expected, greater thermal delay was found in heavier walls, such as stone walls, while the lightweight wood wall revealed less thermal delay. However, the thermal conductivity of the support wall is also relevant for the results, as can be seen by comparing the ceramic brick wall with the granite stone wall. The thermal delay of VIP walls is around 22 to 100 minutes higher than EPS walls, considering the different support walls analysed. Also, the thermal damping of the VIP wall is higher (around 0.6 to 3.6°C) than that of EPS walls. The edge thermal bridging effect is also noticeable on the overall thermal performance of ETICS walls, as slightly lower thermal delay is found in these areas.

## 3.6. Discussion

Edge thermal bridging effects is one of the most critical issues of VIP technology for buildings applications. In this research work, an experimental and numerical investigation was carried out in order to study the impact of the edge thermal bridging effect in vacuum insulation panels suited for ETICS façades.

Experimental measurements showed a range of linear thermal transmittance between 7 to 38 mW/(m·K), depending on the VIP joint assembly. The results for VIP single layer joints (case A), which was the simplest case studied, is in line with other researchers' findings using analytical models for metalized barrier envelopes [4] – values around 10 mW/(m·K). Regarding the encapsulated VIPs which are intended to be used in ETICS, on the one hand, the use of the protective cover layers leads to a reduction of the edge thermal bridging effect. On the other hand, the use of edge material (case D and F) increases the linear thermal transmittance due to the higher thermal conductivity of the material. However, edge material is needed for using anchors without

perforating the VIP, and allow the installation of bonded ETICS with supplementary mechanical fixings, which is the most commonly used ETICS solution.

Numerical modelling results showed a good agreement with the experimental measurements for both steady and unsteady-state boundary conditions. The small differences observed could be related with the simplification of the models, namely regarding the perfect meeting of the different materials, the multilayer barrier envelope which was assumed as a single foil and the overlapping layer being considered as a single foil with twice the thickness. Air gaps between VIPs were assumed to be 0.5 mm in the numerical models. However, this value could easily increase in real construction works, which could greatly decrease the thermal performance of the VIP solutions.

Due to the very low thermal conductivity of the VIP CoP, thermal bridges have a high impact increasing the equivalent thermal conductivity in 10 to 60% (case A) and 19 to 114% (case F), depending of the panel size. These findings showed that using a correction factor of 1.1 on the thermal conductivity of VIPs measured at CoP (for panels higher than 400 mm x 300 mm), as suggested in European Assessment Document for VIP with cover layers [41], could be considered inaccurate when estimating the equivalent thermal conductivity of vacuum panels. A comparison with expanded polystyrene panels showed that the edge thermal bridging of this conventional insulation material is significantly lower than that of VIP products. Furthermore, the point thermal transmittance of VIPs designed for ETICS installation was found to be relevant, even without a plastic anchor fixing device.

Using larger panels (*e.g.* 1200 x 1000 mm) can reduce the edge thermal bridging effects on the equivalent thermal conductivity of VIPs. However, the use of larger panels may not be feasible due architectural constrains or even handling limitations (bigger panels are harder to handle both in the production stage and on the construction site). Commercial solutions with a size as large as 1000 x 600 mm [23] are available. Other effective ways to mitigate the influence of edge thermal bridges consists in reducing the thermal conductivity of the VIP edge material layers. Air gaps between panels should also be avoided.

Specific heat capacity measurements by means of indirect test method on GHP found similar values of fumed silica specific heat determined through differential scanning calorimeter, revealing a good accuracy of the method for non-homogeneous products, such as VIPs. The use of VIP instead of a conventional insulation material (EPS) in ETICS walls showed better response in terms of internal temperatures, namely lower temperature fluctuations, higher thermal delay and higher thermal damping. The effect of VIP is more noticeable on walls with lower thermal delay such as lightweight wooden walls or light steel framing.

It should also be noted that the VIP edge thermal bridging effects studied in this chapter may promote surface temperature variation along the surface of the façades. In order to assess the potential for the occurrence of anomalies, this issue should be further investigated by means of durability tests and/or long-term onsite monitoring, particularly, in the case of VIP based ETICS

walls, where the VIP are covered by a thin rendering system which is subjected to high temperature amplitudes. Also, the viability of purely bonded VIP ETICS solutions (without mechanical fixing devices) should be evaluated further. As shown, VIP assembly case E could be an interesting solution due to its lower linear thermal transmittance value.

### 3.7. Conclusions

The goal of the work presented in this chapter was to provide information to designers, developers and owners about the edge thermal bridging effects of vacuum insulation panels in building applications. For this purpose, experimental and numerical investigations were carried out considering different VIP joint assemblies. A detailed analysis was performed considering an encapsulated VIP solution designed for use in ETICS walls.

The results demonstrated that the thermal bridging effect between panel joints have a significant impact on the overall thermal performance of the walls. Although less relevant, the contribution of point thermal transmittance of the mechanical fixing devices is also noticeable. The size of the panels and the selection of the edge material are key-factors to be considered for minimizing linear thermal bridges in VIPs buildings applications. Furthermore, gaps between panels should be avoided by careful installation and by performing small adjustments to the edge materials, as needed. A balance between what is technically feasible (size, thickness, materials selection, cost-effectiveness) and the goal to maximize the thermal performance of VIPs should be achieved.

Numerical modelling simulations were successfully validated by comparison with the experimental measurements, which allowed for carrying out several sensitivity analyses without laboratorial testing (which is time consuming) and may contribute to the development of new solutions. The linear transmittance depends on a combination of factors, such as the thermal conductivity of the core material, barrier envelope and edge material, as well as the size and thickness of the panels. The results presented were obtained specifically for a fumed silica vacuum panel with a metallized high barrier film. Other VIP products could have different linear thermal transmittance values, as the ones demonstrated here through the sensitivity analysis. Also, the several VIP joint assemblies analysed showed a wide range of results.

Regarding the overall thermal performance of ETICS walls, the use of VIPs (considering the linear, point thermal transmittance values and ageing) allows to achieve a U-value which is around 46 to 61% lower than an EPS ETICS wall with the same insulation thickness, considering standard VIP sizes of 440 mm x 440 mm and 640 mm x 640 mm, respectively. VIP based ETICS walls

also showed high thermal delay when compared with a conventional ETICS wall, which contributes to increasing the thermal comfort of the occupants.

## References

- [1] International Energy Agency, “Long-Term Performance of Super-Insulating Materials in Building Components and Systems”, Report of Subtask I: State of the art and case studies, EBC Annex 65, U. Heinemann, ed., 2020.
- [2] M. Alam, H. Singh, M.C. Limbachiya, “Vacuum insulation panels (VIPs) for building construction industry - a review of the contemporary developments and future directions”, *Appl. Energy*. vol. 88, pp. 3592–3602, 2011, doi:10.1016/j.apenergy.2011.04.040.
- [3] I. Mandilaras, I. Atsonios, G. Zannis, M. Founti, “Thermal performance of a building envelope incorporating ETICS with vacuum insulation panels and EPS”, *Energy Build.* vol. 85, pp. 654–665, 2014, doi:10.1016/j.enbuild.2014.06.053.
- [4] M. Tenpierik, H. Cauberg, “Analytical models for calculating thermal bridge effects caused by thin high barrier envelopes around vacuum insulation panels”, *J. Build. Phys.* vol. 30, pp. 185–215, 2007, doi:10.1177/1744259107073160.
- [5] C. Sprengard, A. H. Holm, “Numerical examination of thermal bridging effects at the edges of vacuum-insulation-panels (VIP) in various constructions”, *Energy Build.* vol. 85, pp. 638–643, 2014, doi:10.1016/j.enbuild.2014.03.027.
- [6] A. Lorenzati, S. Fantucci, A. Capozzoli, M. Perino, “Experimental and numerical investigation of thermal bridging effects of jointed vacuum insulation panels”, *Energy Build.* vol. 111, pp. 164–175, 2016, doi:10.1016/j.enbuild.2015.11.026.
- [7] F. E. Boafu, J. G. Ahn, J. T. Kim, J. H. Kim, “Computing thermal bridge of VIP in building retrofits using DesignBuilder”, *Energy Procedia*, vol. 78, pp. 400–405, 2015, doi:10.1016/j.egypro.2015.11.683.
- [8] K. G. Wakili, T. Stahl, S. Brunner, “Effective thermal conductivity of a staggered double layer of vacuum insulation panels”, *Energy Build.* vol. 43, pp. 1241–1246, 2011 doi:10.1016/j.enbuild.2011.01.004.
- [9] A. Capozzoli, S. Fantucci, F. Favoino, M. Perino, “Vacuum insulation panels: Analysis of the thermal performance of both single panel and multilayer boards”, *Energies*, vol. 8, pp. 2528–2547, 2015, doi:10.3390/en8042528.
- [10] A. Lorenzati, S. Fantucci, A. Capozzoli, M. Perino, “The effect of different materials joint in Vacuum Insulation Panels”, *Energy Procedia*. vol. 62, pp. 374–381, 2014, doi:10.1016/j.egypro.2014.12.399.
- [11] L. Kubina, “ETICS with integrated vacuum insulation”, in *Proc. Int. Conf. Cent. Eur. Towar. Sustain. Build.*, Prague, 2010, pp. 2–5.

- [12] T. Nussbaumer, K. G. Wakili, C. Tanner, “Experimental and numerical investigation of the thermal performance of a protected vacuum-insulation system applied to a concrete wall”, *Appl. Energy*. vol. 83, pp. 841–855, 2006, doi:10.1016/j.apenergy.2005.08.004.
- [13] *Thermal insulation products for buildings - Factory-made vacuum insulation panels (VIP) - Specification*, EN 17140, European Committee for Standardization, 2020.
- [14] F. Isaia, S. Fantucci, A. Capozzoli, M. Perino, “Vacuum insulation panels: thermal bridging effects and energy performance in real building applications”, *Energy Procedia*, vol. 83, pp. 269–278, 2015, doi:10.1016/j.egypro.2015.12.181.
- [15] S. Verbeke, A. Audenaert, “Thermal inertia in buildings: A review of impacts across climate and building use”, *Renew. Sustain. Energy Rev.* vol. 82, pp. 2300–2318, 2018, doi:10.1016/j.rser.2017.08.083.
- [16] A. Tadeu, N. Simões, I. Simões, F. Pedro, L. Škerget, “In-situ thermal resistance evaluation of walls using an iterative dynamic model”, *Numer. Heat Transf. Part A Appl.* vol. 67, pp. 33–51, 2015, doi:10.1080/10407782.2014.901032.
- [17] I. Simões, N. Simões, A. Tadeu, “Thermal delay simulation in multilayer systems using analytical solutions”, *Energy Build.* vol. 49, pp. 631–639, 2012, doi:10.1016/j.enbuild.2012.03.005.
- [18] R. Ji, Z. Zhang, Y. He, J. Liu, S. Qu, “Simulating the effects of anchors on the thermal performance of building insulation systems”, *Energy Build.* vol. 140, pp. 501–507, 2017, doi:10.1016/j.enbuild.2016.12.036.
- [19] *Standard Test Method for Mean Specific Heat of Thermal Insulation*, C351-92b, ASTM International, 1999.
- [20] *Standard Test Method for Determining Specific Heat Capacity by Differential Scanning Calorimetry*, E1216-11, ASTM International, (2018).
- [21] *Advanced technical ceramics. Monolithic ceramics. Thermo-physical properties. Determination of specific heat capacity*, EN 821-3, European Committee for Standardization, 2005.
- [22] B. Marques, A. Tadeu, J. Almeida, J. António, J. de Brito, “Characterisation of sustainable building walls made from rice straw bales”, *J. Build. Eng.* vol. 28, 101041, doi:10.1016/j.job.2019.101041.
- [23] va-Q-tec, “Product Data Sheet – va-Q-vip F-EPS”, 2020.
- [24] *Thermal insulation - Determination of steady-state thermal resistance and related properties - Guarded hot plate apparatus*, ISO 8302, International Organization for Standardization, 1991.
- [25] *Thermal performance of building materials and products - Determination of thermal resistance by means of guarded hot plate and heat flow meter methods - Products of high and medium thermal resistance*, EN 12667, European Committee for Standardization, 2001.
- [26] *Point thermal transmittance of plastic anchors for ETICS*, TR 025, European Organisation for Technical Approvals, 2016.
- [27] *Thermal bridges in building construction - Heat flows and surface temperatures - Detailed calculations*, ISO 10211, International Organization for Standardization, 2017.

- [28] B. Marques, J. Almeida, A. Tadeu, J. António, M. I. Santos, J. de Brito, M. Oliveira, “Rice husk cement-based composites for acoustic barriers and thermal insulating layers”, *J. Build. Eng.* vol. 39, 102297, 2021, doi:10.1016/j.job.2021.102297.
- [29] *Standard Test Method for Determining Specific Heat Capacity by Differential Scanning Calorimetry*, E1269-01, ASTM International, 2011.
- [30] *BISCO - 2D steady state heat transfer*, (version 11.0w). Physibel. <http://www.physibel.be/v0n2bi.htm>.
- [31] *Thermal performance of windows, doors and shutters - Calculation of thermal transmittance - Part 2: Numerical method for frames*, EN ISO 10077-2, European Committee for Standardization, 2012.
- [32] *TRISCO - 3D steady state heat transfer* (version 14.0w). Physibel. <http://www.physibel.be/v0n2tr.htm>.
- [33] Secil Argamassas, “Product data sheet - ISOVIT REV FINO/MÉDIO” (in portuguese), 2020.
- [34] Secil Tek, “Product data sheet – ISOVIT FIBRA” (in portuguese), 2020.
- [35] C. Santos, L. Matias, “ITE 50 - Coeficientes de Transmissão Térmica de Elementos da Envolvente dos Edifícios” (in portuguese), LNEC, Lisboa, 2006.
- [36] Preceram Indústrias de Construção, S.A., “Product data sheet - Tijolo Cerâmico Tradicional”, 2016.
- [37] *BISTRA - 2D transient heat transfer*, (version 4.0w). Physibel. <http://www.physibel.be/bistra.htm>.
- [38] *Thermal performance of building materials and products - Determination of thermal resistance by means of guarded hot plate and heat flow meter methods - Dry and moist products of medium and low thermal resistance*, EN 12664, European Committee for Standardization, 2001.
- [39] The Engineering Toolbox, “Specific heat of solids”, [https://www.engineeringtoolbox.com/specific-heat-solids-d\\_154.html](https://www.engineeringtoolbox.com/specific-heat-solids-d_154.html) (accessed Mar. 17, 2019).
- [40] *Evaluation of measurement data – The role of measurement uncertainty in conformity assessment*, JCGM 106, Joint Committee for Guides in Metrology, 2014, doi:10.1515/ci.2013.35.2.22.
- [41] *European Assessment Document: Vacuum Insulation Panels (VIP) with factory applied protection layers*, EAD 040011-00-1201, European Organisation for Technical Approvals, 2017.





## **CHAPTER 4**

# **ONSITE MONITORING OF VIP BASED ETICS IN WARSAW: RETROFITTING OF A REAL BUILDING**



## **4. Onsite monitoring of VIP based ETICS in Warsaw: retrofitting of a real building**

### **4.1. Introduction**

As previously mentioned, the External Thermal Insulation Composite System (ETICS) is one of the most popular renovation solutions used to improve the thermal resistance of buildings façades. At a relatively low-cost, ETICS have been proven to be a great option [1], with expanded polystyrene (EPS) being the most used insulation material [2]. However, as European legislation [3] pushes insulation requirements to continue to increase, so does the thickness of ETICS solutions. Although this is required, it may not always be desirable or even technically or architecturally viable [4]. Hence, an ETICS solution that incorporates VIPs instead of EPS may present itself as great alternative, as it can significantly improve the thermal performance of the envelope without the need for thicker walls.

While the thermal properties of VIPs may promise a great potential for energy savings in buildings, critical issues such as the fragility of the VIP panels and the uncertainty about their long-term performance have made the widespread application of VIP building solutions difficult, as stated in chapter 2. For this reason, the industry and researchers need to focus on improving the applicability and durability of VIP building products. Regarding the evaluation and prediction of the long-term performance of VIPs, further research is still required [5], as a service life ranging from 10 to 50 years can be found in the literature, depending on the local conditions and the type of VIP technology used [6]. It is known that conserving initial low pressure and low humidity inside VIPs is essential to ensure high thermal resistance during their service life [7]. Nonetheless, other factors such as the barrier envelope properties or the size and thickness of panels can also strongly influence the VIPs service life [8].

Several studies have focused on external wall insulation applications with VIPs using rigid boards which are used to protect the panels, avoid accidental perforation and ensure watertightness. For example, Johansson *et al.* [9] evaluated the VIP performance of a retrofitted building façade

during 5 years. The constructive solution included 20 mm VIPs covered with 30 mm glass wool, an air space of 28 mm and 22 mm wooden board. The temperature and relative humidity measurements showed no sign of deterioration of the VIPs and low risk of condensation. Another study [10] based on onsite measurements and simulations which considered the same VIP constructive solution (with wooden cover boards) stated that, after the retrofitting, the VIP did not increase the moisture content in the wall. Ascione *et al.* [11] used numerical and experimental approaches to assess the VIP performance in a test room by integrating 10 mm VIP covered with 13 mm fibre cement panels and a 15 mm cement coat in a multi-layered wall. The results showed the effectiveness of the VIP solution for Mediterranean climate. However, using temperature and heat flux measurements De Masi *et al.* [12] found an increment of VIP thermal conductivity of 10.6% after 5 years monitoring in the test room.

In VIP based ETICS applications, the insulation is placed externally and a thin (4 to 7 mm) rendering system is used. This solution could impose higher thermal stresses onto the VIP panels. This was demonstrated by Yrieix *et al.* [13] by using analytical models and comparing internal and external VIP wall applications. In this study, VIP ETICS achieved higher degradation level due to external environmental agents. Furthermore, the high thermal resistance specific to vacuum technology, which is highly beneficial in terms of energy savings, is expected to be detrimental in terms of increasing the risk of the anomalies commonly associated with ETICS occurring, as stated in chapter 2. Greater thermal resistance means that the external surface temperature variations are higher. This stress on the thin ETICS rendering can potentiate cracking and ultimately allow for water penetration through the multi-layered coating system. Similarly, as the night-time surface temperatures are expected to be lower with VIPs when compared with conventional insulation material, there is greater risk of surface condensation and consequently, of the development of biological growth on the external surface. The biological growth risk assessment, through the surface condensation evaluation is further explored in chapter 5. Due to the mechanical fragility of the VIPs and the thin rendering system, this type of solution is also vulnerable to superficial mechanical damage, particularly to mechanical impact and perforation, which may result in loss of vacuum and thermal performance. Thus, accidental impacts or vandalism could contribute to reducing the long-term performance of the building façade. Another aspect that needs to be considered is the significant impact that the thermal bridging effect that occurs at the edges between vacuum panels could have on the thermal resistance of the whole walls and needs to be taken into account, as demonstrated in chapter 3, through experimental and numerical investigation.

As the number of real-life applications is still relatively reduced, only a few studies have reported on VIP based ETICS anomalies and long-term performance. Brunner *et al.* [14] studied the reasons for the deterioration of a VIP in an ETICS wall and concluded that a systematic failure in the VIP metallization process was the main cause. A building located in Germany was retrofitted with VIPs coated with an organically based render and even after the replacement of panels that

lost their vacuum, it was registered that one year later a set of panels had been punctured and lost their vacuum [15]. Mandiralas *et al.* [16] explored both experimental and numerical approaches and found a marked difference between the expected and the real performance of an ETICS solution with VIP, highlighting the deviations from VIP design values. The possible increase of the internal pressure of the VIPs and the strong dependence on linear thermal bridges and fasteners were identified as possible causes for the deviations. As the uncertainty about long-term performance affects the general acceptance of VIP solutions [17], studies evaluating the ageing effects are of major importance, particularly in more severe climates.

To evaluate the real thermal performance of ETICS façades, it is crucial to obtain reliable *in situ* thermal characterization rather than theoretical design values. However, the main challenge facing onsite measurements characterization is related with the outdoor climate conditions which are intrinsically dynamic [18]. In order to address this, some authors have proposed dynamic models to investigate the thermal performance of building walls under real exposure conditions with accuracy. Teni *et al.* [19] summarized current experimental approaches for *in situ* measurements, most of which use heat flow meters or infrared thermography. Some of these works following a temperature-based method, *i.e.*, without heat flow meters, show a maximum deviation of 44% between theoretical and measured U-values.

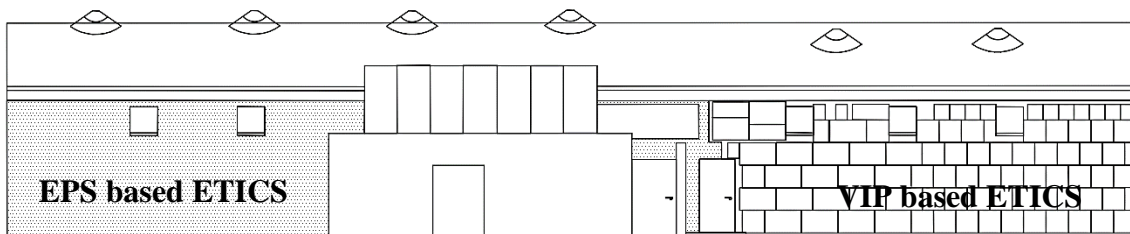
The work presented in this chapter aims to contribute to the evaluation of ETICS walls incorporating a VIP product by reporting the monitoring results of a retrofitted building located in Warsaw, Poland. The main goals set out for this work were: to analyse the hygrothermal behaviour of real onsite VIP based ETICS; to compare the VIP solution with one using a conventional insulation material (EPS); to identify potential anomalies in service conditions; to discuss the contribution of the VIP panels' edge effect; and to estimate the thermal transmittance of the retrofitted wall. Temperatures, relative humidity and heat fluxes were recorded for more than 24 months for both the VIP based ETICS and EPS based one (used as reference). In the VIP wall sensors were placed both at the centre of the panel (CoP) area and at the edges between panels (joint area).

## **4.2. Materials and methods**

In this section, first, the real onsite VIP based ETICS application case study is presented. Then, information on the local weather data and measurement settings is provided. Finally, the methods used to evaluate the hygrothermal performance of ETICS walls are described and a computational algorithm for U-value estimation is presented.

### 4.2.1. Case study

The case study is a façade which was partially renovated with a VIP based ETICS solution, and partially renovated with EPS based ETICS (to be used as a reference wall). The building is the Herpetarium of the Warsaw Zoo, in Poland, the interior of which requires specific temperature and humidity conditions. Throughout the year, the internal set-point temperature is mainly kept constant at around  $28 \pm 3^\circ\text{C}$ . The façade under study has a northeast orientation. Figure 4.1 shows a schematic drawing of the front view of the façade. On the right is the part of the wall that was retrofitted with a VIP based ETICS solution and on the left is the part of the wall which was retrofitted using a conventional ETICS system with EPS and which will be used as a reference.



**Figure 4.1:** Schematic drawing of the case study façades, including EPS reference wall and VIP layout pattern.

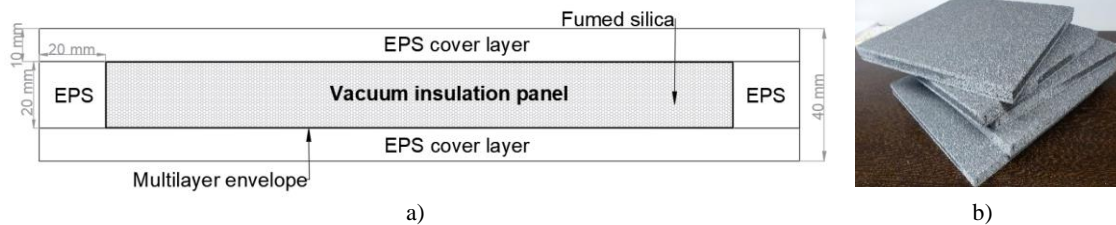
In the VIP wall, different sized panels were arranged in a way so as to maximize the area covered by VIPs, including panels with 440 mm x 440 mm; 440 mm x 340 mm; 640 mm x 440 mm; 640 mm x 640 mm; 1040 mm x 440 mm; and 1040 mm x 640 mm. In the final layout the VIP solution covers 87% of the VIP wall area, while EPS was used to fill out the remaining 13% where it could not be applied (due the VIP size and shape limitations). A photo taken after the renovation was finished is presented in Figure 4.2.



**Figure 4.2:** Photograph after renovation of the case study façades, including EPS and VIP based ETICS.

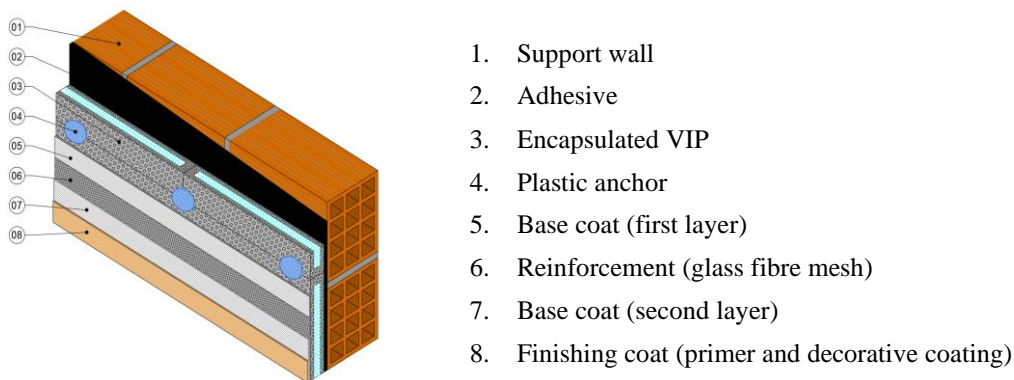
The VIPs used are 20 mm fumed silica panels with a bi-laminate structure with a thin EVOH (ethylene-vinyl alcohol copolymer) envelope. The VIP product, as shown in Figure 4.3, is covered with a protective layer made of graphite EPS with a thickness of 10 mm on each side and 20 mm along the edges. The super-insulating material, referred to as “encapsulated VIP”, has a total thickness of 40 mm. The EPS layer allows for the adhesive bonding of the panels and provides

additional mechanical resistance, minimizing the risk of perforation of the VIPs. The 20 mm of EPS at the edges of the panels also allow for the use of plastic anchors (auxiliary fixing of the panels).



**Figure 4.3:** Encapsulated VIP solution: a) schematic cross-section; b) photography.

The retrofitting of the VIP wall side consisted in the application of around 42 m<sup>2</sup> of a VIP based ETICS solution fixed with suitable adhesive, reinforced with plastic anchors at the EPS-edges of the panels and coated with a 7 mm rendering system. The rendering is made up by a base coat mortar reinforced with a 160 g/m<sup>2</sup> fibre glass mesh, a key-coat and an acrylic finishing coat which contributes to the protection against weathering and provides a decorative finish. Figure 4.4 shows a schematic representation of the layers of the VIP based ETICS wall.



**Figure 4.4:** Representation of VIP ETICS wall layers.

Figure 4.5 shows the installation of the encapsulated VIPs on the façade. To minimize the risk of cracks occurring along the edges, the VIPs are placed in such a way as to avoid superimposed vertical joints. At the joints, any remaining air space between panels was filled with PU foam. Regarding the reference wall (with around 82 m<sup>2</sup>), a similar ETICS solution was applied, where EPS panels with the same thickness (40 mm) were used instead of VIPs. Unlike the conventional ETICS, where the mechanical fixings are placed at the edge and in the centre of the insulation panels, in the case of VIP based ETICS this is not possible. Thus, the plastic anchors were placed only on the corner of each panel, perforating the EPS edge material and assuring around 4 anchors per square meter. The number of mechanical fixing devices used were a little lower than the number suggested by manufactures of ETICS solutions [20] (around 6 to 8 anchors per square meter).



**Figure 4.5:** Installation of VIP based ETICS: a) encapsulated panels with mechanical fixings at the corners; b) reinforced base coat mortar application.

Table 4.1 lists the materials found in the existing wall (two hollow brick layers with EPS in the cavity wall), as well as the ones used during the retrofitting works. The thermophysical properties of the existing materials were obtained using information collected onsite and from technical literature [21]. ETICS properties were obtained from technical data sheets, while the thermal conductivity of the insulation material was obtained in a laboratory using the guarded hot plate method according to EN 12667 [22]. The average thermal conductivity of encapsulated VIP centre of the panel was measured (at 10°C) in 3 different panels, resulting in an average thermal conductivity of 7.5 mW/(m·K).

**Table 4.1:** Thermophysical properties of each wall material.

External wall cross section	Wall parts	Materials	d <sup>(1)</sup> [mm]	λ <sup>(2)</sup> [W/(m·K)]	
	Existing wall <sup>(3)</sup>	Plaster	25	1.0	
		Masonry brick	230	0.77	
		Plaster	25	1.0	
		EPS	100	0.04	
		Masonry brick	120	0.77	
		External render	25	1.0	
	ETICS retrofitting <sup>(4)</sup>	Insulation material	Adhesive	10	0.47
			Encapsulated VIP	40	0.0075
			EPS <sup>(5)</sup>	40	0.0320
			Base coat	5	0.47
	Finishing coat	2	0.40		

<sup>(1)</sup> Thickness;

<sup>(2)</sup> Thermal conductivity;

<sup>(3)</sup> Estimated properties according construction company information and technical data sheets;

<sup>(4)</sup> Properties of ETICS solution, according technical data sheets and guarded hot plate apparatus λ-Meter EP500e measurements at centre of panel at 10°C;

<sup>(5)</sup> Graphite expanded polystyrene insulation panels used in the reference wall.



## 4.2.2. Weather data

Warsaw climate is classified as temperate oceanic climate Cfb under Köppen-Geiger ([23,24]). According to historical data, the mean annual precipitation is 515 mm (93 rainy days per year) and the mean annual sunshine hours are 1589 [25].

Figure 4.6 shows the mean monthly air temperature (maximum, minimum and average), as well as mean air relative humidity, obtained for the year of 2019. It is based on onsite data monitoring results obtained from sensors located in the proximity of the building façade. June was the hottest month, when the mean monthly minimum temperature was 19°C. The maximum daily temperature amplitude found (around 14.1°C) occurred during May and a minimum daily temperature amplitude of around 1°C was found in the winter months, namely in January and December.

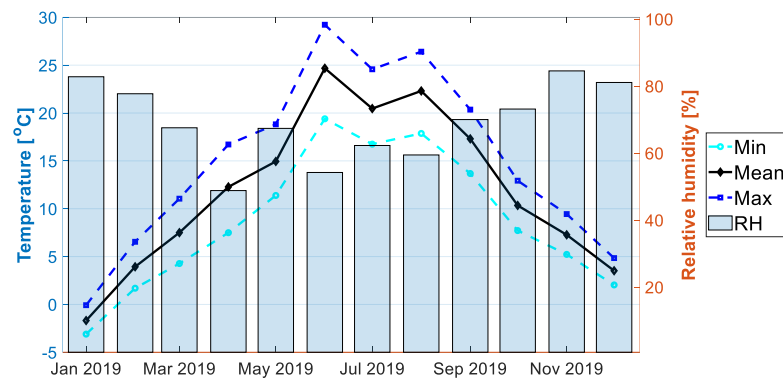
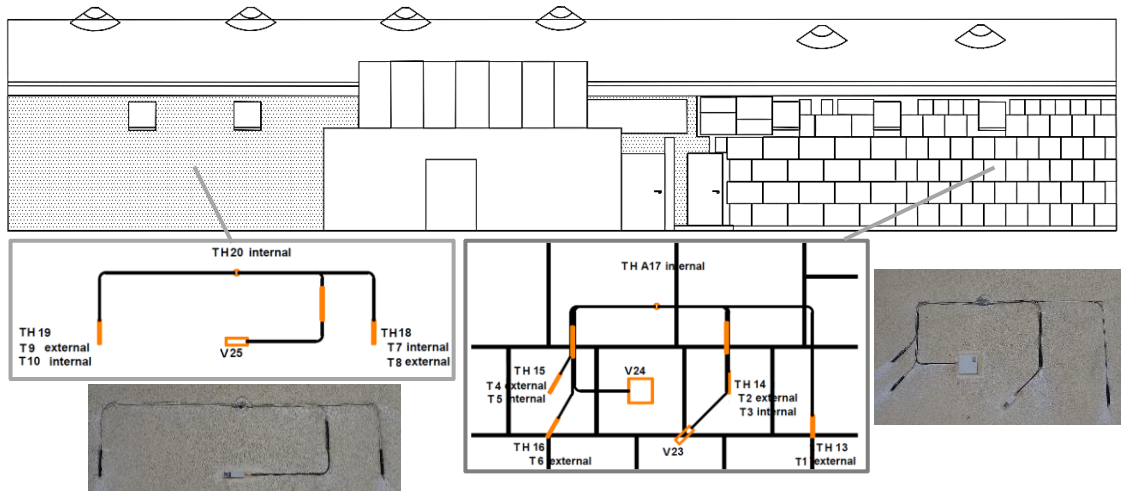


Figure 4.6: Mean monthly weather data monitoring in 2019.

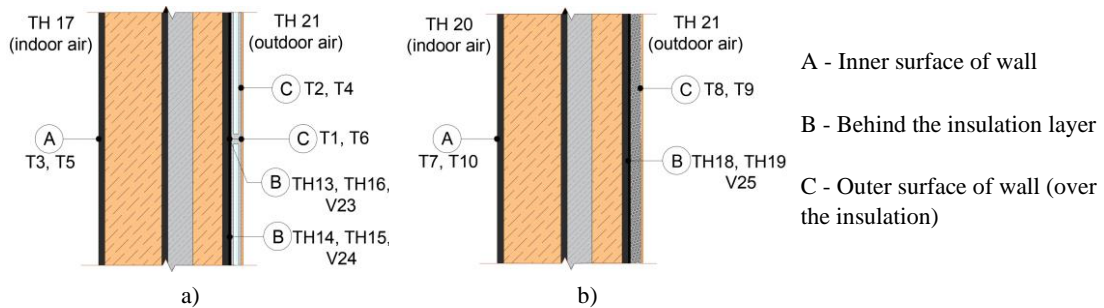
## 4.2.3. Measurement settings

The building façade was monitored for a 24-month period starting in October 2018. Sensors measuring temperature (T), temperature/relative humidity (TH) and heat flux (V) were applied in the two different areas of the external wall under renovation, meaning the VIP side and the reference wall side. For measuring temperature and relative humidity, sensors (45 mm of length and 5 mm diameter) with an accuracy of  $\pm (0.1+0.17\%)^{\circ}\text{C}$  and  $\pm 3\%$  RH were used. Regarding heat flux, sensors with an accuracy of 5% at 25°C were installed, namely the models FQA017C (meander size of 80 mm x 20 mm) and FQA018C (meander size of 90 mm x 90 mm) by ALMEMO. Figure 4.7 gives the location of the sensors.



**Figure 4.7:** Schematic representation and photograph of the location of the sensors in the walls.

Sensors were placed along several interfaces of the walls, namely (from inner to outer surfaces): on the inner wall surface – surface A; behind the insulation (between the existing wall surface and the insulation layer – interface B); and over the insulation (between the insulation layer and the final rendering system – interface C). A schematic representation of the placement of the sensors is given in Figure 4.8a for the VIP wall and in Figure 4.8b for the EPS reference wall. On the VIP wall side, in order to understand the thermal bridging effects that may occur along the edges of the VIP panels, some sensors were positioned at the centre of the panels (CoP) and others at the joints between panels, as can be seen in Figure 4.8.



**Figure 4.8:** Schematic cross-section of the building walls and placement of temperature (T), temperature/humidity (TH) and heat flux (V) sensors: a) VIP wall; b) reference wall.

Additionally, two sensors were placed inside the building to measure indoor air temperature and relative humidity, and one sensor was placed outside the building to measure outdoor air temperature and relative humidity. For this purpose, Temp/RH Data Logger model HOBO U12-012 with accuracy of temperature  $\pm 0.35^{\circ}\text{C}$  (between  $20^{\circ}\text{C}$  to  $70^{\circ}\text{C}$ ) and  $\pm 2.5\%$  (between 5% to 95% RH). All sensors were connected to a data logger programmed to record every 5 minutes, namely an Agilent 34972A. Table 4.2 summarizes each sensor's location in terms of wall area and its placement (inside the wall) according to its reference.

**Table 4.2:** References and locations of the sensors.

Wall area	Indoor air	Inner surface (A)	Behind insulation (B)	Over insulation (C)	Outdoor air
Reference wall	TH20	T7, T10	TH 18, TH 19, V25	T8, T9	
VIP wall	Joint		TH 13, TH 16, V23	T1, T6	TH21
	CoP	TH17	T3, T5	TH 14, TH 15, V24	T2, T4

T1 to T10 are temperature sensors;  
TH 13 to TH 21 are temperature and humidity sensors;  
V23 to V25 are heat flux sensors.

## 4.2.4. Hygrothermal parameters

The temperature and relative humidity sensors described in the previous sub-section were used to evaluate the hygrothermal behaviour of the ETICS façades. Furthermore, these measurements allowed for the evaluation of surface condensation risk via dew point calculation. Risk of condensation occurs when the surface temperature is lower than the dew point. For this purpose, the dew point temperature was estimated according to the Magnus formula [26], which relates the saturation vapour pressure and the dew point. At a temperature,  $T$ , in °C, the saturation vapour pressure,  $P_{ws}$ , expressed in hPa over liquid water is given by equation 4.1:

$$P_{ws} = a \cdot e^{\left(\frac{b \cdot T}{c+T}\right)} \quad [\text{hPa}] \quad (4.1)$$

Where Magnus parameters  $a, b, c$  are 6.11 hPa, 17.62 and 243.12°C, respectively (for the range -45°C to 60°C) [26]. Considering the definition of air relative humidity  $RH$  in %, the vapour pressure,  $P_w$ , is obtained by equation 4.2:

$$P_w = \frac{RH}{100} \cdot P_{ws} \quad [\text{hPa}] \quad (4.2)$$

Restating equation 4.1, the dew-point temperature,  $T_{dp}$ , in °C can be expressed from the vapour pressure  $P_w$ :

$$T_{dp} = \frac{c \cdot \ln\left(\frac{P_w}{a}\right)}{b - \ln\left(\frac{P_w}{a}\right)} \quad [^\circ\text{C}] \quad (4.3)$$

By inserting equation 4.2 into equation 4.3, and by using equation 4.1 the calculation of dew-point temperature,  $T_{dp}$ , from temperature  $T$  and relative humidity  $RH$  is:

$$T_{dp}(T, RH) = \frac{c \cdot \left(\ln\left(\frac{RH}{100}\right) + \frac{b \cdot T}{c+T}\right)}{b - \left(\ln\left(\frac{RH}{100}\right) + \frac{b \cdot T}{c+T}\right)} \quad [^\circ\text{C}] \quad (4.4)$$

Based on air relative humidity and temperature measurements, the absolute humidity can also be obtained. Absolute humidity,  $H$ , was calculated according to equation 4.5 in order to allow a direct comparison between solutions, avoiding the influence of different air temperatures between walls.

$$H = C \cdot \frac{P_w}{c + T} \quad [\text{g/m}^3] \quad (4.5)$$

Where  $C$  is a constant 2.17 gK/J,  $T$  is the surface temperature in °C and  $P_w$ , in Pa, is the vapour pressure resulting from equation 4.2 and 4.3.

## 4.2.5. U-value estimation

The estimation of the thermal transmittance, given by the U-value, was carried out following two approaches: (1) using experimental heat flux and temperature measurements following the international standard ISO 9869-1 [27]; and (2) using a numerical algorithm based on temperature measurements. The results were compared with the theoretically calculated U-value according to ISO 6946 [28]. For this purpose, the properties presented in Table 4.1 and the external and internal surface thermal resistance equal to 0.04 (m<sup>2</sup>·K)/W and 0.13 (m<sup>2</sup>·K)/W, respectively, were used.

### 4.2.5.1. Experimental determination

The thermal transmittance estimation of ETICS walls was carried out based on the heat flow meter method defined in ISO 9869-1 [27]. This method allows the measurement of the thermal transmission properties of plane building components, consisting of opaque layers perpendicular to the heat flow. For analysis of the data collected onsite, the average method was used. This method assumes that the thermal transmittance,  $U$ , can be obtained by dividing the mean density of heat flow rate,  $q$ , expressed in W/m<sup>2</sup>, by the mean temperature difference between interior,  $T_{ij}$ , and exterior,  $T_{ej}$ , environmental temperature, expressed in °C. The average values were taken over one month of monitoring. Considering that the index  $j$  related to individual measurements, the thermal transmittance obtained from experimental measurements is achieved by using equation 4.6:

$$U = \sum_{j=1}^n q_j \cdot \left[ \sum_{j=1}^n (T_{ij} - T_{ej}) \right]^{-1} \quad [\text{W}/(\text{m}^2 \cdot \text{K})] \quad (4.6)$$

### 4.2.5.2. Computational algorithm calculation

A temperature-based method developed by FIW Munich (Research Institute for Thermal Insulation) was used to assess the thermal performance of existing walls after they have been renovated. With this algorithm, it is possible to assess the U-value of the existing wall and the retrofitted wall without prior testing or without knowing the composition in terms of thickness and thermal properties of the layers. This means that it is possible to obtain the thermal transmittance of both new and existing walls, by carrying out temperature measurements after retrofitting. The input parameters for the algorithm are the following:

- $\lambda_{10,\text{ins}}$  - thermal conductivity of the new insulation material at 10°C mean temperature (in W/(m·K));
- $K_{\lambda,\text{ins}}$  - thermal conductivity variation function of temperature (in W/(m·K<sup>2</sup>));
- $d_{\text{ins}}$  - thickness of the new insulation layer (in m);
- $R_{\text{si}}$  and  $R_{\text{se}}$  - interior and exterior surface thermal resistance for horizontal heat flux according ISO 6946 [28], namely 0.13 (m<sup>2</sup>·K)/W and 0.04 (m<sup>2</sup>·K)/W;
- $T_{\text{si}}$  - inner surface temperature (layer surface A in Figure 4.8);
- $T_{\text{m}}$  - temperature in the interface between the new insulation and the existing wall (interface B in Figure 4.8);
- $T_{\text{se}}$  - outer surface temperature (interface C in Figure 4.8).

The monitoring period needs to be long enough so as to make a steady-state estimation of the thermal transmittance possible. Each measurement needs to be performed in time steps of one hour or less. The U-values are updated continuously at each time step over the entire monitoring period. Therefore, the result becomes more accurate over time as periodically changing transient influences are continuously eliminated.

With the above-mentioned input parameters - the material properties (fixed values) and the temperature data (time series) - the calculation is performed for each time step  $n$ . The calculation of the mean temperature (in °C),  $T_{\text{mean}}$ , includes the current time step  $n$  and all previous time steps for the three temperatures  $T_{\text{se}}$ ,  $T_{\text{m}}$  and  $T_{\text{si}}$ , according equation 4.7:

$$T_{mean} = \frac{1}{n} \sum_1^n T_n \quad [^{\circ}\text{C}] \quad (4.7)$$

Next is the calculation of the thermal conductivity,  $\lambda_{ins,mean}$ , and heat flux density ( $\text{W}/\text{m}^2$ ),  $q$ , of the current time step, according equation 4.8 and 4.9, respectively.

$$\lambda_{ins,mean} = \lambda_{10,ins} + (0.5 \cdot (T_{se,mean} + T_{m,mean}) - 10^{\circ}\text{C}) \cdot K_{\lambda,ins} \quad [\text{W}/(\text{m} \cdot \text{K})] \quad (4.8)$$

$$q = (\lambda_{ins,mean} \cdot (T_{se,mean} + T_{m,mean})) \cdot d_{ins}^{-1} \quad [\text{W}/\text{m}^2] \quad (4.9)$$

With

$$T_{e,mean} = T_{se,mean} - q \cdot R_{se} \quad [^{\circ}\text{C}] \quad (4.10)$$

$$T_{i,mean} = T_{si,mean} - q \cdot R_{si} \quad [^{\circ}\text{C}] \quad (4.11)$$

Finally, the thermal resistance of the existing wall (in  $(\text{m}^2 \cdot \text{K})/\text{W}$ ),  $R_w$ , before the renovation (without ETICS) is obtained by:

$$R_w = \frac{T_{m,mean} - T_{i,mean}}{q_{mean}} \quad [(\text{m}^2 \cdot \text{K})/\text{W}] \quad (4.12)$$

Thus, the thermal transmittance coefficient (in  $\text{W}/(\text{m}^2 \cdot \text{K})$ ) of both existing and retrofitted walls are respectively obtained using equation 4.13 and 4.14:

$$U_{old} = (R_{si} + R_{se} + R_w)^{-1} \quad [\text{W}/(\text{m}^2 \cdot \text{K})] \quad (4.13)$$

$$U_{new} = \left( R_{si} + R_{se} + R_w + \frac{d_{ins}}{\lambda_{ins,mean}} \right)^{-1} \quad [\text{W}/(\text{m}^2 \cdot \text{K})] \quad (4.14)$$

## 4.2.6. Infrared thermography

In order to assess the integrity of the VIP panels over time, namely for loss of vacuum, as well as to identify possible rendering anomalies (detachments, cracking, among others) and evaluate wall surface temperatures, an extensive passive thermographic inspection was carried out, based on the infrared method proposed in ISO 6781 [29]. For this purpose, an infrared thermographic camera (FLIR i50), with resolution of 140 x 140 pixels, accuracy  $<0.1^{\circ}\text{C}$  at  $25^{\circ}\text{C}$  and object temperature range of  $20^{\circ}\text{C}$  to  $350^{\circ}\text{C}$ , was used to record thermographic images. This device is able to capture the infrared radiation emitted by any object and, using the Stefan–Boltzmann law,

produce images containing surface temperature patterns. Thermograms were taken periodically (about twice a month) in the early afternoon at a distance from the wall of approximately 7 m (field of view is 2.5 m x 2.5 m). A default emissivity of 0.9 was considered for both wall surfaces [30].

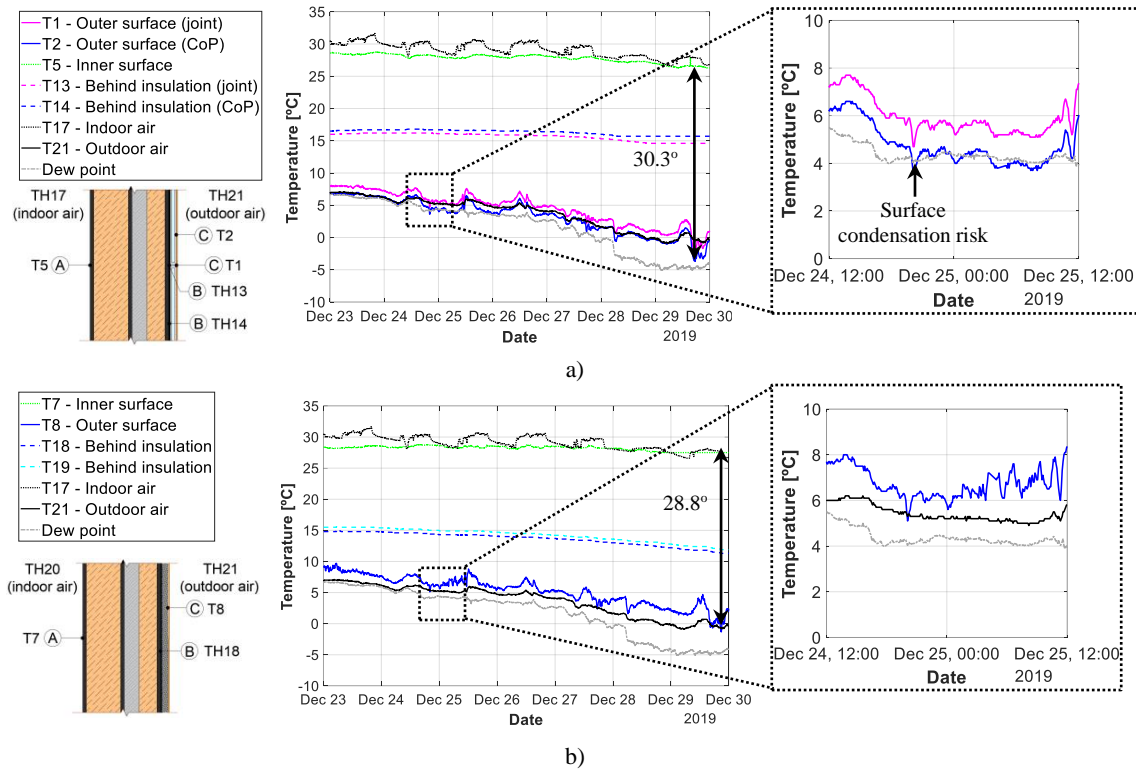
Additionally, a high-resolution camera was used to validate the thermograms recorded with the lower resolution camera. For this purpose, a FLIR T630sc with a resolution of 640 x 480 pixels, accuracy  $\pm 1^{\circ}\text{C}$  or  $\pm 1\%$  at  $25^{\circ}\text{C}$  and object temperature range  $-40$  to  $150^{\circ}\text{C}$ , was used. These thermograms were also used to check the monitoring conditions.

### **4.3. Results and discussion**

This section presents the main results obtained from the onsite monitoring campaign. The results shown have been selected to represent the behaviour of the walls during a typical week in winter (cold season) and a typical week in summer (warm season).

#### **4.3.1. Temperature analysis - cold season**

Figure 4.9 shows temperatures monitored along several layers of the VIP wall (Figure 4.9a) and the reference wall with EPS (Figure 4.9b) from 23<sup>rd</sup> to 30<sup>th</sup> December 2019. The dew point curve can also be observed in both figures. The weather conditions during this week were cloudy and rainy, with an average temperature of  $3.6^{\circ}\text{C}$ , a maximum of  $7.1^{\circ}\text{C}$  and a minimum of  $-0.9^{\circ}\text{C}$ .



**Figure 4.9:** Temperatures during a representative week in the cold season: a) VIP wall with daily detail; b) reference wall with daily detail.

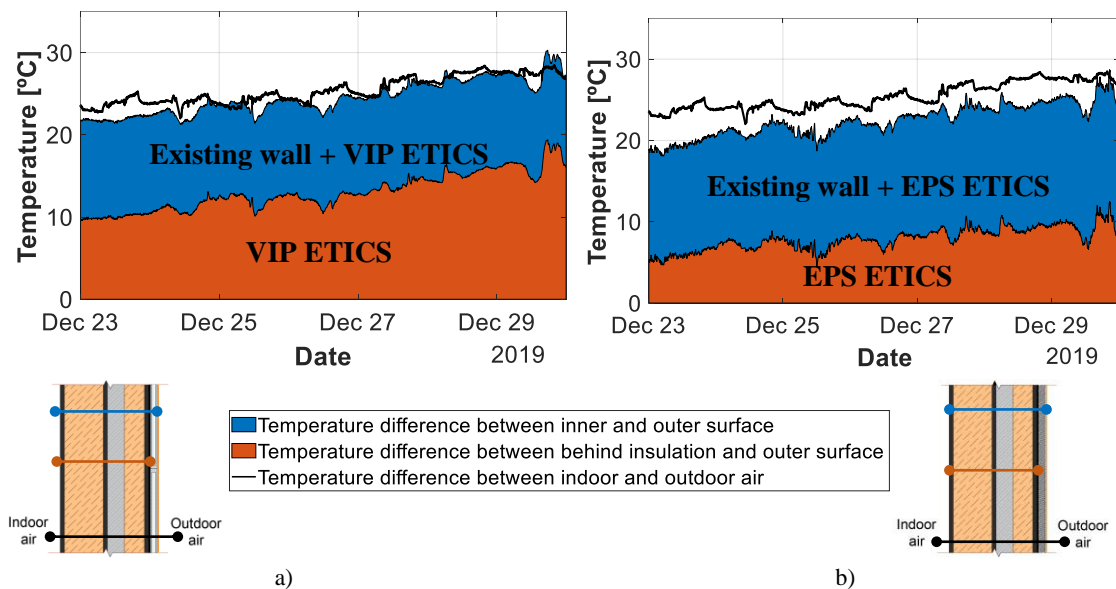
In both ETICS walls (VIP and reference), the daily amplitude in outer surface temperature is higher than the amplitude in outdoor air temperature. Due to radiation, the surfaces of externally insulated walls reach higher and lower temperatures than the outdoor air. When comparing both walls, a higher outer-inner surface temperature gradient is found for the VIP wall, which is to be expected given the higher insulation level. The reference wall outer surface temperatures are higher than the temperatures of the VIP wall. For example, for the same night period (December 29),  $-3.7^{\circ}\text{C}$  was recorded at the VIP CoP surface and  $-0.7^{\circ}\text{C}$  at the EPS surface. These measurements can be justified by higher heat losses of the building in the reference wall. This phenomenon is also visible in the temperatures measured behind the insulation layer, where both joint and CoP VIP area temperatures are slightly higher than for the EPS wall, confirming the high level of insulation provided by VIP.

Regarding the risk of condensation, which occurs when the surface temperature is lower than the dew point, the reference wall did not present risk of condensation during the depicted period, while the VIP wall showed some night periods with external surface condensation, mainly in the CoP area. These lower temperatures are due to the radiative heat loss to the atmosphere and lower heat transfer from the inside, due to the higher level of insulation in the VIP wall, particularly in the CoP area. Temperature below dew point at CoP may result in higher biological growth risk when compared with the VIP edges. Over time, this could ultimately lead to an undesirable squared-pattern to appear on the façade.



Figure 4.9 is also used to highlight the differences between the centre of panel (CoP) and the edge joints area in terms of surface temperatures. Most of the time, the outer surface temperatures are higher along the edges (around 1°C difference). It can be clearly observed that the temperature along the joints (pink line) is higher than the outdoor air temperature (black line), while the CoP (blue line) presents long periods with lower temperatures.

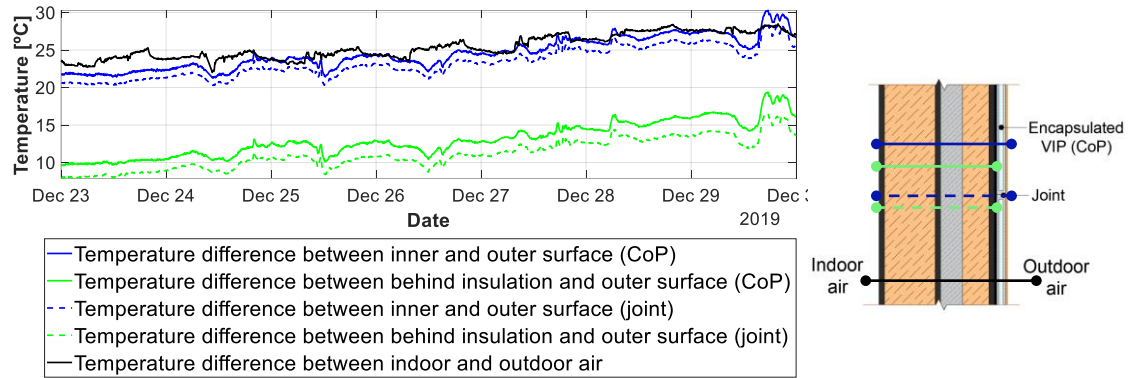
For the same week, Figure 4.10 shows the difference in temperature between inner and outer surface and between the interface located behind the insulation and the outer surface (ETICS solution). The average temperature difference between indoor and outdoor air is 25.1°C. The contribution of the VIP based ETICS solution is around 50%, while the EPS based ETICS solution only has an impact of 30% on temperature reduction (considering the average temperatures presented in Figure 4.10). These results highlight again the higher insulation level provided by the VIP panels.



**Figure 4.10:** Temperature differences between layers during a cold season period: a) VIP wall; b) reference wall.

It should be noted that the temperature difference between inner and outer surface is not only due to the VIP thermal resistance, but also due to the thermal resistance of the pre-existing wall (which includes 100 mm of EPS in the wall cavity).

Figure 4.11 also shows curves of temperature differences, now comparing results obtained at the centre of the VIP panel (CoP) and at the edge of the panels (joint area).

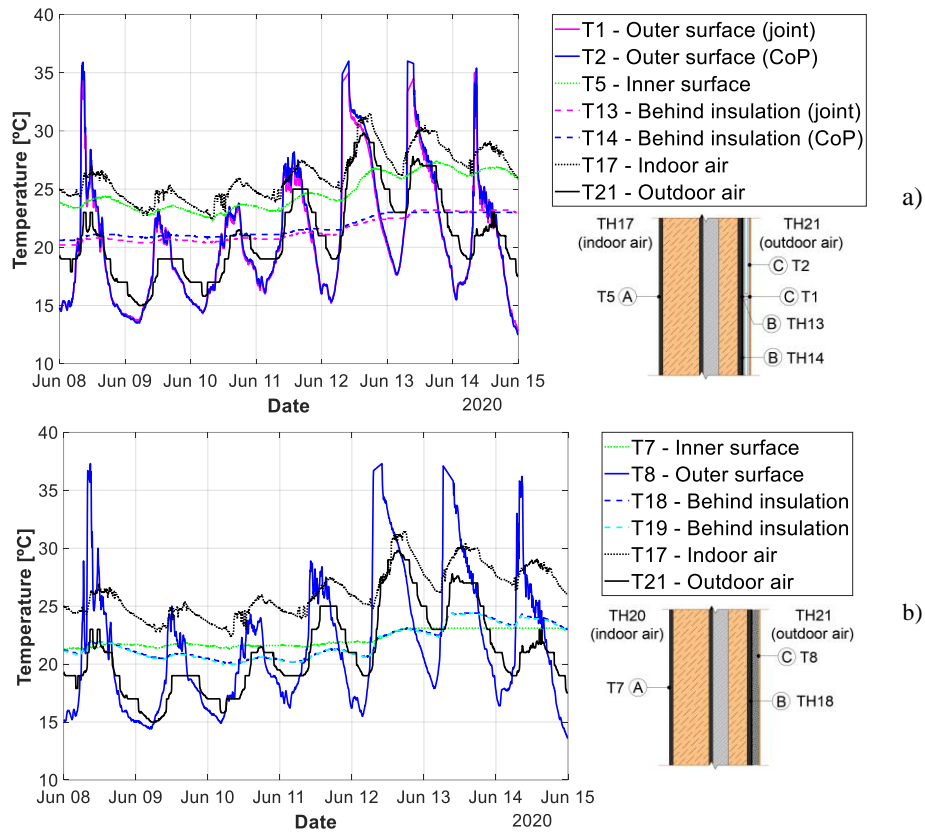


**Figure 4.11:** Temperature differences for VIP based ETICS wall in cold season period – CoP vs joint comparison.

The difference between edge and CoP is noticeable. For both temperature differences (“between inner and outer surface” and “between behind insulation and outer surface”) there is a clear drop in the case of the edge joint area. It can be observed that the edge effect is slightly more noticeable in the temperature difference between behind insulation and outer surface (maximum 2.4°C), when compared with the temperature difference between inner and outer surface (maximum 1.2°C).

### 4.3.2. Temperature analysis - warm season

Figure 4.12 shows the temperatures monitored along different layers of the VIP wall (Figure 4.12a) and reference wall (Figure 4.12b) from 8<sup>th</sup> June 2020 to 15<sup>th</sup> June 2020. The weather conditions during this week were characterized by cloudy and sunny days, an average temperature of 21.1°C, a maximum of 29.8°C, and a minimum of 15.0°C .



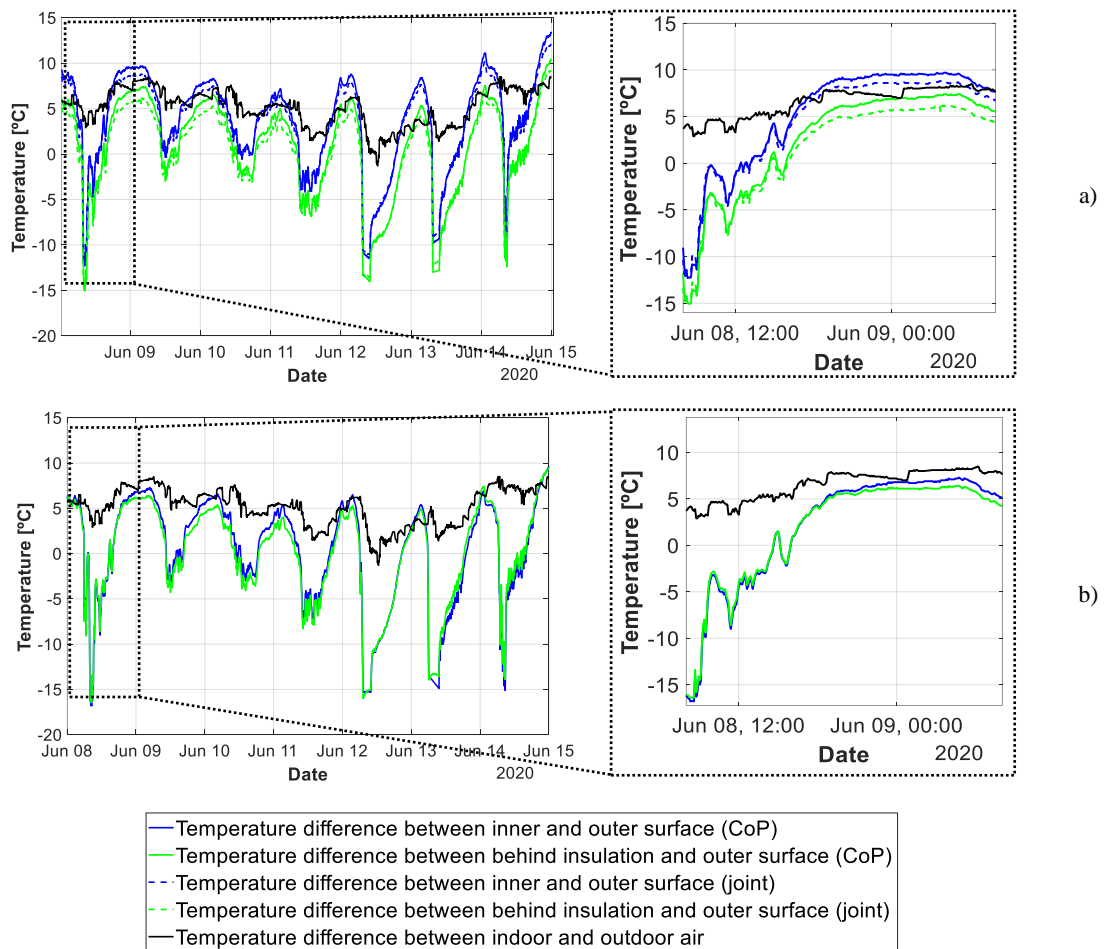
**Figure 4.12:** Temperature curves during a warm season: a) VIP wall; b) EPS wall.

In the warm season period, high outer surface temperatures are observed. For example, during a sunny day (12<sup>th</sup> June), the temperature of the outer surface of the VIP wall was 8°C higher (at the daily maximum temperature) than the outdoor air temperature. This temperature difference is due to the solar radiation from the sun reaching a highly insulated surface. On the 9<sup>th</sup> and 10<sup>th</sup> of June, which were mostly cloudy days, the surface temperature was around 12 to 13°C lower than that which was recorded on the sunny days in both walls. Such an elevated temperature amplitude may be an additional risk regarding the development of anomalies such as cracking of the rendering layer. However, it should be said that no rendering cracks were observed during the 24 months of monitoring.

Similarly, to the cold season period, the recorded surface temperature of the EPS wall was higher than that of the VIP wall. This is due to the heat transfer from indoors, as the air temperature inside was still found to be greater than the outdoor air temperature at all times. The higher heat losses in the EPS wall, when compared to the VIP wall, result in higher outer surface temperature.

For the same week, Figure 4.13 shows the temperature differences between several layers across both walls. During this period, a maximum temperature difference of 8.5°C was registered between indoor and outdoor air. Due to the effect of solar radiation, the outer surface temperature changes much more than the outdoor air temperature. Temperature differences of around 15°C were found between outer and inner surfaces in both walls. As expected, the joint area temperature

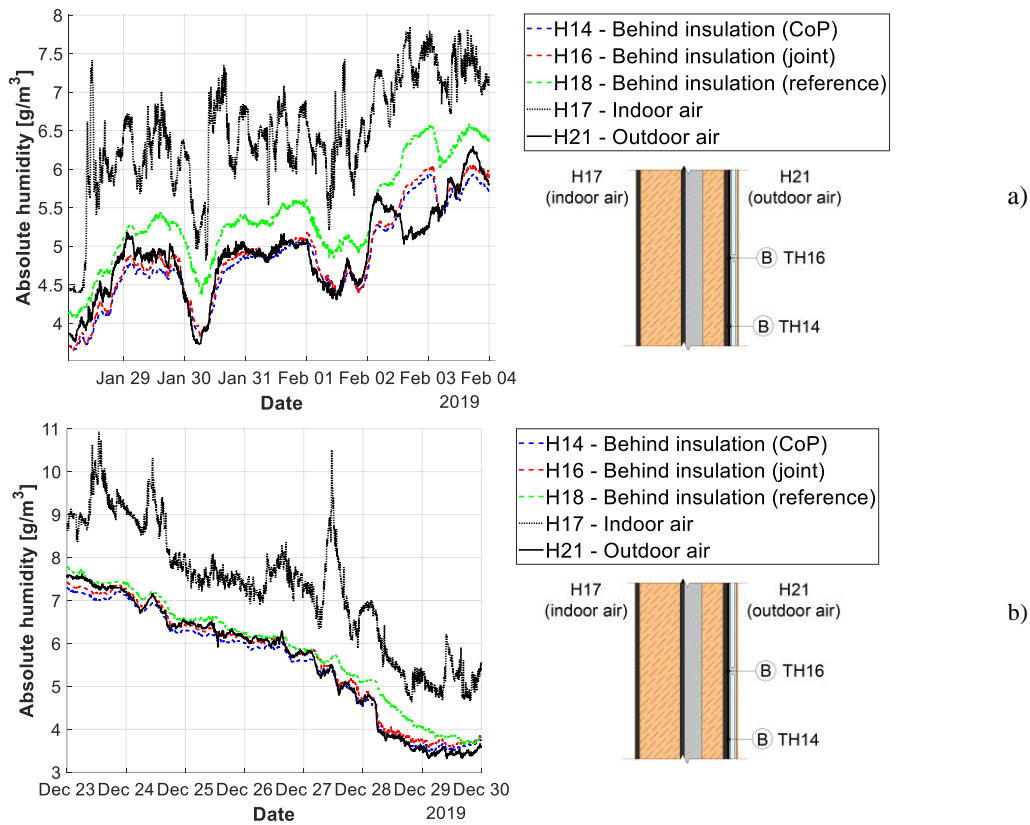
differences are lower (around 1°C) than CoP differences due the edge linear thermal bridging effects.



**Figure 4.13:** Temperature differences between layers during the warm season: a) VIP wall - CoP and joint area with daily detail; b) reference wall with daily detail.

### 4.3.3. Humidity analysis

Figure 4.14 shows the absolute humidity measured behind the insulation layer (interface B) in both walls (VIP and reference) for periods during the cold season.



**Figure 4.14:** Absolute humidity curves for VIP wall and reference wall: a) January 2019 week; b) December 2019 week.

It can be seen that the measured absolute humidity is lower than  $8 \text{ g/m}^3$  in both solutions. For the results in Figure 4.14b, the average absolute humidity calculated according to equation 4.5 is  $5.47 \text{ g/m}^3$  for the VIP wall and  $5.79 \text{ g/m}^3$  for the reference wall, which can be considered to be very similar. This indicates that, when compared to the conventional wall, the VIP solution will not present additional problems regarding internal humidity levels.

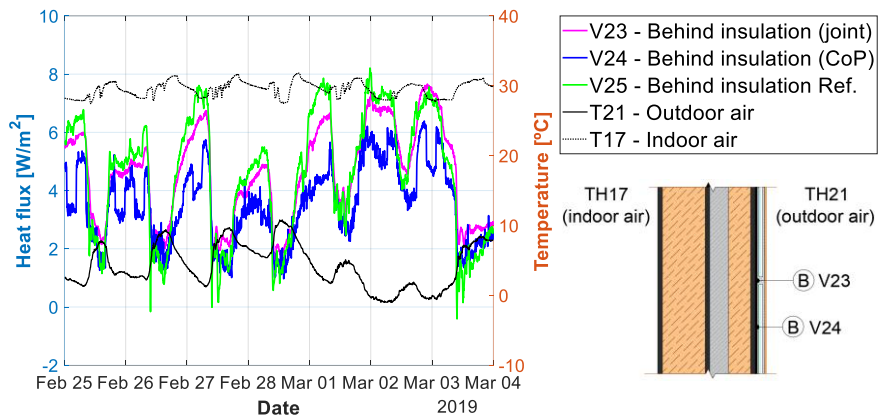
Results in Figure 4.14a and Figure 4.14b are approximately 1 year apart. However, similar absolute humidity levels are found. Thus, it can be said that no continuing built up in moisture levels has occurred.

#### 4.3.4. U-value estimation

This section presents the main results obtained from the heat flux measurements made in both walls. Results for a cold period and a warm period are presented and discussed. Furthermore, the retrofitted wall U-value is estimated using experimental measurements and computational algorithm. Both experimental and numerical results are compared with theoretical values.

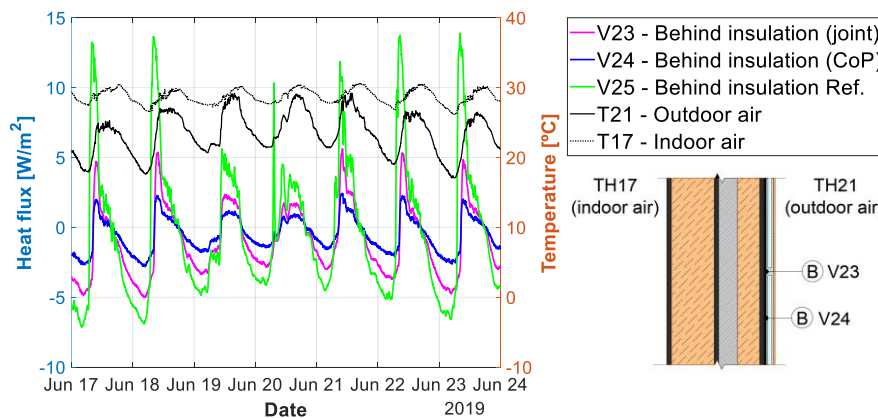
### 4.3.4.1. Heat fluxes measurements

Figure 4.15 shows the heat fluxes measured behind the VIP insulation (at the CoP and the joint area) in the VIP wall, as well as in the reference wall, for a representative week during winter (cold period).



**Figure 4.15:** Heat fluxes and ambient temperatures curves during a cold period.

The reference wall registered higher absolute heat fluxes than the VIP wall due to lower thermal resistance. Also, when comparing the CoP area with the joint area, greater amplitudes in heat flux are observed due to the linear thermal bridging effect at the edges of the panels (joint area). For example, on 1<sup>st</sup> March 2019, the absolute heat flux in the reference wall reached approximately 8.0 W/m<sup>2</sup>, while in the VIP wall the maximum was 6.5 W/m<sup>2</sup> in the joint area, and peaked below 5.5 W/m<sup>2</sup> in the CoP area. Figure 4.16 shows the heat flux measurements made in a warm period.



**Figure 4.16:** Heat fluxes and ambient temperatures curves during a warm period.

As expected, the conclusions are similar to the cold period measurements. The heat fluxes measured in the reference wall are higher than in the VIP wall and the amplitudes are greater. In the VIP wall, higher heat flux amplitudes are observed in the joint area due to the linear edge thermal bridging effect. In the morning period, higher heat flux amplitudes are visible due to the solar radiation. This issue is clearly visible for the EPS wall which has lower thermal resistance.

These heat flux measurements highlight the importance of the edge effects in the VIP solution. This linear thermal bridging effect occurs both due to the barrier envelope used to maintain the vacuum panels and due to the higher thermal conductivity of the edge material used to encapsulate the VIPs (EPS insulation). Furthermore, the eventual gaps that may occur between adjacent panels could contribute to increase the edge thermal bridging effects, even if filled with PUR. Thus, the global thermal performance of VIP ETICS walls is affected by the edge thermal bridging effect.

Throughout the 24 months of monitoring, the heat flux measurements have shown to be within the same range of values, which means that the performance of the VIPs being monitored has been preserved along this time.

Based on the heat fluxes and temperatures measurements from a cold season period (March 2019), the experimental U-value was determined for both walls, as suggested in ISO 9869-1 [27]. The results, presented in Table 4.3, show a relative deviation of 12% to 15% comparing the theoretical U-values calculated according ISO 6946 [28] and the experimental results. According to ISO 9869-1 [27] the uncertainty of *in situ* measurements ranges from 14% to 28%, hence these deviations are considered to be acceptable.

**Table 4.3:** U-values comparison between theoretical and experimental values.

Wall	Theoretical U-value <sup>(1)</sup>	Experimental U-value <sup>(2)</sup>	Relative deviation <sup>(3)</sup>
<b>VIP at CoP</b>	0.117	0.134	14.8%
<b>Reference</b>	0.223	0.195	12.6%

<sup>(1)</sup> Theoretical U-value calculated using data given in Table 4.1 and following the ISO 6946.

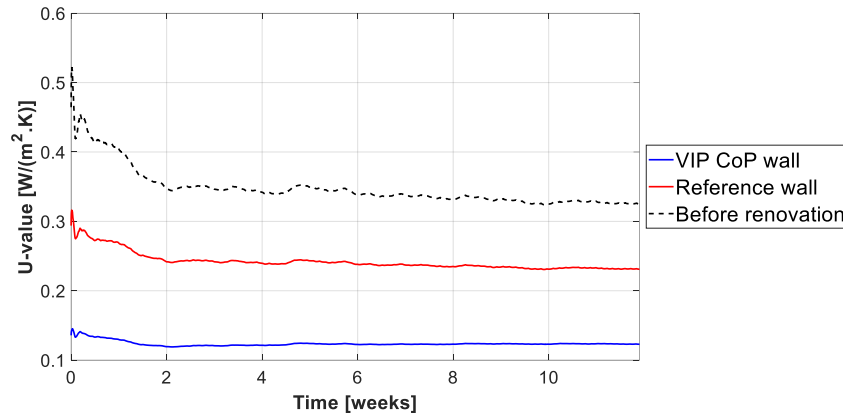
<sup>(2)</sup> U-value obtained using experimental measurements, following the ISO 9869-1.

<sup>(3)</sup> Relative deviation between theoretical U-value and the experimental U-value.

### 4.3.4.2. Computational algorithm results

The results for the U-value estimation of the VIP wall both before and after the renovation of the building are depicted in Figure 4.17. The graphic shows a timespan of approximately twelve weeks (from January to April 2019). At the beginning of the observation period, it is clear that the algorithm is highly influenced by transient effects. However, after approximately two weeks the algorithm starts to stabilize.

The U-value after the VIP based ETICS solution retrofit stabilized at 0.12 W/(m<sup>2</sup>·K) after the first week. The estimated pre-existing wall U-value shows a wider bandwidth, but also tends towards stabilization at 0.32 to 0.33 W/(m<sup>2</sup>·K). The U-value before renovation was calculated back from the results of the reference wall.



**Figure 4.17:** U-value estimation at the VIP wall (centre of VIP panel) and reference wall after the renovation with ETICS and before the renovation.

These results are again compared again with a theoretical U-value calculated following the ISO 6946. Table 4.4 summarizes the comparison between the theoretical U-values and the results obtained using the proposed numerical algorithm.

**Table 4.4:** U-values comparison between theoretical and numerical values.

Wall	Theoretical U-value <sup>(1)</sup>	U-value result <sup>(2)</sup>	Relative deviation <sup>(3)</sup>
<b>Before renovation</b>	0.313	0.325	3.8%
<b>VIP at CoP</b>	0.117	0.123	5.3%
<b>Reference</b>	0.223	0.231	3.7%

<sup>(1)</sup> Theoretical U-value calculated using data given in Table 1 and following the ISO 6946.

<sup>(2)</sup> U-value obtained using the computational algorithm.

<sup>(3)</sup> Relative deviation between theoretical and calculated U-value.

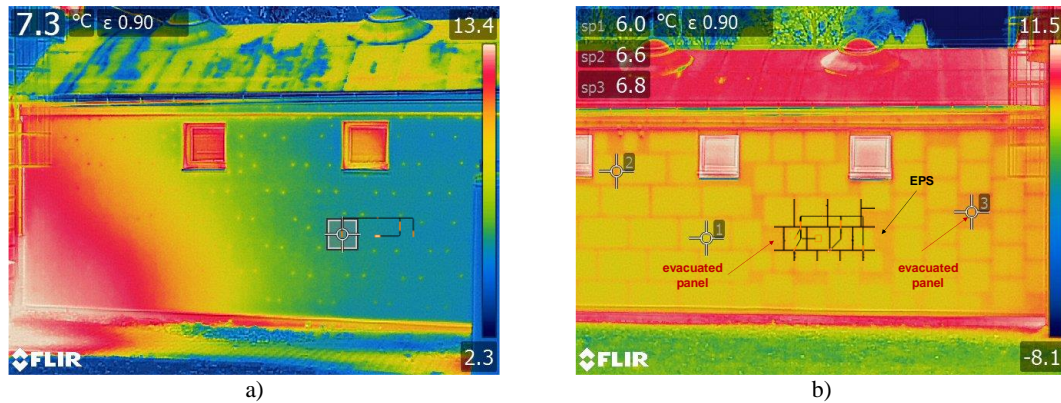
The theoretical U-value before refurbishment amounts to 0.313 W/(m<sup>2</sup>·K), while the numerical result was 0.325 W/(m<sup>2</sup>·K). For the retrofitted wall with VIP based ETICS, a numerical result of 0.123 W/(m<sup>2</sup>·K) was obtained from the computational algorithm, while the theoretical U-value of 0.117 W/(m<sup>2</sup>·K) is estimated. Thus, the relative deviation between the results is around 5%, showing a very good agreement with the proposed algorithm.

### 4.3.5. Infrared thermography inspection

Infrared thermographic inspection was performed to check the monitoring conditions, as well as to identify possible anomalies during the monitoring period. For control, two VIP panels were intentionally perforated (vacuum loss) during installation.



Figure 4.18 shows the surface temperatures of the external insulation VIP solution as well as of the reference wall. Both were recorded on 30<sup>th</sup> October 2019, around 2 pm, at which time the outdoor air temperature was around 7.5°C. Note that, in order to ensure a high enough contrast in each thermogram, the temperature colour scale may vary from image to image, hence the images are not to be compared directly with one another.

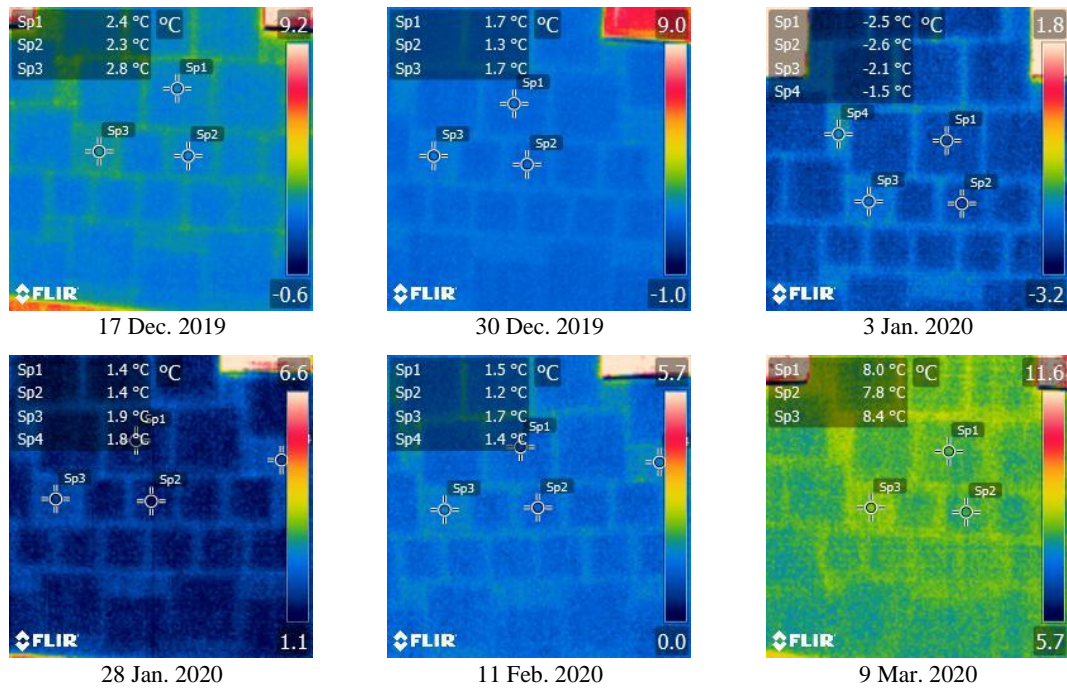


**Figure 4.18:** Thermograms: a) reference external insulation wall; b) VIP external insulation wall application.

Figure 4.18a shows a clear interference on the EPS reference wall due to a vent located in the lower left corner of the image. This effect was minimized by blocking the air and preventing it from going directly in the direction of the wall.

In the VIP wall (Figure 4.18b), the outline of the panels is clearly visible. This is due to the fact that there is more heat transfer around the edges of the panels (the surface temperature appears as higher). These findings are in line with the thermocouple measurements over the insulation. Also visible are areas where EPS panels have been used to fill out gaps that could not be covered by the VIP panels, as well as areas where the VIP panels have been intentionally perforated to produce this effect (allow for a comparison with other intact panels). The outline of the sensors has been superimposed on the images. It can be observed that the panels under monitoring did not lose their vacuum during the installation.

Thermograms of the VIP wall which were taken periodically during the winter are presented in Figure 4.19.



**Figure 4.19:** Thermograms taken of part of the VIP wall on several dates during winter period.

From these images, it is clear that the VIPs have not lost their vacuum during this period. Regarding the appearance of ETICS rendering, no cracking, blistering, or aesthetic anomalies were found. However, it should be noted that the case study wall faces northeast. If this VIP based ETICS wall was facing south, greater thermal amplitudes would be expected, as well as increased risk of cracking.

Due to the intentional loss of vacuum and the accompanying increase of the thermal conductivity, surface temperatures in the perforated panel zone (Sp3) are higher than in the VIP CoP zone (Sp2) by around 0.5°C. This increase in temperature means that the heat transfer through the perforated panel is higher than in the CoP area, as expected. However, when comparing the EPS zone (Sp4) with the perforated panel (Sp3) on the VIP wall, there is a better thermal performance of the perforated panel (lower temperature surface), due to the low thermal conductivity of the fumed silica core. As indicated in Annex B, the thermal conductivity of a perforated VIP (without vacuum) is around 21 mW/(m·K) which is still lower than a thermal conductivity of EPS panels (32 mW/(m·K)), confirming the results of the onsite measurements.

## 4.4. Conclusions

This chapter presented the onsite monitoring results for a retrofitted wall with ETICS built with VIP insulation located Warsaw. The results enabled a quantification of the thermal performance

of the VIP wall - both at the centre of panel and at the panel edges (joint area). Furthermore, a comparison with a conventional insulation material solution (EPS based ETICS) with the same thickness was possible.

The higher thermal performance of VIP ETICS compared to EPS ETICS was confirmed through temperatures and heat fluxes measurements. It was found that the VIP thermal resistance contribution is significantly higher than in EPS based solutions, even when measuring at the joint area where the thermal bridging edge effect occurs. However, slightly higher surface condensation risk was found at the VIP centre of panel, increasing the risk of biological growth. Humidity measurements allowed for the conclusion that this VIP based ETICS wall solution will not likely present significant internal humidity level problems when compared with conventional ETICS solutions with EPS. Furthermore, no continuing built up in moisture levels was verified.

U-value estimations based on heat fluxes measurements showed a deviation of around 12 to 15% when compared to the theoretical U-value of the wall. Later, a computational algorithm was used to determine the U-value of the wall before and after refurbishment with the VIP ETICS solution based only on temperature measurements and the known thermal conductivity of the insulation material. The results found are in line with the estimated theoretical values, showing a maximum deviation of 5%.

The analysis of heat fluxes showed the relevance of the edge thermal bridging effects on the global performance of the ETICS wall. Thus, for an adequate façade design, an estimation of effective thermal transmittance of VIPs will need to take into account the linear thermal bridges at the panel edges. Also, the use of bigger panels is desirable in order to reduce the contribution of edge thermal bridging effects.

Infrared thermograms also confirmed the different behaviours of centre of panel and joint area. This issue, which is vital for the determination of an effective U-value, should be carefully assessed in future studies carried out in a controlled environment. Furthermore, future research should include large scale testing of specimens in laboratory conditions to allow a detailed study of the ageing and hygrothermal behaviour of VIP ETICS solutions under different controlled environment parameters.

After 24 months of monitoring, no visible surface anomalies or panels with vacuum loss (inspected via infrared thermography) were found in the VIP based ETICS wall. Since there are some market uncertainties regarding the long-term performance of VIP solutions, the findings of this study, namely the VIP thermal benefits and the absence of defects, contributes to increasing the confidence of the construction sector in the use of vacuum-based solutions as an ETICS option for walls.

## References

- [1] S. Varela, C. Viñas, A. Rodríguez, P. Aguilera, M. González, “Experimental comparative study of the thermal performance of the façade of a building refurbished using ETICS, and quantification of improvements”, *Sustain. Cities Soc.* vol. 51, 101713, 2019, doi:10.1016/j.scs.2019.101713.
- [2] A. M. Raimundo, N. B. Saraiva, A. V. M. Oliveira, “Thermal insulation cost optimality of opaque constructive solutions of buildings under Portuguese temperate climate”, *Build. Environ.* vol. 182, 107107, 2020, doi:10.1016/j.buildenv.2020.107107.
- [3] European Parliament, “Directive (EU) 2018/844 of the European Parliament and of the Council of 30 May 2018 amending Directive 2010/31/EU on the energy performance of buildings and Directive 2012/27/EU on energy efficiency”, *Off. J. Eur. Union.* pp 75–91, 2018.
- [4] J. Maia, N. M. M. Ramos, R. Veiga, “Evaluation of the hygrothermal properties of thermal rendering systems”, *Build. Environ.* vol. 144 pp. 437–449, 2016, doi:10.1016/j.buildenv.2018.08.055.
- [5] A. Batard, T. Duforestel, L. Flandin, B. Yrieix, “Prediction method of the long-term thermal performance of vacuum insulation panels installed in building thermal insulation applications”, *Energy Build.* vol.178 pp. 1–10, 2018, doi:10.1016/j.enbuild.2018.08.006.
- [6] M. Gonçalves, N. Simões, C. Serra, I. Flores-Colen, “A review of the challenges posed by the use of vacuum panels in external insulation finishing systems”, *Appl. Energy.* vol. 257, 114028, 2020. doi:10.1016/j.apenergy.2019.114028.
- [7] M. Bouquerel, T. Duforestel, D. Baillis, G. Rusaouen, “Mass transfer modelling in gas barrier envelopes for vacuum insulation panels: A review”, *Energy Build.* vol. 55, pp. 903–920, 2012, doi:10.1016/j.enbuild.2012.09.004.
- [8] M. Tenpierik, A. Van Timmen, W. Van der Spoel, H. Cauberg, “Vacuum insulation panels and architecture: cradle-to-cradle façade systems”, in *3<sup>rd</sup> Int. Conf. Smart Sustain. Built Environ.*, 2009.
- [9] P. Johansson, B. Adl-Zarrabi, A. S. Kalagasidis, “Evaluation of 5 years’ performance of VIPs in a retrofitted building façade”, *Energy Build.* vol. 130 pp. 488–494, 2016, doi:10.1016/j.enbuild.2016.08.073.
- [10] P. Johansson, C.E. Hagentoft, A. S. Kalagasidis, “Retrofitting of a listed brick and wood building using vacuum insulation panels on the exterior of the facade: measurements and simulations”, *Energy Build.* vol. 73, pp. 92–104, 2014, doi:10.1016/j.enbuild.2014.01.019.
- [11] F. Ascione, R.F. de Masi, R. M. Mastrullo, S. Ruggiero, G. P. Vanoli, “Experimental investigation and numerical evaluation of adoption of multi-layered wall with vacuum insulation panel for typical Mediterranean climate”, *Energy Build.* vol. 152, pp. 108–123, 2017, doi:10.1016/j.enbuild.2017.07.029.
- [12] R. Francesca, D. Masi, S. Ruggiero, G. Peter, “Multi-layered wall with vacuum insulation panels: results of 5-years in-field monitoring and numerical analysis of aging effect on building consumptions”, *Appl. Energy.* vol. 278, 115605, 2020, doi:10.1016/j.apenergy.2020.115605.

- [13] B. Yrieix, B. Morel, E. Pons, “VIP service life assessment: Interactions between barrier laminates and core material, and significance of silica core ageing”, *Energy Build.* vol. 85, pp. 617–630, 2014, doi:10.1016/j.enbuild.2014.07.035.
- [14] S. Brunner, T. Stahl, K. G. Wakili, “An example of deteriorated vacuum insulation panels in a building façade”, *Energy Build.* vol. 54, pp. 278–282, 2012, doi:10.1016/j.enbuild.2012.07.027.
- [15] P. Johansson, “Vacuum insulation panels in buildings. Literature review”, Report in Building Physics. Department of Civil and Environmental Engineering, Chalmers University of Technology, Göteborg, Sweden 2012.
- [16] I. Mandilaras, I. Atsonios, G. Zannis, M. Founti, “Thermal performance of a building envelope incorporating ETICS with vacuum insulation panels and EPS”, *Energy Build.* vol. 85, pp. 654–665, 2014, doi:10.1016/j.enbuild.2014.06.053.
- [17] S. E. Kalnæs, B. P. Jelle, “Vacuum insulation panel products: a state-of-the-art review and future research pathways”, *Appl. Energy.* vol. 116, pp. 355–375, 2014, doi:10.1016/j.apenergy.2013.11.032.
- [18] M. Ibrahim, H. Sayegh, L. Bianco, E. Wurtz, “Hygrothermal performance of novel internal and external super-insulating systems: in-situ experimental study and 1D/2D numerical modeling”, *Appl. Therm. Eng.* vol. 150, pp. 1306–1327, 2019, doi:10.1016/j.applthermaleng.2019.01.054.
- [19] M. Teni, H. Krstić, P. Kosiński, “Review and comparison of current experimental approaches for in-situ measurements of building walls thermal transmittance”, *Energy Build.* vol. 203, 109417, 2019. doi:10.1016/j.enbuild.2019.109417.
- [20] Associação Portuguesa dos Fabricantes de Argamassas e ETICS, “Manual ETICS” (in portuguese), pp. 1–48, 2018
- [21] J. Gonçalves, J. Graça, “Conceitos Bioclimáticos para os Edifícios em Portugal”, INETI, 2004.
- [22] *Thermal performance of building materials and products - Determination of thermal resistance by means of guarded hot plate and heat flow meter methods - Products of high and medium thermal resistance*, EN 12667, European Committee for Standardization, 2001.
- [23] M. Kottek, J. Grieser, C. Beck, B. Rudolf, F. Rubel, “World map of the Köppen-Geiger climate classification updated”, *Meteorol. Zeitschrift.* vol. 15, pp. 259–263, 2006, doi:10.1127/0941-2948/2006/0130.
- [24] F. Rubel, K. Brugger, K. Haslinger, I. Auer, “The climate of the European Alps: Shift of very high resolution Köppen-Geiger climate zones 1800-2100”, *Meteorol. Zeitschrift.* vol. 26, pp.115–125, 2017, doi:10.1127/metz/2016/0816.
- [25] climatedata.eu, “Temperature - Precipitation – Sunshine”, <https://www.climatedata.eu/> (accessed September 17, 2019).
- [26] Sensirion, “Dew-Point Calculation”, pp. 1–3, 2006, [www.sensirion.com/humidity](http://www.sensirion.com/humidity).
- [27] *Thermal insulation building elements - in-situ measurement of thermal resistance and thermal transmittance. Part 1: Heat flow meter method*, ISO 9869-1, International Organization for Standardization, 2014.

- [28] *Building components and building elements - Thermal resistance and thermal transmittance - Calculation method*, ISO 6946, International Organization for Standardization, 2017.
- [29] *Thermal insulation – qualitative detection of thermal irregularities in building envelopes – infrared method*, ISO 6781, International Organization for Standardization, 1983.
- [30] C. Marino, F. Minichiello, W. Bahnfleth, “The influence of surface finishes on the energy demand of HVAC systems for existing buildings,” *Energy Build.* vol. 95, pp. 70–79, 2015, doi:10.1016/j.enbuild.2015.02.036.







## **CHAPTER 5**

# **ONSITE MONITORING OF VIP BASED ETICS IN COIMBRA: COMPARISON OF DIFFERENT EXPOSURE CONDITIONS AND INSULATION MATERIALS**



## **5. Onsite monitoring of VIP based ETICS in Coimbra: comparison of different exposure conditions and insulation materials**

### **5.1. Introduction**

An External Thermal Insulation Composite System (ETICS) is a popular multi-layered finishing system used to improve the thermal performance of façades and consequently, the energy efficiency of buildings. Due to its known advantages and relative low cost [1] the most used insulation material in ETICS is expanded moulded polystyrene (EPS) [2]. However, other thermal insulation materials such as mineral wool (MW) or expanded cork agglomerate (ICB) are also used. Using vacuum products in ETICS to replace these conventional insulation materials, presents itself as an interesting solution to achieve greater energy efficiency with reduced thickness. However, it is expected that, due to the greater thermal insulation capacity of vacuum panels, the thin rendering layer in VIP based ETICS may be under increased stresses due to a higher temperature gradient.

ETICS with rendering are directly exposed to weathering agents and anthropic factors [3]. For this reason, biological growth is one of the most frequent anomalies in conventional ETICS [4]. In the Mediterranean climate, the occurrence of biological growth has been confirmed by statistical surveys of inspections carried out in ETICS façades [5]. Even though aesthetical anomalies may not influence the system's thermal performance, an issue such as this can contribute to decreasing confidence in the solution. Previous studies ([6],[7]) have shown that biological growth is strongly influenced by surface properties, such as pH, porosity and roughness of the finishing coat, as well as, by air temperature and relative humidity. Barreira *et al.* [8] evaluated experimentally the influence of orientation on surface humidification of EPS ETICS façades through one year onsite monitoring. For the building under this study, the west façade presented higher risk of condensation, followed by the east, north and south façades. In fact, mould growth is linked to high levels of surface moisture content, resulting from the combined

effect of external surface condensation, wind-driven rain, drying process and rendering properties [8].

In addition to wetting from wind-driven rain, external surface condensation occurs due to the exchange of long wave radiation between the façade and the atmosphere, which results in a net heat flux to the sky leading to low temperatures [9]. Condensation occurs when the wall's external surface temperature drops below the dew point of the ambient air. Quantifying the amount of surface condensation due to long wave irradiation is considered to be a good criterion when assessing microbiological growth risk [10] since the availability of water in the material is regarded as a crucial aspect for mould growth on walls surfaces [11].

In ETICS, in addition to the finishing coat properties, the insulation material can also have significant impact. The risk of surface condensation is lower in the case of buildings with low thermal insulation levels [12]. This was also found by Johansson *et al.* [13] when comparing, in terms of mould growth, a lightweight wall (ETICS with EPS over wooden board) and a heavy wall (brick wall placed outside the EPS and the wood board). The results showed that the thin low inertia walls had a higher potential for biological growth. Also, the colour of the wall was highlighted as being one important factor when studying surface humidity levels. Thus, avoiding biological growth in ETICS with VIPs can be expected to be a great challenge facing the industry in the near future.

The biological growth risk on ETICS surface also depends on the climate, the surrounding environment (in regard, for example, the presence of gardens, forest, industries, among others) and the orientation of the walls. For example, in Canada, external condensation in externally insulated walls facing east and west is common during the summer months in cool, clear nights after hot and humid days [14]. In Belgium, researchers [15] observed that a North facing façade experienced longer drying times due to lack of exposure to solar radiation and hence presented a greater risk for biological growth. Regarding VIP walls monitoring, Mandilaras *et al.* [16] collected onsite data for one year of a VIP wall facing North, where 20 mm VIPs covered by 20 mm mineral wool and 50 mm of insulation render were used. The hygrothermal monitoring stated periods of high humidity values and the presence of condensates on the surfaces of the VIP.

In summary, ETICS are constantly exposed to weathering agents, which can lead to physical, mechanical and aesthetic anomalies. The greater thermal resistance provided by the vacuum technology can lead the thin ETICS rendering layer to be subject to higher temperature gradients. This could potentiate cracking and ultimately allow water to penetrate through the walls. Also, night-time surface temperatures are expected to be lower with VIPs due to its the higher thermal resistance level (when compared with conventional insulation materials), increasing the risk for surface condensations and consequently, biological growth.

The literature review presented in chapter 2 showed some studies which have focused on anomalies in conventional ETICS surfaces, highlighting the biological growth issue. Since there

is a gap in the knowledge surrounding the evaluation of the long-term performance of ETICS with super-insulating materials, including comparisons of surface condensation risk against the conventional ETICS solutions, there is a need for onsite monitoring of VIP based ETICS. Furthermore, the use of super-insulating materials could potentiate the risk of the rendering cracking due to the expected higher thermal amplitudes.

This chapter aims to contribute to the evaluation of VIP based ETICS by comparing its thermal behaviour against conventional ETICS solutions. The main goal of the work presented herein is to investigate the influence of finishing coat colour and orientation on the surface condensation risk. For this purpose, this chapter reports the monitoring results for two free-standing walls which incorporate several different insulation materials. The walls were located in Coimbra, Portugal. The temperatures across several layers of the walls were monitored for more than 24 months. During the monitoring period, a passive infrared thermography (IRT) inspection technique was also used to detect early signs of potential anomalies, such as cracking, blistering or water infiltration. Additionally, since a numerical modelling tool may be helpful to understand the condensation risk in other climates or solutions, a finite difference model was used and numerical results were compared against the onsite experimental measurements.

## **5.2. Materials and methods**

In this section, first, the case-studies of onsite ETICS applications are presented. Then, information on the local weather data and measurement settings is provided. Next, the infrared thermography inspection method is detailed. Finally, the methods used to evaluate the surface condensation risk on the ETICS walls are described. Additionally, the 2D numerical model used to simulate the transient thermal behaviour of the case study walls is presented.

### **5.2.1. Case study**

Figure 5.1 shows the two free-standing case study masonry walls built in Coimbra, Portugal. Each is 5 m x 2 m (width x height). The walls were built, in September 2018, in a position so that each has a side facing North and the other facing South. Each wall has sections that incorporate different thermal insulation products. Namely, 8 cm thick layers of expanded polystyrene (EPS),

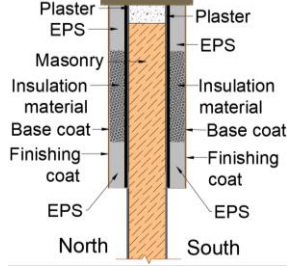
thermal insulation mortar (TIM), and expanded cork agglomerate (ICB) were applied in different areas with 1000 mm x 500 mm (shown in Figure 5.1a). The areas surrounding the different solutions were filled with EPS with the same thickness to guarantee adequate boundary conditions. The insulation materials were bonded to the wall using a suitable adhesive and supplementary mechanical fixing (plastic anchors).



**Figure 5.1:** ETICS walls: a) different thermal insulation materials (EPS, TIM, ICB and VIP); b) different colour finishing coat (black and white).

In the case of the vacuum technology, 440 mm x 440 mm encapsulated VIPs with 4 cm thickness were applied. Due to the reduced number of available VIPs, two VIP products were installed on the south black wall, and one on the south white wall, looking to explore the higher temperature amplitudes on south facing walls. The encapsulated VIP product consists in a 20 mm thick vacuum panel with fumed silica core covered with a graphite EPS protective layer with 10 mm thickness on both sides and 20 mm along the edges. The rendering system consists in a reinforced base coat with around 5 mm thickness, a 160 g/m<sup>2</sup> fibre glass mesh, a primer, and an acrylic finishing coat which protects against weathering and provides a decorative finish [17]. Two different finishing coat colours (white and black) were used in each wall, while the remaining properties such as roughness, size of the aggregates, etc. were kept the same. The ETICS were applied on the masonry walls 1.0 m from the ground up in order to mitigate the floor reflection phenomena and to avoid shading by elements in the vicinity. Table 5.1 shows the thermophysical properties of the materials used in the two free-standing walls.

**Table 5.1:** Thermophysical properties of the materials used in the case-study walls.

External wall cross section	Constructive layer	d <sup>(1)</sup> [mm]	$\lambda$ <sup>(2)</sup> [W/(m·K)]	$\epsilon$ <sup>(3)</sup> [-]	$\rho$ <sup>(4)</sup> [kg/m <sup>3</sup> ]	c <sup>(5)</sup> [J/(kg·K)]	
	Masonry block	190	0.30	0.90	850	840	
	Plaster	10	0.67	0.90	1650	840	
	Adhesive	10	0.47	0.90	1350	840	
	Encapsulated VIP	40	0.0075	0.90	130	900	
	Insulation material	EPS	80	0.036	0.90	20	1430
		ICB	80	0.040	0.90	120	1670
		TIM	80	0.055	0.90	300	1430
	Base coat	5	0.47	0.90	1350	840	
	Finishing coat (white/black colour)	2	0.40	0.91/0.94	1650	1000	

<sup>(1)</sup> Thickness.

<sup>(2)</sup> Thermal conductivity.

<sup>(3)</sup> Emissivity.

<sup>(4)</sup> Density.

<sup>(5)</sup> Specific heat.

The thermal conductivity values of the ETICS components were obtained in a guarded hot plate apparatus ( $\lambda$ -Meter EP500e) for an average temperature of 10°C, as recommended by the EN 12667 [18] and EN 12664 [19]. Finishing coat emissivity was measured onsite by means of TIR100-2 emissometer, which has a measurement uncertainty of  $\pm 0.01$ , mentioned in the standard EN 16012 [20]. Figure 5.2 shows the use of this hand-held portable apparatus on the onsite walls. The solar reflectance of both finishing colours was determined in laboratory samples according to ASTM E903-96 [21], resulting in 0.74 for white finishing coat and 0.04 for black coating. The remaining properties are based in technical datasheets.



**Figure 5.2:** Determination of finishing coat emissivity by means of TIR100-2.

## 5.2.2. Weather data

The weather in Coimbra is classified as warm summer Mediterranean climate Csb, under the Köppen-Geiger classification ([22,23]). According to historical data [24], the mean annual

precipitation is 905 mm (102 rainy days per year) and the mean annual sunshine hours are 2463. There is significantly more rainfall in winter than in summer.

Based on onsite data monitoring from a meteorological station located close to the walls, Figure 5.3 shows the mean monthly temperatures (maximum, minimum and average), as well as mean air relative humidity, obtained for the year of 2019. January was the coldest month, recording a mean monthly minimum temperature of 6.9°C. In opposition, July was the hottest month, with a mean monthly minimum temperature of 18.4°C. The maximum daily temperature amplitude found (around 21°C) occurred during July and a minimum daily temperature amplitude of around 7°C was found in the winter months, namely in January and December.

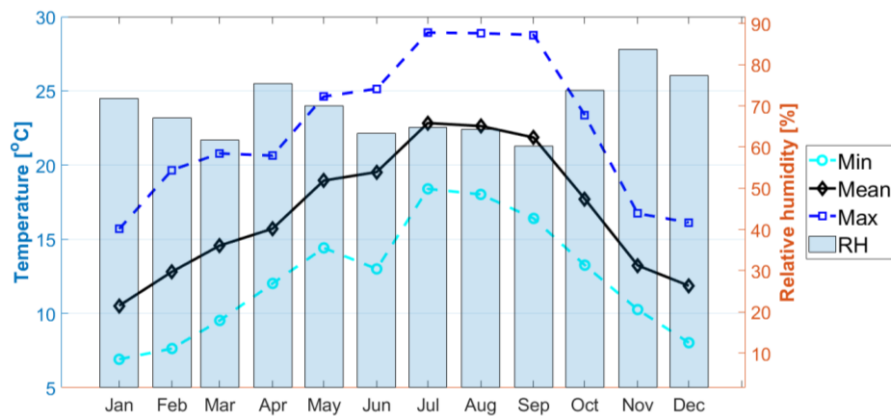
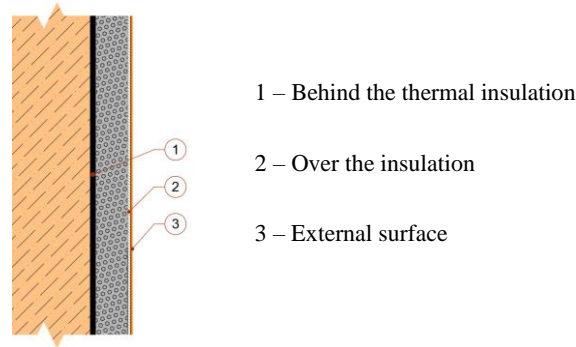


Figure 5.3: Mean monthly weather data monitored in 2019.

### 5.2.3. Measurement settings

The ETICS walls were monitored for more than 24 months, starting in October 2018. Each insulation area was instrumented with thermocouples type T connected to a datalogger Keysight/Agilent, model 34970A (accuracy  $\pm 1^\circ\text{C}$ ) to register temperature over time (30-minute intervals). Temperature sensors were placed, near the centre of each insulation material section, along the different interfaces between the wall layers, namely (from inner to outer surfaces): behind the insulation (meaning between the substrate and the external insulation layer – interface 1); over the insulation (meaning between the insulation layer and the base coat layer – interface 2); and over the external surface – interface 3. A schematic representation of the placement of the sensors is given in Figure 5.4.





**Figure 5.4:** Schematic representation of the location of the thermocouples.

Climate data, such as ambient temperature, air relative humidity, global solar radiation and wind velocity, were recorded continuously, every 30 minutes, using a meteorological station located close to the walls. The meteorological station includes: a temperature and relative humidity sensor, an albedometer Hukseflux SRA01 for global and reflective radiation measurements, a pyranometer with shadow ring Hukseflux LP02 for diffuse radiation measurements, and a wind speed and direction monitor RM Young 05103.

#### **5.2.4. Infrared thermography inspection**

In order to check the monitoring conditions and evaluate the surface temperature distribution for the different insulation products included in the case study walls, a passive infrared thermography (IRT) inspection was carried out, based on the method proposed in ISO 6781 [25]. For this purpose, a FLIR T630sc thermographic camera with a resolution of 640 x 480 pixels, accuracy of  $\pm 1^{\circ}\text{C}$  or  $\pm 1\%$  at  $25^{\circ}\text{C}$ , and object temperature range of  $-40$  to  $150^{\circ}\text{C}$  was used. This device is able to capture the infrared radiation emitted by any object and, using the Stefan–Boltzmann law, produce images containing surface temperature patterns.

Thermograms were taken periodically, in the early afternoon, at a distance from the wall of approximately 3 m (field of view 1.0 m x 1.0 m). In the processing of the thermal images, an emissivity of 0.91 and 0.94 were considered for the white and black wall surfaces, respectively, in accordance with onsite measurements.

IRT was also used to assess the integrity of the VIP panels over time, in particular to detect loss of vacuum, as well as to identify the occurrence of rendering anomalies (detachments, cracking, water infiltration, moisture, etc.).

### 5.2.5. Surface condensation risk assessment

There is risk of surface condensation occurring whenever the temperature of a surface is lower than the dew point temperature. In order to calculate the dew point temperature, the Magnus formula [26], which relates saturation vapour pressure with the dew point, was used.

At an ambient temperature of  $T$ , in °C, the saturation vapor pressure,  $P_{ws}$ , expressed in hPa, is given by the expression in equation 5.1:

$$P_{ws} = a \cdot e^{\left(\frac{b \cdot T}{c+T}\right)} \quad [\text{hPa}] \quad (5.1)$$

where Magnus parameters  $a, b, c$  are 6.11 hPa, 17.62 and 243.12 °C, respectively (for the range -45°C to 60°C) [26].

The dew-point temperature  $T_{dp}$  in °C can be expressed from the vapour pressure  $P_w$ , according to the expression in equation 5.2:

$$T_{dp} = \frac{c \cdot \ln\left(\frac{P_w}{a}\right)}{b - \ln\left(\frac{P_w}{a}\right)} \quad [^\circ\text{C}] \quad (5.2)$$

Considering the definition of air relative humidity  $RH$  in %, vapour pressure can be expressed as:

$$P_w = \frac{RH}{100} \cdot P_{ws} \quad [\text{hPa}] \quad (5.3)$$

Using the vapour pressures given by equations 5.1 and 5.3 in equation 5.2 leads to the calculation of dew-point temperature,  $T_{dp}$ , for an ambient temperature  $T$  and relative humidity  $RH$  is in equation 5.4:

$$T_{dp}(T, RH) = \frac{c \cdot \left(\ln\left(\frac{RH}{100}\right) + \frac{b \cdot T}{c+T}\right)}{b - \left(\ln\left(\frac{RH}{100}\right) + \frac{b \cdot T}{c+T}\right)} \quad [^\circ\text{C}] \quad (5.4)$$

The dew-point curves can be plotted with this calculation of dew-point temperature. The condensation risk,  $Cr$ , is estimated to be the percentage of time during which the surface temperature,  $T_s$ , is lower than the dew-point temperature,  $T_{dp}$ , during the monitoring period,  $M$ :

$$Cr(T_{dp}, T_s) = \frac{\sum(\text{time with } T_s < T_{dp})}{\sum(M)} \times 100 \quad [\%] \quad (5.5)$$

## **5.2.6. Numerical modelling**

Simulations of the case studies temperature behaviour were performed using BISTRA software version 4.0w [27] from Physibel which allows 2D transient heat transfer modelling. This software uses the Cranck-Nicolson finite difference method to formulate the energy balance for all control volumes around material nodes. In order to validate the software calculation procedures, the software was previously used to run the benchmarks provided by EN ISO 13786 Annex D [28], namely a single layer component and a multilayer component. The dynamic thermal characteristics results using the software simulations showed to be in very close agreement with benchmarks values.

For the case study walls, the numerical modelling was performed using a triangular mesh with 55855 nodes with 20 pixels (2 mm) each. The calculation parameters were defined in 5 iteration cycles with a maximum number of 10000 iterations per cycle, considering a maximum temperature difference of 0.0001°C and maximum heat flow divergence of 1% for any node. The meteorological station measurements, namely ambient temperature, global solar radiation, and diffuse radiation were introduced as input data, as well as information regarding the local time zone and geographical coordinates.

Based on preliminary analysis of air movement velocity and direction and following the ISO 6946 Annex C [29], an average convective heat transfer coefficient of 6.9 W/(m<sup>2</sup>·K) for south facing walls was used in the simulations presented in this chapter. Also, a default black radiation heat transfer coefficient of 5.1 W/(m<sup>2</sup>·K) and a ground reflection factor equal to 0.18 were considered in all simulations. The ground reflection factor was obtained based on the average measurements of the albedometer (placed near the walls) during the period simulated. The thermophysical properties of the materials used in the numerical model are presented in Table 5.1.

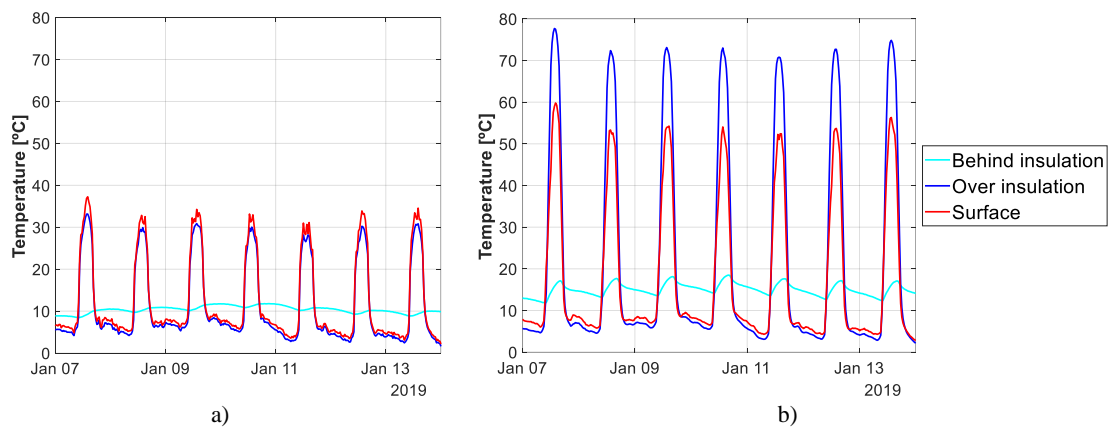
## **5.3. Results and discussion**

In this section, the main results of the onsite monitoring are presented and discussed. First, the temperature monitoring of an innovative solution – VIP based ETICS is presented. The results shown were chosen to represent the behaviour of the walls on a typical week during the heating season (week in January) and the cooling season (week in July). Next, the influence of orientation of the ETICS walls are discussed. Results from the infrared thermographic inspection campaign carried out to assess potential ETICS anomalies are also presented. Then, the condensation risk

estimation for different insulation materials using the temperature and relative humidity measurements is presented and discussed. Finally, a comparison between experimental and numerical modelling results is also presented in this section.

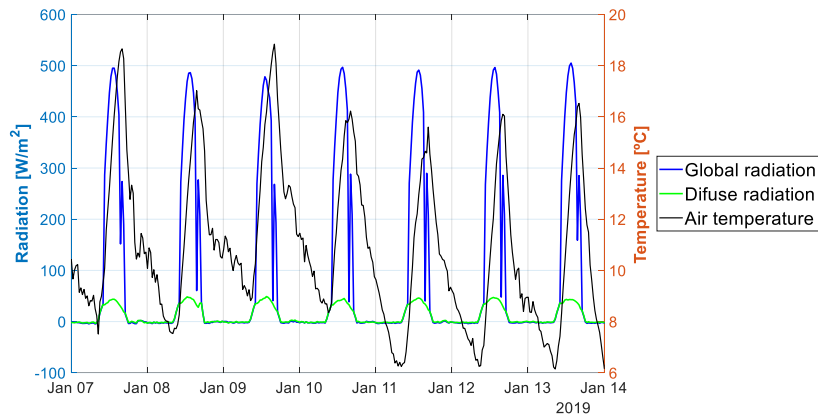
### 5.3.1. Temperature monitoring of VIP based ETICS

Figure 5.5 shows the temperatures recorded along the different layers of the VIP based ETICS solution during a week in a January 2019, for both the white and the black coated walls. This was a sunny week, during which a maximum outdoor temperature of 19°C was reached, as Figure 5.6 shows. As expected, the black wall exhibits higher temperatures, reaching values above 70°C over the insulation layer. The thermal protection provided by the VIP insulation allows a temperature drop behind the insulation of more than 20°C in the white wall (Figure 5.5a) and 40°C in the black wall (Figure 5.5b). In Figure 5.5b it can be seen that “over insulation” temperatures reach higher values than surface temperatures. This phenomenon, occurring only in the black walls, may be related to a greater convective heat transfer generated at the surface caused by a significant difference between surface temperature and air temperature (when compared with the white wall measurements).



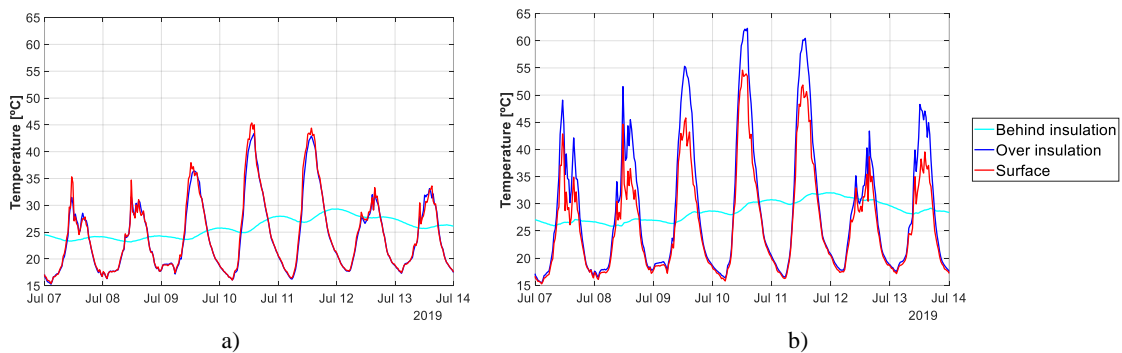
**Figure 5.5:** Temperature measurements in different VIP based ETICS layers during a week in winter: a) white wall (south); b) black wall (south).

*Onsite monitoring of VIP based ETICS in Coimbra: comparison of different exposure conditions and insulation materials*

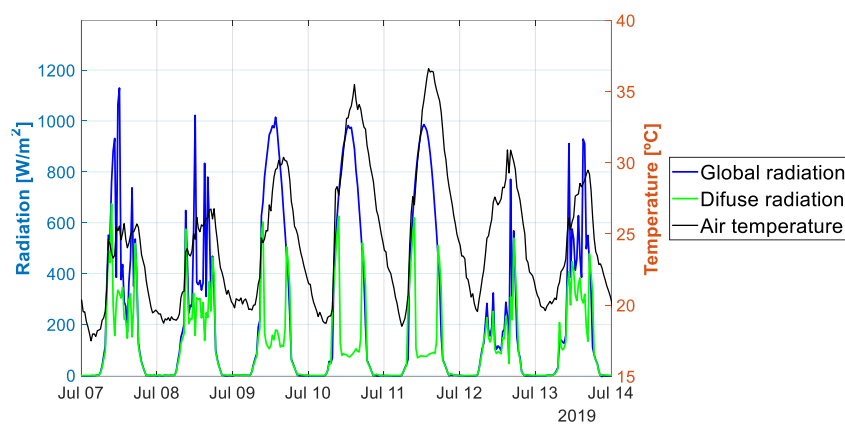


**Figure 5.6:** Temperature and radiation registered during a week in winter.

Figure 5.7 shows the temperatures recorded during a week in July 2019 along the different layers of the VIP based ETICS solution, including white and black finishing coat. During this week, a maximum outdoor temperature of 36°C was achieved. This summer week presented some cloudy days, as can be seen in Figure 5.8.



**Figure 5.7:** Temperature measurements in different VIP based ETICS layers during a week in summer: a) white wall (south); b) black wall (south).



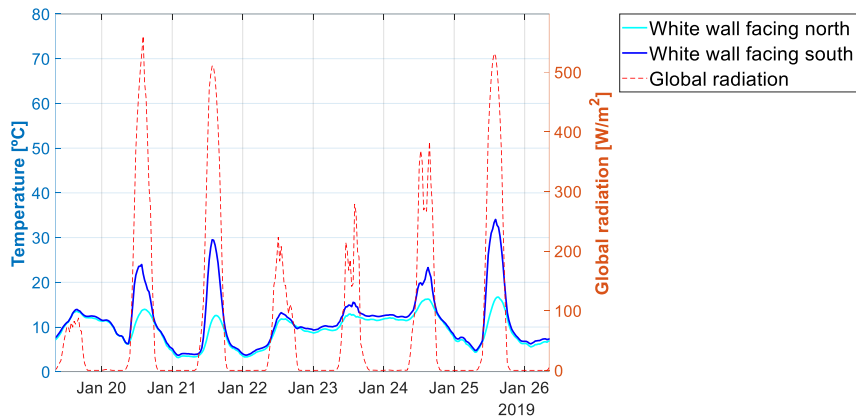
**Figure 5.8:** Temperature and radiation registered during a week in summer.

Once again, the black wall has higher surface temperatures, especially in the interface between the insulation layer and the rendering system (interface 2), where the temperature reaches more than 60°C. Even during the cloudy periods, the black wall presents higher surface temperatures

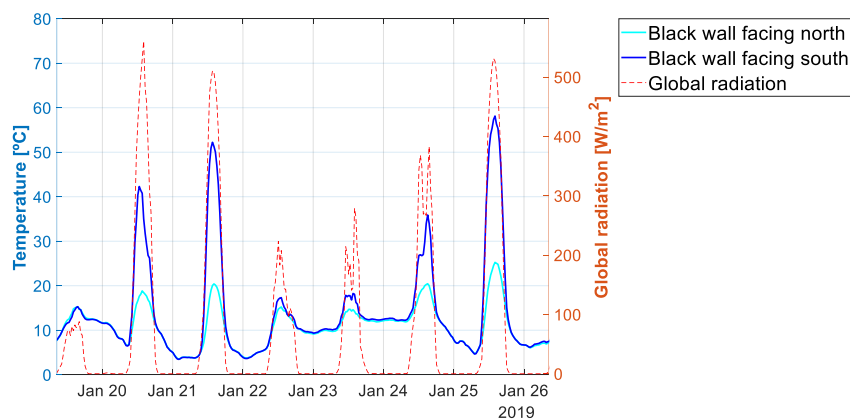
than the white wall, showing that it is more affected by the diffuse radiation. Thus, it can be stated that radiation phenomena largely affect the temperatures of ETICS surfaces.

### 5.3.2. Influence of ETICS walls orientation

To analyse the influence of the orientation on the ETICS temperature behaviour, the exterior surface temperatures are presented in Figure 5.9 and Figure 5.10, for the white ICB ETICS and black ICB ETICS walls, respectively. For this purpose, a winter week with cloudy and sunny days was selected. In order to correlate the surface temperature behaviour with solar radiation, the global solar radiation is also presented.



**Figure 5.9:** Surface temperature and global radiation in the ICB ETICS white walls.



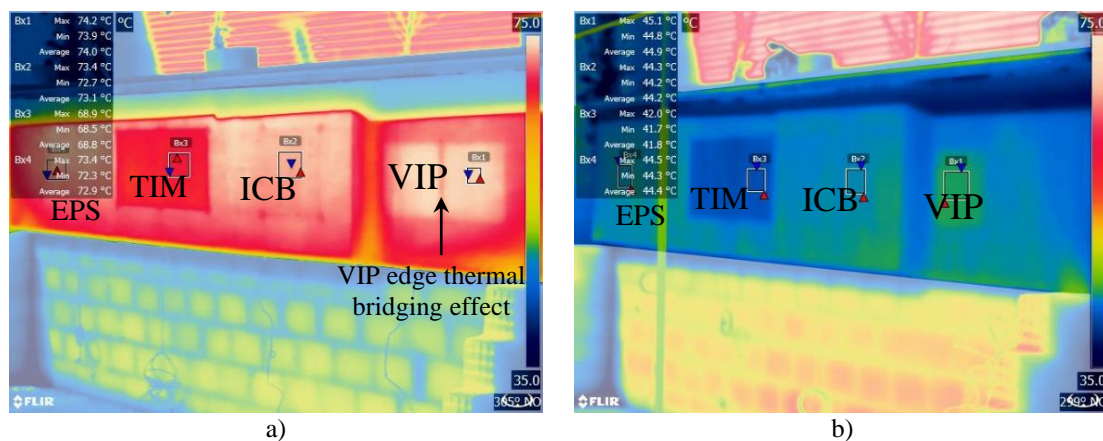
**Figure 5.10:** Surface temperature and global radiation in the ICB ETICS black walls.

The difference in surface temperature between ETICS walls facing North and South is noticeable, for both colours. As expected, in the case of the black wall, this difference is higher. The results measured during low solar radiation days should be highlighted. For instance, on 19<sup>th</sup> January the surface temperatures are similar for both colours and orientations. In opposition, in days with high

solar radiation (e.g. 25<sup>th</sup> January), the surface temperatures reached 58°C and 34°C for the black and white walls facing South, respectively, and 25°C and 17°C for the black and white North facing walls, respectively.

### 5.3.3. Infrared thermograms

Figure 5.11 shows infrared thermograms taken (at around the same time) of the two south-facing ETICS walls. In each, the temperature difference between the several insulation products is clearly visible. Also, the edge thermal bridging between VIPs is noticeable in Figure 5.11a. This is due to the fact that there is more heat transfer around the edges of the VIPs (composed by EPS). These thermograms also show the average apparent surface temperature measured over an area of each insulation material: VIP (Bx1), ICB (Bx2), TIM (Bx3) and EPS (Bx4).

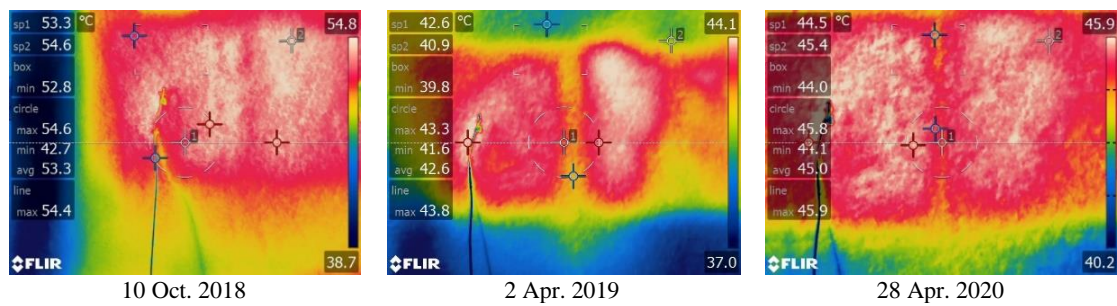


**Figure 5.11:** Thermograms taken of part the VIP south-facing walls: a) black wall; b) white wall.

In the white wall, the area insulated with TIM, identified as Bx3, shows an average surface temperature of 41.8°C, while the VIP panel (Bx1) shows a surface temperature of 44.9°C. At around the same time, the black wall shows a surface temperature of 68.8°C for TIM and 74.0°C for VIP, highlighting the impact that the insulation thermal conductivity and the finishing colour have on the ETICS surface temperatures.

During the monitoring period, periodic thermograms were taken in order to assess an eventual loss of vacuum in the VIP zone. Figure 5.12 illustrate some of the thermograms taken of the VIP area in the black wall. The clear difference in temperature that exists between the centre of the VIP panels and the EPS (surrounding the panels and located in the edge between panels) indicates that the two VIP panels have preserved their vacuum, as their low thermal conductivity is maintained. This finding is relevant since VIP long-term performance is crucial for increasing

confidence in this super-insulating material. The non-homogeneous temperature surface observed in the thermograms are related with the finishing coat roughness.



**Figure 5.12:** Thermograms of VIP black wall facing south on several dates.

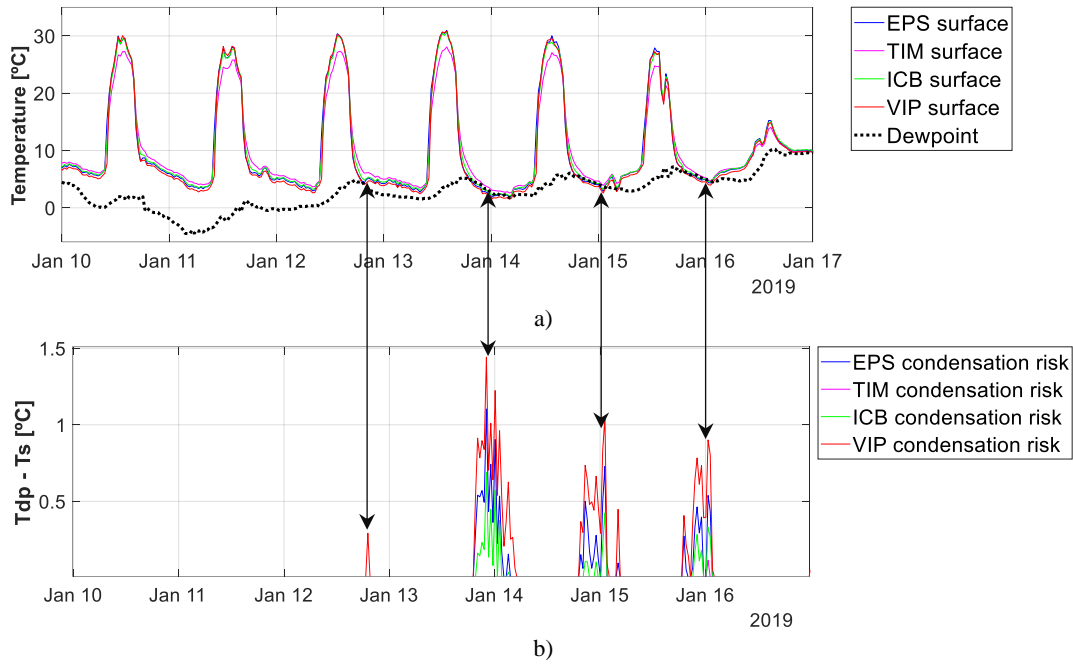
Although the case study walls did not present microbiological growth over the 24-months period of monitoring, some run-off marks were observed on both walls due to the failure of the walls copping. Also, in the south-facing black wall, a vertical crack on rendering system was visually detected. The crack with 20 cm extension and around 0.4 mm thick was observed in the EPS zone.

### 5.3.4. Surface condensation risk

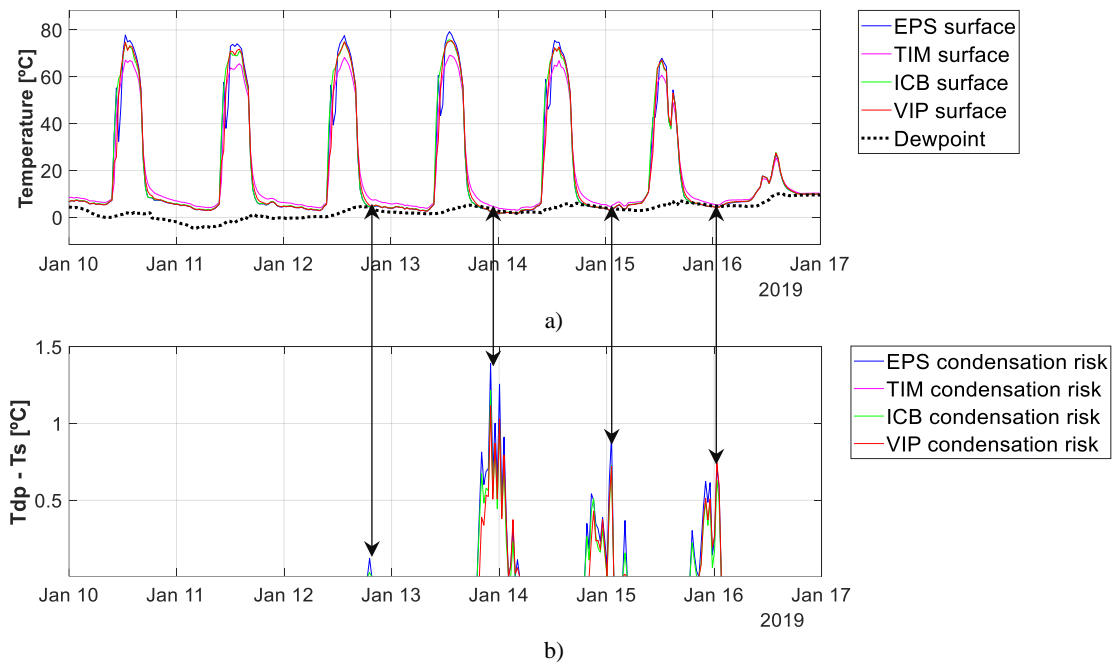
A surface condensation risk analysis was carried out based on the onsite measurements. Figure 5.13a compares the estimated dew point temperatures with the over insulation temperatures registered for each insulation product at the south-facing white ETICS wall. In order to better illustrate the risk of condensation occurring, the positive difference between dewpoint and surface temperatures is presented in Figure 5.13b, for each of the insulation solutions. This graph shows the times when surface condensation risk occurred, *i.e.* the registered surface temperature was lower than the dew point. Similarly, Figure 5.14 provides the same analysis for the black ETICS wall. These results indicate that higher levels of insulation (namely VIP panels) are more prone to surface condensation due to the cooling effect observed during the night-time.



*Onsite monitoring of VIP based ETICS in Coimbra: comparison of different exposure conditions and insulation materials*



**Figure 5.13:** Temperature in ETICS white wall faced south: a) surface curves  $T_s$  and dewpoint curve  $T_{dp}$ ; b) positive temperature difference between dewpoint  $T_{dp}$  and surface temperatures  $T_s$ .



**Figure 5.14:** Temperature in ETICS black wall faced south: a) surface curves  $T_s$  and dewpoint curve  $T_{dp}$ ; b) positive temperature difference between dewpoint  $T_{dp}$  and surface temperatures  $T_s$ .

The percentage of time during which the surface temperatures are lower than the dew point temperature was calculated according to equation 5.5. Table 5.2 shows these condensation risk results for the south-facing walls, for a winter month (with higher condensation risk) and a representative spring month, namely: December 2018, during which an average external temperature of 11.8°C and relative humidity of 85.0% were registered; April 2019, during which the average temperature was 15.7°C and the average relative humidity was 75.3%.

**Table 5.2:** Percentage of time with condensation risk estimated for the south-facing walls in December 2018 and April 2019.

Insulation product	December 2018		April 2019	
	White wall	Black wall	White wall	Black wall
VIP	45.2%	40.3%	8.9%	7.3%
EPS	41.9%	40.5%	7.1%	7.6%
ICB	40.3%	39.8%	5.7%	7.0%
TIM	40.4%	34.8%	0.8%	0.7%

It can be observed that ETICS with higher levels of insulation (*i.e.* VIP solution) and a white coloured finishing coat are more susceptible to condensation phenomena and, consequently, to the development of microbiological growth. In turn, the TIM based ETICS solution presented the lowest risk of condensation due to its higher thermal conductivity (0.055 W/(m·K)).

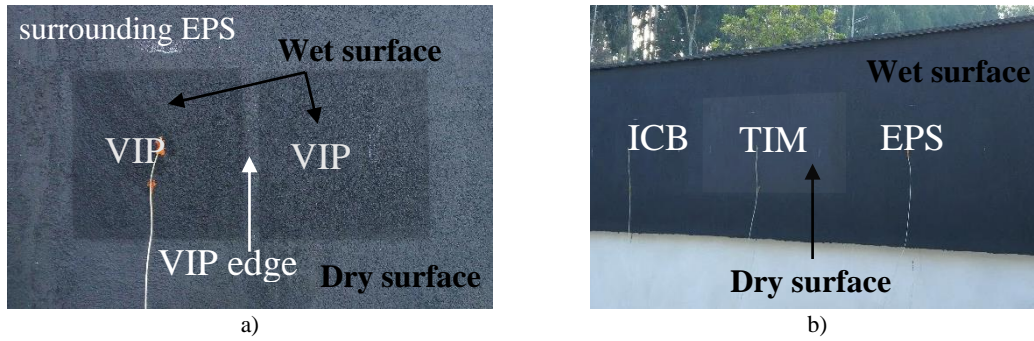
Similarly, Table 5.3 shows the percentage of time during which there was risk of condensation for the same winter month, namely January, in two different years (2019 and 2020). In 2019, January had an average external temperature of 10.5°C and an average relative humidity of 71.9%. In 2020, an average temperature of 10.4°C and an average relative humidity 76.6% were observed in the same month. When comparing both periods, the same conclusions are reached, namely higher condensation risk for higher levels of insulation.

**Table 5.3:** Percentage of time with risk of condensation estimated for the south-facing walls in January 2019 and January 2020.

Insulation product	January 2019		January 2020	
	White wall	Black wall	White wall	Black wall
VIP	25.0%	20.0%	24.4%	19.7%
EPS	19.7%	20.5%	19.5%	20.7%
ICB	16.2%	19.8%	17.0%	19.2%
TIM	9.6%	5.0%	5.9%	5.7%

During certain periods, the higher condensation risk associated with the VIP solution was also clearly visible through visual inspection of the walls. Figure 5.15 shows two photographs taken during the winter period at around 8.30 am. In Figure 5.15a, it is possible to see surface condensation along the outline of the VIP panels. The edge area between the two VIP (composed by EPS) and the area surrounding the panels (also in EPS) do not evidence surface condensation and appear to be dry.

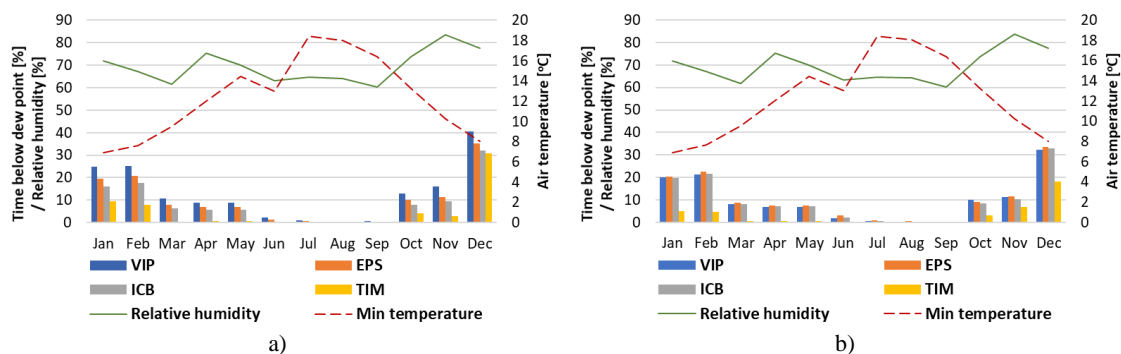
During these inspections, as can be seen in Figure 5.15b, it was also possible to find periods with surface condensation on all solutions except for the thermal mortar (TIM), the solution with highest thermal conductivity. This was also found to happen in the white wall, for both orientations.



**Figure 5.15:** Surface condensation observed during the morning period in winter in the black walls: a) VIP centre of panel condensation; b) TIM without condensation.

These visual findings are in line with the experimental measurements and condensation risk calculations, highlighting the influence of the insulation thermal conductivity on the surface condensation risk.

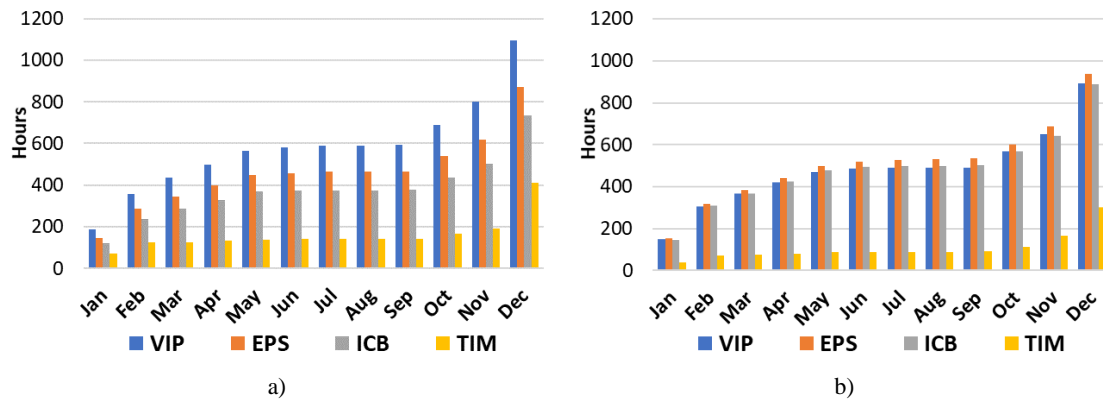
For a more complete analysis, the condensation risk estimated throughout an entire year of 2019 for the south-facing white and black free-standing walls is presented in Figure 5.16. The average relative humidity and mean minimum air temperature for each month are also presented. The surface condensation risk is much higher in the colder months during which the relative humidity is higher. It can be seen that the solution in the white wall have a higher risk of surface condensation than in the black wall. Also, it can be observed that a higher thermal resistance of the insulation layer contributes to increasing the risk of surface condensation. This is notable when comparing the VIP solution with other insulating solutions, particularly in the white wall, during winter time. In opposition, the thermal mortar solution is the one with lowest condensation risk.



**Figure 5.16:** Annual condensation risk analysis for different ETICS solutions: a) white wall; b) black wall.

Although the thermal resistance of both VIP (4 cm) and EPS (8 cm) solutions are quite different ( $5.33 \text{ (m}^2 \cdot \text{K)/W}$  against  $2.22 \text{ (m}^2 \cdot \text{K)/W}$ ), the condensation risk is similar. The long-term monitoring showed that, on a monthly basis, the condensation risk of the conventional EPS based ETICS solution only differed 5.3% at maximum in comparison with the VIP based ETICS. This may be due to the fact that VIP panel is encapsulated in a 10 mm covering layer of EPS. This external layer may be responsible for bringing the results closer to each other.

The accumulated hours of condensation risk estimated for the entire year of 2019 for the south-facing white and black walls are presented in Figure 5.17. The white ETICS wall (Figure 5.17a) revealed some differentiation as a function of the thermal resistance of each insulation material. Accumulated periods of 1095h, 873h, 735h and 412h, were calculated for VIP, EPS, ICB and TIM, respectively. However, there is no clear correlation between the accumulated hours of condensation and the thermal resistance of each insulation material in the black wall (Figure 5.17b).



**Figure 5.17:** Accumulated hours of surface condensation risk for different ETICS solutions: a) white wall; b) black wall.

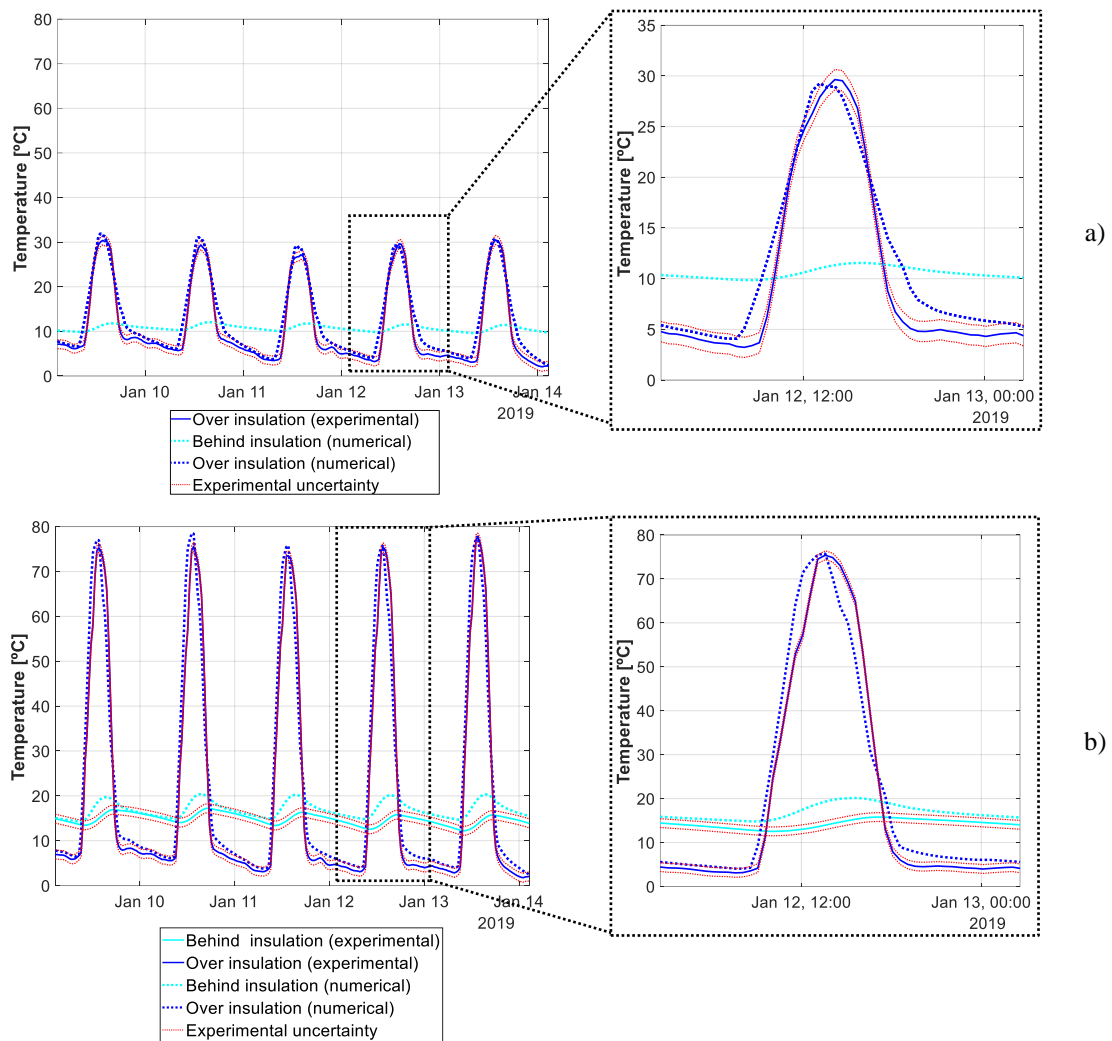
Similar findings were found for the north-facing walls. However, in this case, the percentage of time in which there is risk of condensation increases around 18%, when compared with the south-facing walls.

### 5.3.5. Numerical modelling results

The numerical modelling tool BISTRA was used to simulate transient temperature measurements. By comparing the experimental and numerical results, this study contributes to increasing the confidence in using such tools to assess condensation risk in ETICS based solutions located in different climates and with varying parameters. This section presents numerically obtained temperature results for a homogenous insulation material (EPS) and for the VIP solution, which are compared with the experimentally measured ones.

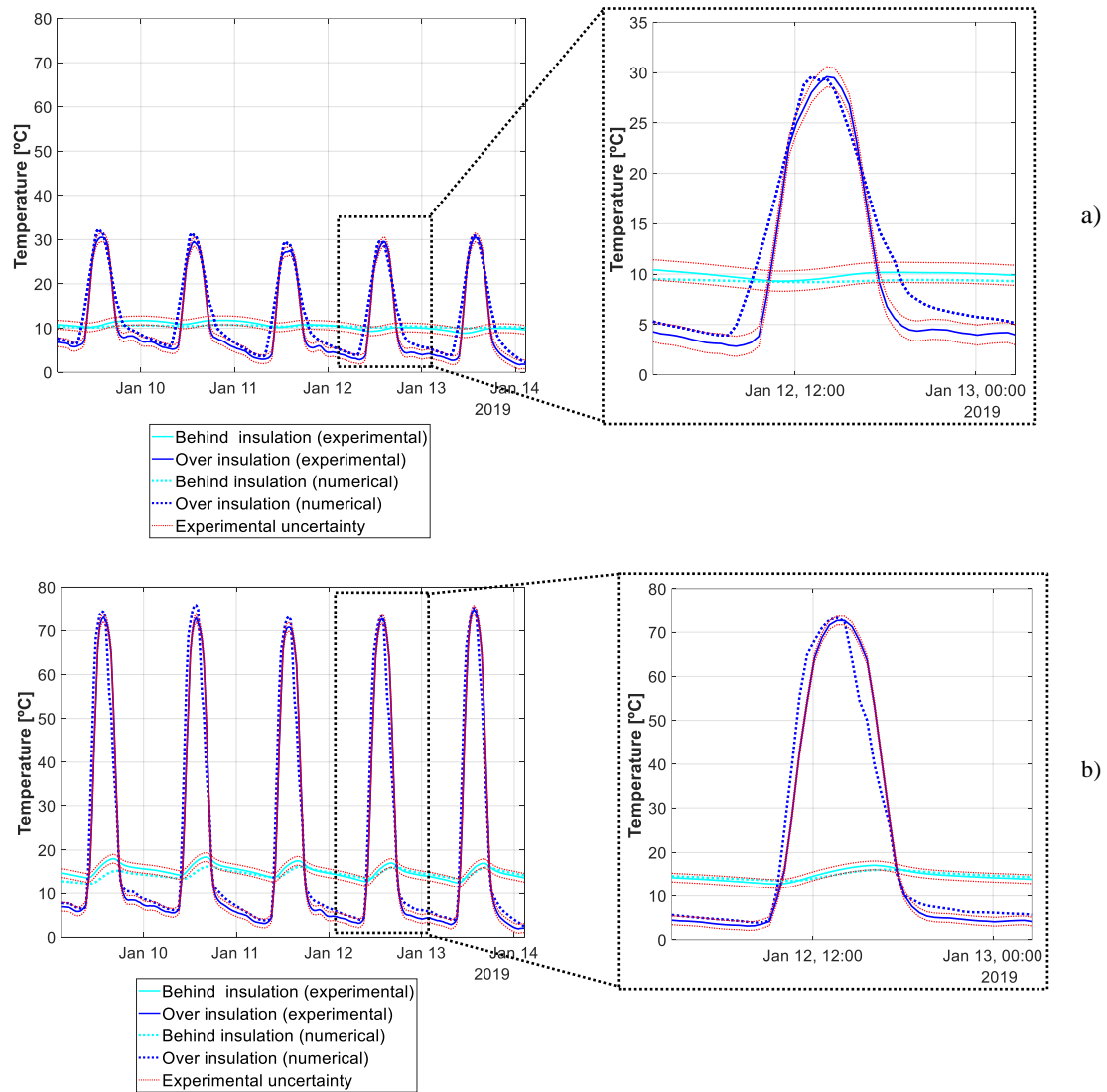
Figure 5.18 shows the comparison between numerical results and experimental measurements for a south-facing EPS wall, considering both a white and a black finishing coat. The temperatures presented in the graphs are for behind the thermal insulation (interface 1) and over the insulation (interface 2). Surface temperatures (interface 3) were not simulated, since there is high

measurement uncertainty related with temperature measurement at the surface of the finishing coat (thermocouple contact with a roughness surface), as well as, with the conditions of exposure.



**Figure 5.18:** Temperatures in a south-facing EPS wall, during winter: a) white colour; b) black colour.

Figure 5.19 shows the comparison between numerical results and experimental measurements, for a VIP based ETICS wall, considering both white and black finishing coats.



**Figure 5.19:** Temperatures in a south-facing VIP wall, during winter: a) white colour; b) black colour.

In general, a good correlation between experimental measurements and numerical results was found. Most of numerical temperature deviations are within the uncertainty of the experimental temperature measurements ( $\pm 1^\circ\text{C}$ ). The greater deviations (around  $3^\circ\text{C}$ ) were found in the late afternoon for both EPS and VIP ETICS walls.

## 5.4. Conclusions

This chapter presented onsite monitoring results for ETICS walls located in Coimbra (Mediterranean climate) which have been built with different insulation materials. Different finishing coat colours and orientations were also analysed.

The thermal conductivity of the insulation material and the optical properties of the finishing coat colour revealed to be a determining factor regarding the thermal behaviour of ETICS walls. During the experimental campaign carried out, the ETICS solution containing the encapsulated VIP showed the highest temperature amplitudes, while the lowest were registered for the material with the highest thermal conductivity (thermal insulation mortar). The highest temperatures were registered during the day on the walls with the dark finishing coat, while the lowest temperatures during the night were registered in the white finishing coat walls. Also, the orientation of ETICS walls was found to be relevant on the surface temperature behaviour, mainly due to the direct solar radiation.

After more than 24 months of monitoring, the VIP based ETICS did not showed early signs of anomalies. However, temperature measurements showed that walls with a greater insulation capacity finished with a white coloured surface are more likely to develop surface condensations, and consequently, microbiological growth. However, the risk of condensation of VIP based ETICS walls was not shown to be significantly higher than EPS based ETICS walls.

Numerical simulations achieved accurate results when compared with experimental measurements. Reliable input data, in particular regarding the optical properties of the finishing coat and the environmental factors, such as convective phenomena and solar radiation, are crucial for a good correlation with the model.

It should be noted that, even though it has been shown that the colour of the finishing coat has significant influence on the behaviour of ETICS, optical properties of the coating are currently not taken into account in the standard assessment methods for ETICS. Optical properties, such as emissivity and solar reflectance, have great impact on surface temperature, particularly in façades exposed to direct solar radiation. Thus, further research should be conducted to assess the impact that solar radiation has on long-term behaviour of innovative ETICS solutions. Also, the monitoring of VIP ETICS façades in real buildings applications could be useful to deepen the knowledge about the behaviour of vacuum products during service life. New accelerated ageing procedures should be developed to better evaluate ETICS performance, namely with different finishing options (*i.e.* colours) and to help developing more resistant rendering systems.

This work focused on some challenges that need to be taken into account when using super-insulating materials in ETICS, namely the greater temperature stress and risk of surface condensation occurring. The results presented may be useful for the industry, since there is growing interest in developing innovative solutions with high thermal performance and reduced thickness. The onsite long-term monitoring will also contribute to improve the confidence of the building sector in the use of ETICS incorporating innovative materials.

## References

- [1] A. M. Raimundo, N. B. Saraiva, A. V. M. Oliveira, “Thermal insulation cost optimality of opaque constructive solutions of buildings under Portuguese temperate climate”, *Build. Environ.* vol. 182, 107107, 2020, doi:10.1016/j.buildenv.2020.107107.
- [2] S. Tadeu, A. Tadeu, N. Simões, M. Gonçalves, R. Prado, “A sensitivity analysis of a cost optimality study on the energy retrofit of a single-family reference building in Portugal”, *Energy Effic.* pp. 1–22, 2018 doi:10.1007/s12053-018-9645-5.
- [3] J. L. Parracha, G. Borsoi, I. Flores-Colen, R. Veiga, L. Nunes, A. Dionísio, M. G. Gomes, P. Faria, “Performance parameters of ETICS: Correlating water resistance, bio-susceptibility and surface properties”, *Constr. Build. Mater.* vol. 272, 121956, 2021, doi:10.1016/j.conbuildmat.2020.121956.
- [4] B. Amaro, D. Saraiva, J. de Brito, I. Flores-Colen, “Inspection and diagnosis system of ETICS on walls”, *Constr. Build. Mater.* vol. 47, pp. 1257–1267, 2013, doi:10.1016/j.conbuildmat.2013.06.024.
- [5] B. Amaro, D. Saraiva, J. de Brito, I. Flores-Colen, “Statistical survey of the pathology, diagnosis and rehabilitation of ETICS in walls”, *J. Civ. Eng. Manag.* vol. 20, pp. 511–526, 2014, doi:10.3846/13923730.2013.801923.
- [6] M. D. Orazio, G. Cursio, L. Graziani, L. Aquilanti, A. Osimani, F. Clementi, C. Yéprémian, V. Lariccia, S. Amoroso, “Effects of water absorption and surface roughness on the bioreceptivity of ETICS compared to clay bricks”, *Build. Environ.* vol. 77, pp. 20–28, 2014, doi:10.1016/j.buildenv.2014.03.018.
- [7] H. Barberousse, B. Ruot, C. Yéprémian, G. Boulon, “An assessment of facade coatings against colonisation by aerial algae and cyanobacteria”, *Build. Environ.* vol. 42, pp. 2555–2561, 2007, doi:10.1016/j.buildenv.2006.07.031.
- [8] E. Barreira, V. P. de Freitas, “Experimental study of the hygrothermal behaviour of External Thermal Insulation Composite Systems (ETICS)”, *Build. Environ.* vol. 63, pp. 31–39, 2013, doi:10.1016/j.buildenv.2013.02.001.
- [9] H. M. Künzle, “Factors determining surface moisture on external walls”, in *Build. X.*, 2007.
- [10] K. Lengsfeld, M. Krus, “Microorganism on façades – reasons, consequences and measures”, Fraunhofer-Institute for Building Physics (IBP), Germany, 2001.
- [11] P. Johansson, A. Ekstrand-tobin, T. Svensson, G. Bok, “Laboratory study to determine the critical moisture level for mould growth on building materials”, *Int. Biodeterior. Biodegradation.* vol. 73, pp. 23–32, 2012, doi:10.1016/j.ibiod.2012.05.014.
- [12] D. Aelenei, F. M. A. Henriques, “Analysis of the condensation risk on exterior surface of building envelopes”, *Energy Build.* vol. 40, pp. 1866–1871, 2008, doi:10.1016/j.enbuild.2008.04.003.
- [13] S. Johansson, L. Wadsö, K. Sandin, “Estimation of mould growth levels on rendered façades based on surface relative humidity and surface temperature measurements”, *Build. Environ.* vol. 45, pp.1153–1160, 2010, doi:10.1016/j.buildenv.2009.10.022.



- [14] M. N. Said, W. C. Brown, I. S. Walker, “Long-term field monitoring of an EIFS clad wall”, *J. Therm. Envel. Build. Sci.* vol. 20 pp. 320–338, 1997, doi:10.1177/109719639702000405.
- [15] I. Dirkx, Y. Grégoire, Evaluation of the resistance to algae growth of ETICS, APFAC, 4<sup>o</sup> Congresso Português de Argamassas e ETICS, Coimbra, (2012).
- [16] I. Mandilaras, I. Atsonios, G. Zannis, M. Founti, “Thermal performance of a building envelope incorporating ETICS with vacuum insulation panels and EPS”, *Energy Build.* vol. 85, pp. 654–665, 2014, doi:10.1016/j.enbuild.2014.06.053.
- [17] *European Assessment Document: External Thermal Insulation Composite Systems with rendering*, EAD 040083-00-0404, European Organisation for Technical Approvals, 2019
- [18] *Thermal performance of building materials and products - Determination of thermal resistance by means of guarded hot plate and heat flow meter methods - Products of high and medium thermal resistance*, EN 12667, European Committee for Standardization, 2001.
- [19] *Thermal performance of building materials and products - Determination of thermal resistance by means of guarded hot plate and heat flow meter methods - Dry and moist products of medium and low thermal resistance*, EN 12664, European Committee for Standardization, 2001.
- [20] *Thermal insulation for buildings - Reflective insulation products -Determination of the declared thermal performance*, EN 16012+A1, European Committee of Standardization, 2012.
- [21] *Standard Test Method for Solar Absorptance, Reflectance, and Transmittance of Materials Using Integrating Spheres*, E903-12, ASTM International, 1996.
- [22] M. Kottke, J. Grieser, C. Beck, B. Rudolf, F. Rubel, “World map of the Köppen-Geiger climate classification updated”, *Meteorol. Zeitschrift.* vol. 15, pp. 259–263, 2006, doi:10.1127/0941-2948/2006/0130.
- [23] F. Rubel, K. Brugger, K. Haslinger, I. Auer, “The climate of the European Alps: Shift of very high resolution Köppen-Geiger climate zones 1800-2100”, *Meteorol. Zeitschrift.* vol. 26, pp.115–125, 2017, doi:10.1127/metz/2016/0816.
- [24] climatedata.eu, “Temperature - Precipitation – Sunshine”, <https://www.climatedata.eu/> (accessed September 17, 2019).
- [25] *Thermal insulation – qualitative detection of thermal irregularities in building envelopes – infrared method*, ISO 6781, International Organization for Standardization, 1983.
- [26] Sensirion, “Dew-Point Calculation”, pp. 1–3, 2006, [www.sensirion.com/humidity](http://www.sensirion.com/humidity).
- [27] *BISTRA - 2D transient heat transfer*, (version 4.0w). Physibel. <http://www.physibel.be/bistra.htm>.
- [28] *Thermal performance of building components - Dynamic thermal characteristics - Calculation methods*, EN ISO 13786, International Organization for Standardization, 2006.
- [29] *Building components and building elements - Thermal resistance and thermal transmittance - Calculation method*, ISO 6946, International Organization for Standardization, 2017.



## **CHAPTER 6**

# **LABORATORY ASSESSMENT OF THE HYGROTHERMAL PERFORMANCE OF THE VIP BASED ETICS**



## **6. Laboratory assessment of the hygrothermal performance of the VIP based ETICS**

### **6.1. Introduction**

Over the recent years, a lot of research has been carried out focusing on vacuum insulation panels (VIPs), namely looking to increase their thermal performance ([1],[2],[3]) and service life ([4],[5],[6]), and to reduce production costs ([7],[8]). Batard *et al.* [9] modelled the long-term hygrothermal performance of a VIP panel and showed the importance that external temperature and humidity conditions have on long-term VIP thermal performance, revealing the need to study further the behaviour of VIPs under real solicitations during their service life. As stated in chapter 2, there is a lack in knowledge regarding long-term performance and potential anomalies when VIPs are used as the thermal insulation layer in External Thermal Insulation Composite Systems (ETICS).

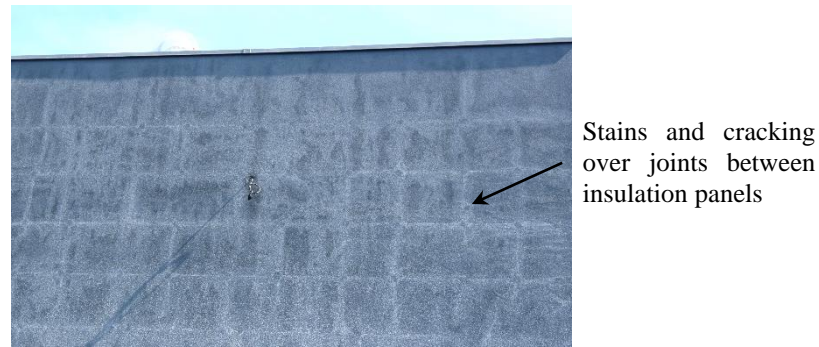
Some researchers have been studying the degradation of onsite conventional ETICS for a long time. Amaro *et al.* [10] inspected 146 ETICS façades located in Portugal aged from 3 to 22 years in which more than 450 anomalies were registered. In Italy, Stazi *et al.* [11] observed the state of conservation of an EPS-based ETICS façade with 20 years and concluded that the ETICS solution was still effective from the hygrothermal performance point of view. However, cracking occurred due to overheating and differential temperature dilatation, particularly when facing south (where higher temperature amplitudes are found). Onsite inspections are useful for understand the real behaviour of innovative solutions under real dynamic agents, such as the research studies presented in chapters 4 and 5. Nevertheless, a longer period of monitoring would be needed to evaluate the natural ageing performance degradation over time. Therefore, in order to properly validate innovative solutions, it is crucial to carry out experimental work and obtain reliable data by means of accelerated ageing tests under controlled conditions.

According to ISO 15686-1 [12] degradation agents can be classified into five categories: thermal (*e. g.* heat, frost and thermal shock); mechanical (*e. g.* impacts); electromagnetic (*e. g.* solar/UV radiation); biological (*e. g.* moulds and fungi) and chemical (*e. g.* carbonic acid). However, the

ageing cycles test method proposed by the European Assessment Document (EAD) for ETICS [13] does not include solar radiation. The proposed method is based on EN 16383 [14] which defines the test procedures for determining the hygrothermal behaviour of ETICS by means of performing heat-rain cycles and freeze-thaw cycles. This standardized hygrothermal cycles test procedure [14] has been used to validate new ETICS and to study innovative solutions. For example Xiong *et al.*, used this procedure to study the temperature field of ETICS cladding system with finishing colourful steel plate [15] and to evaluate the hygrothermal deformation of ETICS cladding system with glazed hollow bead [16]. Nevertheless, optical properties of the rendering, such as emissivity and solar reflectance, have been generally disregarded in laboratory test assessments. A few works have applied accelerated solar ageing using UV radiation, however focusing on small samples only. Parracha *et al.* [17] evaluated the durability of the rendering system of conventional ETICS by exposing small samples to an accelerated ageing procedure, including hygrothermal cycles, UV radiation and air pollutants exposure. The results showed that the combined effect of the ageing cycles changed rendering properties, such as the colour and the surface roughness, hardness and gloss. However, to simulate radiation using only UV is not representative of real solar radiation conditions of weather exposure.

In this chapter, the author is looking to go further in the study of the effects of solar radiation on ETICS walls. Theoretical calculations [18] have shown that walls exposed to direct solar radiation reach surface temperature values that are much greater than the external air temperature. For example, in typical temperate climates, an air temperature range of 10 to 27°C implies surface wall temperatures of up to 45°C. This phenomenon, as also mentioned in chapters 4 and 5, contributes to an early degradation of the rendering system, especially in ETICS with thin rendering.

To mitigate the thermal stress of the ETICS rendering system, and consequently reduce the risk of cracking occurring, ETICS manufacturers [19] do not recommend finishing coat colours with solar absorptance coefficient higher than 0.7. In fact, optical properties such as emissivity and solar reflectance are known to have an impact on the surface temperature (as demonstrated in chapter 5) and, consequently, on the potential degradation of the rendering system. Alonso *et al.* [20] analysed experimentally the influence of these parameters in three case studies, including a reference non-insulated double wall with air cavity and two retrofitting solutions: ventilated façade and ETICS. For similar surface colours, the ETICS case exhibited the highest visible and solar absorptance values, which led to higher external surface temperature (around 50°C) compared with the surface temperature recorded in the case of the double wall with air cavity wall (around 40°C). The solar absorptance of ETICS can be controlled using lighter colours, but an architectural aesthetic demand for dark colours has led to high ETICS surface temperatures [21]. Figure 6.1 shows an example of an EPS ETICS façade coloured with dark finishing coat that presents early anomalies, namely stains, discoloration and cracking associated with the joints between insulation panels.



**Figure 6.1:** Dark coloured ETICS façade with rendering anomalies.

Using super-insulating products will increase the temperature amplitudes endured by the rendering system. This may lead to increased occurrence of anomalies such as cracking, blistering, loss of flatness, amongst others, which calls for deeper research into these types of solutions.

In summary, the literature review reveals a gap in laboratory ageing tests for assessing vacuum-based ETICS applications. In particular, there is a need to explore test methods that analyse the solar radiation effect. Xenon lamps are often used as an artificial light source [22] since they can provide a faithful reproduction of solar energy distribution [23]. However, because of an excessive infrared radiation component and a low radiation efficiency in the UV/visible range, they are not suitable for use in large test chambers. For this reason, a metal halide lamp, which simulates total global radiation, is considered to be the best method for real scale test specimens [24].

The aim of the work presented in this chapter is to carry out an experimental test campaign to adequately assess the hygrothermal behaviour of an ETICS solution with VIPs. For this purpose, a three-stage test was proposed and carried out on a large-scale test specimen. First, temperature and heat flux measurements were performed in steady state conditions. In the second stage, heat-rain and freeze-thaw standardized cycles were performed to assess the solution as resistant to hygrothermal cycles. In the third stage, a new test procedure which includes solar radiation simulation was defined and carried out in order to evaluate the solution behaviour and assess the effect of the finishing colour on the ETICS behaviour. For this purpose, two finishing colours (white and black) were tested. Temperatures and heat fluxes were recorded to evaluate the thermal performance of the VIP based ETICS during and after ageing cycles. Visual and infrared thermography inspections were carried out to identify potential anomalies throughout the tests. Also, a crack microscope, a scanning electronic microscope (SEM) and a spectrophotometer were used to evaluate the surface degradation and colour change in samples removed after ageing tests. In order to assess the safety in use of the ETICS, mechanical tests such as bond strength and impact resistance were performed after the ageing cycles. Additionally, numerical calculations of 2D transient heat transfer were carried out in order to evaluate the accuracy of numerical models when simulating the thermal behaviour of VIP products, including the edge thermal bridging

effects. Numerical results were compared with those obtained experimentally. The validation of numerical modelling can be useful to increase the confidence of using these tools in real VIP applications in the design or use stage.

## **6.2. Materials and methods**

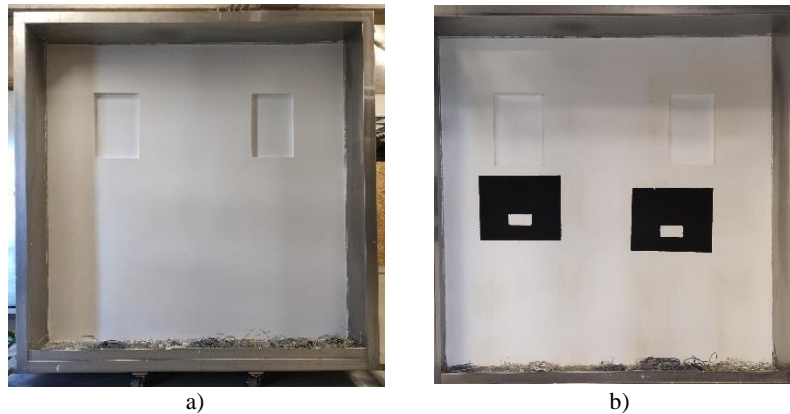
In this section, first, the test specimen consisting in a VIP based ETICS wall is presented, as well as the equipment and sensors used during the experimental campaign. Then, the experimental test methods and equipment used to evaluate the hygrothermal performance of ETICS walls are described. Finally, information is provided about the transient heat transfer simulations used to compare numerical modelling results with experimental measurements.

### **6.2.1. Test specimen and apparatus**

The test specimen is a 2.8 m x 2.8 m ceramic masonry wall with the VIP based ETICS solution. Figure 6.2 shows the test specimen installed in a rigid frame. The application of the ETICS system consisted in fixing an encapsulated vacuum insulation panel onto a base using adhesive and auxiliary mechanical fixing (4 plastic anchors per square meter and placed at VIP edge material) and covering it with a thin rendering system. The encapsulated VIP product consists in 20 mm fumed silica panels covered with a protective layer made of graphite EPS (10 mm thick on each side of the panel and 20 mm thick along the edges). Panels with 640 mm x 640 mm and 440 mm x 440 mm were used. EPS insulation with 40 mm thickness was used to fill out the remaining areas of the wall not covered with VIP product. Some joints between panels were filled with PU foam. Regarding the rendering system, a cement base coat mortar formulated from mixed binders, selected aggregates and additions, and an acrylic finishing coating with siloxane resins and marble granules were applied, including two finishing coat colour, white and black. For this purpose, after testing the white finishing coat specimen (Figure 6.2a), two zones with 700 mm x 550 mm



were painted black (Figure 6.2b). Two symmetrical openings with 400 mm x 600 mm are included in the testing rig to simulate the need for adjustments near a window.



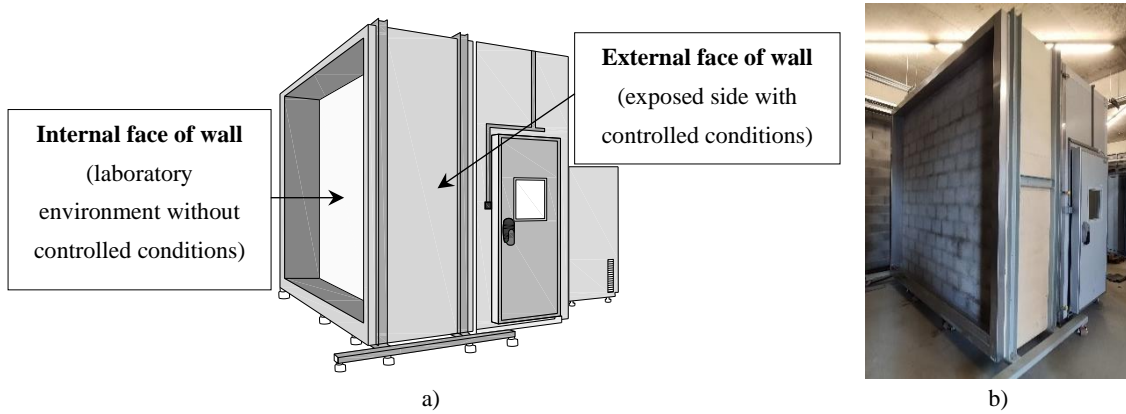
**Figure 6.2:** Test specimen of VIP based ETICS wall: a) photograph of the test specimen at initial state; b) photograph of the test specimen after black painting areas.

Additional information regarding the test specimen characteristics is presented in Table 6.1. The thermal conductivity values of the test specimen components were obtained in a guarded hot plate apparatus ( $\lambda$ -Meter EP500e) for an average temperature of 10°C, as recommended by the EN 12667 [25] and EN 12664 [26]. The solar reflectance of both finishing colours was determined in laboratory samples according to ASTM E903-96 [27], resulting in 0.74 for white finishing coat and 0.04 for black coating. Finishing coat emissivity was measured by means of TIR100-2 emissometer, which has a measurement uncertainty of  $\pm 0.01$ . The remaining properties are based in technical datasheets.

**Table 6.1:** Specimen components characteristics.

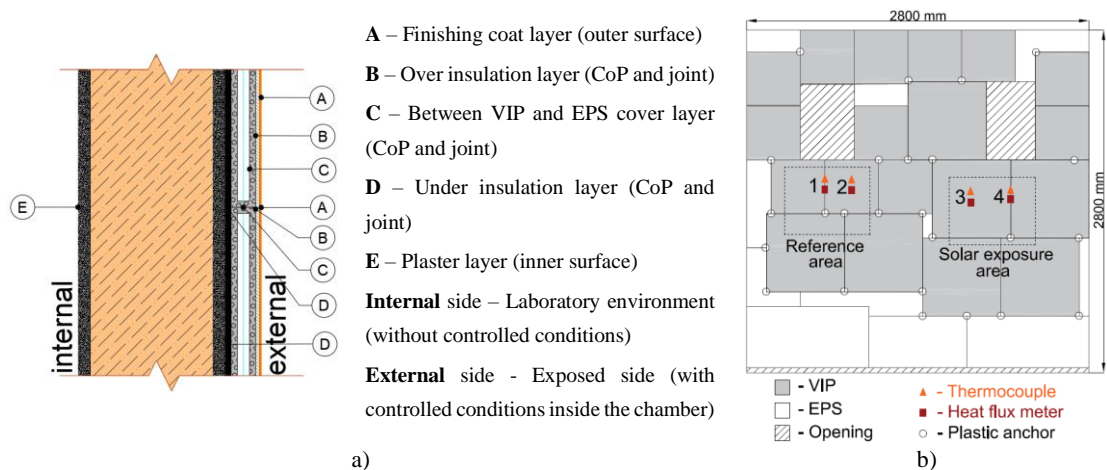
Component	Thickness [mm]	Product usage [kg/m <sup>2</sup> ]	Thermal conductivity [W/(m·K)]	Emissivity [-]	Density [kg/m <sup>3</sup> ]	Specific heat [J/(kg·K)]
Plaster	10	---	1.3	0.90	1650	840
Hollow brick	220	---	0.52	0.90	850	840
Levelling mortar	10	---	1.3	0.90	1650	840
Adhesive	10	5.5	0.45	0.90	1350	840
Encapsulated VIP	40	---	0.0075	0.90	129	900
Base coat	5	8.0	0.47	0.90	1350	840
Primer	<1	0.3	0.40	0.90	--	--
Finishing coat	2	1.4	0.40	0.93	1650	1000

The specimen was attached to a climatic chamber, as shown in Figure 6.3. The rig preparation was carried out by an experienced ETICS installer, following a detailed specimen layout and the recommendations of the products' manufacturers. Before starting the tests, the ETICS specimen was cured in a climate chamber for 28 days at 20°C and 60% relative humidity, as per the EAD 040083-00-0404 requirements [13].



**Figure 6.3:** Hygrothermal cycles apparatus: a) schematic drawing; b) photograph.





In order to monitor the thermal behaviour during the ageing tests, the specimen was instrumented with thermocouples and heat flux sensors. Figure 6.4 shows the specific placement of each sensor, namely at the centre of VIP panels (CoP) area and at the joint between panels area, as can be seen in Figure 6.4b. Thermocouples were placed along several layers of the cross-section of the wall (A to E) and heat flux sensors were placed over the insulation layer (interface B). Surface A sensors were used to control the conditions inside the chamber.



**Figure 6.4:** Sensor locations in the test specimen: a) cross-section; b) layout pattern.

Specifications of the equipment used to monitor and record the hygrothermal cycles resistance test is given in Table 6.2. An infrared thermography camera was used to assess the state of VIPs (*i.e.* check for eventual loss of vacuum) after their installation, as well as after the ageing cycles. Also, an albedometer was used to measure the global radiation provided by the radiation unit in order to help define the solar radiation simulations procedures. Regarding the heat flux sensors, previous validation of the measurements was carried out in a calibrated guarded hot plate (GHP) apparatus, resulting in an uncertainty of heat fluxes around 5%.

**Table 6.2:** Description of the equipment used in the hygrothermal cycles resistance test.

Item (model)	Description	Output	Illustration
Climatic chamber (FitoClima 1000 EC 50)	Climatic chamber with 14.5 m <sup>3</sup> of conditioned volume. Temperature range capacity of -20 to 150°C (± 5°C) and humidity of 10 to 98% (± 10%); Includes a water spraying system with 1±0.1 l/(min.m <sup>2</sup> ). This chamber is annually calibrated to accomplish the test procedure requirements.	Temperature control, relative humidity control and water spraying.	
Thermocouples (Type T thermocouples)	Thermocouple with temperature range between -270 to 370°C and accuracy ±1.0°C or 0.75%.	Temperature (°C)	
Heat flux sensor (FHF02SC-02)	Heat flux sensor with a measurement range (-10 to +10) x 10 <sup>3</sup> W/m <sup>2</sup> , a sensitivity of 5.5 x 10 <sup>-6</sup> V/(W/m <sup>2</sup> ) and an uncertainty of calibration of 5%.	Heat flux (W/m <sup>2</sup> ) and temperature (°C)	
Data logger (Keysight 34970A)	Data acquisition unit.	Data files	
Infrared camera (FLIR T630sc)	Infrared camera with accuracy: ±1°C or ±1% at 25°C; object temperature range: -40°C to 150°C; and resolution: 640 x 480 pixels.	Infrared thermograms	
Albedometer (Hukseflux SRA01)	Two identical pyranometer with measurement rang 0 to 2000 W/m <sup>2</sup> ; spectral range 285 to 3000 x 10 <sup>-9</sup> m and uncertainty <1.8%.	Global solar radiation (W/m <sup>2</sup> )	
Solar radiation simulation system (BF SUN 2500W)	BF SUN 2500W with a Osram HMI 2500W lamp, and an Electronic Power Supply Unit.	Solar radiation: UV-C, UV-B, UV-A, visible and infrared radiation	

## 6.2.2. Test procedures

In this section, the three stages of this work are described: stage (1) with steady state conditions, stage (2) consisting in the ageing hygrothermal cycles, and stage (3) with the cycles including solar radiation. This sequence was first carried out on an all-white finishing coat. Afterwards, two reference zones were painted black and stages 2 and 3 were repeated. Finally, steady state

conditions measurements were again carried out in order to evaluate the final thermal performance of VIPs after the hygrothermal and solar radiation ageing cycles.

### **6.2.2.1. Stage 1: steady-state condition**

The main goal of this stage was to check the monitoring conditions, including temperature and heat flux measurements, using steady state conditions. In this stage, the experimental U-value was estimated and compared with the theoretical U-value determined according to ISO 6946 [28]. For this purpose, the properties presented Table 6.1 were used, as well as the conventional values for internal and external surface thermal resistances of  $0.13 \text{ (m}^2 \cdot \text{K)/W}$  and  $0.04 \text{ (m}^2 \cdot \text{K)/W}$ .

Additionally, to allow for a comparison of the experimental measurements with numerical modelling results, the rig was subjected to some temperature steps:  $(0^\circ\text{C} \pm 5)^\circ\text{C}$ ;  $(20 \pm 5)^\circ\text{C}$ ,  $(30 \pm 5)^\circ\text{C}$ ,  $(40 \pm 5)^\circ\text{C}$  and  $(50 \pm 5)^\circ\text{C}$ . In each step, the temperature was kept constant during a period of at least 5 hours.

### **6.2.2.2. Stage 2: hygrothermal cycles resistance**

Hygrothermal resistance was assessed according to section 2.2.6 of ETICS EAD [13]. The test consists in inducing accelerated ageing on an ETICS sample by exposing the specimen to 80 heat-rain cycles and 5 freeze-thaw cycles. Observations regarding a change in characteristics or performance, such as blistering, detachment, crazing, or formation of cracks were recorded (during and at the end of the test).

First, the rig was subjected to a series of 80 heat-rain cycles, comprising the following stages:

- Heating to  $70^\circ\text{C}$  (increase for 1 hour) and maintaining of the temperature at  $(70 \pm 5)^\circ\text{C}$  and the relative humidity (RH) at 10 to 30% for 2 hours (total of 3 hours);
- Spraying water at  $(15 \pm 5)^\circ\text{C}$  for 1 hour at a rate of  $(1 \pm 0.1) \text{ l}/(\text{m}^2 \cdot \text{min})$ ;
- Drainage during 2 hours keeping the air chamber at  $(23 \pm 5)^\circ\text{C}$ .

Next, after at least 48 hours of conditioning at temperatures between  $10$  and  $25^\circ\text{C}$  and a minimum relative humidity of 50%, the same test rig is exposed to 5 freeze-thaw cycles of 24 hours comprising of the following stages:

- Exposure to  $(50 \pm 5)^{\circ}\text{C}$  (increase for 1 hour) and maximum 30% RH for 7 hours (total of 8 hours);
- Exposure to  $(-20 \pm 5)^{\circ}\text{C}$  (decrease for 2 hours) for 14 hours (total of 16 hours).

Additionally, and similarly to stage 1, the experimental measurements were compared to dynamic numerical modelling results.

### **6.2.2.3. Stage 3: solar radiation cycles resistance**

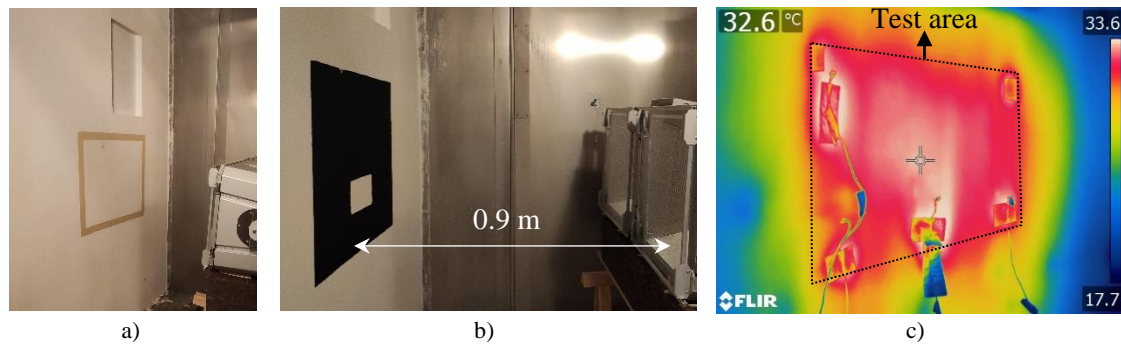
Stage 3 aims to propose a new test procedure to evaluate ETICS, which introduces the simulation of solar radiation. Since colour has a great impact on the surface temperatures due to the radiation effect, this new test method will introduce into the ageing test an additional agent which is sensitive to the coating colour.

The proposed test procedure consists in inducing accelerated ageing by exposing the specimen to controlled temperature, relative humidity and solar radiation intensity. The rig was subjected to 5 cycles, comprising of the following steps:

- Heating to  $35^{\circ}\text{C}$  (increase for 1 hour) and maintaining the temperature at  $(35 \pm 5)^{\circ}\text{C}$  and the relative humidity (RH) at 20 to 30% for 1 hour (total of 2 hours);
- Maintaining the temperature at  $(35 \pm 5)^{\circ}\text{C}$  and turning the solar radiation lamps on at a setpoint of  $(1100 \pm 100) \text{ W/m}^2$  during 5 hours;
- After turning off the solar radiation lamps, cooling the air chamber within 2 h to a temperature of  $(-20 \pm 5)^{\circ}\text{C}$  and maintaining it for 15 hours (total 17 hours).

For this purpose, an apparatus composed by two BF SUN 2500W lighting systems, each with a metal halide lamp Osram HMI 2500 W, and an electronic power supply unit with intensity control 40 to 100% was installed inside the hygrothermal chamber, 0.9 m away from the test specimen. This artificial global radiation system accomplishes the requirements for automobile industry ageing tests [24], simulating the wave length spectral range of 230-3000 nm, which includes UV-C, UV-B, UV-A, visible and infrared radiation.

Based on preliminary tests, a representative area with homogeneous solar radiation incidence of around 700 mm x 550 mm was defined, as can be seen in Figure 6.5. This test area includes monitoring zone 3 (VIP CoP) and zone 4 (VIP joint) shown in Figure 6.4. To help the definition of this representative area, assuring homogenous temperature within the representative area, infrared thermography (Figure 6.5c), as well as, surface thermocouples were used. A similar area which is not directly affected by the lamps and includes zone 1 (VIP joint) and zone 2 (VIP CoP) was also defined to be used as a reference.



**Figure 6.5:** Experimental apparatus to simulate artificial solar radiation: a) white finishing coat; b) black finishing coat c) preliminary infrared thermogram.

An albedometer was used to measure global radiation and help define the intensity control of the lamps. In order to verify the radiation distribution within the radiation test area, the albedometer was placed in 9 different positions located 230 mm away from the wall surface. A standard deviation of  $87 \text{ W/m}^2$  was verified within test area. This deviation is in line with radiation intensity requirement [24] that shall be within 10% of the desirable value, which in this study is  $1100 \text{ W/m}^2$ . This solar radiation set-point was defined based on the maximum solar radiation found in the summer of 2019 in Portugal, according to the onsite measurements recorded at Itecons.

### 6.2.3. Test specimen inspection

In order to identify possible anomalies, such as blistering, cracking, finishing coat pulverulence (superficial loss of cohesion), amongst others, the test specimen was inspected during and after the ageing tests. The cracks width was measured by means of a Controls microscope, model 53-C02018, with 40x magnification and a measuring range of 4 mm.

Also, the thermal performance of VIP panels was assessed after each stage. For this purpose, the heat flux and temperature measurements obtained during steady-state periods were used to calculate the U-value of the ETICS wall.

After the experimental testing campaign, a SEM Phenom, model 800-07334, with resolution  $<17 \text{ nm}$  and an electron optical magnification range of 80-100000x was used to analyse potential degradation of the finishing coat microstructure. Also, the colour change of the finishing coat system was analysed by CIELAB method [29], by means of spectrophotometer Perkin Elmer, model Lambda 35, with an illuminant D65, an observation angle of  $10^\circ$  and a diffuse xenon lamp which simulates daylight. Colour measurements were carried out in the visible spectrum, within 700 to 380 nm.

The colour change was analysed by numerical comparison of the colorimetric parameters of samples removed from both the area exposed to solar radiation and the reference area (not affected by solar radiation). For this purpose, both white and black samples that had been subjected to radiation were removed from the specimen. The absolute differences in colour coordinates between the test samples are expressed as  $\Delta L^*$  (difference in terms of lightness),  $\Delta a^*$  (difference in red and green) and  $\Delta b^*$  (difference in yellow and blue). Finally, the total colour difference,  $\Delta E^*_{ab}$ , using the three coordinates is obtained according to the equation 6.1 [30]:

$$\Delta E^*_{ab} = \sqrt{(\Delta L^*)^2 + (\Delta a^*)^2 + (\Delta b^*)^2} \quad (6.1)$$

Finally, in order to assess the mechanical behaviour of the VIP based ETICS after the hygrothermal cycles campaign, mechanical tests were carried out, namely bond strength test resistance and hard body impact resistance were carried out.

The assessment of the bond strength between the base coat and the encapsulated VIP was carried out in accordance with the test procedure of ETICS EAD section 2.2.11.1 [13] over the test specimen wall. For this purpose, five squares with 50 mm x 50 mm were cut through the base coat and square metal plates of the same size were affixed to these areas with a suitable epoxy adhesive. The pull-off test was performed by means of a portable pull-off equipment, model 58-C02157T by Controls with an accuracy of 2% and a tensioning speed of  $10 \pm 1$  mm/minute. The mean failure resistance was based on the results of five tests. Two bond strength resistance tests after ageing were carried out, namely at the reference area and at the area exposure to solar radiation.

The hard body impact test was performed on the test specimen after ageing cycles campaign, in accordance with ISO 7892 [31] and ETICS EAD section 2.2.8 [13] test procedures. The test consists in carrying out 5 hard body impacts (10 Joules) with a steel ball weighing 1.0 kg from a height of 1.02 m, and 5 impacts (3 Joules) with the steel ball weighing 0.5 kg and from a height of 0.61 m. In each, the diameter of the impact is measured and recorded, as well as the presence of any cracks at the impact point. According to observations ETICS correspond to categories of impact resistance I, II, III in accordance with ETICS EAD [13] classification.

## **6.2.4. Numerical modelling**

Experimental campaigns such as those carried out in this study are time consuming and can become very expensive. Therefore, if reliable, numerical models can be a useful tool in understanding the hygrothermal behaviour of innovative constructive solutions, such as VIP based ETICS, under dynamic boundary conditions. In line with the other chapters of this thesis,

2D transient heat transfer simulations were performed using BISTRA software version 4.0w [32] from Physibel.

The estimated properties of the materials used in the specimen considered in the modelling are presented in Table 6.1. A triangular mesh with around 220000 nodes with 20 pixels (2 mm) each was selected. The calculation parameters were defined in 5 iteration cycles with a maximum number of 10000 iterations per cycle, considering a maximum temperature difference of 0.0001°C and maximum heat flow divergence of 1% for any node. The simulations were performed using, as boundary conditions, the external and internal air temperatures recorded during the tests with timestep of 1 minute. Based on preliminary simulations and considering the ventilation intensity of the climatic chamber, constant heat transfer coefficients of 8 W/(m<sup>2</sup>·K) (internal side) and 11 W/(m<sup>2</sup>·K) (external side) were used.

## **6.3. Results and discussion**

This section presents and discusses the main results of the laboratory assessment of the hygrothermal performance of an external vacuum-insulation composite system, considering the three stages of this work previously described. Also, a complementary analysis which includes cracking measurements, colour change and thermal performance assessment, is presented. Finally, a summary of the main findings of this experimental work is provided.

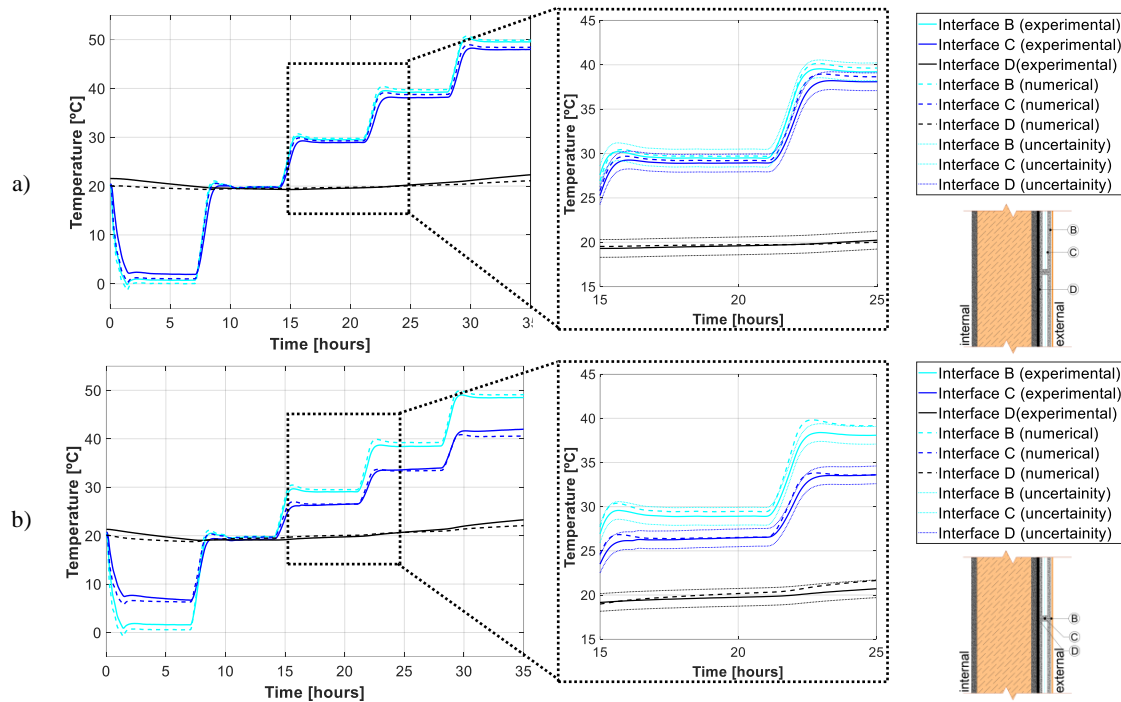
### **6.3.1. Stage 1: steady state condition results**

Stage 1 was carried out to check the monitoring conditions and to assess the real thermal transmittance of the wall system under steady conditions. Furthermore, in order to evaluate the potential use of numerical models to analyse the VIP based ETICS behaviour, the experimental results were compared with the numerically obtained ones, for both centre of panel (CoP) and joint areas.



### 6.3.1.1. Temperature measurements

Figure 6.6 presents temperatures measured both in the centre of panel (CoP) and in the joint between panels. The graphs show results registered at the several interfaces along the wall (B to D), as presented in Figure 6.4. The experimental uncertainty and the numerical results are also provided. The sources for uncertainty are the thermocouples and the datalogger accuracy.



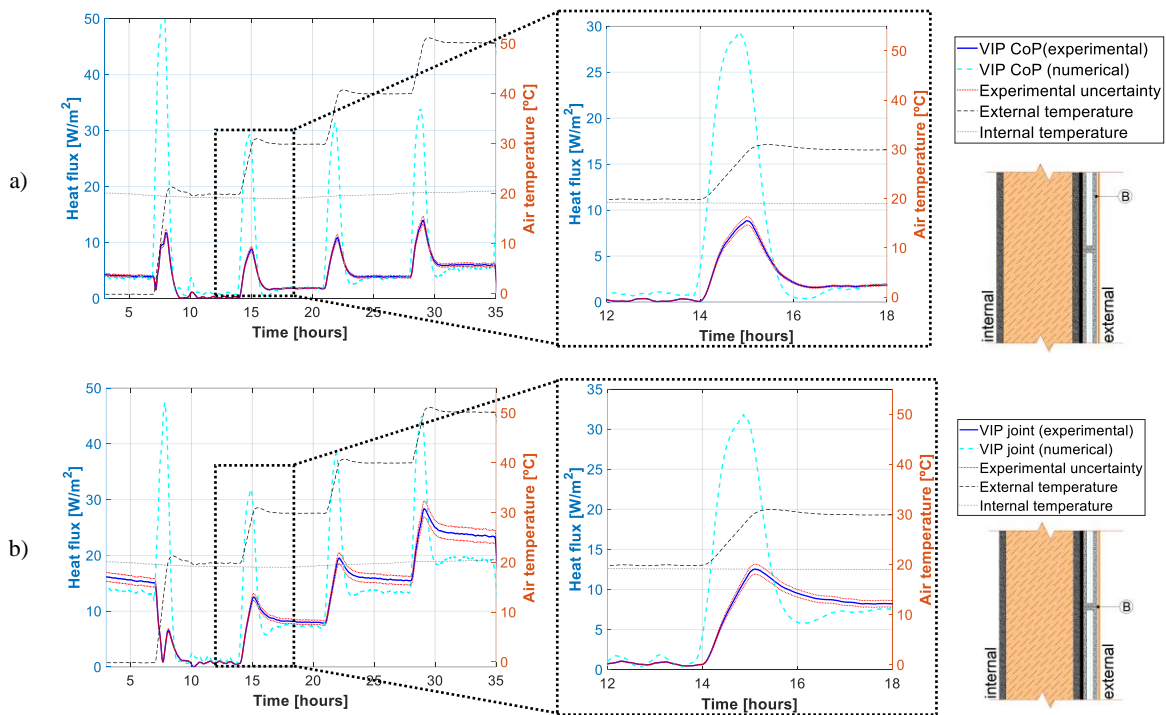
**Figure 6.6:** Temperatures results along the wall with white finishing coat: a) CoP area (zone 3); b) joint area (zone 4).

The numerical results are in good agreement with the experimental measurements over the insulation (interface B), between VIP and EPS cover layer (interface C) and behind the insulation (interface D). Comparing the experimental measurements with numerical results, a maximum difference of around 1.5°C was observed. Most of the temperature differences are within the uncertainty of thermocouples measurements.

### 6.3.1.2. Heat flux measurements

Figure 6.7 shows the heat flux measurements recorded in the CoP and joint areas, as well as the corresponding numerical results. Good agreement is observed in each level of steady state regime. However, it can be seen that the numerical model provided inaccurate results during each

temperature increase. These deviations were found to be greater in the VIP joint areas, possibly due to air gaps between panels not being considered in the model.



**Figure 6.7:** Heat fluxes results in the wall with white finishing coat: a) CoP area (zone 3); b) VIP joint area (zone 4).

It should be noted that heat fluxes measured in the VIP joint area were up to 4x higher than those measured in the centre of panel (CoP) area as a result of the edge thermal bridging effect. This is due to the higher thermal conductivity of the EPS (when compared with the VIP CoP) used to cover the encapsulated VIP product, as well as due to the edge thermal bridging effect caused by the laminate film barrier (envelope of each VIP). Thus, it can be said that the use of larger sized panels is recommended for better overall façade performance. However, the production, transport and installation of larger panels may not always be technically and economically feasible, hence a balance between technical and performance aspects should be achieved.

### 6.3.1.3. Thermal transmittance estimation

Heat fluxes measured over the insulation layer and temperatures recorded inside and outside the chamber (presented in Figure 6.7) were used to estimate the thermal transmittance coefficient (U-value) of the test specimen. For this purpose, the results recorded in the last hour of each steady state level were considered. Table 6.3 compares the theoretical U-values (according to ISO 6946

[28]) with those calculated using the experimental measurements for the different boundary conditions in terms of temperature gradient ( $\Delta T$ ).

**Table 6.3:** Thermal transmittance estimation for several boundary conditions.

	$\Delta T$ [°C]	Heat flux [W/m <sup>2</sup> ]	U-value [W/(m <sup>2</sup> ·K)]	Theoretical U-value [W/(m <sup>2</sup> ·K)]	U-value deviation [%]
	-20.1	-3.426	0.171		1.8%
<b>VIP CoP (zone 3)</b>	10.6	1.924	0.182	0.168	8.3%
	20.0	3.733	0.187		11.3%
	29.7	5.644	0.190		13.1%

When compared with the theoretical values calculated according to ISO 6946, the experimental results show an average difference of around 9%. This can be considered an acceptable deviation, taking into account the experimental measurement uncertainty and the temperature dependence of the material's thermal conductivity which was not considered.

## 6.3.2. Stage 2: hygrothermal cycles results

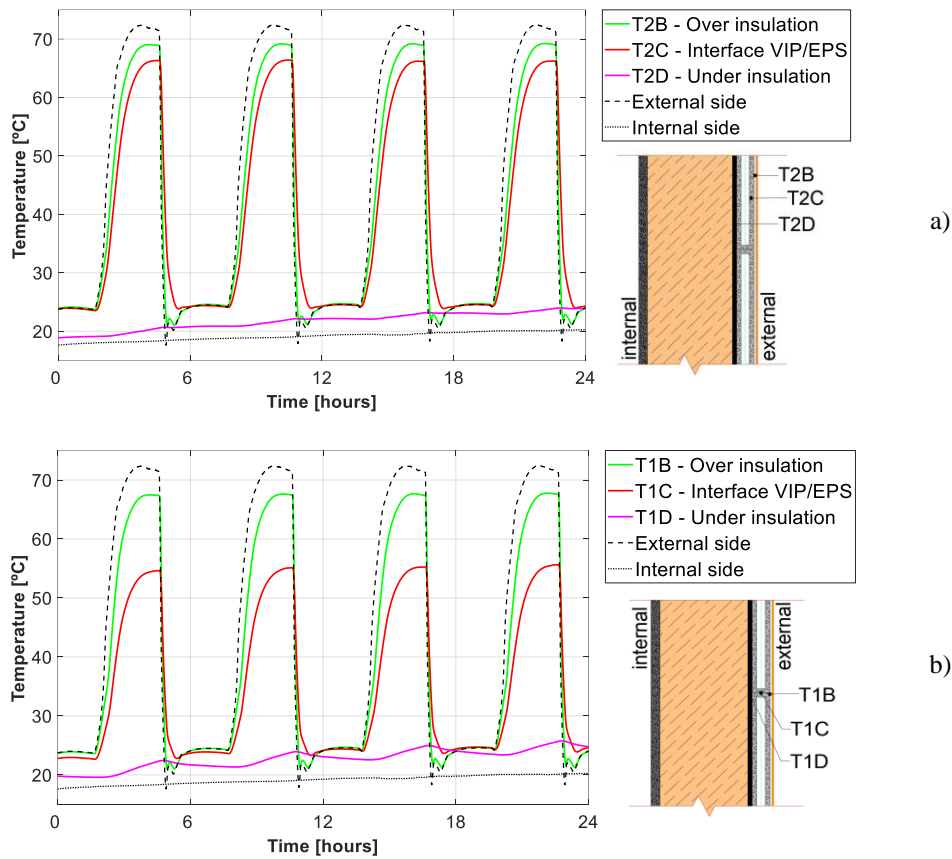
In this stage, heat-rain and freeze-thaw standardized cycles were performed to assess the solution as resistant to hygrothermal cycles, according to ETICS EAD requirements [13]. Temperature and heat flux measurements are presented and discussed. Additionally, dynamic numerical simulation results are compared with experimental measurements, for both CoP and joint areas

### 6.3.2.1. Temperature measurements

This section presents the temperatures measured during the hygrothermal cycles. Firstly, the results obtained during the heat-rain cycles are presented. Then, the results obtained during the freeze-thaw cycles are shown.

#### *i) Heat-rain cycles*

Figure 6.8 shows temperatures registered along several interfaces of the wall in the VIP CoP area (zone 1) and in the joint area (zone 2).



**Figure 6.8:** Temperature monitoring during heat-rain cycles with white finishing coat: a) CoP area (zone 2); b) VIP joint area (zone 1).

The CoP area temperatures at interface C (between VIP and EPS cover layer) reaches 66°C, while for the VIP joint area the maximum temperature at the same interface C is 55°C. This difference is due to the concentrated heat loss that occurs at the edges of the panels. This effect is also observed at interface D (internal side of VIP), where the temperature in VIP CoP area is about 2°C higher than in the joint area. Similar results were observed in other areas of the specimen (also monitored).

Figure 6.9 provides differences between temperatures measured along the wall in a CoP area, namely between the external side of the wall (inside the climatic chamber) and: over the insulation (interface B); between VIP and EPS cover layer (interface C); under the insulation (interface D); and internal side of the wall (laboratory environment without controlled conditions).

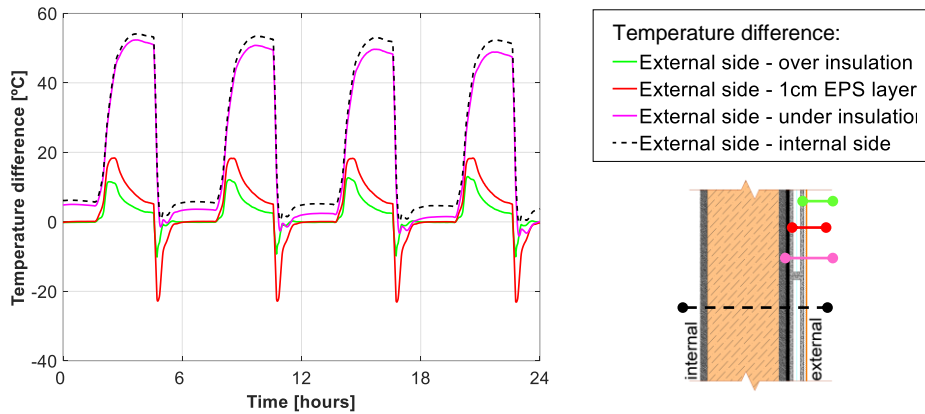


Figure 6.9: Temperature differences in VIP CoP area (zone 2) during heat-rain cycles with white finishing coat.

For a maximum recorded temperature gradient (between internal and external sides of the wall) of 54°C, the temperature difference between the external side and the “under insulation” interface is approximately 50°C, which demonstrates how significant the thermal resistance of the VIP panels is for the overall resistance of the wall. The negative temperature differences occur in periods of rain (water temperature is around 18°C), when the external temperature is lower than the temperature over the insulation layer.

Figure 6.10 shows the temperatures measured at interface B (over the insulation layer) both in the centre of panel area (CoP) and in the area between two adjacent panels (joint) during heat-rain cycles. Results are provided for both finishing coat colours. When comparing the finishing coat colours, both showed similar thermal behaviour.

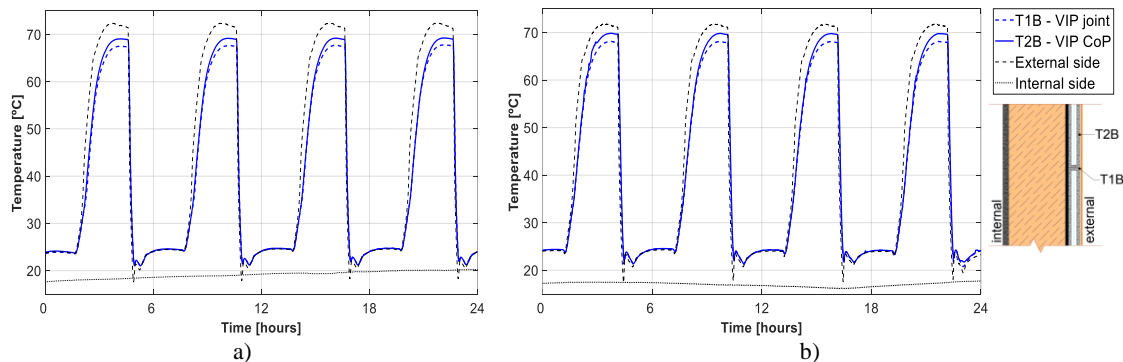
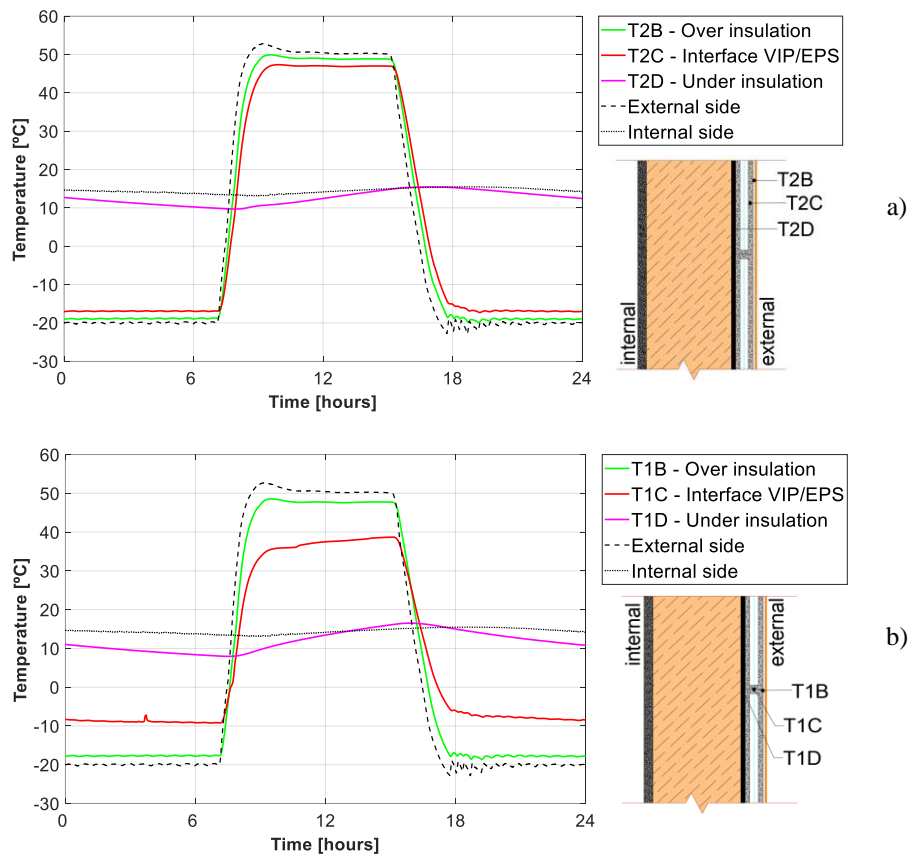


Figure 6.10: Temperature monitoring in interface B, VIP joint area (zone 1) and VIP CoP area (zone 2) during heat-rain cycle: a) white finishing coat; b) black finishing coat.

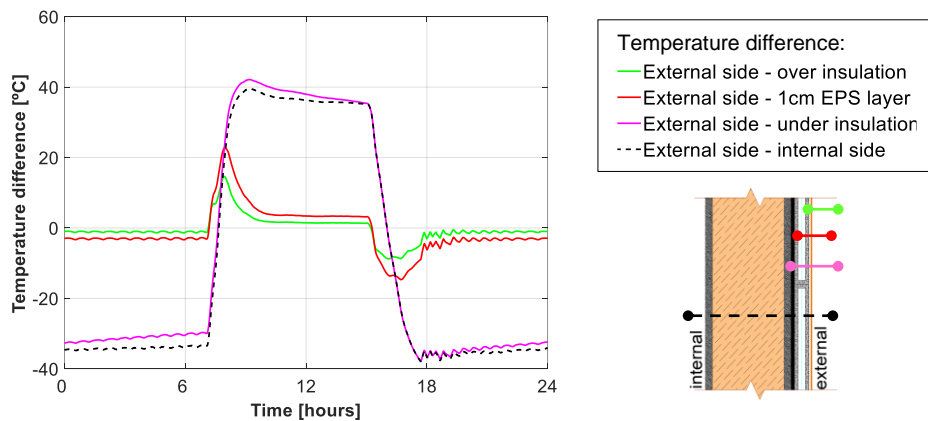
## ii) Freeze-thaw cycles

Figure 6.11 shows the temperatures recorded along several interfaces of the specimen wall, both in the VIP CoP area and in the joint area, during one representative freeze-thaw cycle. In the centre of panel area, the maximum temperature at interface C is 47°C, while in the joint area between panels it is 39°C. Regarding minimum temperatures, -9°C was measured in the joint area, while in the centre of panel a minimum of -17°C was registered.



**Figure 6.11:** Temperature monitoring during freeze-thaw cycles with white finishing coat: a) VIP centre of panel (zone 2); b) VIP joint (zone 1).

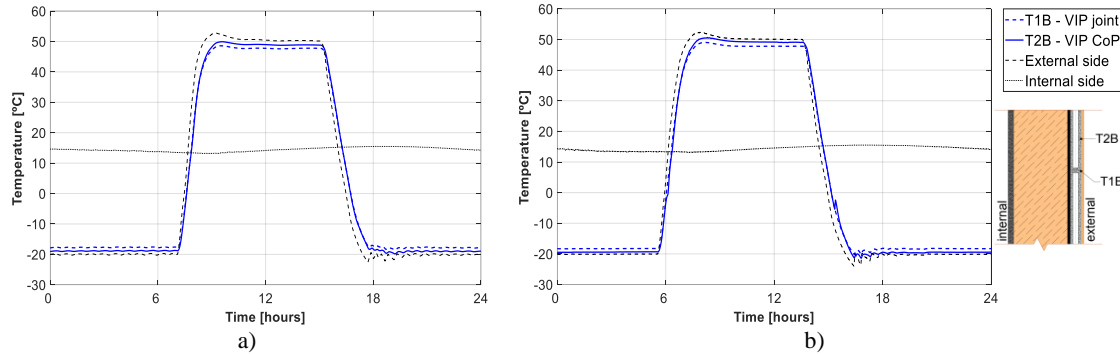
Figure 6.12 presents the temperature differences registered along the several layers of the test specimen in a VIP CoP area. During freeze-thaw cycles, where the chamber temperature has an amplitude between 50°C and -20°C, the temperature difference between external side and under the VIP panel is very close to the internal-external temperature gradient, highlighting again the significance of the influence of the thermal resistance of VIP panels.



**Figure 6.12:** Temperature differences in VIP CoP (zone 2) during freeze-thaw cycles with white finishing coat.

Figure 6.13 shows the temperatures measured at interface B, both in the VIP CoP area and in the joint area, during the freeze-thaw cycles. Results are given for both finishing colours. Likewise,

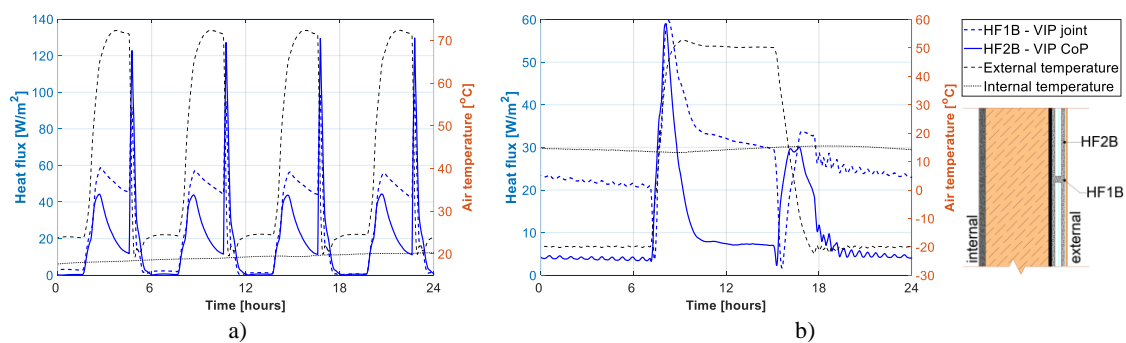
to the heat-rain cycles, similar thermal behaviour is observed for both finishing colours, highlighting that the finishing coat colour had no influence on the temperature measurements during the standard hygrothermal cycles.



**Figure 6.13:** Temperature monitoring in layer B, VIP joint (zone 1) and VIP CoP (zone 2), during freeze-thaw cycles: a) white finishing coat; b) black finishing coat.

### 6.3.2.2. Heat flux measurements

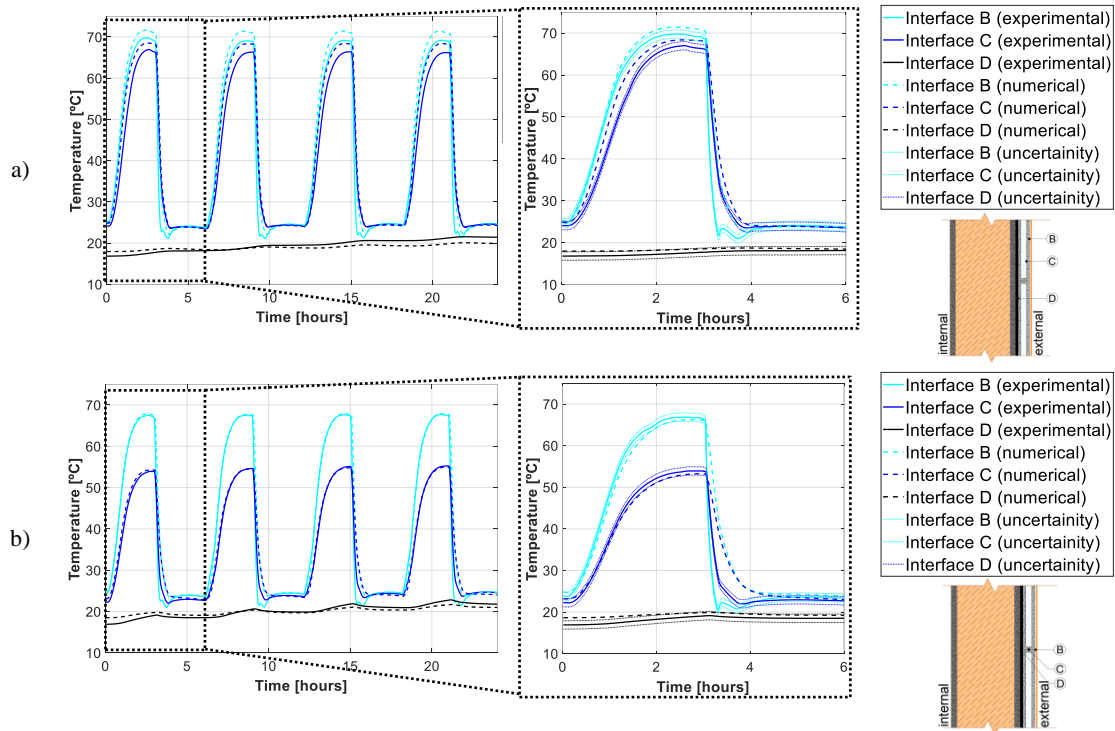
Heat flux meters were placed at interface B of the wall allowed the measurement of heat flux in both VIP CoP and joint areas. Figure 6.14 shows heat flux measurements obtained during representative cycles in stage 2. As expected, higher fluxes were obtained in the joints between VIPs. The peaks in heat flux that occur during the hygrothermal cycles are due to the rainy period, as can be seen in Figure 6.14a.



**Figure 6.14:** Heat flux monitoring: a) during hygrothermal cycles; b) during a freeze-thaw cycle.

### 6.3.2.3. Numerical modelling

A numerical modelling campaign was also performed in order to compare the recorded experimental measurements with the simulation results obtained for the dynamic temperature conditions of the hygrothermal cycles test. Figure 6.15 provides heat-rain cycles numerical results. Also, a zoomed-in image of one representative cycle is presented.



**Figure 6.15:** Temperatures results at different VIP interfaces during hygrothermal cycles with white finishing coat: a) VIP CoP (zone 2); b) VIP joint (zone 1).

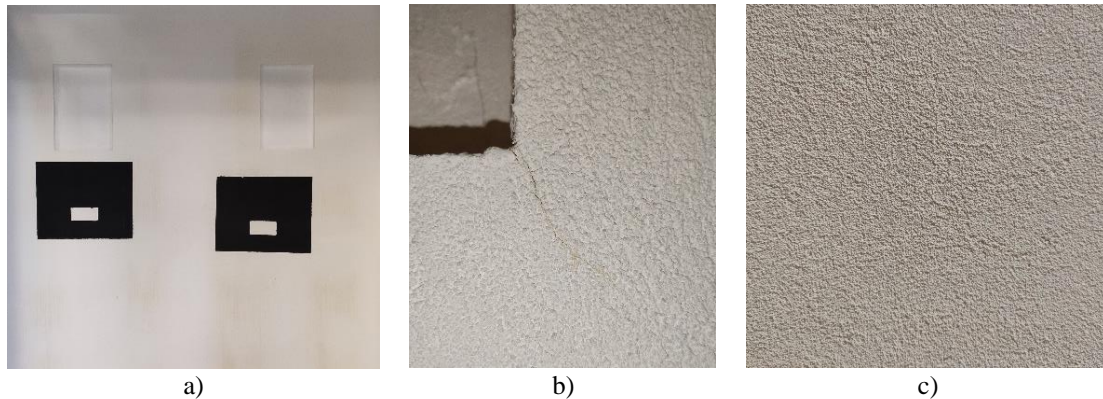
The numerical results were found to be in accordance with the experimental measurements. A maximum difference of 2.4°C was found at interface B. In general, BISTRA software modelling showed good accuracy, with a maximum relative deviation of temperatures under dynamic behaviour of around 7%.

### 6.3.2.4. Visual inspection

Figure 6.16 presents the appearance of the test specimen after the hygrothermal cycles resistance tests. During the freeze-thaw cycles it was observed that microcracking occurred at the corners of both opening areas, as can be seen in Figure 6.16b. This cracking of the finishing coat layer is



0.08–0.12 mm wide and 25 mm to 50 mm in length and follows a diagonal or vertical pattern. According to the EAD for ETICS [13], this kind of defect (crack width lower than 0.2 mm) is admissible since it does not allow penetration of water to the thermal insulation layer. At the end of the test campaign, further investigation was conducted involving the removal of sections containing cracks to observe any water penetration within the ETICS, confirming the watertightness of the rendering system. Also, some staining resulting from the water spraying system was found.



**Figure 6.16:** Appearance of the test specimen after hygrothermal cycles: a) overall view; b) close-up of the corner of the opening; c) close-up of the finishing coat.

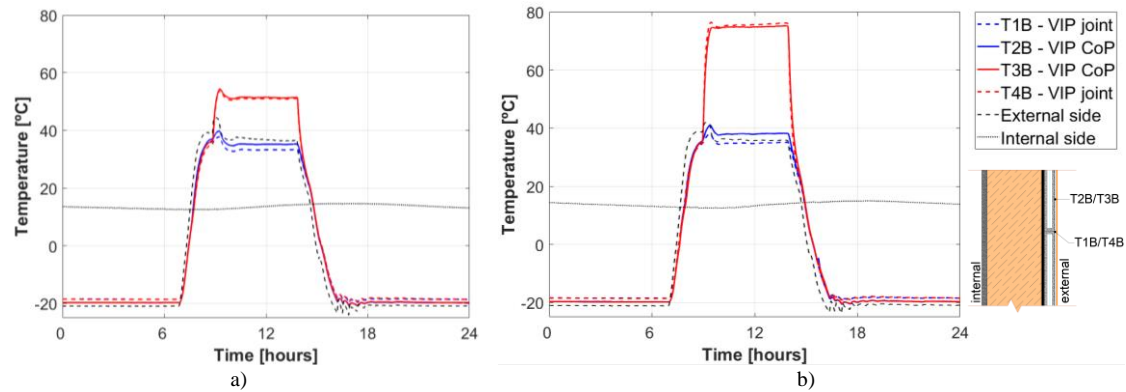
After the hygrothermal cycles, none of the following defects were detected: blistering or peeling of final coating; failure or cracking associated with joints between insulation panels; detachment of the rendering system; and cracking allowing penetration of water into the insulation layer (cracks width over 0.2 mm). Thus, according to the EAD for ETICS [13] this VIP based ETICS solution is assessed as resistant to hygrothermal cycles. Following the hygrothermal cycles after the application of the black finishing, no change was found in the test specimen.

### **6.3.3. Stage 3: solar radiation cycles results**

In stage 3 the new test procedure with solar radiation simulation was carried out. Similar to previous sections, temperature, heat flux and numerical modelling results are presented and discussed.

### 6.3.3.1. Temperature measurements

Figure 6.17 shows the temperature monitoring results obtained at interface B (over the insulation layer) during the solar radiation simulation cycles. These include the test area directly affected by radiation (zone 3 and 4) and the area not affected by the radiation (zone 1 and 2). Results are given for measurements recorded for both finishing colours (white and black).

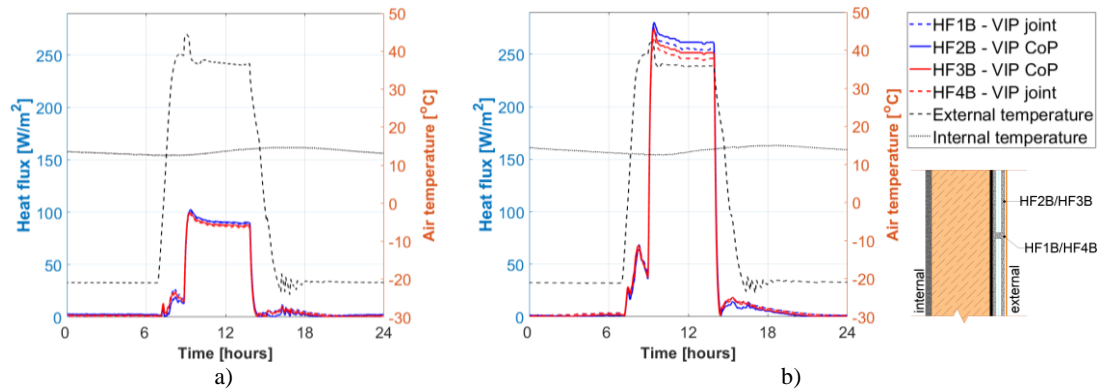


**Figure 6.17:** Temperature monitoring over insulation in VIP centre of panel area (zone 2 and 3) and in VIP joint area (zone 1 and 4) during solar radiation cycles: a) white finishing coat; b) black finishing coat.

During the solar radiation step in the white finishing coat (Figure 6.17a), differences of around  $16^{\circ}\text{C}$  can be found when comparing the areas with (T3B and T4B) and without (T1B and T2B) direct radiation. This demonstrates the fact that solar radiation will increase the temperature stress put on the rendering system layer during the ageing cycles. When analysing the results for the ETICS with a dark finishing coat (Figure 6.17b), higher surface temperatures are observed, namely there is an increase of  $24^{\circ}\text{C}$  when compared with the previous test performed on the white finishing coat. For this reason, it is confirmed that colours with high solar absorptance should be avoided in ETICS solutions, since they contribute to higher thermal stresses on the thin rendering system.

### 6.3.3.2. Heat flux measurements

Figure 6.18 shows the heat flux measurements recorded at interface B during a representative cycle of stage 3. For both finishing colours, a test area affected by radiation (zone 3 and 4) and one which is not (zone 1 and 2) are included.



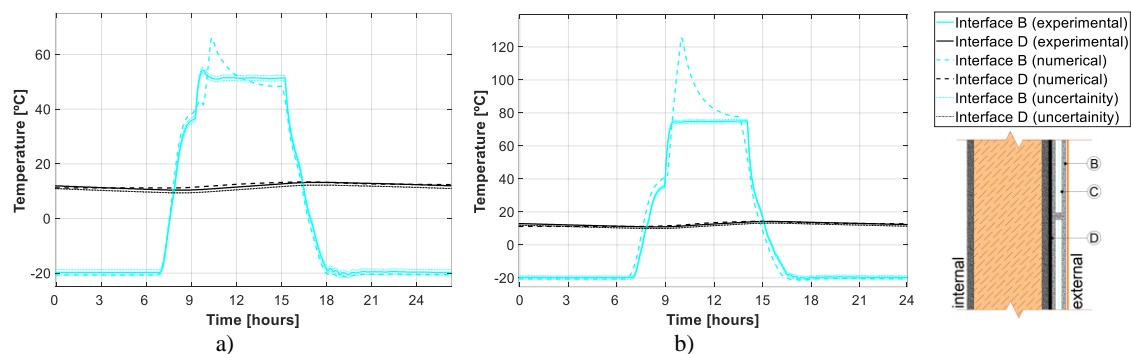
**Figure 6.18:** Heat flux monitoring in VIP centre of panel area (zone 2 and 3) and in VIP joint area (zone 1 and 4) during solar radiation cycles: a) white finishing coat; b) black finishing coat.

Even though similar heat flux behaviour was found, when compared with the previous cycles performed on the white surface (Figure 6.18a), the solar radiation cycles carried out on the black surface (Figure 6.18b) generated results with greater heat fluxes. These results could indicate that some loss of performance of the VIP panels may have occurred during the ageing cycles.

### 6.3.3.3. Numerical modelling results

In order to evaluate the numerical model response under dynamic temperature behaviour and solar radiation stimuli, the solar radiation cycles were numerically simulated by introducing a radiation step with  $1100 \text{ W/m}^2$  in the model. Additionally, a higher convective coefficient of  $50 \text{ W/(m}^2 \cdot \text{K)}$  was considered during the solar radiation step in order to simulate the increase of ventilation that occurs within the test chamber to keep the air temperature at  $35^\circ\text{C}$ .

Figure 6.19 shows the results obtained in the VIP CoP area, at interface B and D, during a representative solar cycle.

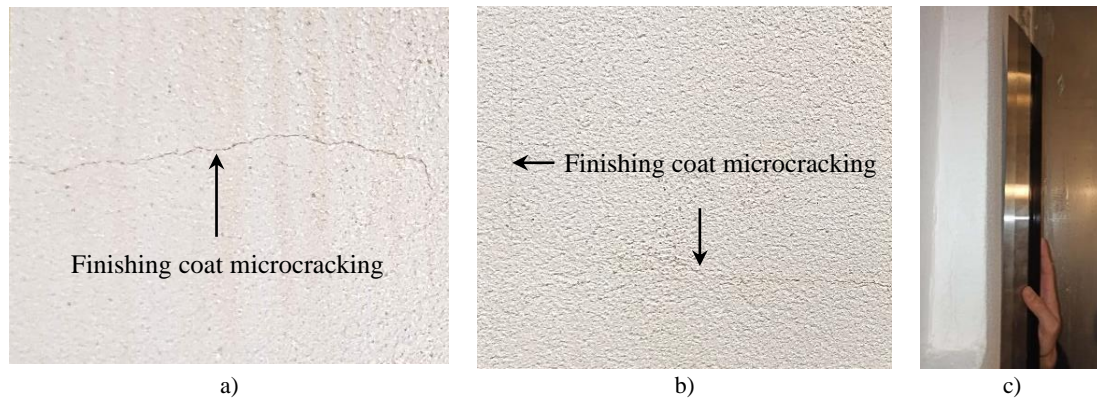


**Figure 6.19:** Temperature results during solar radiation cycles obtained at several VIP interfaces in a VIP CoP area (zone 3): a) white finishing coat; b) black finishing coat.

When compared with the experimental measurements, the numerical results reveal some lack of accuracy, particularly in the first hours of the solar radiation simulation step. This could be related with the limitations in regards to simulating the air convection inside the chamber that occurs in order to reduce the influence of the heat generated by the lamps.

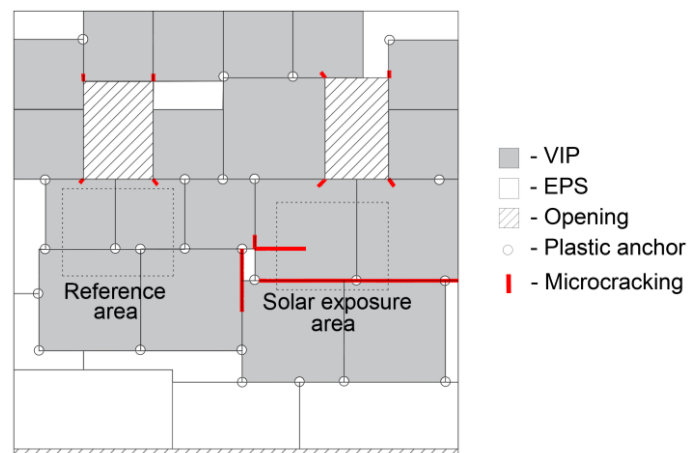
### 6.3.3.4. Visual inspection

Inspection of the specimen after the solar radiation cycles resistance test revealed some anomalies, namely there was some microcracking of the finishing coat and loss of flatness (checked with 1 meter ruler), as can be seen in Figure 6.20.



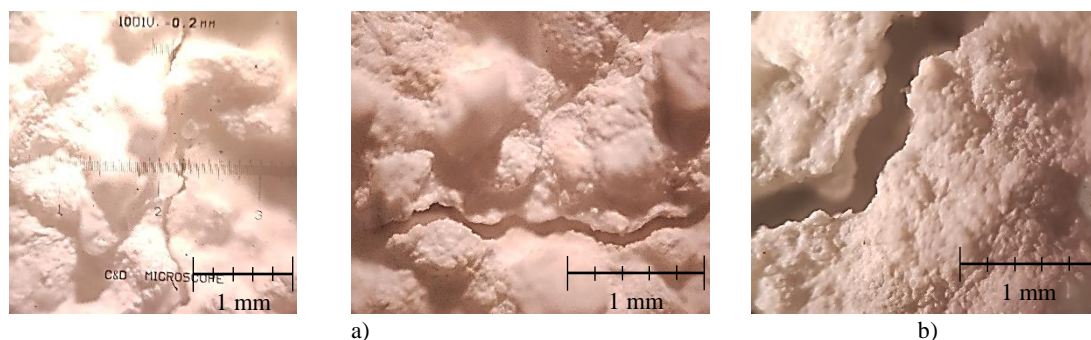
**Figure 6.20:** Visual inspection after solar radiation cycles: a) microcracking on the finishing coat layer; b) microcracking on the finishing coat layer at VIP joints; c) loss of flatness.

Figure 6.21 shows in detail the location of the microcracking on the finishing coat layer. Most of these cracks are located vertically and horizontally along the VIP joints. The cracking occurred only at within the solar radiation exposure area and its surrounding area. Furthermore, lack of flatness was only found in the area exposed to solar radiation (Figure 6.20c).



**Figure 6.21:** Layout pattern scheme of VIPs and location of the microcracking (in red) on the finishing coat layer.

Figure 6.22 illustrates some images taken during measurements of the width of the cracks using a microscope with 40x magnification. The area affected by solar radiation presented microcracking of the finishing coat with width of 0.04 to 0.08 mm and extension of 160 to 800 mm.



**Figure 6.22:** Microscopic image of: a) cracking along joints between panels; b) cracking in the corner of an opening.

The cracking in the corners of the openings that had been observed after the hygrothermal cycles (stage 2) can be seen to have worsened (Figure 6.22b). After the hygrothermal cycles, the cracks associated with the openings were 0.08 to 0.12 mm wide as stated in section 6.3.2.4. In the opening without direct radiation this width remained about the same, while in the opening closer to the radiation area the cracking width increased to 0.38 mm, which allow water penetration to the insulation layer.

It should also be noted that the additional solar radiation cycles test performed after the black finishing coat was applied did not cause any defects beyond those which existed previously. The use of a black acrylic paint, which is more flexible than the textured white acrylic finishing coat used in the ETICS, may have contributed to lessening the risk of cracking, even with the higher temperature amplitudes resulting from the dark colour.

From the test results, it can be concluded that the VIP joints are the critical issue of this solution, in terms of ageing cycles resistance. In addition to higher heat flux measurements verified at the joints, most microcracking of the finishing coat was observed at VIP joints areas, during the solar radiation cycles tests. Furthermore, when dealing with windows and doors the joints of insulation panels should not be aligned with the corners of these openings, due to the higher stress concentration, as explained in Annex A of this thesis. In the case of vacuum technology, this issue is not always avoidable, since panels cannot be adapted and cut onsite. This may lead to additional stress concentration and, consequently, to higher risk of cracking of the rendering (as it was verified in the hygrothermal cycles stage). For these reasons, the risk of rendering cracking is higher in VIP based ETICS solutions than in other conventional ETICS solutions that employ only one insulation material. Additional reinforcements of the rendering system, or use of new rendering products should be studied to minimize the cracking risk.

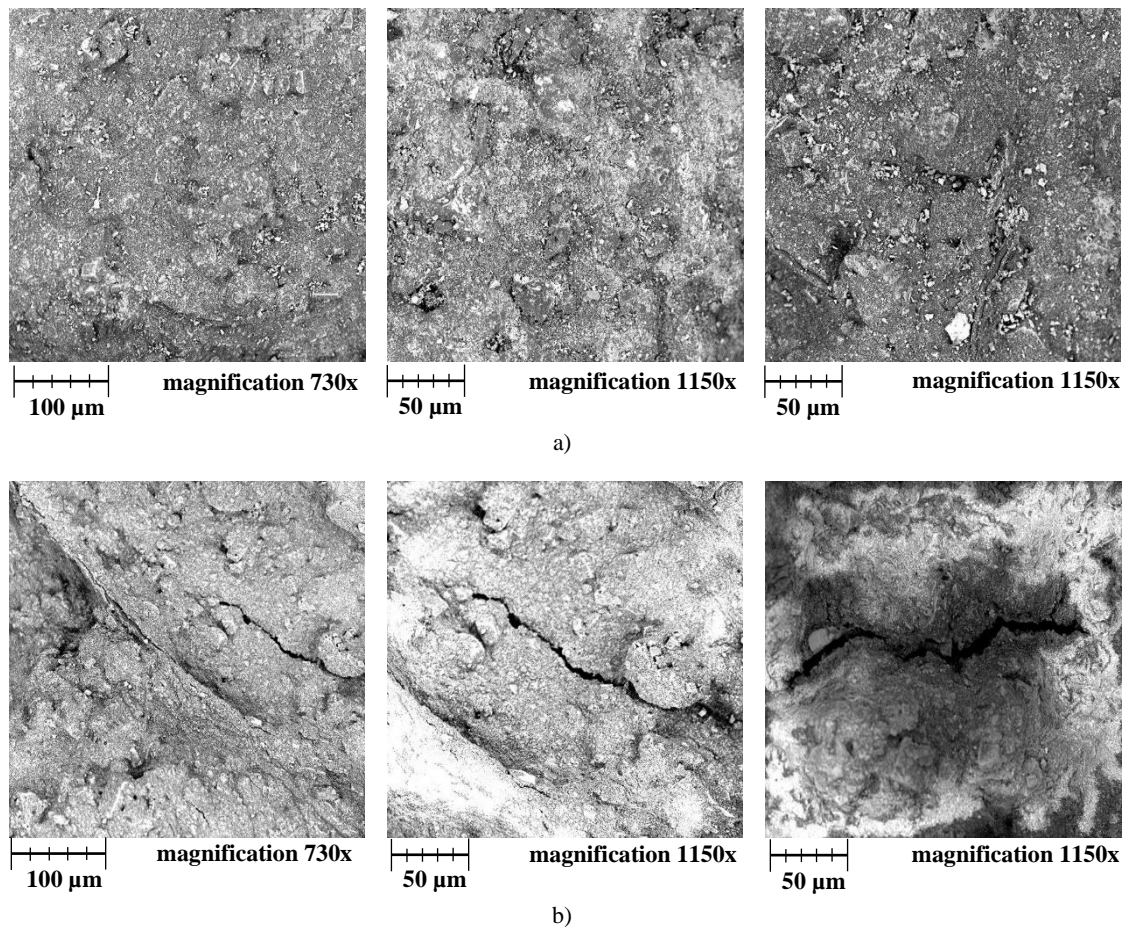


### 6.3.4. Test specimen inspection

In this section, an additional inspection of the specimen is presented. It includes SEM images, colour change analysis, mechanical behaviour assessment, and thermal performance evaluation of the test specimen. Finally, the main findings of this experimental campaign are summarized.

#### 6.3.4.1. Scanning electron microscope

Figure 6.23 shows the results of image analysis by means of a scanning electron microscope (SEM) for samples removed from the test area directly exposed to solar radiation simulation and the test area not exposed to solar radiation.



**Figure 6.23:** Scanning electron microscope images: a) rendering system not exposed to solar radiation; b) rendering system exposed to solar radiation.

From the images in Figure 6.23, it is clear that the solar radiation cycles have led to degradation of the finishing coat layer in the exposed area (when compared with the area not exposed to solar radiation). This type of cracks on the finishing coat are not perceptible with a naked eye, however they were found in multiple samples of the test areas. These observations also indicate particles without cohesion of the finishing coat.

### **6.3.4.2. Colour change**

Table 6.4 shows the results of the change in colour analysis performed by numeric comparison of colorimetric parameters for one sample removed from the test area directly exposed to solar radiation simulation and one sample removed from the area not exposed to solar radiation (reference area).

**Table 6.4:** Change in colour determined by numeric comparison of colorimetric parameters.

<b>Colorimeter parameters</b>	<b><math>\Delta L^*</math></b>	<b><math>\Delta a^*</math></b>	<b><math>\Delta b^*</math></b>	<b><math>\Delta E^*_{ab}</math></b>
White colour change	-1.45	-0.84	0.36	1.71
Black colour change	-1.01	0.06	0.18	1.03

For both finishing colours, the results showed a slight colour change after the solar radiation cycles. However, since only differences over  $\Delta E^*_{ab} > 2$  are detectable by an unexperienced observer [33], it can be said that the change in colour is not noticeable.

### **6.3.4.3. Thermal performance**

With the aim of assessing the thermal performance of the VIP after the ageing test campaign, the test specimen was subjected to steady state boundary conditions. Table 6.5 shows the VIP CoP thermal transmittance calculated using heat flux measurements in steady-state regime. The results are given for several external-internal temperature gradients during steady-state periods of the ageing test campaign. The theoretical U-values calculated according to ISO 6946 (considering the thermal properties of Table 6.1) are also presented.

**Table 6.5:** VIP CoP thermal transmittance estimation for different ageing test periods.

	$\Delta T$ [°C]	Heat flux [W/m <sup>2</sup> ]	U-value [W/(m <sup>2</sup> ·K)]	Theoretical U-value [W/(m <sup>2</sup> ·K)]	Deviation from initial state U-value [%]
<b>Initial state</b>	20.0	3.733	<b>0.187</b>	0.168 <sup>(1)</sup> (initial state)	11.4%
<b>After hygrothermal cycles (white colour)</b>	12.7	2.553	<b>0.201</b>	0.206 <sup>(2)</sup> - 0.235 <sup>(3)</sup> (after VIP ageing according test procedure of EN 17140)	19.7%
<b>After hygrothermal cycles (black colour)</b>	35.5	8.083	<b>0.228</b>		35.5%
<b>Final state (after hygrothermal and solar radiation cycles)</b>	17.2	4.913	<b>0.286</b>	0.469 <sup>(4)</sup> (VIP without vacuum)	70.0%

<sup>(1)</sup> Considering thermal conductivity results (4.2 mW/(m·K)) for VIP panel.

<sup>(2)</sup> Considering thermal conductivity results (5.5 mW/(m·K)) after ageing for VIP panel with 600 mm x 600 mm.

<sup>(3)</sup> Considering thermal conductivity results (6.6 mW/(m·K)) after ageing for VIP panel with 400 mm x 400 mm.

<sup>(4)</sup> Considering thermal conductivity results (21.6 mW/(m·K)) after intentional perforation of VIP panel.

When comparing the initial steady state results with the results during and after the ageing test campaign, an increase of the thermal transmittance was found. This indicates that the VIPs may have lost their initial thermal performance during the ageing cycles. This was expected, since it is known that vacuum products lose some performance during their service life. For this reason, the specification standard for VIP - EN 17140 [34] indicates that the declared thermal conductivity should include the ageing effect. The thermal conductivity of a VIP product over the first 25 years is estimated based on accelerated ageing test according to Annex C of EN 17140. This was done by storing the panel at 50°C and 70% relative humidity over a period of 180 days. The VIP thermal conductivity increased from 4.2 mW/(m·K) - initial state - to 5.5 mW/(m·K) - after accelerated ageing of a panel with 600 mm x 600 mm, measured at 10°C in GHP apparatus in accordance with EN 12667 [25]. Considering this thermal conductivity, the expected theoretical U-value of the wall should be 0.206 W/(m<sup>2</sup>·K).

Also, thermal conductivity measurements in intentionally perforated panels were carried out, resulting in a thermal conductivity of 21.6 mW/(m·K). Thus, if the test specimen was to be completely without vacuum, the U-value should be around 0.469 W/(m<sup>2</sup>·K).

We may conclude that after the hygrothermal and solar radiation cycles (final state) the system has reached a higher thermal transmittance than the one expected after standardised ageing testing on small samples. Namely, the VIP thermal conductivity increase during the proposed ageing tests cycles (around 4.5 mW/(m·K)) was higher than the thermal conductivity increase estimated with the ageing test method purposed in EN 17140 for individual panels (1.3 to 2.4 mW/(m·K)).



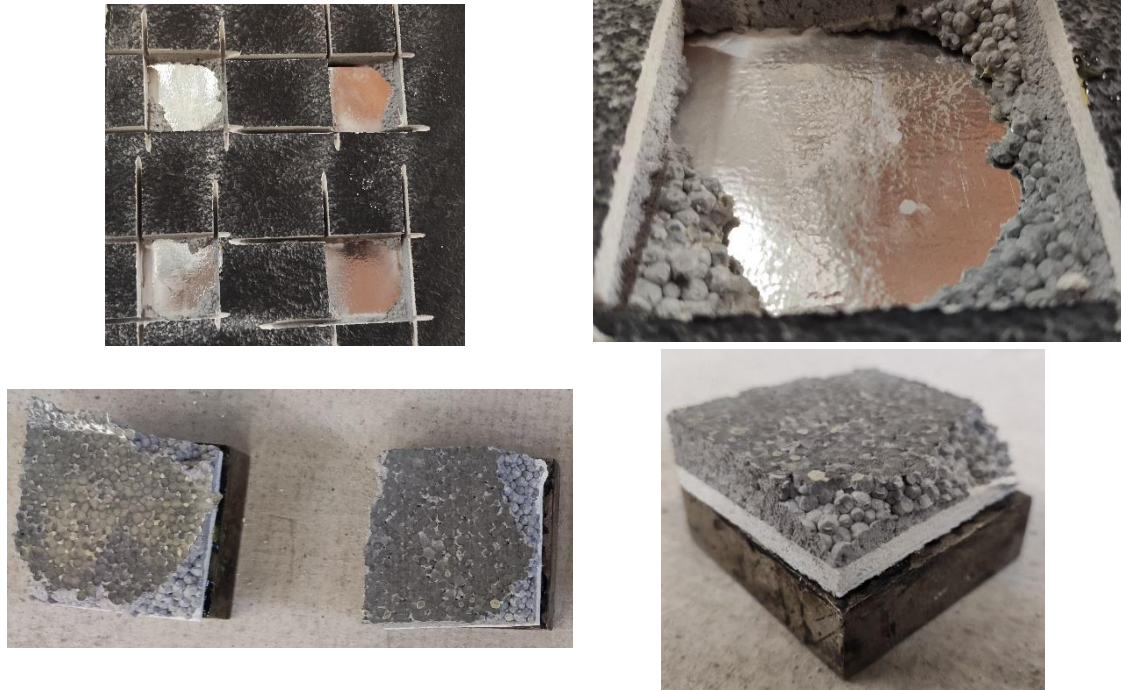
### 6.3.4.4. Bond strength resistance

Bond strength resistance tests (between the base coat and the encapsulated VIP) were performed in the area subjected to solar radiation (close to zones 3 and 4) and the area not exposed, called previously as reference area (close to the zones 1 and 2). Table 6.6 presents the results obtained, as well as the result uncertainty based on the repeatability and acceptance criterion of the test equipment.

**Table 6.6:** Test results of the bond strength tests between the base coat and the thermal insulation product.

Zone	Test no.	Tensile strength [kPa]	Failure pattern	Failure location	Mean value [kPa]
Reference area	1	102	80% adhesive/ 20% cohesive	Between EPS cover layer and VIP (adhesive failure) / EPS cover layer (cohesive failure)	100 (± 20)
	2	125	82% adhesive/ 18% cohesive		
	3	87	90% adhesive/ 10% cohesive		
	4	89	85% adhesive/ 15% cohesive		
	5	98	85% adhesive/ 15% cohesive		
Solar radiation exposure area	1	113	85% adhesive/ 15% cohesive	Between EPS cover layer and VIP (adhesive failure) / EPS cover layer (cohesive failure)	113 (± 18)
	2	97	87% adhesive/ 13% cohesive		
	3	124	90% adhesive/ 10% cohesive		
	4	123	81% adhesive/ 19% cohesive		
	5	109	90% adhesive/ 10% cohesive		

The bond strength test results showed mostly an adhesive failure between the EPS cover layer and the VIP panel, which means that the failure of the system was in the PU glue (used to bond the cover layer to the VIP). All the results are higher than the ETICS EAD requirement (> 80 kPa). No noticeable differences between the results of solar radiation exposure area and the reference area were found. The representative failure pattern is showed in Figure 6.6.

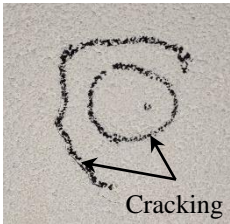
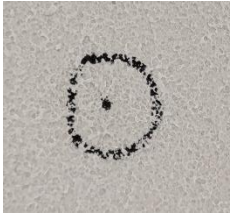
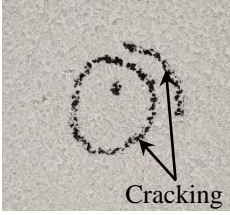




**Figure 6.24:** Adhesive failure pattern after bond strength tests.

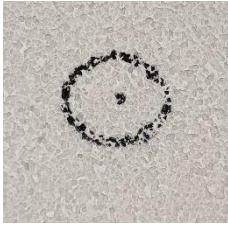
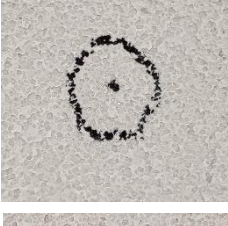
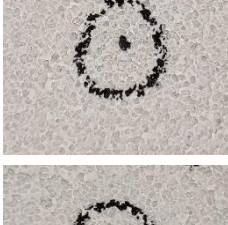
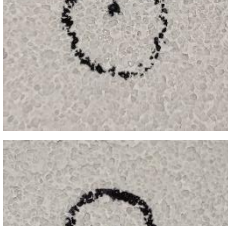
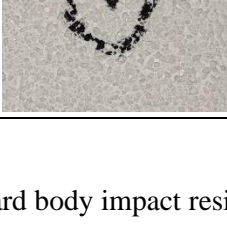
### **6.3.4.5. Resistance to hard body impact**

Table 6.7 and Table 6.8 present the results obtained for the hard body impacts of 10 J and 3 J, respectively. Most of impacts resulted in superficial damage without cracking of the rendering system. However, some of them (10 J impacts) resulted in cracking of the finishing coat, without reaching the encapsulated VIP.

**Table 6.7:** Hard body impact test results – 10 Joules.

<b>Impact zone No.</b>	<b>Photo</b>	<b>Diameter of the impact [mm]</b>	<b>Observations</b>
1		36.08	Existence of cracks without reaching the insulation product
2		19.41	Superficial damage without cracking
3		26.38	Existence of cracks without reaching the insulation product
4		20.33	Superficial damage without cracking
5		27.84	Superficial damage without cracking

**Table 6.8:** Hard body impact test results – 3 Joules.

Impact zone No.	Photo	Diameter of the impact [mm]	Observations
1		15.31	Superficial damage without cracking
2		16.53	Superficial damage without cracking
3		13.20	Superficial damage without cracking
4		14.83	Superficial damage without cracking
5		14.99	Superficial damage without cracking

In terms of hard body impact resistance, the test specimen fits in category II, according to Table 3 of the ETICS EAD [13]. Thus, this VIP based ETICS is suitable to be installed in a zone liable to impacts from thrown or kicked objects, but in public locations where the height of the ETICS will limit the size of the impact; or at lower levels where access to the buildings primarily to those with some incentive to exercise care.

### 6.3.4.6. Summary of results

Table 6.9 summarizes the ageing test results for several parameters inspected during the ageing tests.

**Table 6.9:** Summary of ageing tests results.

Parameter	Before ageing tests	After hygrothermal cycles (stage 2)	After solar radiation cycles (stage 3)
Finishing coat pulverulence	No	No	No
Blistering or peeling of final coating	No	No	No
Detachment of the rendering coat	No	No	No
Cracking	No	Microcracking in openings corners	Microcracking along VIP joints and cracking allowing the water penetration in one opening corner
Loss of flatness	No	No	Yes
Vacuum loss (heat flux measurements)	No	Loss of performance	Loss of performance
Image analysis (by means of SEM)	--	--	Microcracking
Colour change (CIELAB method)	--	--	Not noticeable
Impact resistance (ETICS EAD section 2.2.8)	--	--	Category II
Bond strength resistance (ETICS EAD section 2.2.11.1)	--	--	107 kPa

The VIP based ETICS was considered to be resistant to hygrothermal cycles. However, solar radiation cycles were found to be sensitive to the finishing colour and caused anomalies that were not observed with the hygrothermal standard test method, namely microcracking of the finishing coat layer and loss of flatness. SEM inspection revealed microcracking only on samples exposed to solar radiation, highlighting the effect of this degradation agent. Change in colour was considered to be unnoticeable. Heat flux measurements revealed a loss of VIP thermal performance during hygrothermal cycles.

Regarding the mechanical tests, the bond strength resistance after hygrothermal cycles tests accomplished the ETICS EAD requirements. However, the bonding adhesion of the graphite EPS cover layer to the VIP could be improved. The impact resistance tests resulted in Category II, which is the most usual category for the ETICS systems available in the market.

## 6.4. Conclusions

The goal of this study was to carry out an experimental test campaign to assess the hygrothermal behaviour of ETICS solution that uses vacuum technology instead a conventional insulation material. The test specimen was instrumented with thermocouples and heat flux sensors to analyse the thermal behaviour along the different layers of the wall, as well as in different areas, including VIP centre of panel and VIP joints.

The test procedures included a first stage with steady-state boundary conditions to allow the U-value estimation. Next, the standard test procedures defined in the EAD for ETICS were carried out. Finally, a new test procedure was implemented by using a solar radiation simulation system. The proposed test method allowed the assessment of the influence of the finishing colour on the thermal behaviour of the ETICS wall, which is currently not included in the standard test procedures, and the assessment of possible degradation of the system over time.

Although the system evaluation according to the standardized methods resulted in it being considered to be resistant to hygrothermal cycles, the solar radiation cycles caused defects which were not found after the standard procedures, namely anomalies such as loss of flatness and finishing coat microcracking. This reveals the importance of studying the radiation effect on ETICS systems. VIP joints could be considered the critical issue of the VIP based ETICS solution, since in addition to higher heat flux measurements verified at the joints, most of finishing coat microcracking occurred over joints.

Also, the differences found between initial test specimen U-value and U-value after the ageing cycles reveal an increase of the VIP thermal conductivity when compared with the accelerated ageing tests. These findings revealed that the standard declared thermal conductivity of VIP products, could be inaccurate when compared to the real thermal performance of VIP solutions after being exposed to repeated external environmental agents, in particular in solutions such as ETICS.

In general, numerical modelling results showed good accuracy, in particular during the steady state conditions. However, the numerical model revealed imprecision regarding the simulation of the solar radiation input. The main limitations of the model, and of respective comparison to experimental measurements, are related with the difficulty to simulate the convective phenomena generated to control the temperature inside the test chamber. Due to the large volume of the test chamber, temperature stratification may occur, resulting in a non-homogenous temperature along the height of the test specimen, and, ultimately in measurement deviations, so further research is needed. Future studies may also include mass transfer phenomena in order to assess moisture transport through the different VIP based ETICS layers and evaluate condensation risk.

The proposed test method may also be used to evaluate existing ETICS solutions with conventional materials, in particular with the aim of evaluate the use of finishing coat with different optical properties. For this purpose, an increase of the solar exposition area could be relevant for achieving a more realistic laboratory test. Also, since the solar radiation simulation caused finishing coat degradation, as shown by the experimental tests results, it will be relevant to this degradation agent more in depth, looking to better understand the combination of factors such as the effect of UV, visible and infrared radiation and the variation of the temperature and humidity levels.

The main findings of this work revealed that, in the context of predicting the durability and performance during service life, solar radiation simulation should be considered when assessing the hygrothermal behaviour of an ETICS systems, complementing the existing standard procedures. Also, there is a challenge facing manufacturers in regards to developing rendering systems that are able to mitigate the cracking risk that was observed as a result of the proposed ageing tests.

Since real onsite applications are still few and recent, it is important to further the knowledge on VIP based ETICS solutions by making developments in a laboratorial environment. The experimental validation of these innovative solutions will lead to continuous improvements of vacuum products and will consequently increase the confidence of builders, designers and users. For this purpose, this work contributed by presenting the experimental results of a real scale wall in laboratory conditions and proposing a new accelerating ageing test procedure.

## References

- [1] A. Lorenzati, S. Fantucci, A. Capozzoli, M. Perino, “Experimental and numerical investigation of thermal bridging effects of jointed Vacuum Insulation Panels”, *Energy Build.* vol. 111, pp. 164–175, 2016, doi:10.1016/j.enbuild.2015.11.026.
- [2] J. S. Kwon, C. H. Jang, H. Jung, T. H. Song, “Effective thermal conductivity of various filling materials for vacuum insulation panels”, *Int. J. Heat Mass Transf.* vol. 52, pp. 5525–5532, 2009, doi:10.1016/j.ijheatmasstransfer.2009.06.029.
- [3] S. Treml, M. Engelhardt, C. Sprengard, W. Butko, “Determination of the internal pressure of vacuum insulation panels with the envelope lift-off technique – methods for analysing test data”, *Energy Build.* vol. 184, pp. 44–52, 2019, doi:10.1016/j.enbuild.2018.11.027.
- [4] J. H. J. T. Kim, F. E. Boafu, S. M. Kim, J. H. J. T. Kim, “Aging performance evaluation of vacuum insulation panel (VIP)”, *Case Stud. Constr. Mater.* vol. 7, pp. 329–335, 2017, doi:10.1016/j.cscm.2017.09.003.

- [5] B. Yrieix, B. Morel, E. Pons, “VIP service life assessment: Interactions between barrier laminates and core material, and significance of silica core ageing”, *Energy Build.* vol. 85, pp. 617–630, 2014, doi:10.1016/j.enbuild.2014.07.035.
- [6] U. Berardi, M. Nikafkar, S. Wi, S. Kim, “Experimental verification of the theoretical aging of vacuum insulated panels”, *J. Ind. Eng. Chem.* vol. 90, pp. 300–304, 2020, doi:10.1016/j.jiec.2020.07.027.
- [7] B. Chang, L. Zhong, M. Akinc, “Low cost composites for vacuum insulation core material”, *Vacuum*, vol. 131, pp. 120–126, 2016 doi:10.1016/j.vacuum.2016.05.027.
- [8] J. Wang, Y. Zhan, W. Wei, S. Chen, R. Wang, “A new cost effective composite getter for application in high-vacuum-multilayer-insulation tank”, *Vacuum*, vol. 131, pp. 44–50, 2016, doi:10.1016/j.vacuum.2016.05.025.
- [9] A. Batard, T. Duforestel, L. Flandin, B. Yrieix, “Modelling of long-term hygro-thermal behaviour of vacuum insulation panels”, vol. *Energy Build.* vol. 173, pp. 252–267, 2018, doi:10.1016/j.enbuild.2018.04.041.
- [10] B. Amaro, D. Saraiva, J. de Brito, I. Flores-Colen, “Statistical survey of the pathology, diagnosis and rehabilitation of ETICS in walls”, *J. Civ. Eng. Manag.* vol. 20, pp. 511–526, 2014, doi:10.3846/13923730.2013.801923.
- [11] F. Stazi, C. Di Perna, P. Munafò, “Durability of 20-year-old external insulation and assessment of various types of retrofitting to meet new energy regulations”, *Energy Build.* vol. 41, pp. 721–731, 2009, doi:10.1016/j.enbuild.2009.02.008.
- [12] *Buildings and constructed assets -- Service life planning -- Part 1: General principles and framework*, ISO 15686-1, International Organization for Standardization, 2011.
- [13] *European Assessment Document: External Thermal Insulation Composite Systems with rendering*, EAD 040083-00-0404, European Organisation for Technical Approvals, 2019.
- [14] *Thermal insulation products for building applications - Determination of the hygrothermal behaviour of external thermal insulation composite systems with renders (ETICS)*, EN 16383, European Committee for Standardization, 2016.
- [15] H. Xiong, J. Xu, K. Yuan, “Experimental study on the temperature field of ETICS cladding system with finishing colorful steel plate”, *J. Build. Eng.* vol. 18 pp. 438–447, 2018, doi:10.1016/j.jobbe.2018.04.015.
- [16] H. Xiong, J. Xu, Y. Liu, S. Wang, “Experimental Study on Hygrothermal Deformation of External Thermal Insulation Cladding Systems with Glazed Hollow Bead”, *Adv. Mater. Sci. Eng.* 2016, doi:10.1155/2016/3025213.
- [17] J. L. Parracha, G. Borsoi, R. Veiga, I. Flores-Colen, L. Nunes, A. R. Garcia, L. M. Ilharco, A. Dionísio, P. Faria, “Effects of hygrothermal, UV and SO<sub>2</sub> accelerated ageing on the durability of ETICS in urban environments”, *Build. Environ.* vol. 204, 108151, 2021, doi:10.1016/j.buildenv.2021.108151.
- [18] B. M. Marino, N. Muñoz, L. P. Thomas, “Calculation of the external surface temperature of a multi-layer wall considering solar radiation effects”, *Energy Build.* vol. 174 pp. 452–463, 2018, doi:10.1016/j.enbuild.2018.07.008.
- [19] European Association for External thermal insulation composite systems, “European Guideline for the application of ETICS”, 2011.



- [20] C. Alonso, F. Martín-Consuegra, I. Oteiza, E. Asensio, G. Pérez, I. Martínez, B. Frutos, “Effect of façade surface finish on building energy rehabilitation”, *Sol. Energy*. vol. 146, pp. 470–483, 2017, doi:10.1016/j.solener.2017.03.009.
- [21] N. M. M. Ramos, A. R. Souza, J. Maia, R. M. S. F. Almeida, “Solar reflectance of ETICS finishing coatings - A comparison of experimental techniques”, in *Proceedings of E3S Web Conference*, vol. 172, pp. 1–7, 2020, doi:10.1051/e3sconf/202017221003.
- [22] G. Wypych, “Laboratory Degradation Studies”, in *Handbook of Material Weathering (Sixth Edition)*, 2018, pp. 159-194, doi:10.1016/b978-1-927885-31-4.50009-1.
- [23] B. J. Finlayson-Pitts, J. N. Pitts, “Applications of Atmospheric Chemistry”, *Chem. Up. Low. Atmos.* pp. 871–942, 2000, doi:10.1016/b978-012257060-5/50018-6.
- [24] *Ageing of automotive components in solar simulation units*, DIN 75220 , Deutsches Institut für Normung E.V., 1992.
- [25] *Thermal performance of building materials and products - Determination of thermal resistance by means of guarded hot plate and heat flow meter methods - Products of high and medium thermal resistance*, EN 12667, European Committee for Standardization, 2001.
- [26] *Thermal performance of building materials and products - Determination of thermal resistance by means of guarded hot plate and heat flow meter methods - Dry and moist products of medium and low thermal resistance*, EN 12664, European Committee for Standardization, 2001.
- [27] *Standard Test Method for Solar Absorptance, Reflectance, and Transmittance of Materials Using Integrating Spheres*, E 903, ASTM International, 1996.
- [28] *Building components and building elements - Thermal resistance and thermal transmittance - Calculation method*, ISO 6946, International Organization for Standardization, 2017.
- [29] CIE 1976 ( $L^*$ ,  $u^*$ ,  $v^*$ ) color difference equation. in *Gooch J. W. (eds) Encyclopedic Dictionary of Polymers*. Springer, New York, 2007. [https://doi.org/10.1007/978-0-387-30160-0\\_2346](https://doi.org/10.1007/978-0-387-30160-0_2346).
- [30] *Standard Practice for Calculation of Color Tolerances and Color Differences from Instrumentally Measured Color Coordinates*, D 2244, ASTM International, 2002.
- [31] *Vertical building elements - Impact resistance tests - Impact bodies and general test procedures*, ISO 7892, International Organization for Standardization, 1988.
- [32] BISTRA - 2D transient heat transfer, (version 4.0w). Physibel. <http://www.physibel.be/bistra.htm>.
- [33] W. Mokrzycki, M. Tatol, “Color difference Delta E - A survey, Machine Graphic & Vision”, in *Machine Graphics and Vision*, pp. 383–411, 2012.
- [34] *Thermal insulation products for buildings - Factory-made vacuum insulation panels (VIP) - Specification*, EN 17140, European Committee for Standardization, 2020.



## **CHAPTER 7**

### **WHOLE-LIFE COST ASSESSMENT OF VIP**



## 7. Whole-life cost assessment of VIP

### 7.1. Introduction

The worldwide demand for energy savings has called for improvements in the thermal performance requirements set for buildings. In Europe, the Energy Performance of Buildings Directive (EPBD), first published in 2002 [1], was recast in 2010 by the Directive 2010/31/EU [2], which imposed a set of minimum performance requirements based on cost-optimal levels and established nearly zero-energy buildings targets. More recently, the EPBD was recast as Directive 2018/844 [3]. Throughout its iterations, the EPBD has been pushing countries towards the implementation of higher standards for energy efficiency requirements. For example, maximum thermal transmittance coefficient (U-value) of walls of  $0.28 \text{ W}/(\text{m}^2 \cdot \text{K})$  in Germany and  $0.17 \text{ W}/(\text{m}^2 \cdot \text{K})$  in Finland are required [4]. These requirements are defined by each Member State using a general common framework ([5],[6]) with a view towards achieving the cost-optimal balance between the investments involved and the energy costs saved throughout the life-cycle of the building. However, it is highly recommended that building owners acting as landlords do their own detailed cost-optimality evaluations. In particular, if they are offering a full-service leasing arrangement (*i.e.*, all the costs and benefits of energy investments accrue to the landlord alone), envelope solutions and technical systems selection should be done following the Net Present Value (NPV) criterion which takes into account series of cash flows occurring at different times.

As established in the previous chapters, in order to meet the increasingly stricter thermal requirements being put upon the building envelope, designers and builders are being forced to use thicker layers of insulation material. Currently, thermal insulation materials with 300 mm thick [7] are being used in some countries to meet the thermal performance requirements and ensure indoor thermal comfort. As the thickness of the building envelope wall increases, the ratio of net to gross floor area calculated on a building perimeter basis is adversely affected. As a result, the rental or sale value of the building may change. From an economic point of view, in buildings with high rental values the savings achieved from the increased insulation material (less energy use) may not make up for the global costs due to the loss of rental value (area reduction). Furthermore, an excessively thick envelope layer may not be desirable for a number of technical

and aesthetic reasons such as architectural/design limitations, application difficulties, higher risk of anomalies due to mechanical failure, amongst other issues [8]. Consequently, a new generation of super-insulating materials, such as those using vacuum technologies [9], are entering into the market looking to achieve higher levels of thermal resistance with lower thickness.

Vacuum insulation panels (VIPs) are mainly applied to niche markets, with their total market share in insulating materials being of less than 1% [10]. This is primarily related with the relatively high market price of VIPs, which is due to their production costs being higher [11]. Issues related with the challenges of designing and executing construction works with non-adjustable and fragile panels also contribute to the high cost for current VIPs building products. This is evident in the fact that only 10% of the VIPs used worldwide are for building applications [12]. Since investment profitability in buildings depends on the cost of the insulation material [13], a great challenge facing the vacuum industry and researchers is the development of high performance products for buildings applications with lower costs. Besides initial investments costs, there are also uncertainties surrounding the long-term thermal performance of VIP products, as well as around the thermal bridging effect. Since the VIPs are encased in a metallized barrier against permeation of moisture and gas, special attention has to be given to the edge effect at the joints of the panels [14], where the higher thermal conductivity of the barrier material promotes additional heat losses. As stated in chapter 3, edge thermal bridging effects have a strong impact on the effective thermal conductivity of VIPs, especially in smaller panels. These issues can influence the profitability of energy efficiency measures and, therefore, should be considered in the economic studies.

The global market for VIPs was estimated at €6.1 billion in the year 2020, and is projected to reach €8.5 billion by 2027, growing at a Compound Annual Growth Rate (CAGR) of 4.8% [15]. Therefore, the deployment of this insulation solution for new and existing buildings has inherently great potential. Additionally, integrating VIPs into already well-known building products and solutions (for example External Thermal Insulation Composite Systems – ETICS) that could facilitate their fast and wide-scale commercialisation is considered to be key to the further development of VIP building products. The advantages and challenges posed by this solution have been thoroughly described in chapter 2.

From a capital investment point of view, VIPs struggle to compete with cheaper conventional insulation materials. However, in some applications the gain of rentable floor area due to the slimness of the solution could outweigh the higher initial investment cost. In the case of non-residential buildings, and, in particular, in offices located in high-priced areas, such as the business centres in European capital cities, rental gains could be maximized without compromising the thermal performance of the building by using VIPs. Annual rental prices in offices are very dependent on location and population density. For example, real full-service leasing rental prices of 300 €/m<sup>2</sup>.year) in Warsaw, 456 €/m<sup>2</sup>.year) in Berlin and 882 €/m<sup>2</sup>.year) in London can be found [16]. Given these values, the potential for achieving

higher ratios of rentable floor space relative to overall building area and higher land use rates should be considered at the planning and design stage, particularly for bigger developments. Additionally, it is known that implementing energy efficiency measures in existing buildings can further increase the rental value, benefiting the landlords [17].

There are several research studies focused on the assessment of the profitability and the cost-optimal thickness of the insulation materials in building applications [18–25]. However, few studies consider the use of super-insulating materials such as vacuum-based products. The economic feasibility of vacuum technology application in buildings has been recently investigated by following different approaches. Jelle [9] published an insulation materials review paper, which included a simplified approach to quantify the potential cost savings when applying VIPs in the middle of the walls construction. Alam *et al.* [26] analysed the payback period for VIP and expanded polystyrene (EPS) and concluded that EPS payback is always lower than VIP solutions. However, space savings were not taken into account. Cho *et al.* [27] showed the economic benefit of VIPs over conventional insulation materials in the Korean market. However, they compared different levels of insulation, which will lead to different levels of thermal comfort and energy savings. A multi-story office building located in Saudi Arabia was also studied regarding the energy performance and economic feasibility of a nano VIP [28]. They concluded that the profitability of VIP in walls is strongly influenced by climate and in the case of high cooling needs it may not be economically viable. Di Giuseppe *et al.* [29] stated that the benefit from super-insulating materials was not enough to achieve optimal costs due to the high investment cost of the solution.

The benefits of space floor savings were considered in few studies. Alam *et al.* [30] concluded that fumed silica VIPs were found to be economically viable in high rental value locations assuming a service life of up to 60 years. In this case, the object of the study was a residential reference building and the energy needs were based on steady-state calculations, potentially leading to unrealistic energy use estimations. Fantucci *et al.* [31] proposed the evaluation of office buildings using the test room from ISO 52016 as a reference [32]. The authors calculated the discounted payback period and break-even rental value and found that VIPs can be cost-effective. However, the energy prices evolution during the period of calculation were not included, and the economic indicators for different cities remained fixed. Such economic data can be decisive to evaluate the economic feasibility of investments in insulation materials. These previous studies show a wide disparity of outcomes. Differences like these may be considered acceptable since economic studies such as these depend on a great number of factors such as: methodology approach, climate data, reference building typology, energy carrier, VIPs market prices, energy prices and other economic indicators that strongly influence the results. Only one study [29] used the global cost method proposed in EN 15459 [33] which was subsequently adopted by European cost-optimal methodology framework, published in the Delegated Regulation no. 244/2012

([5],[6]). However, a macroeconomic perspective including costs of greenhouse gas emissions was not present in this study.

There is a gap in the literature for analysing the cost-effectiveness of vacuum-based ETICS applications, addressed in this chapter. Furthermore, the different methodological approaches and assumptions used have led to outcomes that are difficult to compare, with only one study using the global cost methodology framework proposed by the EU.

The aim of the work presented in this chapter was to assess the cost-effectiveness of using VIPs in ETICS façades by using a comparative methodology based on the European cost-optimal methodology ([5],[6],[34]). Even though the EU cost-optimal methodology does not take into account the embodied energy of insulation materials and focuses solely on the buildings use phase, adopting this standardised methodology will allow for the results to be replicable and comparable, effectively contributing to future decision-making processes by the end users of these solutions through providing transparent information regarding their investment. Regarding macroeconomic point of view, the greenhouse gas costs were also introduced in the methodology.

The cost-optimal methodology is based on calculations of initial investment and annual energy needs for heating and cooling. For these calculations, a reference building is often used to represent the building stock. Methodologies for reference buildings definition have been discussed by researchers ([35],[36]). Different assumptions regarding parameters such as window-wall ratio, internal loads, airflow rate, etc. strongly affect the calculations, leading to inconsistent results with different best solutions [37]. The present work proposes to go around this issue by means of an alternative approach considering the energy balance based on transient heat transfer calculations for a unit area of a wall. This methodology allows for a more direct and easier comparison between insulation materials since it avoids other parameters that influence energy use calculations. This is a novel approach when compared with the state-of-the-art.

The main goal of this chapter is to perform a comprehensive whole-life costing (WLC) analysis looking to assess the cost-effectiveness of using VIPs in ETICS façades in office buildings. The study uses a comparative methodology based on the European cost-optimal methodology framework published in the Delegated Regulation no. 244/2012 ([5],[6]), with the added benefits of the rental income taken into account, as made possible by WLC approach of ISO 15686-5 [34].

While building owners and developers will often only consider the cost of construction, other costs should be considered in order to evaluate the optimal cost of construction. This is particularly relevant from the landlords' perspective for the case of a full-service lease where the landlord takes care of all operating costs, including energy costs. Such comprehensive WLC analyses support the decision makers and investors when considering VIPs as an option in the early stages of design for new building or retrofitting scenarios. In particular, this can be used to evaluate the viability of VIP solutions when compared with conventional thermal insulation materials.



In the following section, the external wall under study is presented and characterized followed by detailing of the methodology employed for estimating the energy performance of the wall. As mentioned, instead of calculating energy needs using a reference building, it is proposed that energy balance through walls is used to evaluate the impact of changing the insulation level. The energy balance between heat losses and solar gains through the walls is calculated using dynamic thermal simulation and is used directly in the WLC analysis. Then, the methodology used to calculate the whole-life costs is presented. Since this analysis is performed from the landlord perspective considering full-service leasing, the beneficial aspect obtained from increasing rental area (when using VIPs) is considered in the calculations. The results are compared with those obtained for a conventional EPS based ETICS solution, as one of the most commonly used insulation materials on the market due to its low cost [18]. Then, the results are discussed and some limitations are identified. Finally, the main conclusions from the study are drawn up.

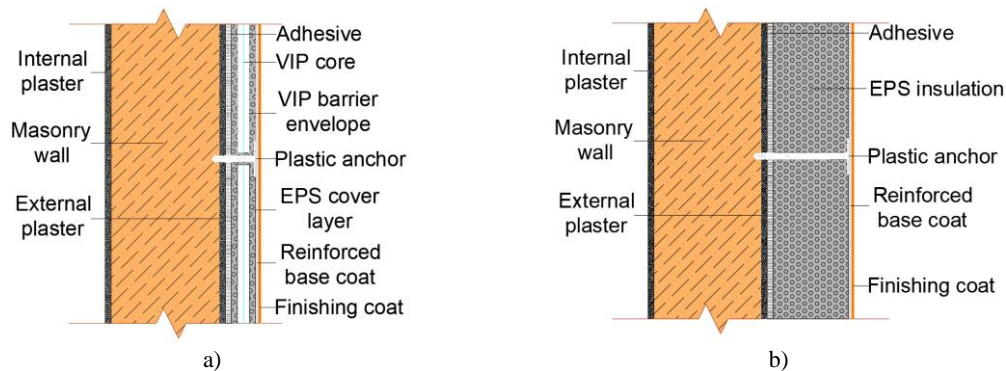
## **7.2. Materials and methods**

The present study performs a whole-life cost analysis (including the life-cycle cost and economic benefits) to assess the cost-effectiveness of using VIPs in ETICS façades in office buildings. Several factors that may affect the outcome of economic calculations, in accordance with the cost optimal methodology, are taken into account. These factors include variables that affect the thermal performance of the VIP solution (degradation with time, the edge effect and varying panel size), maintenance costs, energy costs, rental incomes and residual values. Additionally, a sensitivity analysis is carried out to include variations of initial investment costs, energy carriers, energy price predictions, service life of VIPs and rental prices.

Unlike the European common framework methodology which requires the calculation of the energy needs for a reference building, the energy balance calculations are performed at the level of the construction solution (ETICS wall). These calculations are performed for different VIP sizes using a dynamic thermal simulation software (BISTRA [38]). The ETICS wall is considered to be located in Berlin, London and Helsinki as representative climatic zones. These results are compared to those obtained for an ETICS wall with EPS. This research discusses not only a financial perspective but also a macroeconomic perspective. It also presents other financial indicators such as discounted Payback Period (dPB) and Internal Rate of Return (IRR).

### 7.2.1. Definition of the external wall

The solution under study is an external wall with an ETICS application that incorporates: a) VIP product (Figure 7.1a); and b) expanded polystyrene panel (Figure 7.1b). The product is a fumed silica vacuum panel with multi-layered metalized barrier (thermal conductivity at centre of panel of  $0.0042 \text{ W}/(\text{m}\cdot\text{K})$ ) encapsulated in EPS. The EPS cover layer (10 mm thick layers at the faces of the panels and 20 mm thick at the edges) provides protection against mechanical damage which, along with adhesive and supplementary mechanical fixings, allows for the application of the ETICS. The standard size of the encapsulated VIP product is assumed to be 640 mm x 640 mm. Additionally, a sensitivity analysis was performed and calculations were also made for smaller panels (440 mm x 440 mm) and larger panels (1040 mm x 640 mm). The ETICS solution is applied onto a conventional ceramic masonry wall (220 mm) plastered on both sides. The wall is 3 meters tall.



**Figure 7.1:** Cross-section of external walls: a) VIP ETICS solution; b) EPS ETICS solution.

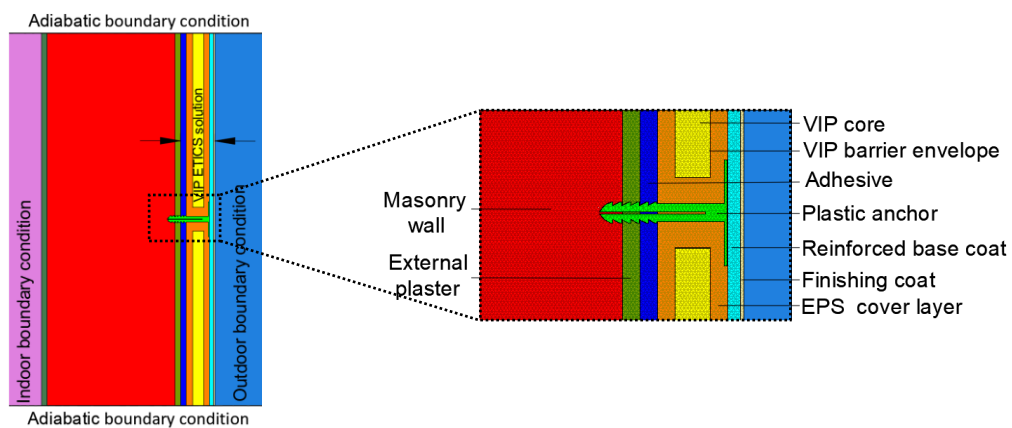
The thermophysical properties of the external wall materials are shown in Table 7.1. A solar reflectance of 0.72 is considered for the finishing coating.

**Table 7.1:** Thermophysical properties of the materials.

Construction layer	Thickness [mm]	Thermal conductivity [ $\text{W}/(\text{m}\cdot\text{K})$ ]	Emissivity [-]	Density [ $\text{kg}/\text{m}^3$ ]	Specific heat [ $\text{J}/(\text{kg}\cdot\text{K})$ ]
Internal plaster	10	1.3	0.90	1350	900
Masonry block	220	0.52	0.90	850	840
External plaster	10	1.3	0.90	1350	900
Adhesive	10	0.45	0.90	1650	900
VIP core	10 - 60	0.0042	0.90	210	900
VIP barrier	0.097	0.90	0.10	2800	880
EPS cover layer	20	0.036	0.90	20	1450
Plastic anchor	70	0.17	0.90	1390	900
Base coat	5	0.45	0.90	1650	900
Finishing coat	2	0.40	0.91	1650	1000

## 7.2.2. Energy performance assessment

The energy performance of the external walls was performed considering a transient regime. The energy balance over one year was calculated using the hourly dynamic thermal simulation software BISTRA version v4.0w [38], by Physibel, considering detailed thermal characteristics (presented in Table 7.1), different orientations and representative climate data (temperature and solar radiation provided in DesignBuilder software). BISTRA is a thermal analysis software for calculating transient heat transfer in two-dimensional free-form objects based on finite elements methods (FEM). A detailed schematic representation of the model considered in the numerical modelling is presented in Figure 7.2.



**Figure 7.2:** Detailed drawing of the 2-D model using a triangular mesh.

In order to evaluate the cost-effectiveness of incorporating the vacuum products in ETICS, the solution is compared with EPS, a widely used insulation material. The comparison is made on the basis of the equivalent thickness of EPS required to achieve the same thermal resistance as the encapsulated VIP. Over time, the thermal performance of VIPs deteriorates due to increase of inner gas pressure, moisture content and possible changes to the core material of the structure [39]. Based on the literature, a 2% thermal conductivity increase per year during the VIPs service life was considered ([40],[41]). For the EPS product, no degradation of performance was considered.

### 7.2.2.1. Effective thermal conductivity of the VIP

The energy performance calculations are presented in terms of the effective thermal conductivity of the VIP solution to account for the thermal bridging effect that occurs at the edges of the encapsulated panels. The effective thermal conductivity of the VIP product is determined

according to equation 7.1, where  $A_{VIP}$  is the VIP surface area,  $\lambda_{CoP}$  is the thermal conductivity at the centre of VIP,  $d$  is the thickness of the encapsulated VIP,  $\psi$  is the linear thermal transmittance of the joint area (between encapsulated panels),  $l$  is the length of the linear thermal bridge and  $A_p$  is the surface area of the VIP product (including the EPS edge cover).

$$\lambda_{eff} = \left[ \left( A_{VIP} \cdot \frac{\lambda_{CoP}}{d} + \psi \cdot l \right) \cdot d \right] \cdot A_p^{-1} \quad [\text{W}/(\text{m}\cdot\text{K})] \quad (7.1)$$

The linear thermal transmittance,  $\psi$ , was determined with BISCO software version v11.00w [42], by Physibel, which allows for steady-state heat transfer simulations in two-dimensional free-form objects based on FEM. Table 7.2 provides the thermal properties results for a wall with the encapsulated VIP product (640 mm x 640 mm size) with varying VIP thickness.

The effective thermal conductivity including the edge thermal bridging effects, as well as the EPS equivalent thickness, were used in WLC calculations. The effective thermal conductivity was calculated according to equation 7.1, and the wall U-values was calculated according to ISO 6946 [43], taking into account the layered structure of the wall presented in Table 7.1. The EPS thicknesses were calculated in order to achieve the same thermal resistance obtained with the encapsulated VIPs:

$$\begin{aligned} R_{EPS} = R_{VIP} &\Leftrightarrow R_{wall} + R_e + \frac{d_{EPS}}{\lambda_{EPS}} + R_i = R_{wall} + R_e + \frac{d_{VIP}}{\lambda_{effVIP}} + R_i \Leftrightarrow \\ &\Leftrightarrow d_{EPS} = \frac{d_{VIP}}{\lambda_{effVIP}} \times \lambda_{EPS} \quad [\text{m}] \quad (7.2) \end{aligned}$$

where  $R$  is the thermal resistance of the external wall (with EPS or VIP),  $d$  is the insulation thickness,  $\lambda$  is the thermal conductivity and  $R_e$  and  $R_i$  are the external and internal conventional surface thermal resistances. For the external and internal surface thermal resistances, respective values of 0.04 (m<sup>2</sup>·K)/W and 0.13 (m<sup>2</sup>·K)/W were considered, according to ISO 6946 [43].

The equivalent EPS thickness required for a conventional ETICS solution is also shown in Table 7.2. It should be noted that simulations were also performed to confirm that the thermal bridging effect occurring between EPS boards in a conventional EPS based ETICS solution is negligible, as showed in chapter 3.

**Table 7.2:** Thermal properties of an encapsulated VIP with 640 mm x 640 mm.

VIP thickness	Encapsulated VIP thickness	$\lambda_{CoP}$ [W/(m·K)]	$\psi$ [W/(m·K)]	$l$ [m]	$A_{VIP}$ [m <sup>2</sup> ]	$A_p$ [m <sup>2</sup> ]	$\lambda_{eff}$ [W/(m·K)]	EPS equivalent thickness	U-value wall
---------------	----------------------------	------------------------------	---------------------	------------	--------------------------------	----------------------------	------------------------------	--------------------------	--------------

[mm]	[mm]						[mm]	[W/(m <sup>2</sup> ·K)]	
10	30	0.0102	0.0225				<b>0.0132</b>	82	0.34
15	35	0.0085	0.0209				<b>0.0120</b>	105	0.28
20	40	0.0075	0.0190				<b>0.0114</b>	127	0.24
25	45	0.0069	0.0184				<b>0.0112</b>	144	0.22
30	50	0.0065	0.0171				<b>0.0111</b>	163	0.19
35	55	0.0062	0.0159	2.56	0.36	0.41	<b>0.0109</b>	182	0.18
40	60	0.0060	0.0146				<b>0.0107</b>	202	0.16
45	65	0.0058	0.0134				<b>0.0105</b>	223	0.15
50	70	0.0056	0.0121				<b>0.0102</b>	246	0.13
55	75	0.0055	0.0109				<b>0.0099</b>	272	0.12
60	80	0.0054	0.0095				<b>0.0095</b>	304	0.11

In order to account for the effect of varying the dimensions of the VIP product, these calculations were also performed for encapsulated VIP panels with 440 mm x 440 mm (Table 7.3) and 1040 mm x 640 mm (Table 7.4).

**Table 7.3:** Thermal properties of an encapsulated VIP with 440 mm x 440 mm.

VIP thickness [mm]	Encapsulated VIP thickness [mm]	$\lambda_{CoP}$ [W/(m·K)]	$\Psi$ [W/(m·K)]	$l$ [m]	$A_{VIP}$ [m <sup>2</sup> ]	$A_p$ [m <sup>2</sup> ]	$\lambda_{eff}$ [W/(m·K)]	EPS equivalent thickness [mm]	U-value wall [W/(m <sup>2</sup> ·K)]
10	30	0.0102	0.0225				<b>0.0146</b>	74	0.37
15	35	0.0085	0.0209				<b>0.0136</b>	92	0.31
20	40	0.0075	0.0190				<b>0.0131</b>	110	0.27
25	45	0.0069	0.0184				<b>0.0132</b>	123	0.25
30	50	0.0065	0.0171				<b>0.0131</b>	137	0.22
35	55	0.0062	0.0159	1.76	0.16	0.19	<b>0.0130</b>	152	0.21
40	60	0.0060	0.0146				<b>0.0129</b>	168	0.19
45	65	0.0058	0.0134				<b>0.0127</b>	185	0.17
50	70	0.0056	0.0121				<b>0.0123</b>	204	0.16
55	75	0.0055	0.0109				<b>0.0119</b>	226	0.14
60	80	0.0054	0.0095				<b>0.0114</b>	254	0.13

**Table 7.4:** Thermal properties of an encapsulated VIP with 1040 mm x 640 mm.

VIP thickness [mm]	Encapsulated VIP thickness [mm]	$\lambda_{CoP}$ [W/(m·K)]	$\Psi$ [W/(m·K)]	$l$ [m]	$A_{VIP}$ [m <sup>2</sup> ]	$A_p$ [m <sup>2</sup> ]	$\lambda_{eff}$ [W/(m·K)]	EPS equivalent thickness [mm]	U-value wall [W/(m <sup>2</sup> ·K)]
--------------------	---------------------------------	---------------------------	------------------	---------	-----------------------------	-------------------------	---------------------------	-------------------------------	--------------------------------------

10	30	0.0102	0.0225				<b>0.0126</b>	86	0.33
15	35	0.0085	0.0209				<b>0.0113</b>	111	0.27
20	40	0.0075	0.0190				<b>0.0106</b>	136	0.23
25	45	0.0069	0.0184				<b>0.0104</b>	156	0.20
30	50	0.0065	0.0171				<b>0.0102</b>	177	0.18
35	55	0.0062	0.0159	3.36	0.60	0.67	<b>0.0100</b>	199	0.16
40	60	0.0060	0.0146				<b>0.0098</b>	221	0.15
45	65	0.0058	0.0134				<b>0.0096</b>	244	0.13
50	70	0.0056	0.0121				<b>0.0093</b>	270	0.12
55	75	0.0055	0.0109				<b>0.0091</b>	298	0.11
60	80	0.0054	0.0095				<b>0.0087</b>	331	0.10

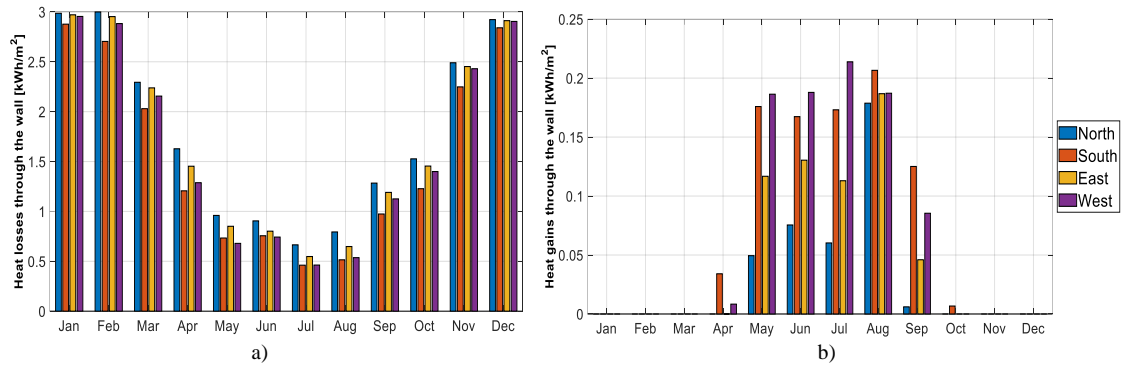
### 7.2.2.2. Energy balance through walls

In this study, the focus is to perform a comparative analysis at the level of the wall solution. This approach will allow for comparative global costs results that are dependent on climate data (location and wall orientation), but that are mostly independent of other variables.

Following ISO 52016-1 [32], an hourly method for assessing the heat flow through the wall was adopted. This method takes into account thermal capacity, internal air temperature, area of the building element, internal convective surface, thermal properties of the wall components, internal surface temperature, external air temperature and solar radiation.

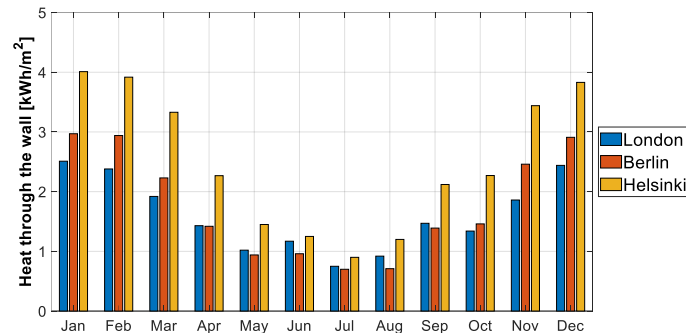
As mentioned before, the hourly energy balance was calculated using BISTRA software. The heat flow obtained per hour expressed in W/m was converted in kWh/m<sup>2</sup> considering a time integral during one year using the multiple application of the trapezoidal rule. In order to account for the effect of varying the dimensions of the VIP product, these calculations were also performed for encapsulated VIP panels with 440 mm x 440 mm and 1040 mm x 640 mm.

The internal temperature set-point is 25°C from June to September and 20°C for the remaining months. Calculations were performed for North, South, East and West-facing walls. As an example, Figure 7.3 shows the monthly heat losses (Figure 7.3a) and gains (Figure 7.3b) through the one square meter of external wall for Berlin, for the case of a ETICS solution with 40 mm of encapsulated VIP. Figure 7.3 demonstrates that for Berlin, heat losses are dominant when compared with heat gains by a factor of 6.



**Figure 7.3:** Heat flow through ETICS wall (with 40 mm encapsulated VIP) located in Berlin, expressed in kWh per square meter of façade: a) heat losses; b) heat gains.

Figure 7.4 shows the calculated monthly average energy balance (difference between losses and gains) for three different locations (Berlin, London and Helsinki). As expected, in Helsinki, which is located in a Nordic climate, the balance of losses over gains is more significant.

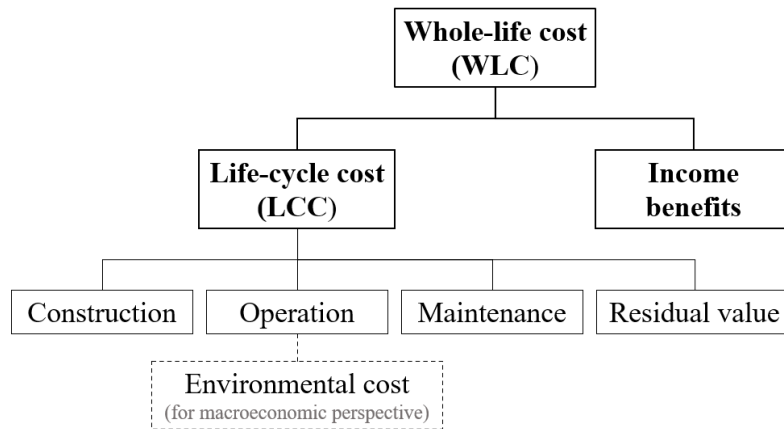


**Figure 7.4:** Average difference between losses and gains through ETICS wall (40 mm encapsulated VIP) for three locations, expressed in kWh per square meter of façade.

The estimated energy balances are dominated by the heat losses, which are quite similar for the different orientations as presented in Figure 7.3. Thus, the energy performance of the wall was simulated considering the average energy balance between all four orientations. Final energy use was calculated considering two different systems: an air conditioning unit (AC) with seasonal coefficient of performance of 5.1, class A+++ according to the Energy Label Directive [44], and an electric heater (EH) with an efficiency of 1.0. As recommended in the Commission Delegated Regulation no. 244/2012 the results are expressed in terms of primary energy. A primary energy conversion factor (PEF) of 2.0 kWh<sub>PE</sub>/kWh for electricity was used ([45],[46]). This value reflects the latest growing share of renewable energy sources and technological progress in the electricity generation sector [47]. Literature review shows different methods for PEF calculation and a forecast of it decreasing in the next few years [48]. However, to avoid uncertainties regarding this parameter, a constant PEF value was considered during the period of calculation.

### 7.2.3. Whole-life costing methodology

The proposed WLC methodology was adapted from the cost-optimal methodology framework established in the Commission Delegated Regulation no. 244/2012 ([5],[6]) and the whole-life costing methodology proposed in ISO 15686-5 [34]. Figure 7.5 presents a graphical representation of the costs considered in the calculations, namely the life-cycle cost assessment, that included the ETICS installation, operation and maintenance costs, and the economic benefits through the additional rental income due to the space savings of VIP solution.



**Figure 7.5:** Stages of the whole-life cost assessment (adapted from [34]).

Calculations are given from both the financial and macroeconomic perspectives. A period of calculation of 20 years was used, as suggested by the Regulation for non-residential buildings [5]. As the calculation period is shorter than the service life of insulation panels, disposal costs were not considered. Instead, the residual value at the end of the calculation period was included in the calculations. The environmental cost was included on the macroeconomic perspective via the costs of greenhouse gas emissions during the operation phase.

As mentioned previously, it is considered that the building owner will be paying all costs (initial investment, maintenance and energy costs) and will benefit from an annual rent paid by the tenant. An additional space savings benefits for VIPs, due to their thinner nature, is considered in the calculations. This is represented by an additional rental income,  $\Delta R$ .

From a financial perspective, the global cost,  $GC$ , expressed in € per square meter of ETICS façade, over the calculation period  $p$ , is calculated by:

$$GC(p) = \left[ C_I + \left[ \sum_{i=1}^p (C_a(i) \cdot D_f(i)) - (V_p \cdot D_f(p)) \right] \right] \cdot A_f^{-1} \quad [€/m^2] \quad (7.3)$$

Where  $V_p$ , is the residual value at the end of the calculation period  $p$ ;  $A_f$  is the façade area;  $D_f(i)$  is the discount factor for year  $i$ , calculated according equation 7.7,  $C_I$  is the initial investment



cost of a ETICS solution calculated according to equation 7.4 for a specific thickness,  $d$ , expressed in m, including material costs,  $C_{ETICS}$ , in €/m<sup>3</sup> and installation costs  $C_{installation}$  in €/m<sup>2</sup>.  $C_a$  is the annual cost during year  $i$ , calculated as presented in equation 7.5.

$$C_I = [(C_{ETICS} \cdot d) + C_{installation}] \cdot A_f \quad [€] \quad (7.4)$$

$$C_a(i) = C_e(i) + C_m - \Delta R \quad [€/year] \quad (7.5)$$

where  $C_e$  is the annual energy cost;  $C_m$  is the annual maintenance cost, defined as 1% of initial investment;  $\Delta R$  is the additional rental income related with the floor area savings for VIP in comparison with EPS, for the same thermal transmittance (U-value). The rental income is calculated according to equation 7.6:

$$\Delta R = L \cdot \Delta d \cdot R_c \quad [€/year] \quad (7.6)$$

Where the  $L$  is the length of the wall (1.0 m for a unit surface area);  $\Delta d$  is difference of wall thickness between VIP solution and corresponding U-value EPS solution and  $R_c$  is the rental price for a specific city expressed in €/m<sup>2</sup> of useful area.

The discount factor for year  $i$ , based on real discount rate  $r$  is calculated as [6]:

$$D_f(p) = \left( \frac{1}{1 + r/100} \right)^p \quad (7.7)$$

Where  $p$  is the number of years from the starting period and  $r$  is the real discount rate.

For the calculations at the macroeconomic level, an additional cost category related with the costs of greenhouse gas emissions,  $C_{ghg}$ , was introduced. The cost of greenhouse gas emissions is defined as the monetary value of environmental damage caused by CO<sub>2</sub> emissions related to the energy use in a building. For this purpose, a CO<sub>2</sub> emission intensity for electricity generation of 0.30 kgCO<sub>2</sub>/kwh [49] and carbon prices based on emission trading system from EU prediction [50] were considered (see Figure 7.6). In this perspective, applicable charges and taxes, such as value-added tax (VAT) are to be excluded. Thus, from a macroeconomic perspective, the global cost  $GC_m$  over a calculation period  $p$ , is calculated by equation 7.8:

$$GC_m(p) = \left[ C_I + \left[ \sum_{i=1}^p (C_a(i) \cdot D_f(i) + C_{ghg}) - (V_p \cdot D_f(p)) \right] \right] \times A_f^{-1} \quad [€/m^2] \quad (7.8)$$

Additionally, the discounted Payback Period (dPB) and the Internal Rate of Return (IRR) from the additional investment on VIP insulation are calculated according to equation 7.9 to 7.11.

$$dPB = i + CF_i \cdot (CF_i - CF_{i+1})^{-1} \quad [years] \quad (7.9)$$

Where  $i$  is the year before accumulated cash flows become positive, and  $CF_i$  is the discounted accumulated cash flow based in annual global costs calculations (equation 7.3) for the year  $i$  expressed by:

$$CF_i = C_I + \sum_{i=1}^t (C_a(i) \cdot D_f(i)) \quad [€] \quad (7.10)$$

Where  $C_I$  is the initial investment at the starting year,  $D_f(i)$  is the discount factor for the year  $i$  and the net cash inflow-outflows, namely the annual costs  $C_a(i)$ , are calculated according to equation 7.5 until the year before the accumulated cash flow becomes positive,  $t$ .

The IRR is the interest rate that makes the Net Present Value, NPV, of all cash flows (payments) and incomes from the investment equal to zero, where  $CF_i$  is the discounted accumulated cash flow for the year  $i$  and  $C_I$  is the initial investment at the starting year.

$$\text{IRR: NPV} = \sum_{i=1}^p (CF_i) - C_I = 0 \quad [\%] \quad (7.11)$$

## 7.2.4. Economic parameters

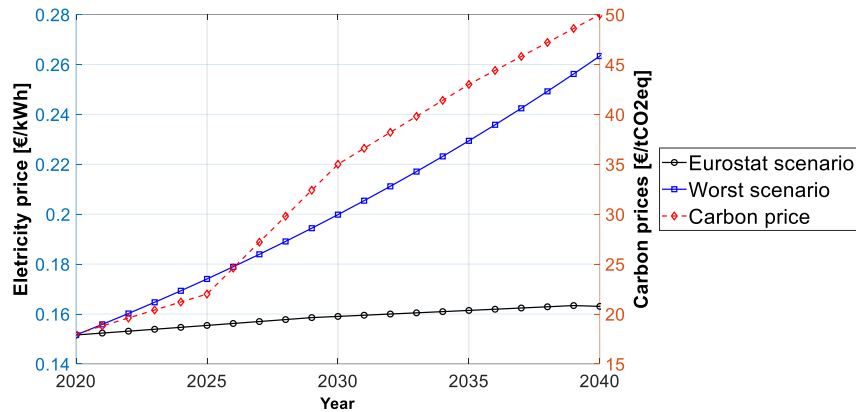
Table 7.5 presents the economic parameters used in the WLC analysis regarding the cost of the ETICS installation and the insulation materials, as well as their estimated service life for VIP [51] and EPS [37]. The insulation material and installation costs were indicated by the manufacturers. The high installation cost for the VIP solution is due to the need for previous planning (unlike EPS, VIPs cannot be cut to size onsite) and for careful handling to avoid damage to the panels, which implies higher labour costs. The land price, earthworks, cost of lifts, and other materials costs were not considered, since they are the same for EPS and VIP based solutions. Since the period of calculation is 20 years for office buildings, insulation panels service life will impact the residual value according to equations 7.3 and 7.8, considering a linear depreciation during the lifetime.

**Table 7.5:** Economic parameters used in WLC for the different ETICS solutions.

Product	Insulation cost [€/m <sup>3</sup> ]	Installation cost [€/m <sup>2</sup> ]	Service life [years]
Encapsulated VIP	3000	62.5	25
EPS	120	50	50

The economic parameters of the three investigated cities were considered. Electricity prices for non-residential buildings were obtained from the Eurostat database for the reference year of 2018 [52]. Since WLC analysis is a long-term study, it is necessary to consider the future development of energy prices during the calculation period. The evolution of energy prices was determined

according to the Eurostat predictions [50]. Additionally, in order to reflect the impact of a larger energy price increase in the future, a sensitivity analysis was performed considering an increase of 2.8% per year. Figure 7.6 shows the predicted electricity prices considered in the WLC calculations for both scenarios, regarding Berlin case study, as well as, the carbon prices based in EU projections [50].



**Figure 7.6:** Carbon price and energy price prediction for Berlin for both scenarios.

All of the economic parameters considered in calculations are summarized in Table 7.6. In order to focus on the profitability assessment of the VIP panels, the same discount rate was considered, avoiding the uncertainty of this rate.

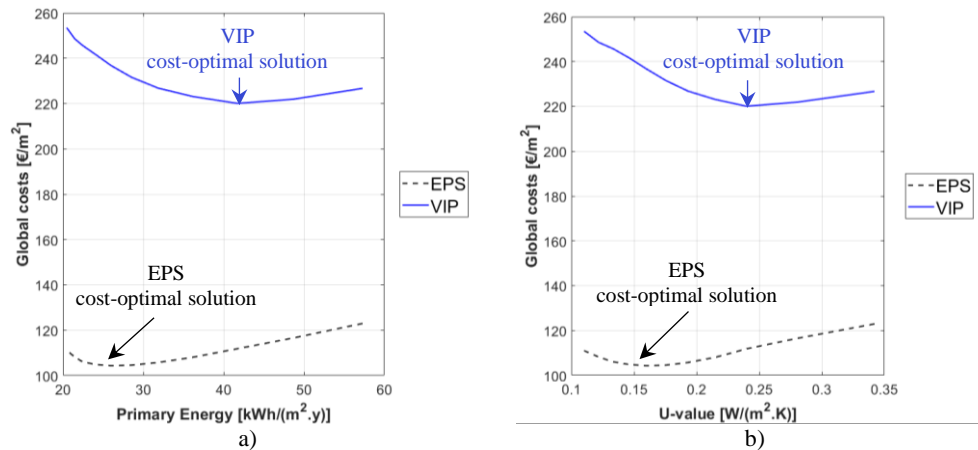
**Table 7.6:** Economic parameters used in WLC analysis for different cities at starting year.

Indicators	Berlin	London	Helsinki
Real discount rate	4%	4%	4%
VAT	19%	20%	24%
Electricity cost (without VAT)	0.1516 €/kWh	0.1423 €/kWh	0.0707 €/kWh

As the calculation period is shorter than the service life of insulation panels, disposal costs are not considered. Since the rental prices (full-service leasing) depend on the city zone, WLC calculations were performed for a range between 150 €/(m<sup>2</sup>.y) and 800 €/(m<sup>2</sup>.y).

## 7.3. Results

In this section, the main results obtained from applying the proposed methodology are presented. Figure 7.7 is used to present an example of the cost-optimal curve obtained for several insulation levels of the VIP ETICS solutions, as well as for the corresponding EPS solutions.



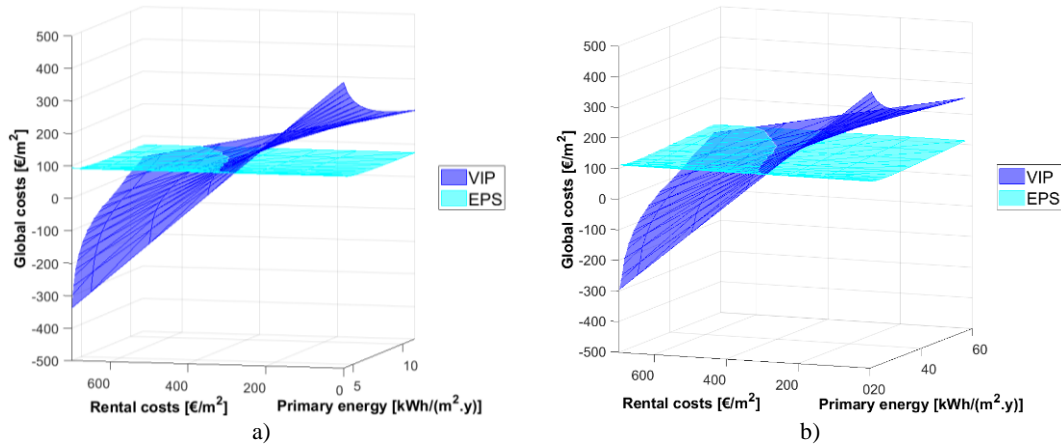
**Figure 7.7:** Berlin cost-optimal curves for VIP and corresponding EPS equivalent thickness curve for financial perspective: a) primary energy on horizontal axis; b) corresponding U-values of wall on horizontal axis.

The results shown are for an ETICS wall located in Berlin under financial perspective, with a low efficiency system (EH) and a rental price of 150 €/m<sup>2</sup>.y). These results show a VIP cost-optimal thickness of 40 mm (U-value=0.24 W/(m<sup>2</sup>.K)), representing a global cost of 220 € per m<sup>2</sup> of façade for the next 20 years. The best EPS solution, for an identical scenario is 220 mm insulation (U-value=0.15 W/(m<sup>2</sup>.K)) for a global cost of 104 € per m<sup>2</sup>. All EPS solutions have lower global costs due their lower investment costs in the given example using a relatively low rental value of (150 €/m<sup>2</sup>.y)).

Over the following subsections, the influence that changing certain parameters has on these cost optimal curves is analysed. Parameters such as rental cost, cost of VIP, size of panels, as well as VIP service life duration are explored. Different energy price scenarios and heating systems are also considered. Additionally, the outcomes of the sensitivity analyses considering different climate zones and taking on a macroeconomic perspective are also presented.

### 7.3.1. Rental costs variation

To better perceive the influence of rental costs, the graphs in Figure 7.8 show the relationship between primary energy use, rental costs and global costs considering the two different heating systems, a highly efficient air conditioning unit (AC) and a lower efficiency electric heater (EH).

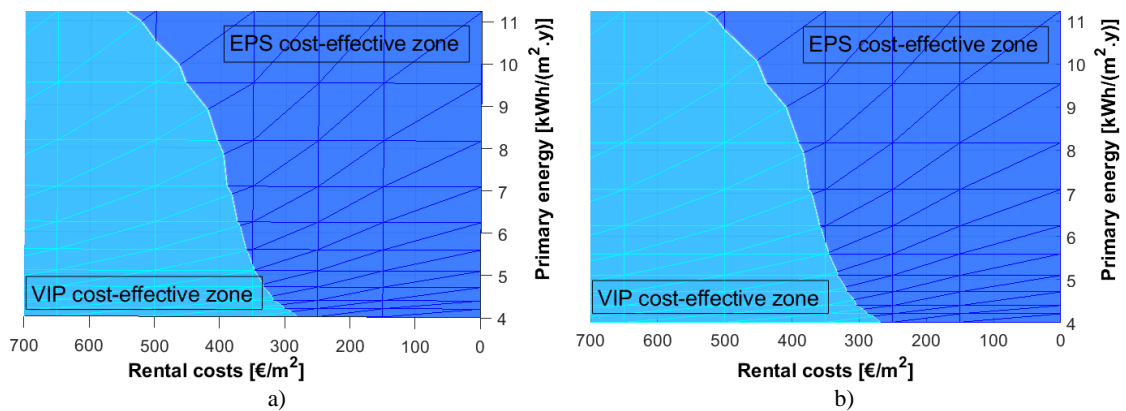


**Figure 7.8:** Rental cost analysis for Berlin for financial perspective: a) AC system; b) EH system.

Negative global costs in these graphs mean a positive benefit for the landlord. This happens when the rental income due the space savings achieved from using the VIP solution exceeds the VIP investment, maintenance and energy costs during the period of calculation. It can be seen that, for both systems, VIP is generally not a profitable solution when rental prices are lower than 350 €/m<sup>2</sup>.y). However, if the city zone has higher rental incomes, which is the case for Berlin city centre, VIPs could be a cost-optimal solution, especially when transitioning to lower energy demands (nZEB targets).

By comparing Figure 7.8a (AC system) with Figure 7.8b (EH system), slightly lower overall costs can be seen for AC system, which is expected, as it is a more energy efficient system. However, the VIP and EPS curves intersect roughly in the same zone, highlighting the relevance of rental costs over building energy use.

A top of view of the 3D graph given in Figure 7.8a is shown in Figure 7.9a. This allows for a clear view of the EPS and VIP cost effectiveness zones in the graphs. In Figure 7.9, the WLC results obtained for the AC system considering both a financial and macroeconomic perspective can be compared.

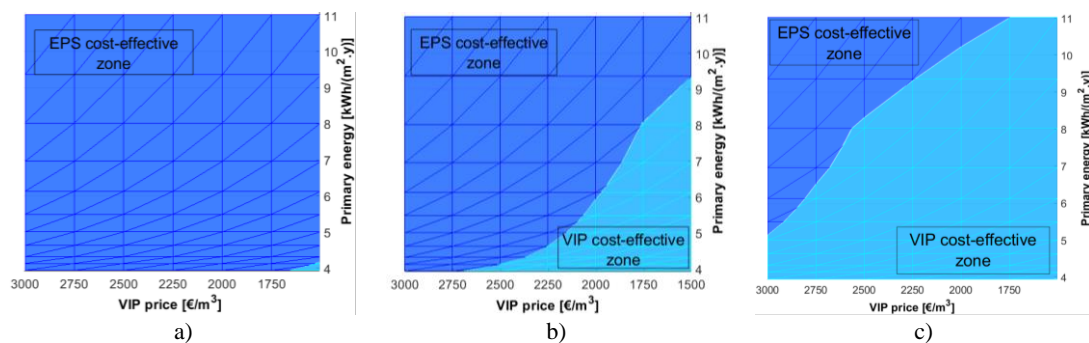


**Figure 7.9:** Rental cost analysis for Berlin: a) financial perspective; b) macroeconomic perspective.

Although the rental incomes are reduced in macroeconomic perspective, due the exclusion of VAT, it can be seen that the profitability of VIP solutions slightly benefits from a macroeconomic point-of-view (Figure 7.9b). On one hand, this is due to the fact that the costs of greenhouse gas emissions decrease for higher insulation levels. On the other hand, the investment in VIPs is substantially reduced when not taking into account applicable charges and taxes, such as VAT, benefiting its cost-effectiveness when compared with EPS. Nonetheless, the profitability of the VIP solution is still dependent on rental prices. As can be seen in Figure 7.9b, for rental prices below 260 €/m<sup>2</sup>.y, the investment in VIPs is not justifiable.

### 7.3.2. VIP price variation

In addition to the rental prices of each zone, the cost-effectiveness of VIP solutions is also dependent on initial investment costs. Figure 7.10 shows the results for the calculations performed considering an AC system, a rental price area of 150, 250 and 350 €/m<sup>2</sup>.y and a range in VIP prices between 1500 €/m<sup>3</sup> and 3000 €/m<sup>3</sup>.

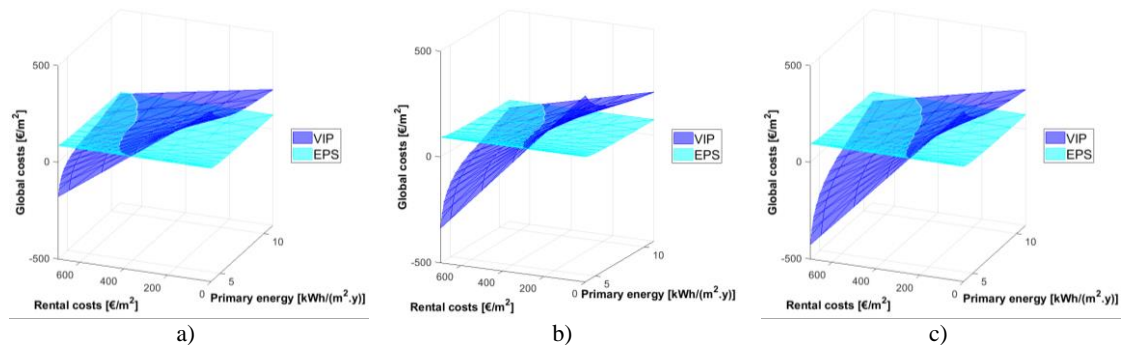


**Figure 7.10:** VIP price analysis for Berlin for financial perspective: a) fixed rental cost of 150 €/m<sup>2</sup>.y; b) fixed rental cost of 250 €/m<sup>2</sup>.y; c) fixed rental cost of 350 €/m<sup>2</sup>.y.

Considering a low rental price area (150 €/m<sup>2</sup>.y) - Figure 7.10a) it can be observed that the VIP is not profitable even when the VIP price is lower than 1750 €/m<sup>3</sup>. For a fixed value of rental cost of 250 €/m<sup>2</sup>.y (see Figure 7.10b), if the cost of VIPs is reduced to less than 2600 €/m<sup>3</sup>, it may become a competitive solution against EPS, depending on the insulation level required. As expected, when the rental price is higher (350 €/m<sup>2</sup>.y) - Figure 7.10c) the VIP profitability is increased. For example, a VIP price of 1750 €/m<sup>3</sup>, all the VIP thicknesses are cost-effective compared with EPS solutions.

### 7.3.3. VIP panel size variation

Due to the influence that the edge thermal bridging effects have on VIP equivalent thermal conductivity, panel size variation needs to be considered in the WLC analysis. It is expected that, due to better overall thermal performance, larger panels will lead to lower global costs. Figure 7.11 shows the influence of panel size on results considering a VIP price of 3000 €/m<sup>3</sup> and an AC system.



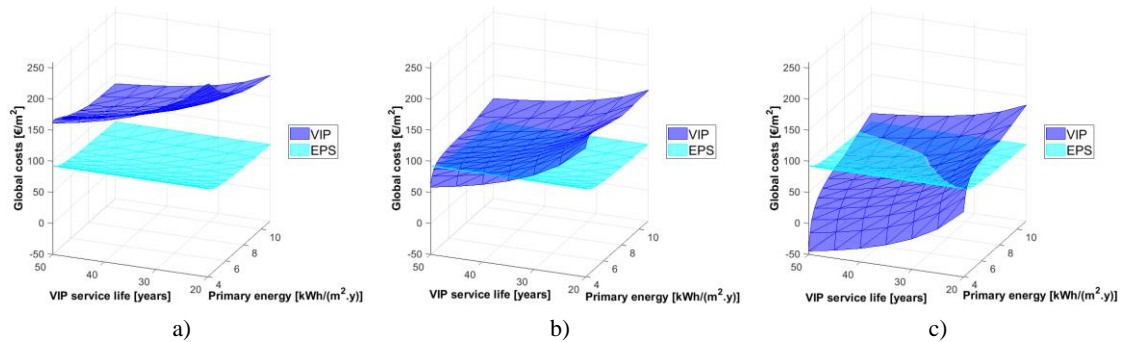
**Figure 7.11:** Panel size analysis for Berlin for financial perspective: a) 440 mm x 440 mm; b) 640 mm x 640 mm; c) 1040 mm x 640 mm.

Bigger panels result in lower primary energy use due to lower equivalent thermal conductivity (reduced linear thermal bridges effect), as well as in lower global cost, as they are strongly affected by the additional rental incomes due the higher corresponding equivalent EPS thickness. Therefore, higher rental income is achieved in larger panels. The EPS curves correspond to the different thicknesses of insulation needed to ensure the same thermal transmittance as the VIP products with different sizes of panels. In this case, global costs are affected by the large investment in insulation material required to achieve such high levels of thermal insulation. It can be said that VIP products with 1040 mm x 640 mm (Figure 7.11c) could compete against EPS when rental prices are around 300 €/m<sup>2</sup>.y, especially if there is a need for high levels of insulation, such as in nZEB buildings. For smaller panels (Figure 7.11a), only in high rental price areas (over than 460 €/m<sup>2</sup>.y) could VIP become cost-effective.

### 7.3.4. VIP service life analysis

The service life duration of VIPs is still an uncertainty for the building industry. However, the influence of VIP durability has relevance on the whole-life cost analysis. If manufacturers improve the service life of VIP products, the economic feasibility of the use of VIP in buildings

could be improved, as shown in Figure 7.12. The graphs in Figure 7.12 are for a highly efficient system (AC system) and a rental price range between 150 to 350 €/m<sup>2</sup>.y).



**Figure 7.12:** VIP service life analysis for Berlin for financial perspective: a) fixed rental cost of 150 €/m<sup>2</sup>.y; b) fixed rental cost of 250 €/m<sup>2</sup>.y; c) fixed rental cost of 350 €/m<sup>2</sup>.y).

For rental price areas of 150 €/m<sup>2</sup>.y, VIPs with current market price (3000 €/m<sup>3</sup>) are not cost-effective, even if the VIP service life is increased to 50 years (as can be seen in Figure 7.12a). However, for the highest rental price areas (350 €/m<sup>2</sup>.y) VIP products with service life of 20+ years could be a cost-effective solution (see Figure 7.12c). For rental price areas with 250 €/m<sup>2</sup>.y (Figure 7.12b) only panels with a service life year of 35+ years could make the VIP products a feasible solution. These results support the need to develop super-insulating materials with long-term performance. Only then will the investment in VIPs in buildings instead of conventional insulation materials become economically feasible.

### 7.3.5. Payback period and internal rate of return

Other financial indicators could be used to evaluate the cost-effectiveness of the VIP ETICS products. The discounted payback period resulting from additional investment on VIP insulation (in comparison with EPS insulation) are presented in Figure 7.13 and Figure 7.14, considering Berlin location with AC system. For the rental price analysis in Figure 7.13, a VIP investment was fixed at 3000 €/m<sup>3</sup>. For the VIP price analysis in Figure 7.14, a rental price was fixed at 350 €/m<sup>2</sup>.y). The vertical axes were defined for a maximum of 25 years, corresponding to the considered VIP service life. Thus, bars with 25 years of payback period suggest that the additional VIP investment will not be recovered before the service span of the VIP (25 years). For these same assumptions, the internal rate of return results are presented in Figure 7.15 and Figure 7.16.



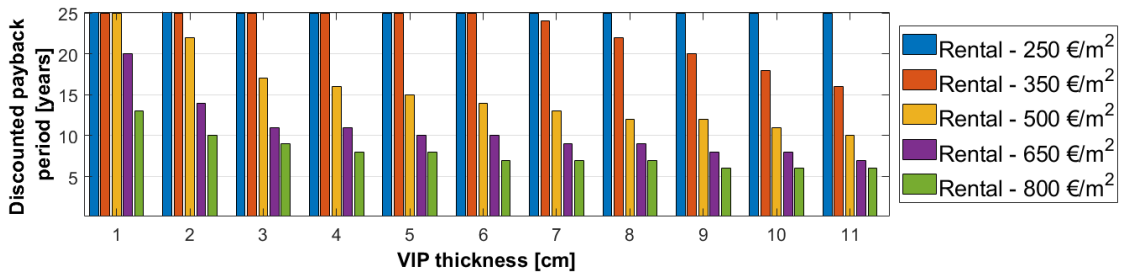


Figure 7.13: Discounted payback period for Berlin results for financial perspective. – Rental costs analysis.

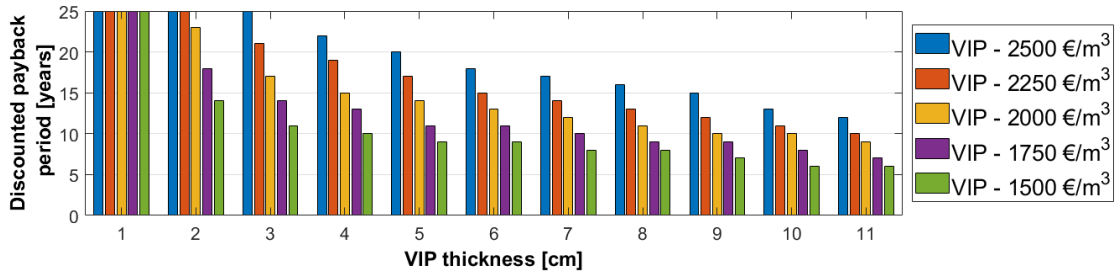


Figure 7.14: Discounted payback period for Berlin results for financial perspective – VIP price analysis.

The discounted payback period results are in accordance with the previous results. The VIP investment price should be reduced in order to achieve a dPB that is less than 20 years. Naturally, if the rental price is high, for example an area where it is 500 €/m<sup>2</sup>, the actual VIP price (3000 €/m<sup>2</sup>) could be cost-effective as shown in Figure 7.13. Similarly, the IRR results state the same conclusions. IRR higher than 5% would be considered a good investment, since the considered discounted rate was 4%.

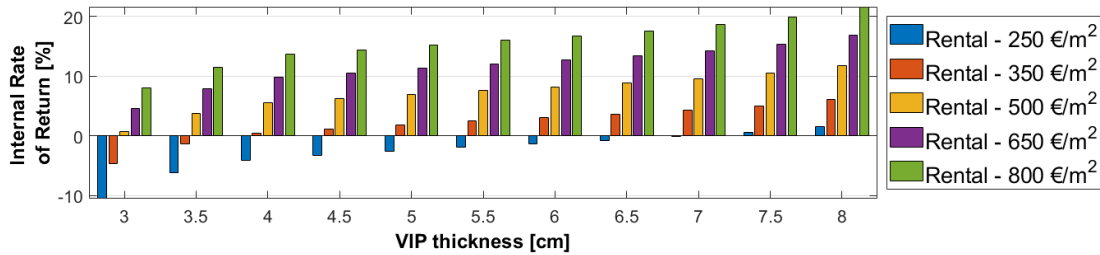


Figure 7.15: Internal rate of return for Berlin results for financial perspective – rental price analysis.

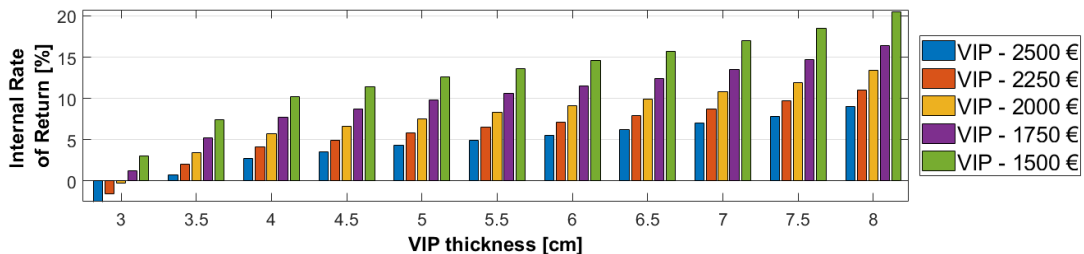
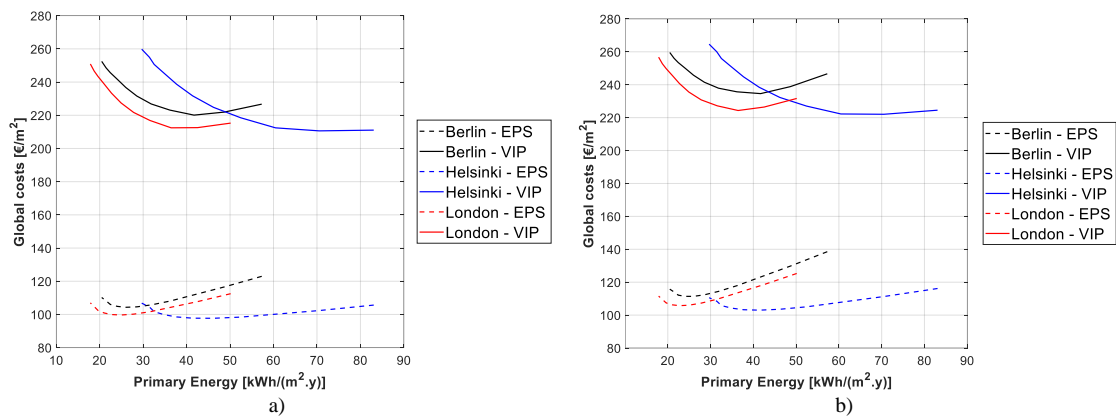


Figure 7.16: Internal rate of return for Berlin results for financial perspective – VIP price analysis.

### 7.3.6. Influence of location

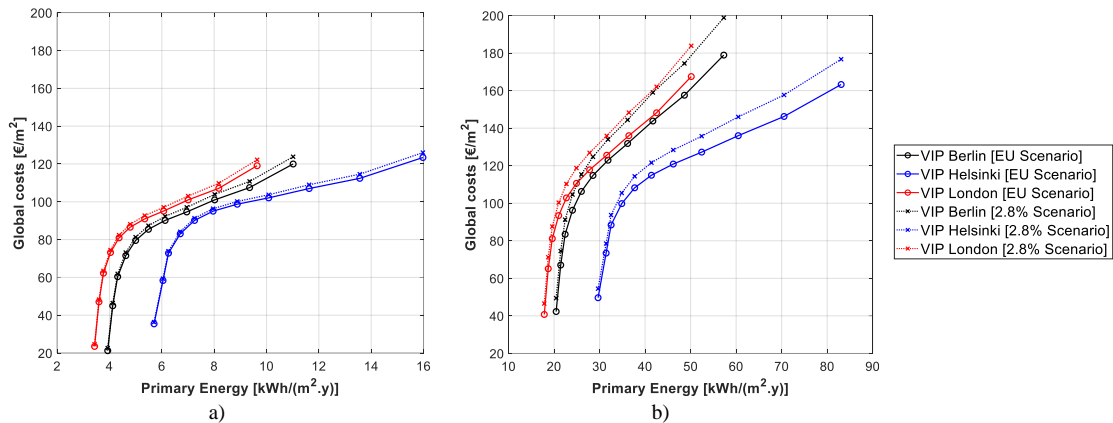
The WLC analysis was extended to consider weather data for buildings located not only in Berlin, but also in Helsinki and London. Figure 7.17 shows the WLC results for these different locations, all considering an EH system and a rental cost of 150 €/m<sup>2</sup>.y. Two different scenarios are presented: a) the Eurostat energy prices prediction; and b) a worst-case scenario with an increase of 2.8% per year.



**Figure 7.17:** VIPs cost-optimal curves for different locations and corresponding EPS equivalent thickness curves for financial perspective (rental cost of 150 €/m<sup>2</sup>.y): a) Eurostat electricity prices prediction b) Electricity price with an increase of 2.8% per year.

Although Helsinki has higher heat losses through the walls due to the colder climate, it ends up having a global cost similar to Berlin and London. This is due to the considerable difference between the electricity prices charged in these cities (see Table 7.6). This is noticeable when the curves intersect, where the investment in high VIP thicknesses in Helsinki is not economical feasible due to the reduced cost of energy used for heating (electricity). Thus, for a 20-year service life, a higher level of insulation is more cost-effective in Berlin than in Helsinki. The cost-optimal EPS equivalent thickness for Berlin is 230 mm (U-value of 0.15 W/(m<sup>2</sup>·K)) against 180 mm in Helsinki (U-value of 0.17 W/(m<sup>2</sup>·K)). This last U-value is the same as the current national thermal requirements in Finland [53], while for Berlin it is considerably lower, as the maximum U-value allowed in Germany is 0.28 W/(m<sup>2</sup>·K) [53]. The results for London are close to Berlin due to similar energy costs and energy balances.

With these results, it can be concluded that, in addition to the influence from climate data, the economic factors of each country/city are particularly relevant in the WLC analysis. That is the reason why strict parameters must be taken into account in this type of studies. Note that the analysis in Figure 7.17 is for a reduced rental cost of 150 €/m<sup>2</sup>.y. In city zones with high rental costs, VIP becomes a competitive solution, as shown in Figure 7.18, in which a rental cost of 350 €/m<sup>2</sup>.y was considered.



**Figure 7.18:** VIPs cost-optimal curves for different locations and energy prices prediction for financial perspective: a) with AC system; b) with EH system.

Similar conclusions can be reached no matter the energy price evolution over the next 20 years. However, higher global costs are obtained, especially when lower levels of insulation along with a system with lower energy efficiency are considered (Figure 7.18b). For example, with EH system, a 30 mm VIP solution in London results in a global cost of 167 €/m<sup>2</sup> and 184 €/m<sup>2</sup>, considering EU predictions and worst-case scenario, respectively. For a high efficiency energy system (Figure 7.18a) the influence of energy prices predictions is lower, resulting in a global cost of 119 €/m<sup>2</sup> (EU predictions [50]) and 122 €/m<sup>2</sup> (worst-case scenario) for the same case.

## 7.4. Discussion

A whole-life cycle analysis was performed in order to compare the VIP based ETICS solutions with conventional EPS based solutions. This section summarizes and discusses the main results of the WLC calculations. Limitations of this study are also discussed and future works are proposed.

For the energy use calculations, this chapter proposed an alternative model by using a numerical software to calculate the unsteady energy balance of a square meter of façade instead of performing a full analysis of a reference building, which typically used in WLC studies. This method allows for the direct comparison of the thermal performance of insulated walls and avoids interference from other factors, such as windows-wall ratio or the geometry of the building.

A large number of parameters important for determining VIPs economic viability in the building sector were analysed. The assumptions made in each presented case and the most important outcomes are summarized in Table 7.7.

**Table 7.7:** Summary of WLC results and assumptions.

Figure no.	Goal of analysis (perspective)	Location	Heating system	Rental price [€/m <sup>2</sup> .y]	VIP Price [€/m <sup>3</sup> ]	Main results
7.7	EPS and VIP cost-optimal curves (financial)	Berlin	EH	150	3000	VIP is not cost-effective for low rental prices.
7.8a and 7.9a	Rental costs variation (financial)	Berlin	AC	200-800	3000	VIP is cost-effective for rental prices higher than 350 €/m <sup>2</sup> .y.
7.8b	Rental costs variation (financial)	Berlin	EH	200-800	3000	VIP is cost-effective for rental prices higher than 350€/m <sup>2</sup> .y)
7.9b	Rental costs variation (macroeconomic)	Berlin	AC	200-800	3000	VIP is cost-effective for rental prices higher than 330 €/m <sup>2</sup> .y).
7.10a	VIP price variation (financial)	Berlin	AC	150	1500-3000	VIP is not cost-effective for low rental prices.
7.10b	VIP price variation (financial)	Berlin	AC	250	1500-3000	VIP is cost-effective for VIP price lower than 2600 €/m <sup>3</sup> .
7.10c	VIP price variation (financial)	Berlin	AC	350	1500-3000	VIP could be cost-effective for VIP market price (3000 €/m <sup>3</sup> ).
7.11	VIP panel size variation (financial)	Berlin	AC	200-800	1500-3000	Biggest panels are cost-effective for rental prices around 300 €/m <sup>2</sup> .y), while smaller panels only become cost-effective for areas over 460 €/m <sup>2</sup> .y).
7.12	VIP service life variation (financial)	Berlin	AC	150-350	3000	For rental prices areas with 250 €/m <sup>2</sup> .y), VIP service life needs to assure more than 35 years, to be cost-effective.
7.17	Influence of location analysis (financial)	Berlin Helsinki London	EH	150	3000	Economic factors of each location have greater influence on WLC results. Rental prices overlap energy use influence.
7.18	Influence of location analysis (financial)	Berlin Helsinki London	AC and EH	350	3000	Energy prices prediction could change the GC results, especially with lower insulation levels and inefficient energy supply system.

The technical and economic variables, such as climate data, energy costs, taxes, product service life, panel size, edge thermal bridging effects or costs (including material and application), and rental prices may lead to different results, as demonstrated in this work, suggesting that a direct comparison with the previous studies might not be possible. However, in general, the results obtained are in line with previous studies where the VIP was used in internal wall insulation and in which a reference building was considered.

Results showed that VIPs can be a cost-effective alternative to conventional insulation materials when different rental incomes are considered. These results are aligned with previous study [31] that considered a reference building and other methodological approaches. In this case [31], VIPs are cost-effective for a rental price range of 220 to 320 €/( $m^2 \cdot y$ )), depending on the climate zone. However, if lower rental costs are considered, the VIP is not cost-effective when compared with EPS, as demonstrated in previous works that did not consider space savings benefits ([26],[29]).

Regarding service life sensitivity analysis, the findings support the need to develop super-insulating materials with effective long-term performance. Only then, will the investment in VIPs be economically feasible, as suggested by Alam *et al.* [30], although based on different assumptions.

Depending on rental price and initial VIP costs, the investment in VIP products were evaluated in terms of other financial indicators, such as the discounted payback period or the internal rate of return. The additional investment in VIP ETICS solution showed a discounted payback period between 6 to 20 years. This range of payback periods for VIP investment are close to those found by Alam *et al.* [30] of 3 to 17 years for VIP fumed silica, depending on rental income of the building.

In addition to factors reflected in the cost-optimal methodology framework, a macroeconomic analysis was also considered taking into account the greenhouse gas emissions. Further research could focus on gathering life cycle inventory for VIP products and processes providing a more holistic analysis for investors and policy makers to consider a life cycle energy approach. Future work could investigate further a sensitivity analysis considering different geometrical models with implications on the energy calculation, such as linear junctions between different building elements. This methodology could also be used to assess the cost-effectiveness of other novel insulation materials, such as aerogels-based products or gas filled panels.

## 7.5. Conclusions

The present chapter aimed to provide information to owners, developers, designers and manufacturers about the cost effectiveness of using VIPs in ETICS instead of EPS, the insulation material most commonly used in conventional ETICS. In particular, the focus of the whole-life cost analysis presented in this study are ETICS wall applications in office buildings that offer full-service leasing. Many relevant economic parameters were considered, such as the VIP performance degradation over time, the thermal bridging effects and the economic benefits from saving floor area by using a slim solution. Also, a sensitivity analysis was carried out in order to

better understand the influence of factors like rental price, VIP investments cost, service life of VIP, location, scenario of energy prices prediction, as well as of performing a financial or a macroeconomic perspective.

The proposed WLC methodology allowed for a comparative analysis of the cost-effectiveness of using VIPs in buildings, as opposed to another conventional insulation material that requires a significantly thicker layer in order to achieve the same thermal performance. For this purpose, the additional floor area savings, expressed by additional rental incomes values, were introduced in the global cost calculations. The energy balances were determined based on transient calculations of the heat transfer between a unit area of an ETICS wall. This approach avoids the variability of office buildings characteristics and user profiles, focusing mainly on comparing the performance of the thermal insulation materials. Even though this chapter presents an WLC study applied to an VIP ETICS wall, the same methodology could be easily applied to other kinds of constructive solutions, such as internally insulated walls, considering new or retrofitted buildings. Since the results are expressed by square meter of façade, the size of the building is irrelevant for the application of these results.

The results have demonstrated the cost-effectiveness of using VIPs in buildings, in particular in cities where office full-leasing rental costs are high. In comparison with EPS, one of the cheaper insulation materials, and considering actual VIP prices, in cities with rental costs that are higher than  $350 \text{ €}/(\text{m}^2 \cdot \text{y})$  VIP solutions can be cost-effective for a current market VIP price of  $3000 \text{ €}/\text{m}^3$ , depending on the level of insulation required. Naturally, if manufacturers together with researchers are able to improve the service life and/or reduce the production costs, they will promote economic competitiveness in areas with lower rental prices, as shown in this chapter. It can be stated that rental prices have shown to have a stronger influence on results than building energy use (insulation levels). This is because the contribution of net floor savings is more relevant, especially in high density cities such as Berlin or London. However, unrealistic energy prices predictions may significantly alter the global costs values. Depending on rental price and initial VIP costs, the additional investment in VIP products has a discounted payback period between 6 to 20 years. Similarly, promising internal rate of return results have also been found. The analysis performed in different locations highlighted the influence of economic factors such as energy costs. Due the high electricity price in Berlin, the estimated global costs were higher than for Helsinki, even though the energy losses in the colder climate are greater. Accurate economic data is also essential for performing an adequate whole-life cycle assessment.

From the point of view of decision makers and environmental politics, the profitability of VIP solutions is slightly improved when a macroeconomic perspective is taken. Thus, it can be said that using VIPs in building façades can contribute to achieving nZEB targets while ensuring economic competitiveness. However, further studies using a whole system approach which includes the material's embodied energy should be carried out.

The understanding of the actual thermal performance of the insulation is also fundamental for achieving a realistic whole-life cycle approach and reliable results. Especially in the case of VIP technology, where uncertainties remain about the actual global thermal performance due the edge thermal bridging effects and about the panels' performance throughout their service life. WLC results showed to be significantly influenced by panel size. These parameters are decisive when assessing the cost-effectiveness of super-insulating materials struggling to compete with other insulation materials on the market.

## References

- [1] European Parliament, “Directive 2002/65/EC of the European Parliament and of the Council of 16 December 2002 on the energy performance of buildings”, *Off. J. Eur. Communities*. pp. 65–71, 2002, doi:10.5040/9781782258674.0021.
- [2] European Parliament, “Directive 2010/31/EU of the European Parliament and of the Council of 19 May 2010 on the energy performance of buildings (recast)”, *Off. J. Eur. Union*. pp. 13–35, 2010, doi:10.3000/17252555.L\_2010.153.eng.
- [3] European Parliament, “Directive (EU) 2018/844 of the European Parliament and of the Council of 30 May 2018 amending Directive 2010/31/EU on the energy performance of buildings and Directive 2012/27/EU on energy efficiency”, *Off. J. Eur. Union*. pp. 75–91, 2018.
- [4] S. Resalati, C. C. Hendrick, C. Hill, “Embodied energy data implications for optimal specification of buildings envelopes”, *Build. Res. Inf.* vol. 48, pp. 429–445, 2020, doi:10.1080/09613218.2019.1665980.
- [5] European Commission, “Commission Delegated Regulation (EU) No 244/2012 of 16 January 2012 supplementing Directive 2010/31/EU of the European Parliament and of the Council on the energy performance of buildings by establishing a comparative methodology framework for calculating”, *Off. J. Eur. Union*. vol. pp. 1-38, 2012, doi:10.3000/1977091X.C\_2012.115.eng.
- [6] European Commission, “Guidelines accompanying Commission Delegated Regulation (EU) No 244/2012 of the European Parliament and of the Council on the energy performance of buildings by establishing a comparative methodology framework for calculating cost-optimal levels of minimum energy performance requirements for buildings and building elements”, *Off. J. Eur. Union*. pp. 1–28, 2012.
- [7] M. Mihai, V. Tanasiev, C. Dinca, A. Badea, R. Vidu, “Passive house analysis in terms of energy performance”. *Energy Build.* vol. 144, pp. 74–86, 2017, doi:10.1016/j.enbuild.2017.03.025.
- [8] J. Maia, N. M. M. Ramos, R. Veiga, “Evaluation of the hygrothermal properties of thermal rendering systems”, *Build. Environ.* vol. 144, pp. 437–449, 2016, doi:10.1016/j.buildenv.2018.08.055.

- [9] B. P. Jelle, “Traditional, state-of-the-art and future thermal building insulation materials and solutions – Properties, requirements and possibilities”, *Energy Build.* vol. 43, pp. 2549–2563, 2011, doi:10.1016/j.enbuild.2011.05.015.
- [10] M. Koebel, J. Wernery, W. Malfait, “Energy in buildings—Policy, materials and solutions”, *MRS Energy & Sustainability*, vol. 4, E12, 2017, doi:10.1557/mre.2017.14.
- [11] S. S. Alotaibi, S. Riffat, “Vacuum insulation panels for sustainable buildings: a review of research and applications”, *Int. J. Energy Res.* vol. 31, pp. 135–147, 2013, doi.org/10.1002/er.3101.
- [12] S. Brunner, K. G. Wakili, T. Stahl, B. Binder, “Vacuum insulation panels for building applications - Continuous challenges and developments”, *Energy Build.* vol. 85, pp. 592–596, 2014, doi:10.1016/j.enbuild.2014.09.016.
- [13] O. Kaynakli, “A review of the economical and optimum thermal insulation thickness for building applications”, *Renew. Sustain. Energy Rev.* vol. 16, pp. 415–425, 2012, doi:10.1016/j.rser.2011.08.006.
- [14] T. Nussbaumer, K. G. Wakili, C. Tanner, “Experimental and numerical investigation of the thermal performance of a protected vacuum-insulation system applied to a concrete wall”, *Appl. Energy.* vol. 83, pp. 841–855, 2006, doi:10.1016/j.apenergy.2005.08.004.
- [15] Research and Markets, “Vacuum Insulation Panels - Global Market Trajectory & Analytics”, <https://www.researchandmarkets.com/reports/4806375/vacuum-insulation-panels-global-market> (accessed Sept. 17, 2020).
- [16] Statista, “Rental prices of prime office properties in selected European cities as of the fourth quarter of 2019”, <https://www.statista.com/statistics/431672/commercial-property-prime-rents-europe/> (accessed Jun. 17, 2020).
- [17] A. Kamal, S.G. Al-Ghamdi, M. Koc, “Revaluing the costs and benefits of energy efficiency: A systematic review”, *Energy Res. Soc. Sci.* vol. 54, pp. 68–84, 2019, doi:10.1016/j.erss.2019.03.012.
- [18] M. F. Alsayed, R. A. Tayeh, “Life cycle cost analysis for determining optimal insulation thickness in Palestinian buildings”, *J. Build. Eng.* vol. 22, pp. 101–112, 2019, doi:10.1016/j.jobe.2018.11.018.
- [19] R. Idchabani, A. Khyad, M. El Ganaoui, “Optimizing insulation thickness of external walls in cold region of Morocco based on life cycle cost analysis”, *Energy Procedia.* vol. 139, pp. 117–121, 2017, doi:10.1016/j.egypro.2017.11.183.
- [20] P. A. Fokaides, A. M. Papadopoulos, “Cost-optimal insulation thickness in dry and mesothermal climates: Existing models and their improvement”, *Energy Build.* vol. 68, pp. 203–212, 2014, doi:10.1016/j.enbuild.2013.09.006.
- [21] D. D. Agostino, F. de Rossi, M. Marigliano, C. Marino, F. Minichiello, “Evaluation of the optimal thermal insulation thickness for an office building in different climates by means of the basic and modified “cost-optimal” methodology”, *J. Build. Eng.* vol. 24, pp. 100743, 2019, doi:10.1016/j.jobe.2019.100743.
- [22] J. Nyers, L. Kajtar, S. Tomić, A. Nyers, “Investment-savings method for energy-economic optimization of external wall thermal insulation thickness”, *Energy Build.* vol. 86, pp. 268–274, 2015, doi:10.1016/j.enbuild.2014.10.023.



- [23] A. Aïssani, A. Chateaneuf, J. P. Fontaine, P. Audebert, “Cost model for optimum thicknesses of insulated walls considering indirect impacts and uncertainties”, *Energy Build.* vol. 84, pp. 21–32, 2014, doi:10.1016/j.enbuild.2014.07.090.
- [24] A. Dombayci, Ö. Atalay, Ş. Güven Acar, E. Yilmaz Ulu, H. Kemal Ozturk, “Thermoeconomic method for determination of optimum insulation thickness of external walls for the houses: Case study for Turkey”, *Sustain. Energy Technol. Assessments*, vol. 22, pp. 1–8, 2017, doi:10.1016/j.seta.2017.05.005.
- [25] A. M. Raimundo, N. B. Saraiva, A. V. M. Oliveira, “Thermal insulation cost optimality of opaque constructive solutions of buildings under Portuguese temperate climate”, *Build. Environ.* vol. 182, 107107, 2020, doi:10.1016/j.buildenv.2020.107107.
- [26] M. Alam, H. Singh, M.C. Limbachiya, “Vacuum insulation panels (VIPs) for building construction industry - a review of the contemporary developments and future directions”, *Appl. Energy*. vol. 88 pp. 3592–3602, 2011, doi:10.1016/j.apenergy.2011.04.040.
- [27] K. Cho, Y. Hong, J. Seo, “Assessment of the economic performance of vacuum insulation panels for housing projects”, *Energy Build.* vol. 70 pp. 45–51, 2014, doi:10.1016/j.enbuild.2013.11.073.
- [28] M. Abdul Mujeebu, N. Ashraf, A. Alsuwayigh, “Energy performance and economic viability of nano aerogel glazing and nano vacuum insulation panel in multi-story office building”, *Energy*, vol. 113, pp. 949–956, 2016, doi:10.1016/j.energy.2016.07.136.
- [29] E. Di Giuseppe, M. Iannaccone, M. Telsoni, M. D’Orazio, C. Di Perna, “Probabilistic life cycle costing of existing buildings retrofit interventions towards nZE target: Methodology and application example”, *Energy Build.* vol. 144 pp. 416–432, 2017, doi:10.1016/j.enbuild.2017.03.055.
- [30] M. Alam, H. Singh, S. Suresh, D. A. G. Redpath, “Energy and economic analysis of Vacuum Insulation Panels (VIPs) used in non-domestic buildings”, *Appl. Energy*, vol. 188, pp. 1–8, 2017, doi:10.1016/j.apenergy.2016.11.115.
- [31] S. Fantucci, S. Garbaccio, A. Lorenzati, M. Perino, “Thermo-economic analysis of building energy retrofits using VIP - Vacuum Insulation Panels”, *Energy Build.* vol. 196, pp. 269–279, 2019, doi:10.1016/j.enbuild.2019.05.019.
- [32] *Energy performance of buildings - Energy needs for heating and cooling, internal temperatures and sensible and latent heat loads*, ISO 52016-1, International Organization for Standardization, 2017.
- [33] *Energy performance of buildings - Economic evaluation procedure for energy systems in buildings*, EN 15459, European Committee for Standardization, 2007.
- [34] *Buildings and constructed assets -- Service life planning – Part 5: Life-cycle costing*, ISO 15686-5, International Organization for Standardization, ISO 15686-5, 2017.
- [35] S. P. Corgnati, E. Fabrizio, M. Filippi, V. Monetti, “Reference buildings for cost optimal analysis: Method of definition and application”, *Appl. Energy*. vol. 102, pp. 983–993, 2013, doi:10.1016/j.apenergy.2012.06.001.
- [36] A. B. Vasconcelos, M. D. Pinheiro, A. Manso, A. Cabaço, “A Portuguese approach to define reference buildings for cost-optimal methodologies”, *Appl. Energy*. vol. 140, pp. 316–328, 2015, doi:10.1016/j.apenergy.2014.11.035.

- [37] S. Tadeu, A. Tadeu, N. Simões, M. Gonçalves, R. Prado, “A sensitivity analysis of a cost optimality study on the energy retrofit of a single-family reference building in Portugal”, *Energy Effic.* pp. 1–22, 2018, doi:10.1007/s12053-018-9645-5.
- [38] *BISTRA - 2D transient heat transfer*, (version 4.0w). Physibel. <http://www.physibel.be/bistra.htm>.
- [39] *Vacuum Insulation Panels (VIP) with factory applied protection layers*, EAD 040011-00-1201, European Organisation for Technical Approvals, 2018.
- [40] E. Wegger, B. P. Jelle, E. Sveipe, S. Grynning, A. Gustavsen, R. Baetens, J. V. Thue, “Aging effects on thermal properties and service life of vacuum insulation panels”, *J. Build. Phys.* vol. 35 pp. 128–167, 2011, doi:10.1177/1744259111398635.
- [41] European Association for ETICS, 5<sup>th</sup> European ETICS Forum, online, 2021.
- [42] *BISCO - 2D steady state heat transfer*, (version 11.0w). Physibel. <http://www.physibel.be/v0n2bi.htm>.
- [43] *Building components and building elements - Thermal resistance and thermal transmittance - Calculation method*, ISO 6946, International Organization for Standardization, 2017.
- [44] European Commission, “Commission Delegated Regulation (EU) No 626/2011 of 4 May 2011 supplementing Directive 2010/30/EU of the European Parliament and of the Council with regard to energy labelling of air conditioners”, *Off. J. Eur. Union.* pp. 1–72, 2011.
- [45] European Commission, “Annex to the proposal for a directive of the European Parliament and of the Council amending Directive 2012/27/EU on energy efficiency”, 2016.
- [46] EURELECTRIC, “European Commission proposal to revise the Energy Efficiency Directive EURELECTRIC proposals for amendments”, 2017, <https://www.eurelectric.org/media/2444/key-amendments-to-the-energy-efficiency-directive.pdf>.
- [47] European Parliament, “Directive 2018/2002/EU amending Directive 2012/27/EU on Energy Efficiency”, *Off. J. Eur. Union.* vol. 328 pp. 210–230, 2018, <https://eur-lex.europa.eu/legal-content/EN/TXT/PDF/?uri=CELEX:32018L2002&from=EN>.
- [48] A. Esser, F. Sensfuss, “Evaluation of primary energy factor calculation options for electricity”, 2016, [https://ec.europa.eu/energy/sites/ener/files/documents/final\\_report\\_pef\\_eed.pdf](https://ec.europa.eu/energy/sites/ener/files/documents/final_report_pef_eed.pdf).
- [49] European Environment Agency, “CO2 emission intensity”, 2018, <https://www.eea.europa.eu/data-and-maps/daviz/co2-emission-intensity-5> (accessed 7 May 2020).
- [50] P. Capros, A. De Vita, N. Tasios, P. Siskos, M. Kannavou, A. Petropoulos, S. Evangelopoulou, M. Zampara, D. Papadopoulos, C. Nakos et al., L. Paroussos, K. Fragiadakis, S. Tsani, P. Karkatsoulis et al., P. Fragkos, N. Kouvaritakis et al., L. Höglund-Isaksson, W. Winiwarter, P. Purohit, A. Gomes-Sanabria, S. Frank, N. Forsell, M. Gusti, P. Havlík, M. Obersteiner, H.P. Witzke, M. Kesting, “EU Reference Scenario 2016: Energy, Transport and GHG emissions trends to 2050”, 2016, doi:10.2833/9127.
- [51] *Thermal insulation products for buildings - Factory-made vacuum insulation panels (VIP) - Specification*, EN 17140, European Committee for Standardization, 2020.

- [52] Eurostat, “Electricity and natural gas price statistics - Statistics Explained”, 2019, [http://epp.eurostat.ec.europa.eu/statistics\\_explained/index.php/Electricity\\_and\\_natural\\_gas\\_price\\_statistics](http://epp.eurostat.ec.europa.eu/statistics_explained/index.php/Electricity_and_natural_gas_price_statistics).
- [53] Global Buildings Performance Network, “Building Policies for a Better World”, 2020. <https://www.gbpn.org/databases-tools/> (accessed July 12, 2020).



## **CHAPTER 8**

### **CONCLUSIONS AND FUTURE WORKS**



## **8. Conclusions and future works**

### **8.1. Overview and final statements**

The use of efficient thermal insulation materials plays a key role when it comes to increasing the energy efficiency of the building stock. Therefore, developing and using advanced materials, such as vacuum insulation panels, will contribute to the large-scale up-take of nearly zero-energy buildings. Combining the known advantages of External Thermal Insulation Composite Systems (ETICS) with the super-insulating qualities of vacuum insulation panels (VIPs) has potential to creating an outstanding thermal insulation solution. Nevertheless, the use of VIPs in buildings is, at this moment, a niche market, since there still are some limitations/challenges regarding this recent technology. In this context, this research presented herein looked to contribute to the literature by studying the performance of a novelty encapsulated VIP panel designed to be used in ETICS façades. For this purpose, a multidisciplinary investigation was conducted focusing mainly on the experimental evaluation of a VIP based ETICS solution, including laboratorial testing and onsite measurements.

The work began with the literature review (presented in chapter 2), which included the identification of the main challenges posed by the use of VIP in buildings, and in ETICS solutions in particular. The focus was to find VIP products suited for use in ETICS, to identify the relevant case studies in the state-of-art and to learn with the main findings that drawn from these cases. The literature review showed that the edge thermal bridging effects; the long-term performance uncertainty; and the high costs of VIP products are the main challenges preventing the widespread use of VIPs in buildings. Also, VIP installation, with the impossibility of being perforated and adapted onsite, is identified as an additional limitation of the VIP when compared to conventional insulation materials. In order to address this, a guideline for VIP based ETICS installation was proposed in Annex A of this thesis. This document provides information regarding the design, planning, installation, maintenance and waste disposal works required, and includes considerations about the application procedure and constructive details. The main concerns regarding VIP based ETICS, which are explored and discussed in chapter 2 serve as motivation for the research work presented in this thesis.

The selection of a VIP panel suited to be used in ETICS solutions was carried out on the first stages of the work. With the production of the first test specimens, a laboratory test campaign was performed, aiming to characterize the selected VIP regarding their mechanical and hygrothermal behaviour. The summary of the test results was presented in Annex B. The test results showed that the VIP solution complies with the requirements set out in the European Assessment Document (EAD) for ETICS and in the VIP specification standard, attesting their suitability for the use in buildings façades. However, lower mechanical behaviour of panels without vacuum (intentionally perforated panels) was found, which could be a problem for the long-term behaviour of the solution in case of failure of the barrier envelope.

A study of the edge thermal bridging effect of VIPs is presented in chapter 3. For this purpose, experimental and numerical approaches were conducted, quantifying and demonstrating that the thermal bridging effect between panel joints have a significant impact on the overall thermal performance of the walls. Thus, the edge thermal bridging effect, as well, as the thermal conductivity after ageing, needs to be taken into account at the design stage, in order to ensure a long-term high thermal performance and avoid unexpected increase of energy demands during the service life. The installation, the size of the panel, the multilayer barrier envelope and the edge material design are determinant factors for reducing linear thermal transmittance values, and consequently, for promoting better overall thermal performance. A balance between these parameters should be striven for, looking to allow an easy installation, assure the long-term thermal performance and minimize the edge thermal bridging effects.

After evaluating the VIP product, the super-insulating ETICS was studied under real weather conditions. For this purpose, a long-term monitoring of real VIP based ETICS walls was carried out in two case studies, located in different climatic conditions, namely: a retrofitted wall located in Warsaw (presented in chapter 4) and two free-standing walls located in Coimbra (presented in chapter 5). After more than 24 months of onsite monitoring, the VIP based ETICS solution did not revealed remarkable anomalies when compared with conventional ETICS, which is a promising indicator for this innovative solution. The higher thermal performance of VIP, compared to conventional insulations, was confirmed through temperatures and heat fluxes measurements, even when measuring at the joint area where the thermal bridging edge effect occurs. However, in comparison with other insulation materials, higher surface temperature amplitudes were found in the VIP solutions, increasing the risk of the rendering system cracking. Also, the condensation risk was found to be slightly higher when compared with an EPS ETICS solution, leading to higher biological growth risk on VIP based ETICS façades. For this reason, manufacturers should look into developing optimized rendering system products with properties that reduce the risk of early anomalies in super-insulating solutions.

To study the accelerated ageing of the constructive solution under controlled environmental parameters, a novel laboratory test campaign to assess the hygrothermal performance of the VIP based ETICS was proposed and carried out using a large-scale test specimen. The ageing test



campaign included the standard hygrothermal cycles for ETICS and a new test procedure that introduces solar radiation. In order to recreate real environmental conditions in the laboratory, the new ageing test method included a radiation system that simulates a large wavelength range of radiation (UV-C, UV-B, UV-A, visible and infrared radiation). This experimental set-up enabled the assessment of the system's performance and durability and was able to potentiate early-stage anomalies on the solution considering different finishing coat colours. The experimental results revealed loss of VIP thermal performance during the ageing cycles and microcracking over the VIP joints, in particular when the solution was exposed to solar radiation.

While the resistance to hygrothermal cycles testing according to ETICS EAD is considered essential to evaluate the compatibility of the ETICS components, the introduction of the solar radiation degradation agent in this type of ageing tests proved to be fruitful. In fact, the use of solar radiation allowed for the evaluation of different finishing coat colours. This agent (which is closer to the real conditions of use) promoted degradations which were not verified in the standard ageing tests. Furthermore, it can be concluded that the EAD ETICS is not fully adequate for performing the assessment of this novelty insulation panel. For example, the hygrothermal cycles resistance is only focused on the rendering system anomalies, neglecting the evaluation of thermal performance (due to potential loss of vacuum) of the VIPs.

From the experimental test results, it can be concluded that the VIP joints are one of the most critical issues of the solution. In addition to linear thermal transmittance found in VIP joints, which increase the overall thermal performance of VIP walls, most of microcracking was observed at VIP joints areas and connections with openings. This issue is potentiated by the difficulty of carrying out a perfect layout pattern design (minimizing cracking risk) due to the production panel's size available.

During this research, numerical modelling was used to simulate the temperature behaviour of the VIP solution. The goal was analyse the accuracy of available software to simulate the thermal performance of VIP and model not only the centre of panel area, but also the joints between panels. For this purpose, the numerical results were compared with experimental measurements for both laboratory and onsite monitoring campaigns. In general, the numerical results showed a good agreement with the experimental measurements, even for real unsteady conditions. The environmental data collection, namely air temperature, convection phenomena and solar radiation are determinant for the results. Also, accurate material properties such as thermal conductivity, solar reflectance, amongst others, are key-factors for the quality of the numerical modelling results.

Finally, the economic feasibility of using VIP in façades was analysed in chapter 7. Since the high initial VIP costs is one of the main reasons for the lack of VIP applications in buildings, performing a life cycle costs assessment is a relevant way to evaluate the economic feasibility of the use of this super-insulating material. In this study, a whole-life costing methodology that

compares the cost-effectiveness of VIPs against conventional insulation materials that takes into account the additional rental income due to space savings was proposed. The results showed that, at the current price VIPs are only cost-effective in cities where the economic benefit of saving space is decisive. For this reason, the use of VIPs is cost-effective in particular locations and in climates with high heating needs, such as central Europe and Nordic countries. Whole-life cost results showed to be significantly influenced by panel size, VIP service life and initial costs, taking into account the global costs of 20 years. These parameters are decisive when assessing the cost-effectiveness of VIPs struggling to compete with other traditional insulation materials. If manufacturers are able to improve the service life and/or reduce the panels production costs, they will promote economic competitiveness and, consequently the more widespread use of vacuum technology.

It should be noted that the main conclusions drawn in this thesis are valid for the encapsulated VIP product selected, which was specifically developed for use in external insulation finishing systems. The use of other products should be carefully studied, since the performance of vacuum technology is highly dependent on the components of the panels, such as the multilayer barrier envelope, the core material, the use of getters/desiccants, the edge material design, amongst other characteristics.

The research works conducted during this doctoral thesis, of which the onsite evaluation and experimental tests on large-scale test specimen stand out, indicate that VIPs can be successfully used in ETICS with a rendering finishing. Nevertheless, such integration needs to be meticulously performed, since concerns specific to VIP installation need to be taken into account. Scientific investigations of this super-insulating material will lead to continuous improvements and will, consequently, increase the confidence of builders, designers and users. In this context, this work has presented a positive contribution towards the more wide-spread use of VIPs in buildings, and consequently towards promoting the improvement of the energy efficiency of building stock.

## 8.2. Future works

This research could be considered an ongoing work, since there are several aspects that deserve further research for a more in-depth knowledge on the use of vacuum technology in ETICS façades. Therefore, the following future studies are suggested:

- To study the viability of using different VIP solutions, for example a solution without materials along the edges of the panels (face cover layers only). This type of solution could be studied for a purely bonded VIP based ETICS which could be an interesting

solution to minimize the linear thermal transmittance value and the point thermal transmittance (no mechanical fixing devices);

- To continue the long-term onsite monitoring campaign in order to evaluate the degradation of the thermal performance of the VIPs over time, as well as to assess the performance of the rendering system along the service life of the system. In this context, establishing a correlation between laboratorial ageing tests and real on-site degradation could be useful to estimate service life of the solution and define adequate laboratorial tests duration;
- To develop laboratorial test procedures to assess the biological growth resistance by means of accelerating ageing cycles;
- To study more in depth the effects of solar radiation on the rendering system, looking to better understand the combination of the effect of UV, visible and infrared radiation, as well as the temperature and humidity daily cycles;
- To use numerical models to simulate mass transfer phenomena in order to assess moisture transport and evaluate condensation risk;
- To carry out detailed life cycle assessments (cradle to grave analysis) of VIP based ETICS. In this context, a preliminary work<sup>1</sup> has been done regarding the evaluation of the environmental impact of different VIP core materials (cradle to gate analysis).

---

<sup>1</sup> S. Resalati, T. Okoroafor, P. Henshall, N. Simões, M. Gonçalves, M. Alam, “Comparative life cycle assessment of different vacuum insulation panel core materials using a cradle to gate approach”, *Building and Environment*, vol. 188, 107501, 2021. <https://doi.org/10.1016/j.buildenv.2020.107501>



**ANNEX A**

**GUIDELINES FOR VIP BASED ETICS  
SOLUTIONS**



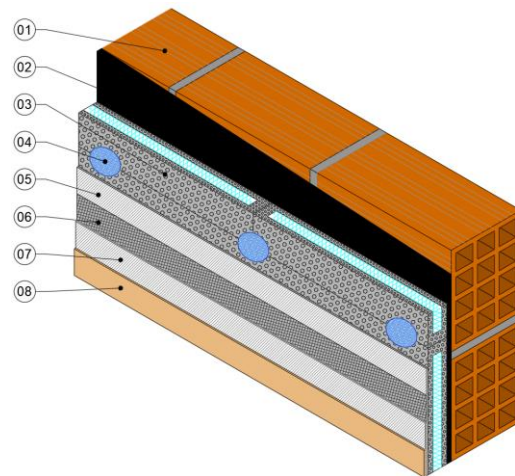
## **Table of contents**

Table of contents .....	1
1. Introduction .....	2
2. Design and planning.....	3
3. Installation.....	5
4. Maintenance .....	7
5. Disassembly and waste disposal .....	8
6. Application procedure .....	8
6.1. Environmental conditions .....	9
6.2. Support preparation .....	9
6.3. Base connection.....	10
6.4. Fixing VIP panels.....	10
6.5. Bonding of VIP .....	11
6.6. Anchoring.....	12
6.7. Base coat with reinforcement.....	13
6.8. Finishing coat application .....	15
7. Constructive details .....	16
8. Conclusion.....	25
References.....	25

# 1. Introduction

External Thermal Insulation Composite Systems (ETICS) are a widely accepted solution in the construction industry for both new buildings and retrofitting actions. ETICS kits are comprised of a thermal insulation material that is applied onto an exterior wall using an adhesive product and/or mechanical fixing (anchors). The insulation product is faced with a rendering consisting of one or more layers (site applied), one of which contains a reinforcement. The rendering is applied directly to the insulating panels, without any air space or disconnecting layer. Figure A.1 shows composition of VIP based ETICS solution, using encapsulated vacuum insulation panels (VIP encapsulated in expanded polystyrene).

1. Support wall
2. Adhesive
3. Encapsulated VIP
4. Plastic anchor
5. Base coat (first layer)
6. Reinforcement (glass fibre mesh)
7. Base coat (second layer)
8. Finishing coat (primer and decorative coating)



**Figure A.1:** VIP based ETICS scheme.

The popularity of this technology has grown due to its advantages when compared to other techniques for façades insulation. The main advantages of ETICS are:

- Increased thermal comfort;
- Thermal bridges and internal surface condensation elimination;
- Interstitial condensations mitigation;
- Protection of masonry and structural elements;
- Aesthetic renovation of facades;
- Reparation/hiding of pre-existing anomalies.

However, only by ensuring the quality of the materials and their correct application is it possible to guarantee good performance and durability. Problems associated with the application include inadequate/insufficient constructive detailing, application of poor-quality materials, poorly qualified labour, application under unfavourable environmental conditions, etc.



This document provides information about the installation of VIP products in ETICS façades, aiming to assure the successful performance of this innovative solution. First, design and planning recommendations are described. Next, a brief information about VIPs installation, maintenance works and waste disposal procedures are provided. In section 6, an application procedure guideline is presented, which includes all the stages of ETICS installation. Considering the most current constructive details, some detailed drawings of ETICS façades using VIP are proposed in section 7. Finally, some final considerations are made.

The guidelines proposed in this document are based on the current technical recommendations by ETICS associations, namely the European Association of ETICS (EAE) [1] and the Portuguese Association of Mortars & ETICS (APFAC) [2] and by ETICS companies [3].

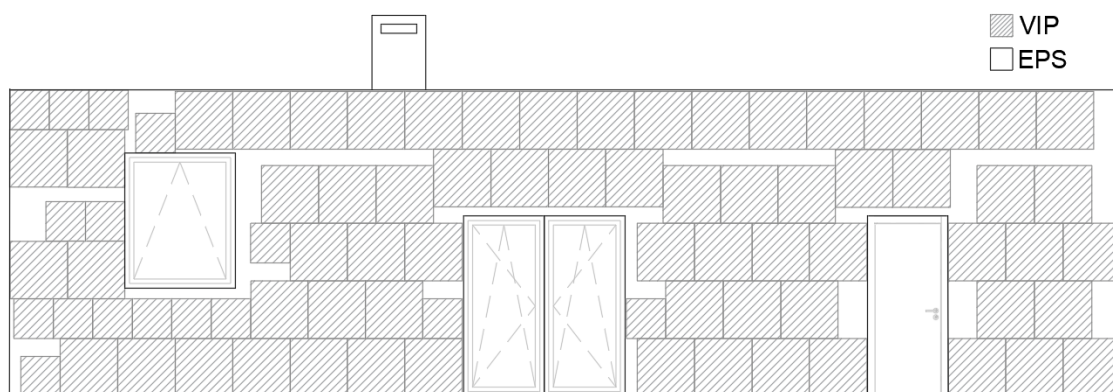
## **2. Design and planning**

Designers and builders must be aware of the special requirements of the VIP products early on in the design process. At this stage, the following topics are recommended:

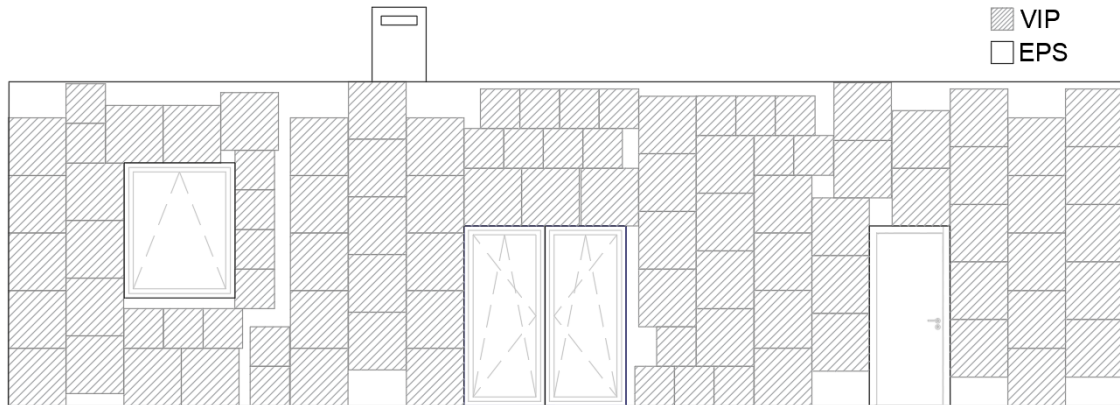
- The installation of VIP products shall comply with national regulations and other relevant documentation specific to the construction site;
- Fire protection requirements must be taken into account;
- Compliance with thermal resistance requirements needs to be ensured;
- The construction project and the chosen constructive solutions need to be carefully analysed and checked for accurate dimensions and adequate surfaces for application of the VIP products;
- All connections between construction elements, attachments of elements that penetrate the building envelope (air conditioning and other equipment), openings (windows, doors, vents) and other singularities should be planned in a way so that clear specifications on their execution are provided;
- Detailed drawings of all singularities must be provided;
- The size and placement of the panels must be labelled so as to ensure an easy and speedy execution of the work;
- The layout pattern should minimize areas without VIPs (maximize VIP area);

- Areas without panels, since they cannot be avoided completely, should be filled with other insulation materials, such as polyurethane (PU) or expanded polystyrene (EPS). Note that compatibility between materials (support and finishing layers) needs to be ensured;
- The use of large vacuum panels instead of smaller panels shall be prioritized, in order to reduce the edge thermal bridging effect;
- All insulation materials must have exactly the same thickness;
- Other relevant documentation for the construction site may include a detailed description of the VIP installation, specifying the required procedures, their sequence and timing of operations, the methods of application, amounts of materials needed, drying times, etc.;
- Only VIP based ETICS which have been experimentally validated should be used. Validation should be made according to the adequate specifications such as the ETICS EAD [4]. The use of ETICS kits with European Technical Assessment (ETA) (while not harmonised VIP based ETICS specification standard) is the only way to guarantee the adequate compatibility between the VIP panels and the different products that compose the ETICS kit, such as base coat mortar, primers, finishing coat materials, amongst others.

Since vacuum insulation panels cannot be adapted on-site, planners must supply detailed drawings of the installation. Figure A.2 and Figure A.3 show examples of an arrangement of panels for a VIP application in ETICS façade (considering only panels with 660 mm x 660 mm and 440 mm x 440 mm are available). It should be noted that the panels should not be aligned (mosaic pattern) to mitigate the risk of cracks occurring.



**Figure A.2:** Layout pattern of a façade (35 m<sup>2</sup> surface) with VIP panels - option 1 with VIP area covering 86.1% of the total wall area.



**Figure A.3:** Layout pattern of a façade (35 m<sup>2</sup> surface) with VIP panels - option 2 with VIP area covering 84.6% of the total wall surface.

Figure A.4 shows a real VIP application in a building façade located in Warsaw. In this case, the VIP solution was bonded by adhesive with plastic anchors for supplementary mechanical fixing. The anchors were installed on EPS edge material of each panel, to avoid VIP perforation.



**Figure A.4:** Real façade using VIP products, applied according to a similar layout pattern planning – Warsaw Zoo.

There are several combinations of panels to achieve the layout pattern of a façade. Thus, the definition of the layout pattern should be carefully defined in order to minimize the U-value of the solution. This parameter is a key-factor to achieve a good layout pattern.

### 3. Installation

Unlike most conventional insulation materials available in the market, VIPs cannot be adapted onsite, as they cannot be cut to size and onsite panel manufacturing is not possible. Also, they are sensitive to mechanical damage and special care must be taken during all stages of the construction process to prevent a loss of the vacuum, which significantly affects the VIPs' performance (thermal conductivity increases 4 to 6 times).

VIP applications should be performed by trained installers with knowledge of how to handle these products. Adequate tools and construction details must be made available to them. VIPs should also be labelled to warn all workers to take special care with these materials.

During the installation phase, the following considerations should be taken into account:

- All applicable regulations regarding work safety shall be complied;
- Panels should be checked at the moment of reception to ensure that they have not been damaged;
- Mechanical damaged panels should be rejected and sent to waste disposal and recycling;
- Panels must be protected from environmental conditions (rain, direct sunlight and wind);
- Panels should be stored in a dry place over a flat surface. Temperatures should not exceed 30°C;
- It must be ensured that the panels are installed according to the previously defined layout plan;
- The VIP products must be applied on a flat surface without sharp irregularities that may potentially puncture the envelope of the panels;
- Before installation, an initial inspection of the building shall be carried out to ensure adequateness of the surface and to identify other issues;
- If needed, regularization of the surface must be performed;
- No cutting, drilling or other processing of the panels is possible, except for possible trimming of the edge material (EPS);
- Avoid mechanical stresses;
- Avoid flames around the panels;
- Only use recommended products and accessories to apply VIP solutions (i.e. adhesives, mortars, finishing coatings, anchors, etc.);
- In case of doubt, contact the designer/project planner.

In ETICS façades with conventional insulation materials, often times early anomalies have been reported. Installation errors or inadequate constructive detailing frequently lead to these anomalies, such as cracking, blistering, aesthetic anomalies, amongst others. For this reason, section 6 presents an application procedure guideline to help installers and construction supervisors avoiding the occurrence of such anomalies in VIP based ETICS façades. In section 7, several detailed drawings of ETICS constructive solutions using the VIP based ETICS solution are proposed.

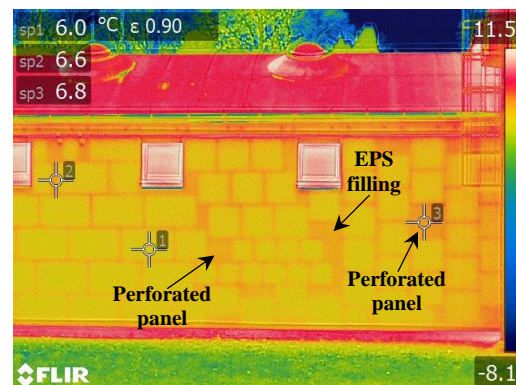
## 4. Maintenance

Sufficient maintenance of the VIP based ETICS applications shall be performed in order to preserve the performance of the ETICS. Maintenance works can include:

- Periodic visual inspection;
- Infrared thermographic (IRT) inspection;
- Periodic cleaning of the finishing coats;
- Repair works on all accidentally damaged areas.

A detailed maintenance plan should be defined by the building designer. The frequency of inspections and periodic works should be planned according the location and use of the building, as well as, following the recommendations of the manufactures of the used ETICS components. The maintenance plan needs to include a detailed schedule and the ETICS façade characterization: estimation of the components service life; define and verify the levels of performance; and monitor the degradation of the system [5].

If required, repairs or replacements should be carried out as soon as the need is identified. Infrared thermography can be a useful tool to help identify anomalies in the construction, such as infiltrations, detachment and loss of vacuum. Figure A.5 shows a thermogram of a building façade with VIP product. It can be seen that the IRT technique allowed the identification of two perforated panels (without vacuum).



**Figure A.5:** Infrared thermogram of ETICS façade with VIP.

The loss of vacuum in the VIP panels negatively affects the thermal performance of the building envelope. Also, the mechanical behaviour of a perforated panel is lower than a VIP in its initial state. This problem can be potentiated due to accidental perforation, vandalism or extreme weather events (hurricanes, earthquakes, storms, floods, forest fires, etc.). If a significant area percentage (*e.g.* 20%) of the building envelope has perforated panels, the full replacement of the solution is recommended. It is important that the maintenance is carried out as best as possible using available products and equipment and without causing harm the building's appearance.

## 5. Disassembly and waste disposal

In order to ensure a proper treatment of VIPs after use, it is crucial to separate the panels from other construction waste. As currently done for EPS panels, which also have to be collected separately, this could be performed using excavators, which scrape the panels off the wall. The separated VIPs should then be collected in closed containers to protect the material from rainfall and to prepare it for the transportation to specialized recycling facilities. The recycling of the core material can help to reduce the environmental impact and it should be carried out at this stage [6].

## 6. Application procedure

The laying of the ETICS may only be commenced once:

- All installations in the substrate have been laid and the resulting openings carefully sealed;
- All joints and slits in the substrate have been carefully sealed;
- All surfaces which are not to be coated, such as glass, wood, aluminium, window ledges, drainage tiles etc. are protected by means of corresponding coverings;
- The substrate shows no visible signs of dampness;
- All horizontal surfaces such as parapets, coping, cornices, etc. have been provided with suitable coverings in order to avoid any penetration of moisture into the ETICS during and after installation;
- Clear installation specifications have been provided for all connections, edges and detail structures;
- Penetrations have been planned in such a way that it can be ensured that connections are permanently protected against driving rain;
- The substrate has been inspected for suitability and appropriate measures taken where necessary;
- In the case of old buildings, the causes of rising damp, efflorescence and similar problems have been corrected and the masonry has dried out sufficiently;

- Where scaffolding is used, it must be ensured that the length of the scaffolding anchors is matched to the system thickness in such a way that the distance from the wall surfaces is adequately guaranteed and that no water can penetrate along these anchors (drill obliquely upwards);
- Suitable scaffolding nets should be provided in order to protect the facade, the substrate and the individual layers against external weather influences (sun, wind, rain).

## **6.1. Environmental conditions**

The application of an ETICS should take into account environmental conditions. The atmospheric temperature shall not exceed 30°C or be lower than 5°C. In the presence of strong wind, rain and direct sunlight, the system should not be applied.

## **6.2. Support preparation**

Checking and preparation of the substrate is of crucial importance. The substrate surface should be mechanically resistant without any detached areas, perfectly clean and free from dust, dirt, dampness, greases, formwork release oil residues, harmful efflorescence, or any other substance that may compromise the bonding of the VIP panels. The walls should not have irregularities of planimetry (greater than 10 mm when controlled with a ruler for a length of 2 m). To ensure adequate stability and drying of the masonry, concrete and plaster, the walls need to be finished for at least four weeks before applying the ETICS components. Whenever the deviation of the support plane is verified, the wall must be corrected with adequate plaster according to EN 998-1 [7].

## 6.3. Base connection

To start the application of the system, it is necessary ensure a flush installation, as well as the mechanical protection of insulation panels. This may be achieved by using a base connection profile.

The base connection profiles are fixed with suitable anchors at intervals of approximately 30 cm. Irregularities in the substrate should be compensated with spacers and profile joins should be fixed with suitable connecting pieces. Gaps between the wall and the base connection profile should be sealed by means of suitable measures (e.g. bonding mortar, sealing strips) in order to ensure a wind-tight execution of the lower edge.

## 6.4. Fixing VIP panels

From the design point of view, ETICS are differentiated according to the methods of fixing [4]:

### *i) Bonded system:*

- Purely bonded systems - The load is totally distributed by the bonding layer. Systems may be fully bonded (over the entire surface) or partially bonded in strips and/or dabs. No mechanical fixings are used;
- Bonded systems with supplementary mechanical fixings - The load is totally distributed by the bonding layer. ETICS may be fully bonded or partially bonded. The mechanical fixings are used primarily to provide the stability and flatness of the outer face of the thermal insulation panel until the adhesive has dried and has reached the final mechanical strength and act as a connection to avoid the risk of detachment. Supplementary mechanical fixings can also provide the stability in case of fire.

### *ii) Mechanically fixed system:*

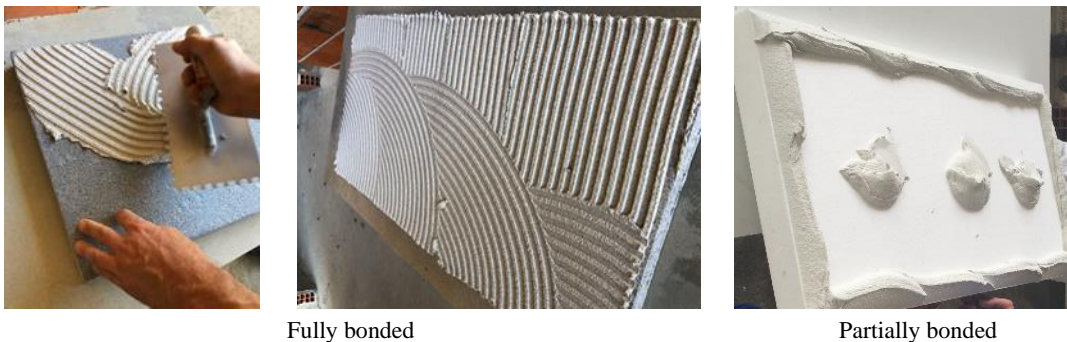
- Mechanically fixed systems with supplementary adhesive - The load is distributed to the substrate by the mechanical fixings and the supplementary bonding. Mechanical fixings shall carry the horizontal load;
- Purely mechanically fixed systems - The load is totally distributed by mechanical fixings. The ETICS are secured to the wall by mechanical fixings only. ETICS with the bonded area less than 20% are also considered to be purely mechanically fixed.



## 6.5. Bonding of VIP

The adhesive should be prepared according to the manufacturer's instructions. The adhesive should be applied in such a way that air leakages between the insulation panels and the support are avoided. ETICS may be fully bonded (over the entire surface) or partially bonded. Thus, adhesive should only be applied to the VIP panels in two ways (see Figure A.6):

- **Fully bonded** - The adhesive can be applied using a notched trowel and it should cover the whole surface of the insulation panel.
- **Partially bonded** - The adhesive should assure a minimum bonding area of 60%. The adhesive should be spread on the perimeter of the panel and transverse points or strips in the centre of the panel.



**Figure A.6:** Adhesive application on thermal insulation panels.

Whenever possible, full surface bonding should be used in order to minimize the possible curvature of the panels. The partially bonded option is only recommended if the substrate is not completely flat such as in masonry walls.

The panels should be laid from bottom to top and tightly butted together to form a flush bond. It must be ensured that the insulation panels are laid flat and evenly. Minimal joints should be created between panels. Any unavoidable joints must be filled with insulation material of the same type as the edge material. If the width of the joint does not allow for this, an appropriate foam filler may be used. In any case, the filling must extend over the full thickness of the insulation material. The wall areas without vacuum panels (which cannot be completely avoided) should be filled with an insulation material of the same type as that of the edge material. In this case, it is essential to ensure that the both insulation materials have the exact same thickness. In order to avoid thermal bridges, special care should be taken when laying the insulation panels so that the adhesive does not flow back into the joints between panels.

The panels should be applied immediately after spreading the adhesive. After they are bonded, slight pressure should be exerted with a trowel to increase grip adhesion by adjusting alignment with adjacent panels. Since a high degree of flatness is required by the system, it must be ensured

that the VIP panels will be as levelled as possible during the gluing process. Thus, it is important to frequently control the flatness of the entire surface with a level ruler. Damaged panels (broken, perforated or compressed edges/cover layers) must not be used.

When gluing the last row of insulation panels bordering the eave, the floating-buttering method may be applied. This method consists of two steps: in the first step, the adhesive is applied vertically to the panel with the notched trowel (at least 10 mm, depending on the substrate). In the second step, the adhesive is applied horizontally to the substrate with the notched trowel. The insulation panel is then brought into position with adequate pressure and in sliding movements. This bonding method helps to prevent water penetration into the wall in case of possible infiltration. The system at the top should always be protected.

As general rule, when dealing with windows or doors openings the joints of VIPs shall not be aligned with the corners of these openings, due to the higher stress concentration. However, with VIP insulation this issue could not be fully avoided. Thus, the layout pattern should be designed with the aim to minimize the panel's corners coinciding with the opening's corners.

Expansion joints on the façade must be respected and should never be covered with panels. The use of specified profiles for expansion joints is recommended. In connections between VIP panels and rigid contour elements (frames, sills, eaves, walls, etc.), a joint of at least 5 mm shall be provided so that it can be filled with waterproof elastic material compatible with the edge material.

If insulated surfaces are exposed to UV radiation for a longer period of time without protection due to delays in the progress of construction work, the surface should be lightly sanded before applying the base coat.

## **6.6. Anchoring**

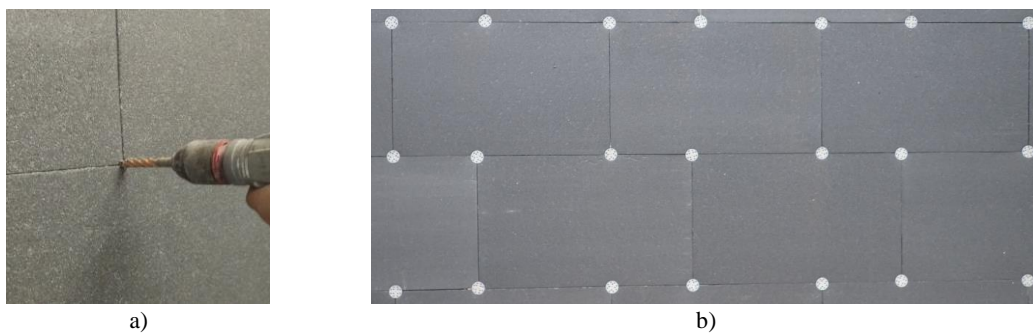
For VIP based ETICS, the use of a bonded system with mechanical fixings (plastic anchors) is highly recommended. The anchors should be applied after the adhesive has hardened. Only anchors that comply with the requirements of EAD 330196-00-0604 – Plastic anchor for fixing External Thermal Insulation Composite Systems with rendering [8] should be used. The selection of the fixings should be made according to the substrate and the thickness of the VIP panels, following the manufacturer's instructions.

Drilling should be done by the following methods:

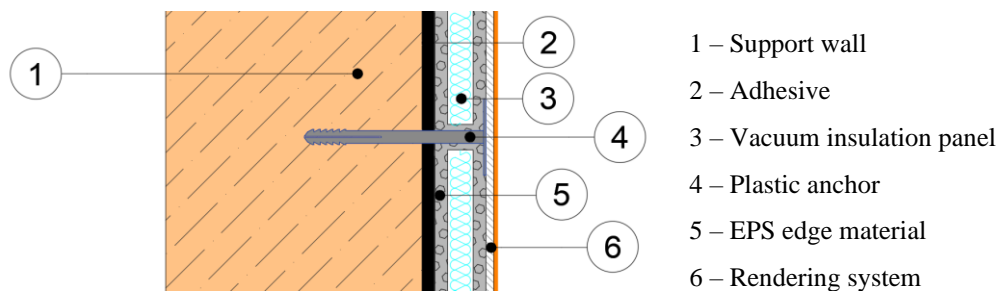
- Hammer/percussion method - for concrete and solid brick substrates;
- Standard method for perforated brick supports.

The depth of the hole should not exceed the length of the anchor in more than 1.5 cm. The anchors must be embedded in the cover layer material to assure a flush surface. Depending on the type of anchoring, the screw will be hammered or screwed. Next, it is necessary to check the correct attachment to the substrate. If any anchor has been damaged or becomes loose for any reason, it must be removed and replaced using a new hole.

Regarding the anchoring pattern, anchors must only be applied in the edge material in order to avoid the perforation of vacuum panel in all the joints between panels (according to planner's specifications) as shown in Figure A.7. Figure A.8 shows a cross-section of the mechanical fixing installation in VIP based ETICS solutions.



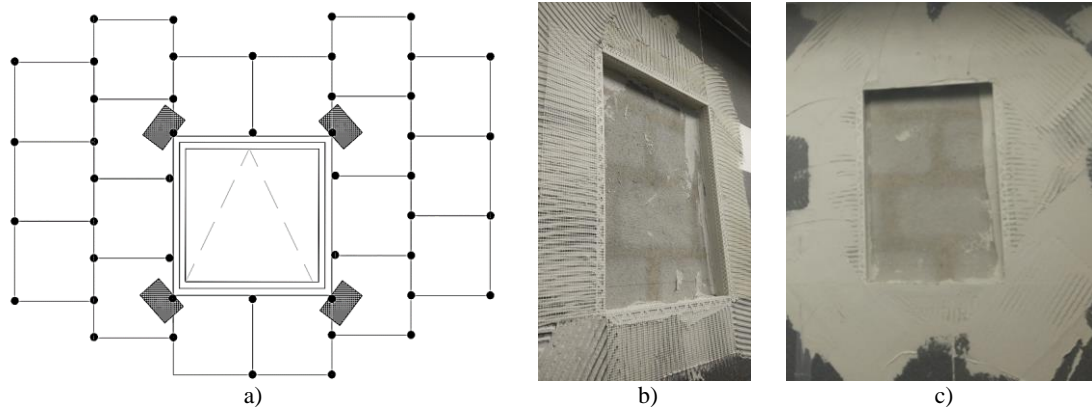
**Figure A.7:** Anchoring of encapsulated VIPs: a) Drilling the hole at the edge material; b) anchoring pattern of VIPs.



**Figure A.8:** Cross-section of the plastic anchor positioned between panels joints.

## 6.7. Base coat with reinforcement

After anchoring, the reinforcement of singularities, such as windows and doors openings, should be carried out. Diagonal reinforcements are necessary in corners and should be embedded in the base coat before applying the surface reinforcement. Figure A.9 shows an example of reinforcement of corners apertures. The diagonal reinforcements should be fixed so that the edge of the strip is applied directly to the corner at an angle of approximately 45°. The dimensions of the reinforcement strips are usually approximately 200 mm x 300 mm. Prefabricated mesh elements are also permitted.



**Figure A.9:** Reinforcement of windows apertures: a) diagonal reinforcement scheme; b) use of specific PVC profiles with glass fibre mesh; c) diagonal reinforcement with glass fibre mesh.

To protect the façade from particular mechanical loads, the reinforcement of elements of the facade edges (corners, drip pans and contour of spans) will be applied, glued with the base coat mortar used for rendering the insulation panels. These accessories (specific PVC profiles as presented in Figure A.9b) should not be fixed with dowels or nails, but instead glued to the insulation board by pressing against the corner and refluxing excess adhesive through the pre-existing holes in the profiles. There is no overlap of profiles and the application is prior to the full reinforcement of the insulation layer.

The base coat mortar is applied in two layers with a stainless-steel trowel in a uniform thickness of approximately 4 mm. The first layer (see Figure A.10) is made with a 50 cm toothed trowel (6 mm or 8 mm tooth) to obtain a layer thickness of about 2 mm on which a mesh is freshly incorporated.



**Figure A.10:** First layer of reinforced base coat.

For glass fibre meshes, a differentiation is made between:

- **Standard mesh:** embedded all over the area of the base coat and tied positively at joints.
- **Reinforced mesh:** embedded in the base coat additionally to the standard mesh to improve the impact resistance. If two layers of glass fibre mesh are laid, it must also be ensured that overlaps are offset.

The standard mesh of anti-alkaline fiberglass has a mesh width of 4 mm and weighs more than  $145 \text{ g/m}^2$  (usually  $160 \text{ g/m}^2$ ). It must be perfectly stretched and soaked in the mortar and should

never be crushed to be positioned midway through the full thickness of the base coat mortar. To ensure continuity of effort, there must be a minimum overlap of 100 mm between mesh strips, even when connecting the mesh to the edges and reinforcement profiles. The mesh must meet the requirements specified in ETICS EAD [4].

After hardening of the first layer, the second layer is applied (also 2 mm thick), forming a homogeneous surface, hiding the fiberglass mesh completely.

## **6.8. Finishing coat application**

After allowing the base coat sufficient time to harden and given suitable weather conditions, the final coating can be applied. The final coating must accomplish the specifications established in EN 15824 [9].

Reduced solar radiation absorption coefficient values are recommended in order to avoid excessive thermal heating of the ETICS surface, especially when super insulation materials such as the VIP products are used. Thus, the use of dark colours in final coatings is not recommended. If the finishing layer option consists of a dark colour, it should be carefully validated by always ensuring a solar radiation absorption coefficient ( $\alpha$ ) less than 0.7.

Different types of finishing coat can be used (previously validated in laboratory conditions). Usually, the finishing rendering system is composed by a key coat (very thin coat which may be applied to the base coat and is intended to act as a preparation for the application of the finishing coat) and a finishing coat (which contributes to the protection against weathering and can provide a decorative finish).

The finishing coat should be applied according to the manufacturer's specifications. A wide range of surface effects can be achieved. Depending on the type of render and the desired structure, the surface can be structured using a suitable tool. The manufacturer's application guidelines should be followed, such as drying period, product usage, thickness, etc.

The finishing coat must be applied from top to bottom. In case of high buildings, the use of sufficient workers for each scaffolding level avoids visible lap marks. Working swiftly, wet-on-wet, avoids the possible risk of an uneven render surface in terms of colour and structure. Interrupting the work on individual surfaces should therefore be avoided. In order to avoid visible lap marks between the scaffolding levels, coatings should be offset.

After the finishing coat has been dried sufficiently, the surface finishing and the contour elements (e.g. frames) must be sealed by applying a bead of elastic mastic or other specific materials.

## 7. Constructive details

In this section, several detailed drawings of ETICS constructive solutions using the encapsulated VIPs are proposed. Although these details are recommended to achieve a long-term performance of the building envelope and mitigate potential anomalies, other techniques may be applied if carefully evaluated. Furthermore, the practical applicability of the proposed details should be checked on site. The constructive detailed drawings include:

- Façade in contact with the ground (Figure A.11);
- Façade starting above ground (Figure A.12);
- Façade contacting a balcony (Figure A.13);
- Corner connection (Figure A.14);
- Connection to windows (jamb) (Figure A.15);
- Connection to windows (lintel) (Figure A.16);
- Connection to windowsill (Figure A.17);
- Connection to roller shutter box (Figure A.18);
- Connection to back-ventilated roof (Figure A.19);
- Parapet façade (Figure A.20).

## Façade in contact with the ground

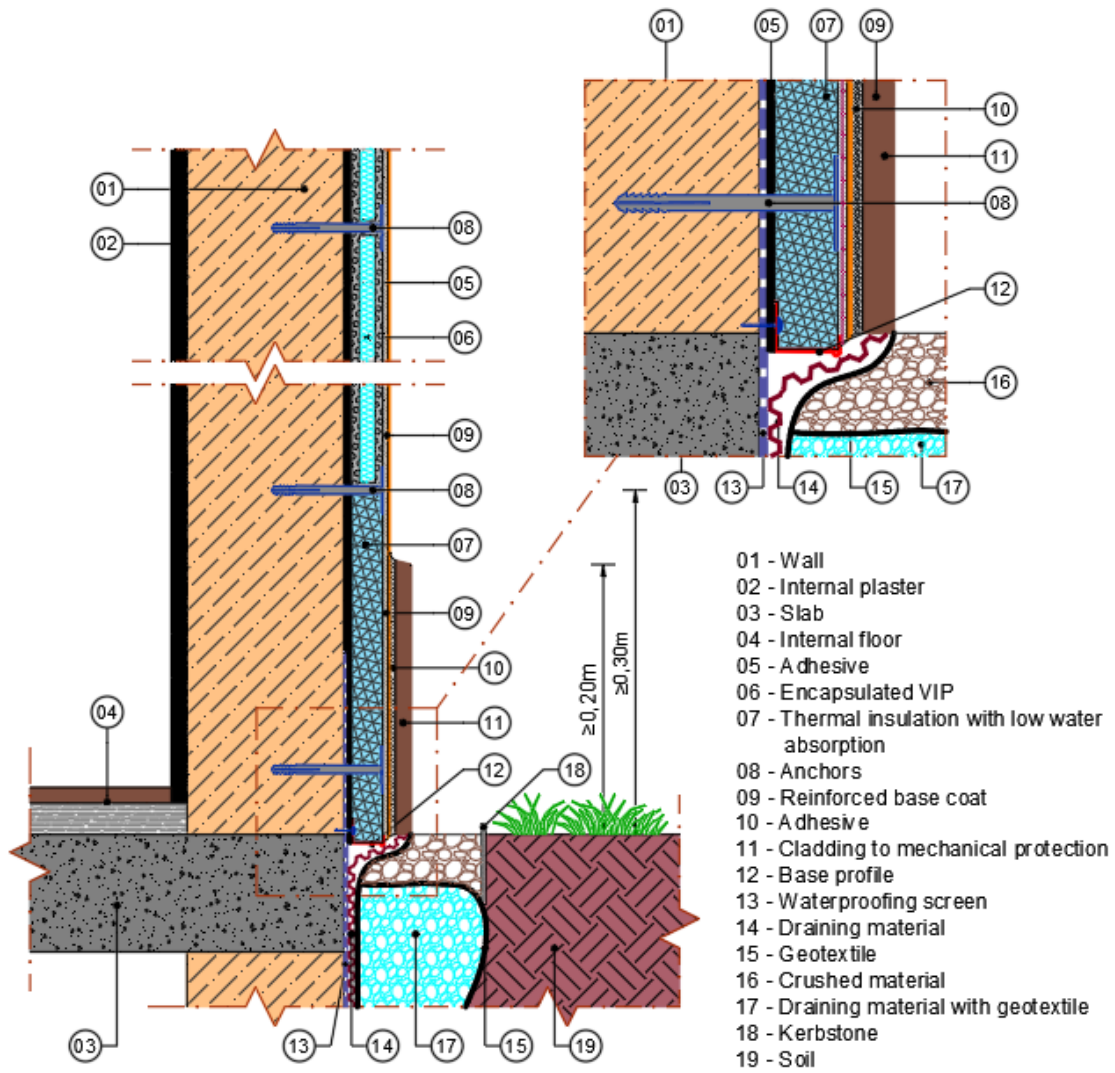
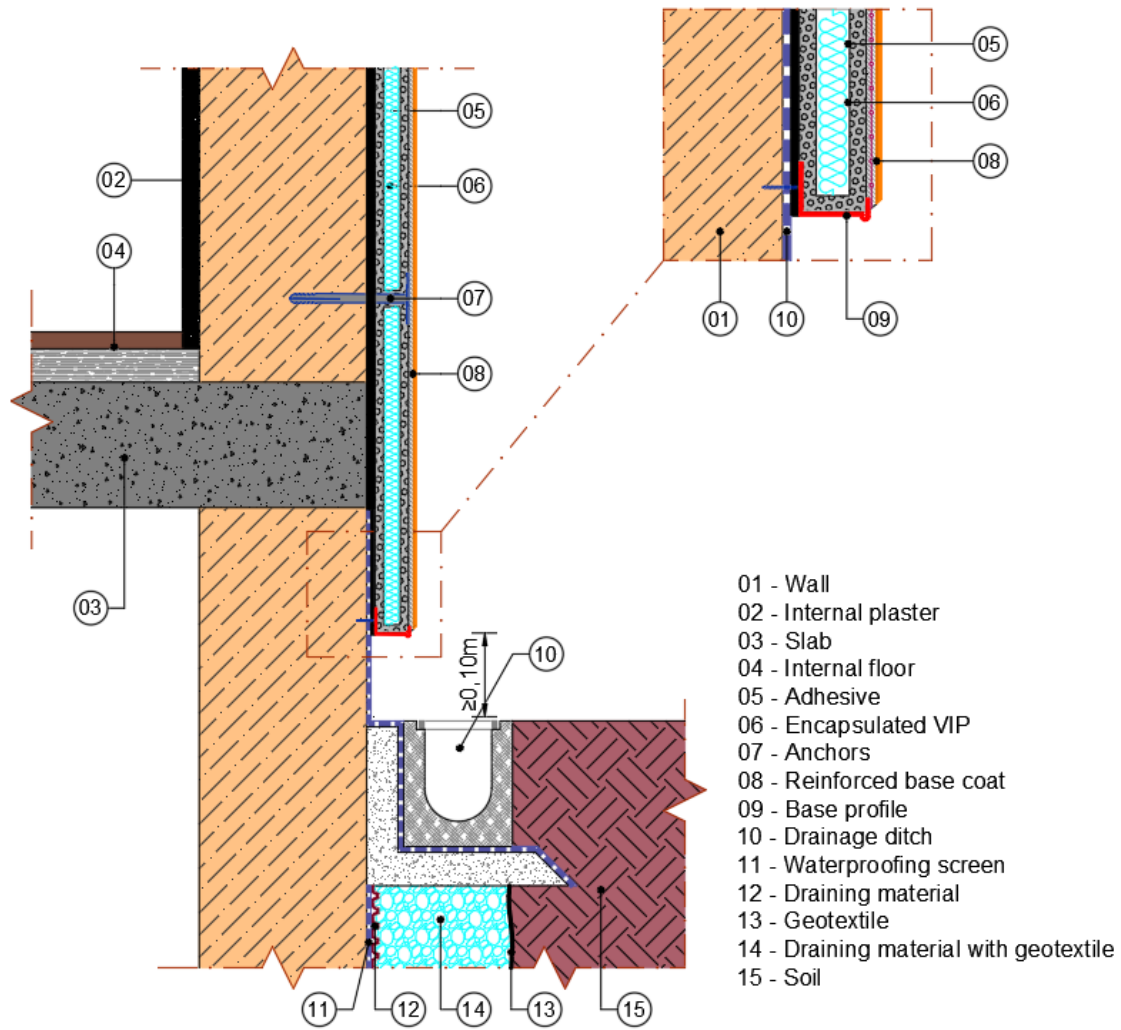


Figure A.11: Sectional drawing - façade in contact with the ground.



## Façade starting above ground



**Figure A.12:** Sectional drawing - façade starting above ground.



## Façade contacting a balcony

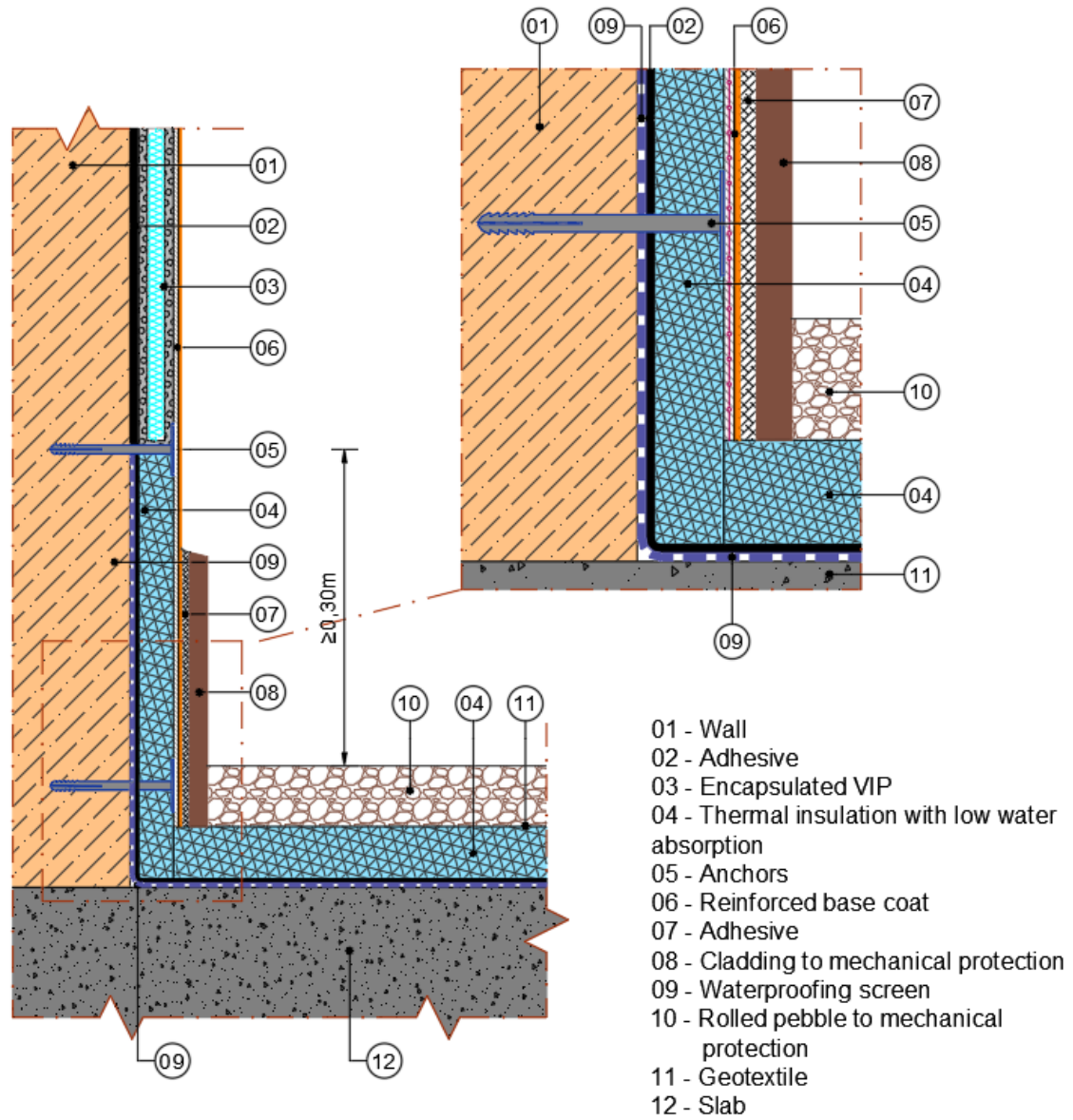


Figure A.13: Sectional drawing - façade contacting a balcony.

### Corner connection

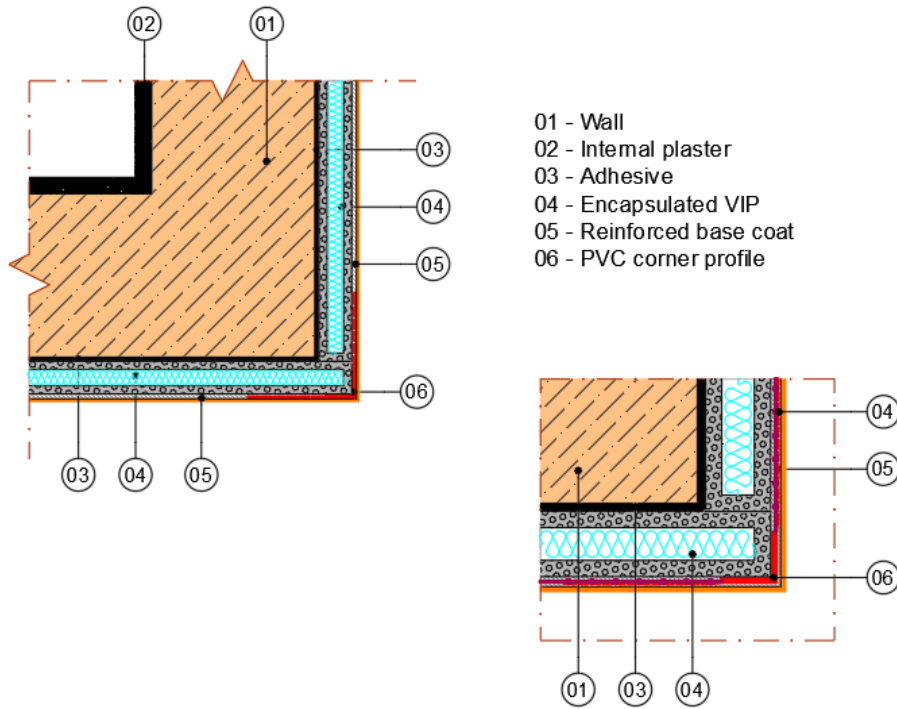


Figure A.14: Sectional drawing - corner connection.

### Connection to windows (jamb)

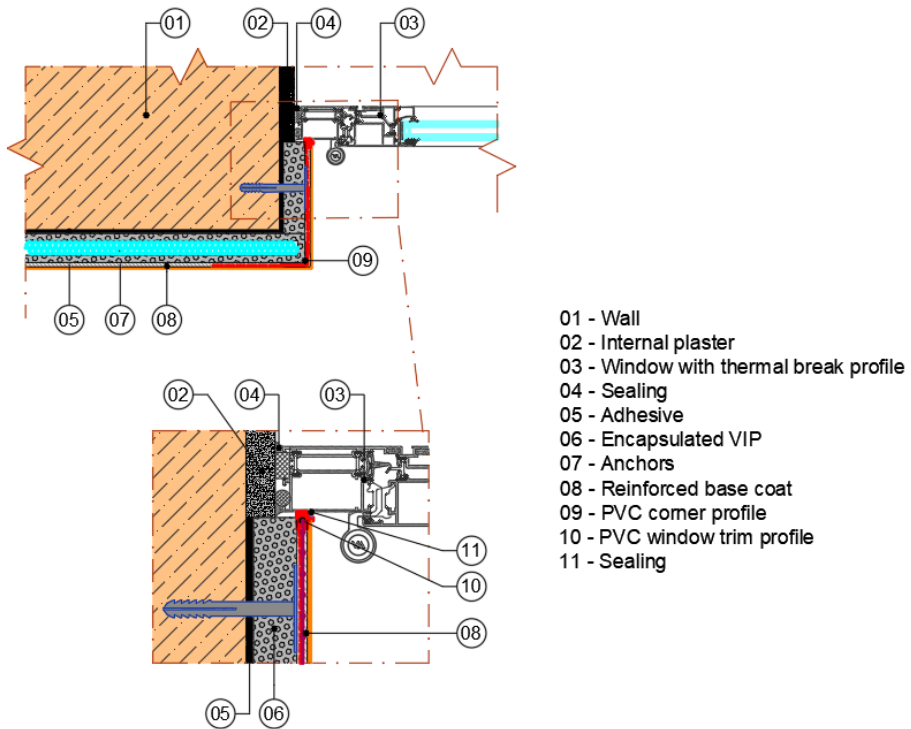


Figure A.15: Sectional drawing – connection to windows (jamb).

### Connection to windows (lintel)

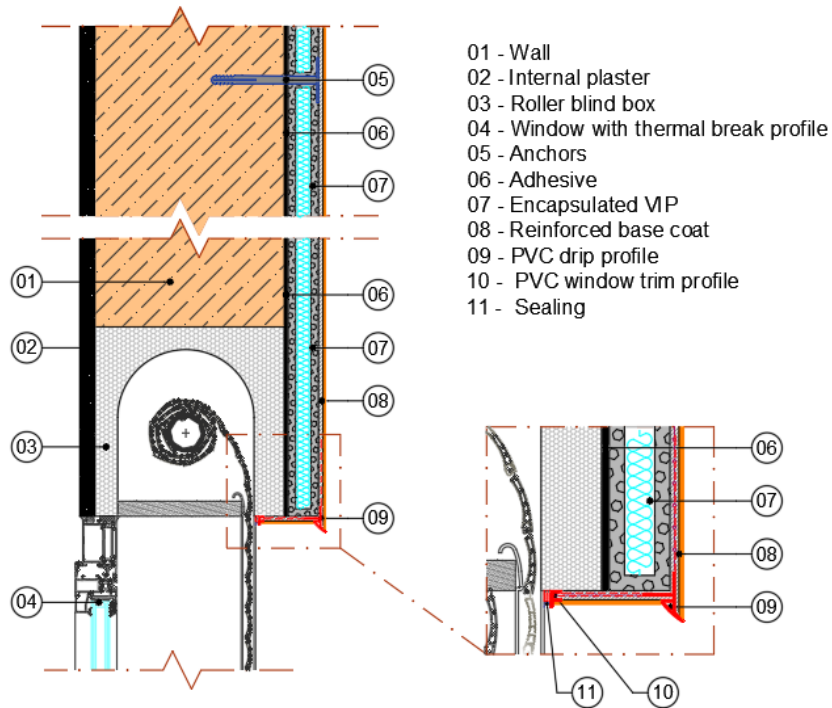


Figure A.16: Sectional drawing – connection to windows (lintel).

### Connection to windowsill

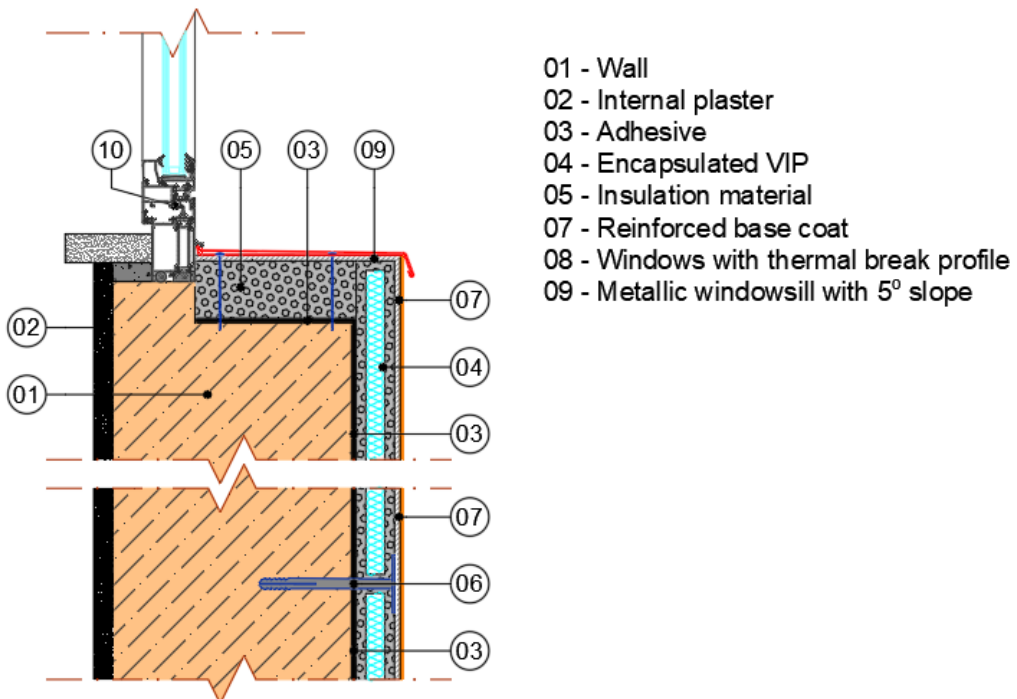


Figure A.17: Sectional drawing – connection to windowsill.

### Connection to roller shutter box

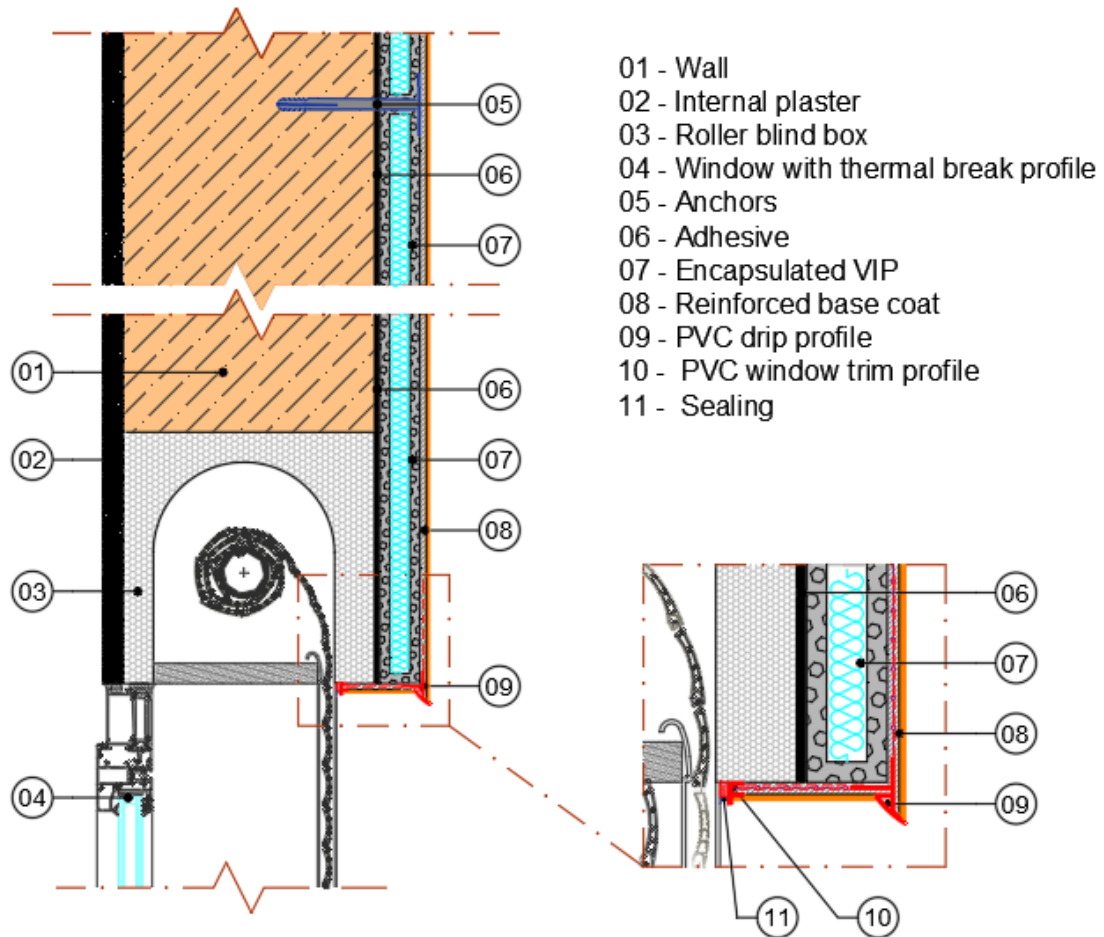


Figure A.18: Sectional drawing – connection to roller shutter box.

## Connection to back-ventilated roof

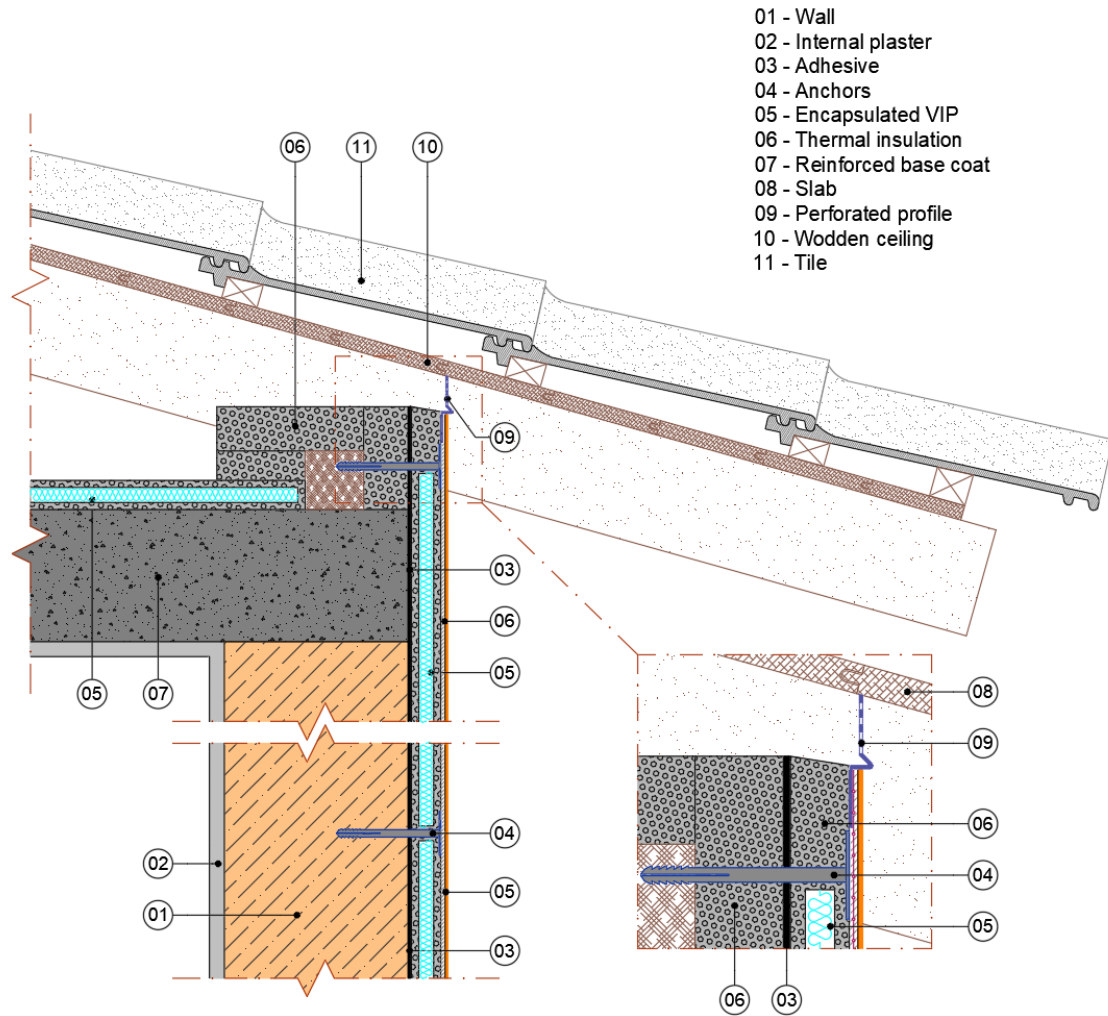


Figure A.19: Sectional drawing – connection to back-ventilated roof.

## Parapet façade

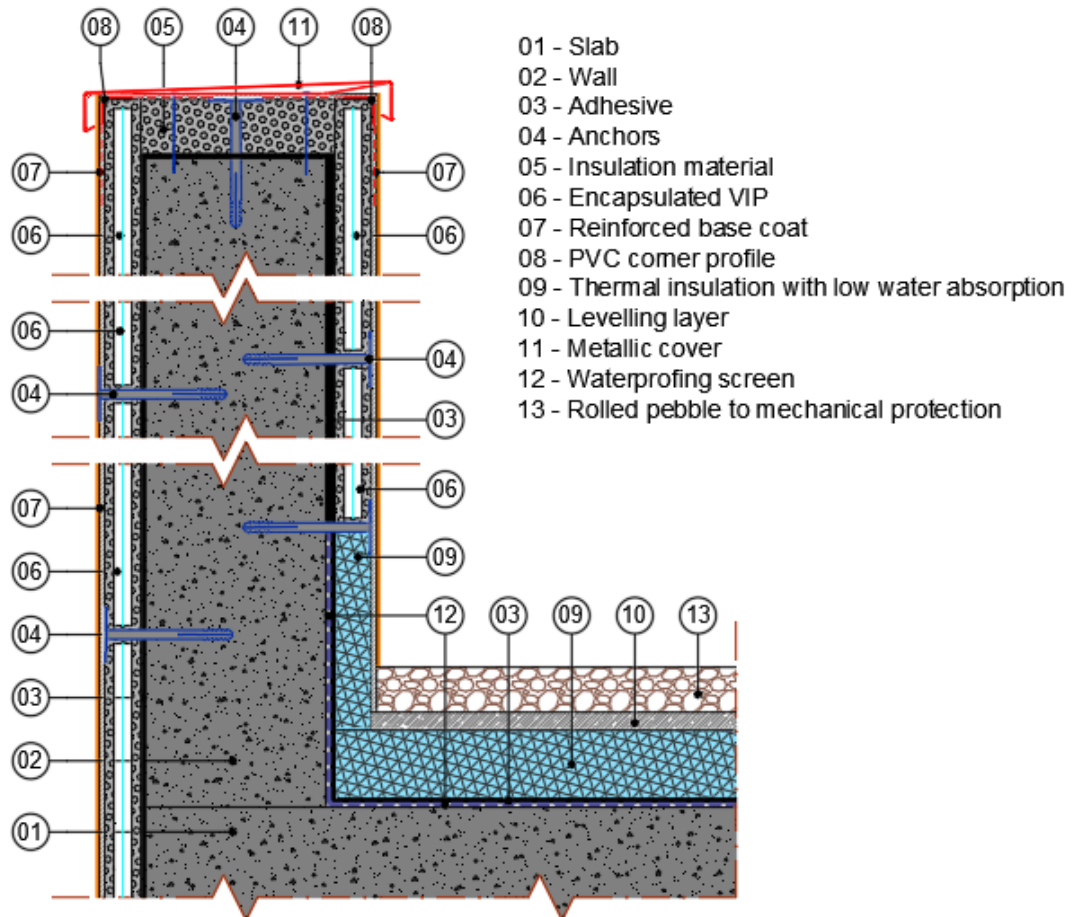


Figure A.20: Sectional drawing – parapet façade.

## 8. Conclusion

This document provides guidelines for the use of VIP products in ETICS. Information regarding all stages of the construction using VIP products is provided, such as design and planning, installation, maintenance, disassembly and waste disposal. To help installers, several recommendations and detailed drawings are given. These aim to ensure the successful implementation of VIP products in buildings façades.

Compared with conventional insulation materials, the vacuum panels impose some specificities which should be taken into account. For example, since VIPs cannot be adapted onsite there is a need to previously define the layout design. Also, they are sensitive to mechanical damage and special care must be taken during their handling.

In terms of the ETICS kit, if the VIPs are encapsulated in expanded polystyrene (the most used insulation material in ETICS), the main installation procedures and type of suitable components are similar to those for traditional ETICS. Nonetheless, the mechanical fixing stage should be carefully performed in order to avoid perforating the panels. The use of VIP based ETICS with CE marking (*i.e.* previous validated in laboratory conditions according standardized test methods) is essential to guarantee the successful performance of the system during service-life. In particular, the rendering system needs to be evaluated, since VIPs will impose higher temperature amplitudes on the surfaces, increasing the risk of cracking.

This document could be particularly useful to promote the use of VIP base ETICS solutions, minimizing common installation errors and adveting installers regarding the additional requirements imposed by vacuum technology.

## References

- [1] European Association for ETICS – EAE, “European Guideline for the application of ETICS”, pp. 1-98, 2011,
- [2] Portuguese Association of Mortar & ETICS - APFAC, “Manual ETICS” (in portuguese), pp. 1-48, 2018.



- [3] Weber Saint-Gobain, “O guia weber 2018” (in portuguese), 2018.
- [4] *European Assessment Document: External Thermal Insulation Composite Systems with rendering*, EAD 040083-00-0404, European Organisation for Technical Approvals, 2019.
- [5] J. Falorca, “Modelo para plano de inspeção e manutenção em edifícios correntes” (in portuguese), PhD thesis. Faculty of Sciences and Technology of the University of Coimbra, 2004. <http://hdl.handle.net/10316/15709>.
- [6] S. Resalati, T. Okoroafor, P. Henshall, N. Simões, M. Gonçalves, M. Alam, “Comparative life cycle assessment of different vacuum insulation panel core materials using a cradle to gate approach”, *Build. Environ.* vol. 188, 107501, 2021, doi:10.1016/j.buildenv.2020.107501.
- [7] *Specification for mortar for masonry - Part 1: Rendering and plastering mortar*, EN 998-1, European Committee for Standardization, 2010.
- [8] *European Assessment Document: Plastic Anchors Made of Virgin or Non-Virgin Material for Fixing of External Thermal Insulation Composite Systems With Rendering*, EAD 330196-00-0604, European Organisation for Technical Approvals. 2016.
- [9] *Specifications for external renders and internal plasters based on organic binders*, EN 15824, European Committee for Standardization, 2017.





## **ANNEX B**

# **CHARACTERIZATION OF THE VACUUM INSULATION PANEL**



# Table of contents

1. Introduction .....	3
2. Test specimens .....	3
2.1. VIP product .....	4
2.2. Encapsulated VIP .....	4
3. Test procedures .....	5
3.1. Dimensional measurements.....	6
3.2. Dimensional stability under specified temperature and humidity conditions .....	6
3.3. Compressive stress at 10% compressibility .....	7
3.4. Behaviour under point load .....	7
3.5. Shear behaviour .....	8
3.6. Resistance to perforation .....	9
3.7. Tensile strength perpendicular to faces .....	9
3.8. Bending .....	10
3.9. Thermal conductivity .....	10
3.10. Water absorption .....	11
4. Test results .....	12
4.1. Dimensional measurements.....	12
4.2. Dimensional stability under specified temperature and humidity conditions .....	13
4.2.1. VIP panel.....	13
4.2.2. Encapsulated VIP .....	14
4.3. Compressive stress at 10% compressibility .....	14
4.3.1. VIP panels .....	14
4.3.2. Encapsulated VIP .....	15
4.4. Behaviour under point load .....	17
4.4.1. VIP panel.....	17

4.4.2.	Encapsulated VIP .....	18
4.5.	Shear behaviour .....	20
4.5.1.	VIP panel .....	20
4.5.2.	Encapsulated VIP .....	21
4.6.	Resistance to perforation .....	22
4.6.1.	VIP panel .....	22
4.6.2.	Encapsulated VIP .....	22
4.7.	Tensile strength perpendicular to faces .....	24
4.7.1.	VIP panel .....	24
4.7.2.	Encapsulated VIP .....	25
4.8.	Bending .....	26
4.8.1.	VIP panel .....	26
4.8.2.	Encapsulated VIP .....	27
4.9.	Thermal conductivity .....	28
4.9.1.	VIP panel .....	28
4.9.2.	Encapsulated VIP .....	30
4.10.	Water absorption .....	30
5.	Summary of experimental test results .....	31
6.	Performance comparison with conventional insulation materials .....	33
7.	Final statements .....	35
8.	References .....	35

# **1. Introduction**

In this document the laboratory characterization of the vacuum insulation panel (VIP) under study is presented. Since VIPs have several specificities that must be considered in buildings applications, there was a need to identify a product capable of being applied on external walls. Handling, technical viability and architectural concerns were taken into account. To ensure the successful integration of VIP in External Thermal Insulation Composite Systems (ETICS), their properties regarding physical, mechanical and hygrothermal performance were evaluated. For this purpose, a laboratory test campaign was carried out. Mechanically, parameters such as flatness, compressive stress, deformation under specified load and temperature and, tensile strength perpendicular to faces, were determined. Properties such as dimensional stability (under specified temperature and humidity conditions) and water absorption were also obtained. The determination of thermal conductivity under specific temperature conditions was also performed, including the edge thermal bridging effect, which is presented in detail in chapter 3 of this thesis.

Regarding the assessment of VIP products to be introduced to the market, specification documents have recently been made available. Namely, a European Assessment Document – EAD 0040011–00- 1201 [1] for VIPs with factory applied protection layers was published in 2018 and the VIP product specification standard EN 17140 [2] was approved in October 2020. These documents define characteristics for factory made VIPs used for the thermal insulation of buildings, attesting to the innovative character of VIP products and confirming the market’s interest in their use in building systems, such as the ETICS solutions.

Considering the specificities of VIPs, it was necessary to establish and adapt test methods and laboratorial equipment in order to enable the characterization campaign of the VIP product. Furthermore, to deeply understand the behaviour of this insulation material some additional measurements to the standardized procedures were assumed. Tests were performed at Itecons’ facilities.

## **2. Test specimens**

In this section, the VIP solution developed within the INNOVIP project and used in this thesis is described, including the VIP product and the encapsulated VIP (vacuum insulation panel encapsulated in graphite expanded polystyrene).

## 2.1. VIP product

The test specimens consist in a vacuum insulation panel composed by loose fill fumed silica powder encapsulated in a metallized high barrier film. The VIP powder core is based on silicon dioxide. Other components of the loose powder panel besides silica are an opacifier, such as iron oxide, and cellulose fibres. Figure B.1 shows some samples of the VIP product.



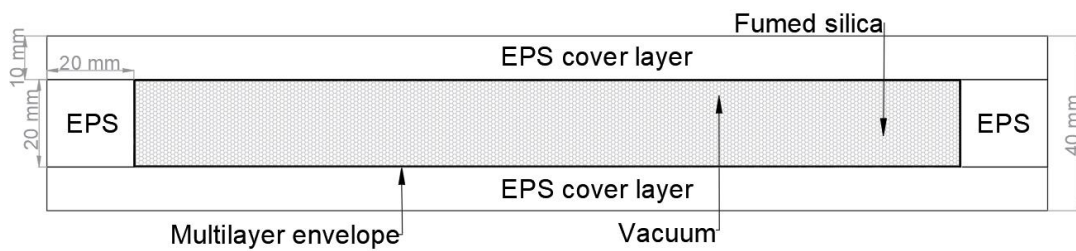
**Figure B.1:** Vacuum insulation panels.

This product is a result of the INNOVIP project that aimed to reinvent the top-of-the-line vacuum insulation materials by improving their thermal performance over the lifetime by at least 25% and by reducing their embodied energy by at least 25%, when compared with other commercial VIP products. This product allows the use of different cover layers to fulfil different functions, such as roof, floor and external walls insulation (ETICS).

The nominal thickness of the VIP product is 20 mm. Panels with 200 mm x 200 mm, 300 mm x 300 mm, 400 mm x 400 mm and 600 mm x 600 mm were used in the laboratory testing assessment.

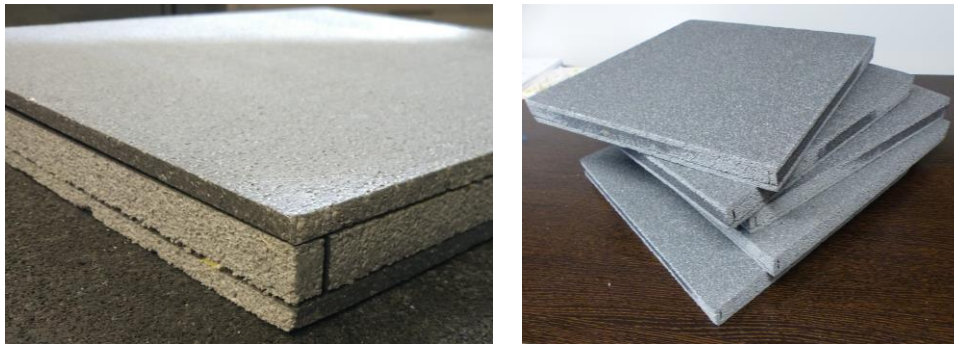
## 2.2. Encapsulated VIP

To allow for an External Thermal Insulation Composite System (ETICS) application, the VIP product is fully encapsulated with a protective cover layer made of graphite expanded polystyrene (EPS) with a thickness of 10 mm on each side and 20 mm along the edges, as can be observed in Figure B.2.



**Figure B.2:** Schematic cross-section of encapsulated VIP.

The EPS layers are bonded to VIP surfaces with a polyurethane adhesive. Figure B.3 shows samples of this same type of solution, referred to as “encapsulated VIP”. The EPS cover layer allows for the adhesive bonding of the panels onto substrate and provides additional mechanical resistance, minimizing the risk of perforation of the VIPs. The 20 mm of EPS at the edges of the panels also allow for the use of auxiliary mechanical fixing (plastic anchors) and to allow for small size adjustments.



**Figure B.3:** Encapsulated VIPs.

The total thickness of the encapsulated VIP is 40 mm. Encapsulated panels with 440 mm x 440 mm and 640 mm x 640 mm were used in the laboratory testing assessment.

### 3. Test procedures

The physical, mechanical and hygrothermal performance evaluation of the VIP product was based on test procedures specified in test standards, namely the VIP specification standard EN 17140 [2] and the European Assessment Document (EAD) for VIP with factory applied protection layers EAD [1]. These documents provide characteristics for factory-made VIP intended to be used for the thermal insulation of buildings. Due to the specificities of VIP products and the dimensions of the test specimens available, some of the test standardized procedures and laboratorial equipment were adapted. In addition, intentionally perforated panels (without vacuum) were



tested, in order to verify the changes regarding the panel's mechanical and thermal performance in case of loss of vacuum. In the following subsections, a brief description of each test is presented.

### **3.1. Dimensional measurements**

The length,  $l$ , and the width,  $b$ , were measured in accordance with EN 822 [3]. The thickness of the specimen was measured in accordance with EN 823 [4]. The apparent mass density was determined according to EN 1602 [5]. The deviation from squareness of the length and width ( $S_b$ ) was measured in accordance with the procedure given in EN 824 [6]. The deviation from flatness ( $S_{\max}$ ) is defined following EN 825 [7].

### **3.2. Dimensional stability under specified temperature and humidity conditions**

Dimensional stability under specified temperature and relative humidity was determined in accordance with EN 1604 [8]. In this test, the changes in linear dimensions which occur when the test specimens have been conditioned, subjected to specified environments for a given period, and then reconditioned are determined. The test was carried out at out at  $(70 \pm 2)^\circ\text{C}$  and  $(90 \pm 5)\%$  relative humidity. In the same atmosphere as used for conditioning, the initial length and width of each test specimen ( $l_0$  and  $b_0$ ) were determine by taking readings at three positions ( $l_{01}$ ,  $l_{02}$ ,  $l_{03}$ , and  $b_{01}$ ,  $b_{02}$ ,  $b_{03}$ ) and the initial thickness ( $d_0$ ) at five positions ( $d_{01}$ ,  $d_{02}$ ,  $d_{03}$ ,  $d_{04}$ ,  $d_{05}$ ), using the appropriate methods described in EN 12085 [9], to an accuracy of 0.1 mm.

### 3.3. Compressive stress at 10% compressibility

The compressive stress at 10% compressibility was performed based on EN 826 [10]. The test is conducted applying a compressive force at a given rate of displacement perpendicular to the major faces of test specimen and the maximum stress supported by the specimen calculated. If no failure is observed before the 10% strain has been reached, the compressive stress at 10% strain is calculated. Figure B.4 shows the equipment used for compressive stress tests. Each compression test was performed with a circular indenter with an area of  $0.0697 \text{ m}^2$  and a load cell of 150 kN.

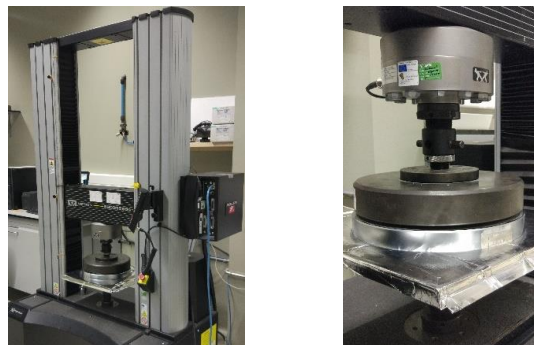


Figure B.4: Compressive stress test apparatus.

### 3.4. Behaviour under point load

The behaviour under point load was performed based on EN 12430 [11]. In this test, a point load is applied with an indenter at a given speed in an axial direction perpendicular to the major faces of a squarely cut test specimen and the compressive force at the critical point and the force for a given deformation is calculated. All the specimens were tested with the apparatus depicted in Figure B.5 with the same position and face.

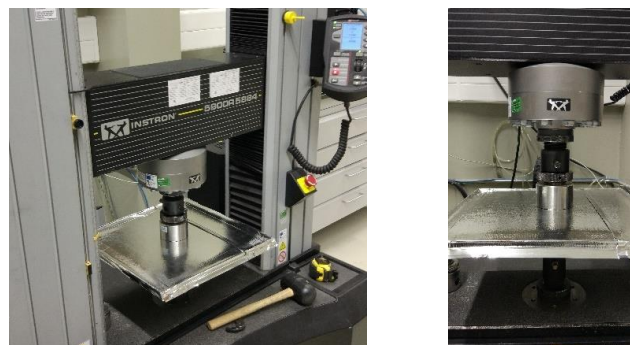
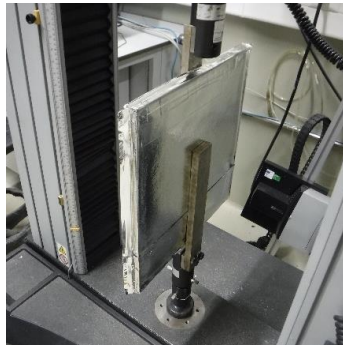


Figure B.5: Test apparatus used for point load.

### 3.5. Shear behaviour

The shear behaviour test was performed based on EN 12090 [12]. A test specimen is subjected to a shear stress transmitted to the test specimen through rigid supports to which it is bonded, as it showed in Figure B.6. The corresponding force-displacement curve was determined.



**Figure B.6:** Shear behaviour test apparatus.

Additionally, the shear strength modulus,  $G$  in kPa, was calculated according the equation presented in the EN 12090 [12]:

$$G = \frac{d \cdot \tan \alpha}{A} \quad [\text{kPa}] \quad (\text{B.1})$$

Where,

$d$  is the initial thickness of the test specimen, in m;

$A$  is the test specimen area, in  $\text{m}^2$ ;

$\tan \alpha$  is the slope of the linear portion of the force-displacement curve, in kN/m, given by equation B.2:

$$\tan \alpha = \frac{F_e}{\gamma_e} \quad [\text{kN/m}] \quad (\text{B.2})$$

With,

$\gamma_e$  is the displacement in the elastic zone (well-defined straight portion of the force-displacement curve);

$F_e$  force corresponding to  $\gamma_e$  (limit of proportionality).

### 3.6. Resistance to perforation

The resistance to perforation test, also called “Perfotest”, was performed according to Itecons’ internal procedure based on ETAG004:2011 [13]. Figure B.7 shows the Perfotest apparatus which enables perforating impacts to be reproduced. It is calibrated with a hemispherical indenter reproducing the impact of a steel sphere weighing 0.5 kg falling from 0.765 m (3.75 J). The test consists of the evaluation of the diameter of the perforating cylindrical indentors that can puncture the panel.

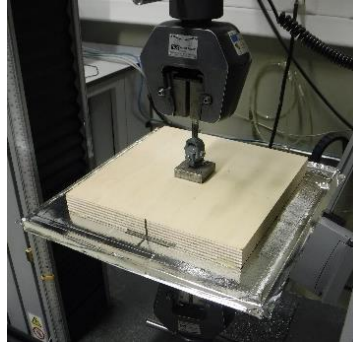


**Figure B.7:** Perfotest equipment with 10 indentors.

First, an equipment calibration was conducted. For this purpose, an impact with a steel sphere weighing 0.5 kg falling from 0.765 m was performed on a conventional ETICS solution (with EPS). The diameter of the impact was measured (33.5 mm). Next, an impact with the perfotest apparatus was performed with calibrated hemispherical indenter. The diameter of perfotest impact was measured (34.2 mm), resulting in a difference of 2%, which is an acceptable value for equipment calibration, since this difference must be lower than 10% to accomplish the requirement).

### 3.7. Tensile strength perpendicular to faces

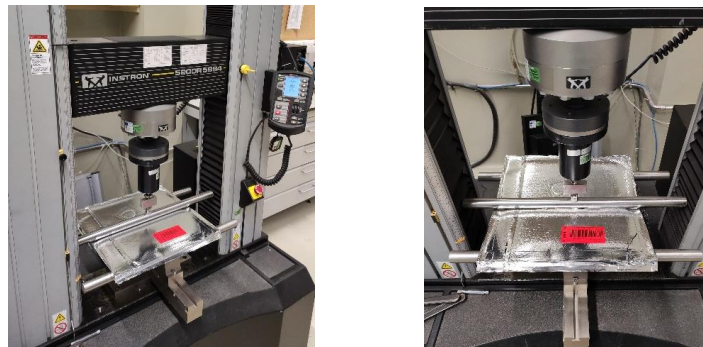
The tensile strength perpendicular to faces test was performed based on EN 1607 [14]. In this test, a specimen is attached between two rigid plates or blocks, fastened in a tensile testing machine and pulled apart at a given speed. The tested area was 300 mm x 300 mm for all specimens, which is the maximum area recommended in EN 1607. For this purpose, a wood plate of 300 mm (width) x 300 mm (height) x 30 mm (thickness) was bonded with epoxy glue to each face of the panel. To perform the tensile strength test perpendicular to faces, a metallic plate fixed with four screws to the wooden plate was pulled out by the apparatus equipment.



**Figure B.8:** Tensile strength test apparatus.

### 3.8. Bending

Bending tests were performed based on EN 12089 [15]. The test method consists of applying a force at a given speed by means of a loading edge in an axial direction to faces of a squarely cut rectangular test specimen, which is placed on two support edges. The force is applied to the test specimen at a position midway between the supporting position. Figure B.9 shows the test apparatus used for bending tests.



**Figure B.9:** Test apparatus of bending tests.

### 3.9. Thermal conductivity

The measurements of thermal conductivity were carried out using a guarded hot plate (GHP) apparatus - Lambda Meter EP500, as well as using a heat flow meter (HFM) apparatus - Lambda Meter HFM 436. The test procedure is standardized in ISO 8302 [16] and EN 12667 [17]. In this method, the specimen is exposed to a unidirectional uniform density of the heat flow rate. From

the temperature gradient between the specimen faces, the thermal resistance can be estimated and, therefore, the mean thermal conductivity of the specimen can be derived.

To determine the linear thermal transmittance of the VIP joint (edge thermal bridging effect) two panels were assembled within the GHP apparatus so that their joint was within the metering area. Finally, using the formulas in Annex C of EN 17140 [2], the linear thermal transmittance was determined by comparing a thermal conductivity measurement in the centre of a panel with a measurement of the joint assembly on panels.

Since the thermal conductivity of vacuum products increases with time during service life, ageing tests must be performed. Ageing effects of vacuum products are due to air and moisture permeating through the barrier envelope. For this purpose, the ageing procedures described in Annex C of EN 17140 [2] were carried out to calculate a mean value of thermal conductivity at centre of panel over a period of 25 years. Therefore, the VIP specimens were stored at 50°C/70 % relative humidity over a period of 180 days. The thermal conductivity measurements were carried out periodically over the 180 days. The thermal conductivity after ageing was determined at the LNE - *Laboratoire National de Métrologie et d'Essais* facilities and at the FIW München - Research Institute for Thermal Insulation.

### 3.10. Water absorption

The determination of long-term water absorption by immersion was conducted following method 2A of EN 12087 [18]. The water absorption by total immersion is determined by measuring the change in mass of the test specimen totally immersed in water over a period of 28 days. The excess water adhering to the surface, which is not absorbed by the test specimen, is removed by drainage. Based on the mass measurements of the specimen, the water absorption as volume percentage is calculated according equation B.3:

$$W_{it} = \frac{m_{28} - m_0}{V} \times \frac{100}{\rho_w} \quad [\%] \quad (\text{B.3})$$

Where,

$m_0$  is the initial specimen mass, expressed in kilograms;

$m_{28}$  is the specimen mass after immersion, expressed in kilograms;

$V$  is the initial volume of the specimen, in cubic meters;

$\rho_w$  is the density of water, which is assumed as 1000 kg/m<sup>3</sup>.

## 4. Test results

In this section, the test results are presented for both products studied: the vacuum insulation panel and encapsulated VIP. Some of the results are also given for VIP without vacuum.

### 4.1. Dimensional measurements

The length and the width of the VIPs, as well as, the deviation from the squareness of the length and width  $S_b$  and the deviation from flatness  $S_{max}$  are presented in Table B.1.

**Table B.1:** Dimensional results.

<b>Properties</b>	<b>VIP</b>	<b>Encapsulated VIP</b>
<b>Length [mm]</b>	401	437
<b>Width [mm]</b>	401	437
<b>Thickness [mm]</b>	21	41
<b>Squareness <math>S_b</math> [mm/m]</b>	---	<5
<b>Flatness <math>S_{max}</math> [mm/m]</b>	---	<6
<b>Density [kg/m<sup>3</sup>]</b>	241	129

The encapsulated VIP product dimensional properties accomplish the VIP EAD [1] requirements. In detail, the length and width measurements are within the EN 13171 [19] requirements, namely  $\pm 2\%$  in the direction of length and  $\pm 1,5\%$  in the direction of width. The thickness tolerance can be classified as T4 (-3 mm lower tolerance, + 5% upper tolerance), according to EN 13171 [19], as required in VIP EAD [1] for panels between 20 to 50 mm thickness. Also, the deviation from squareness,  $S_b$ , on length and width shall not exceed 5 mm/m the deviation from flatness,  $S_{max}$ , shall not exceed 6 mm/m.

## 4.2. Dimensional stability under specified temperature and humidity conditions

### 4.2.1. VIP panel

Three VIP panels with 200 mm x 200 mm (see Figure B.10) were used for dimensional stability testing. The results are shown in Table B.2. According EN 17140, the relative changes in length and width shall not exceed 1%, and the relative reduction in thickness shall not exceed 3%. Thus, VIP panels accomplish these requirements.

**Table B.2:** Test results of dimensional stability on VIP panel.

Test specimen	Specimen 1		Specimen 2		Specimen 3		Average
	Initial value ( $l_0, b_0, d_0$ ) [mm]	Final value ( $l_t, b_t, d_t$ ) [mm]	Initial value ( $l_0, b_0, d_0$ ) [mm]	Final value ( $l_t, b_t, d_t$ ) [mm]	Initial value ( $l_0, b_0, d_0$ ) [mm]	Final value ( $l_t, b_t, d_t$ ) [mm]	
<b>Length (l)</b>	200.0	200.0	199.8	200	200.4	199.6	200.0
<b>Width (b)</b>	201.2	200.4	200.8	200.8	201.4	200.4	200.8
<b>Thickness (d)</b>	21.2	21.0	21.1	20.9	21.1	21	21.1
<b>Relative changes length, <math>\Delta\epsilon_l</math> [%]</b>	0.0%		0.1%		-0.4%		-0.1%
<b>Relative changes width, <math>\Delta\epsilon_b</math> [%]</b>	-0.4%		0.0%		-0.5%		-0.3%
<b>Relative changes thickness, <math>\Delta\epsilon_d</math> [%]</b>	-0.9%		-0.9%		-0.5%		-0.8%



**Figure B.10:** Test specimen used for dimensional stability measurements.



## 4.2.2. Encapsulated VIP<sup>1</sup>

Three encapsulated panels were used for dimensional stability testing. The results are shown in Table B.3. According to EN 13171 [19], the relative changes in length and width accomplishes class DS(70,90)1, since the reduction in length, width and thickness is lower than 1%.

**Table B.3:** Test results of dimensional stability on encapsulated panels.

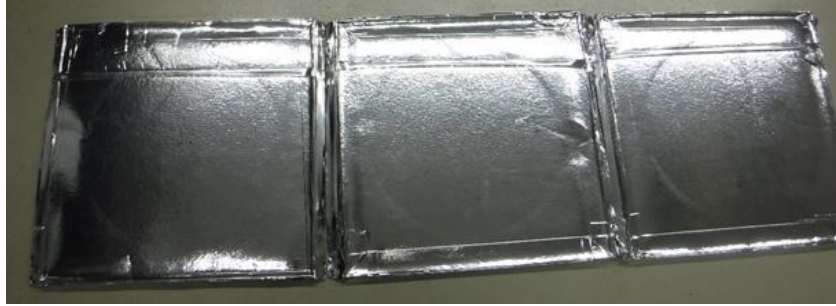
Test specimen	Specimen 1		Specimen 2		Specimen 3		Average
	Initial value (l <sub>0</sub> , b <sub>0</sub> , d <sub>0</sub> ) [mm]	Final value (l <sub>t</sub> , b <sub>t</sub> , d <sub>t</sub> ) [mm]	Initial value (l <sub>0</sub> , b <sub>0</sub> , d <sub>0</sub> ) [mm]	Final value (l <sub>t</sub> , b <sub>t</sub> , d <sub>t</sub> ) [mm]	Initial value (l <sub>0</sub> , b <sub>0</sub> , d <sub>0</sub> ) [mm]	Final value (l <sub>t</sub> , b <sub>t</sub> , d <sub>t</sub> ) [mm]	
<b>Length (l)</b>	437.9	437.0	437.9	436.9	438.1	437.6	437.6
<b>Width (b)</b>	437.9	437.3	437.4	436.9	438.2	437.1	437.5
<b>Thickness (d)</b>	41.8	41.7	41.1	40.9	41.8	42.1	41.6
<b>Relative changes length, <math>\Delta\epsilon_l</math> [%]</b>		-0.2%		-0.2%		-0.1%	-0.2%
<b>Relative changes width, <math>\Delta\epsilon_b</math> [%]</b>		-0.1%		-0.1%		-0.3%	-0.2%
<b>Relative changes thickness, <math>\Delta\epsilon_d</math> [%]</b>		-0.4%		-0.5%		0.9%	-0.01%

## 4.3. Compressive stress at 10% compressibility

### 4.3.1. VIP panels

Five specimens were tested including one perforated panel (panel without vacuum). All tests were performed with the same position and face of the VIP panel. Additionally, two specimens (specimen 4 and 5) were tested for an extension higher than 50% (rupture). The test specimens after compressive stress at 10% strain test are presented in Figure B.11.

<sup>1</sup> Dimensional stability under specified temperature and humidity conditions of encapsulated VIP was carried out at the LNE – *Laboratoire National de Métrologie et d'Essais* facilities.



**Figure B.11:** Test specimens after compressive stress at 10% strain test.

Table B.4 shows the results of compressive stress tests. The results showed a compressive stress at 10% strain of 134 KPa (CS(10\Y)125 - classification according EN 17410).

**Table B.4:** Compressive stress results – VIP panels.

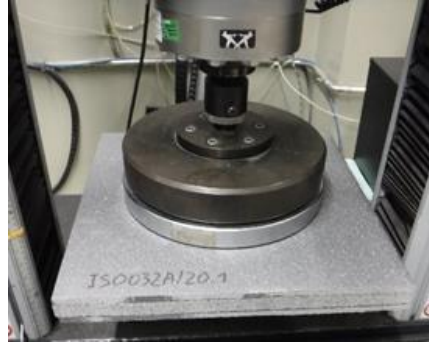
Test specimen	Specimen 1	Specimen 2	Specimen 3	Specimen 4	Specimen 5 <sup>(1)</sup>	Average <sub>(2)</sub>
<b>Compression force at 10%, F<sub>10</sub> [N]</b>	9201	8988	9610	9523	6575	9331
<b>Compressive stress at 10% strain <math>\sigma_{10}</math> [kPa]</b>	<b>132</b>	<b>129</b>	<b>138</b>	<b>137</b>	<b>94.2</b>	<b>134</b>
<b>Thickness after test [mm]</b>	21.3	22.1	21.2	21.3	29.7	21
<b>Compression force at rupture [N]</b>	--	--	--	144394	151982	--
<b>Compressive stress at rupture [kPa]</b>	--	--	--	2070	2179	--
<b>Compressive strain at rupture [%]</b>	--	--	--	52	59	--
<b>Thickness after rupture [mm]</b>	--	--	--	14.3	21.7	--

<sup>(1)</sup> Perforated panel.

<sup>(2)</sup> Average value without perforated panel.

### 4.3.2. Encapsulated VIP

For VIP with EPS cover layers, five specimens were tested. Figure B.12 show photography taken of a test specimen during a compressive test.



**Figure B.12:** Encapsulated VIP during compressive stress test.

Table B.5 shows the results of compressive stress tests encapsulated VIP panels as can be observed in Figure B.12. Test results show a compressive stress at 10% strain of 143 kPa (classification according EN 13171 [19] - CS (10\Y)100).

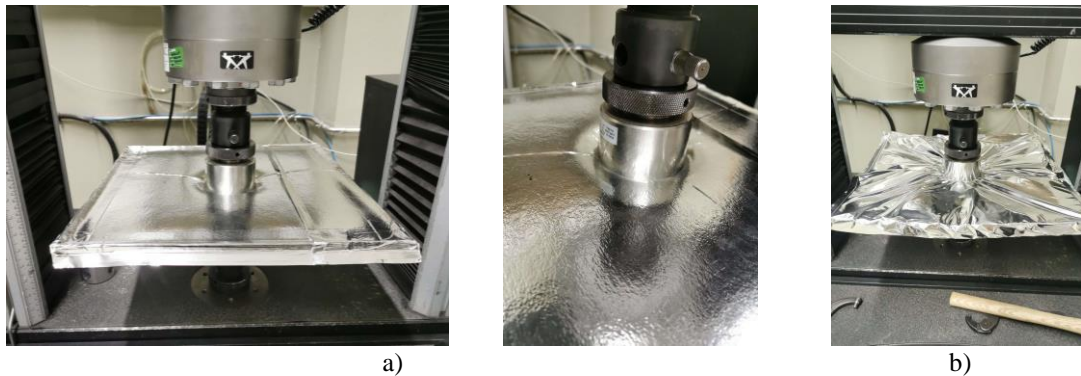
**Table B.5:** Compressive stress results – encapsulated VIP panels.

Test specimen	Specimen 1	Specimen 2	Specimen 3	Specimen 4	Specimen 5	Average
Length [mm]	436	438	437	437	437	437
Width [mm]	436	438	437	437	436	437
Thickness [mm]	41.4	41.1	43.5	40.0	41.4	41.5
Mass after conditioning [g]	1049.8	996.5	1078.2	957.2	1007.6	1020
Apparent density [kg/m <sup>3</sup> ]	133.5	126.4	129.9	125.3	127.8	129
Speed of the test [mm/min]	4.13	4.11	4.35	4.0	4.14	4.2
Compression force at 10%, F <sub>10</sub> [N]	10029	9655	10864	9424	10040.9	10002
Compressive stress at 10% strain, $\sigma_{10}$ [kPa]	<b>144</b>	<b>138</b>	<b>156</b>	<b>135</b>	<b>144</b>	<b>143</b>
Thickness after test [mm]	40.1	40.1	42.3	39.0	39.7	40.4
Compressive stress at rupture [kPa]	--	--	--	<b>966</b>	<b>1205</b>	<b>1085</b>
Compressive strain at rupture [%]	--	--	--	61.1	61.26	61.2
Thickness after rupture [mm]	--	--	--	26.2	26.6	26.4

## 4.4. Behaviour under point load

### 4.4.1. VIP panel

Three specimens, including one perforated panel (specimen 3), were tested for their behaviour under point load. After recording the compressive force at deformation of 5 mm and at strain of 20%, the test continued until rupture (deformation defined at 50%). Figure B.13 shows the specimens during the point load test at rupture. The specimens after testing are presented in Figure B.14. The compressive force at strain 50% was around 13kN. It should be noted that the panels apparently have not lost their vacuum (excluding the specimen 3, which had been perforated previously).



**Figure B.13:** Specimens during rupture test: a) VIP panel; b) perforated VIP panel.



**Figure B.14:** Specimens after rupture test.

Table B.6 shows the behaviour under the point load of VIP panels. Test results show a compressive force at a deformation strain of 20% of 2.7 kN.

**Table B.6:** Point load test results – VIP panels.

Test specimen	Specimen 1	Specimen 2	Specimen 3 <sup>(1)</sup>	Average
Length [mm]	401	400	400	400
Width [mm]	400	400	400	400
Thickness [mm]	22.2	23.0	29.5	24.9
Mass after conditioning [g]	799.1	858.0	956.0	871.0
Apparent density [kg/m <sup>3</sup> ]	224.4	232.9	202.7	220.0
Speed of the test [mm/min]	50	50	50	50
Pre-load [N]	2.5	2.5	2.5	2.5
Compressive force at deformation of 5 mm, [kN]	2.6	3.1	2.4	2.7
Compressive force at strain 20%, critical point [kN]	<b>2.3</b>	<b>2.8</b>	<b>3.0</b>	<b>2.7</b>
Compressive force at the rupture [kN]	12	14	13	13.2
Compressive strain at rupture [%]	49.5	50.0	50.0	49.8
Thickness after test [mm]	14.9	15.3	27.8	19.3

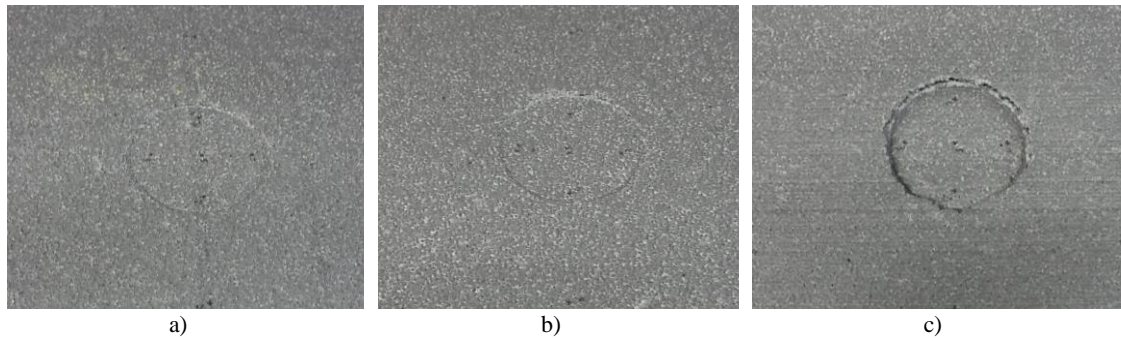
<sup>(1)</sup> Perforated panel.

#### 4.4.2. Encapsulated VIP

Three encapsulated VIP panels were tested. The point load test of encapsulated VIPs can be observed in Figure B.15. The damage of the point load in each panel can be seen in Figure B.16.



**Figure B.15:** Specimen 1 during point load test.



**Figure B.16:** Specimens after point load test: a) Specimen 1; b) Specimen 2; c) Specimen 3 after rupture test.

Table B.7 shows the behaviour under the point load of encapsulated VIP panels. Test results show a compressive force at deformation at 20% strain of 1.5 kN.

**Table B.7:** Point load test results – encapsulated VIP panels.

Specimen	Specimen 1	Specimen 2	Specimen 3	Average
Length [mm]	436	437	437	437
Width [mm]	437	434	436	436
Thickness [mm]	40.5	40.2	42.2	41.0
Mass before conditioning [g]	1087.9	1052.6	1049.3	1063.3
Mass after conditioning [g]	1088.2	1088.2	1088.2	1088.2
Apparent density [kg/m <sup>3</sup> ]	141.1	142.7	135.4	139.7
Speed of the test [mm/min]	50	50	50	50.0
Pre-load [N]	2.5	2.5	2.5	2.5
Compressive force at the at deformation of 5 mm, [kN]	1.1	1.1	1.1	1.1
Compressive force at strain 20 %, critical point [kN]	<b>1.6</b>	<b>1.5</b>	<b>1.6</b>	<b>1.5</b>
Compressive force at the rupture [kN]	--	--	7	7
Compressive strain at rupture [%]	--	--	54	54.0

## 4.5. Shear behaviour

### 4.5.1. VIP panel

Five specimens were tested (including two perforated panels). All tests were performed with the same position of the panel. Figure B.17 show some specimens during the shear test.

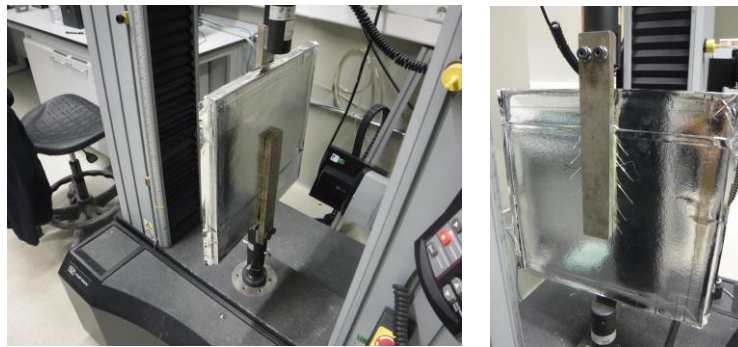


Figure B.17: Specimens during shear strength tests.

Table B.8 shows the dimensional characteristics of VIPs used in shear behaviour tests, as well as the test results. The average shear strength of VIP panels (without perforated panels) was found to be 161.5 kPa (1.7 kN).

Table B.8: Shear strength test results – VIP panels.

Test specimen	Specimen 1 <sup>(1)</sup>	Specimen 3 <sup>(1)</sup>	Specimen 2	Specimen 4	Specimen 5	Average <sup>(2)</sup>
Length [mm]	400	400	399	401	400	400
Width [mm]	400	402	400	401	400	400
Mass [g]	835.9	818.1	882.8	863.4	868.3	871.5
Thickness [mm]	23.2	21.1	22.0	22.7	23.2	22.6
Maximum force applied, $F_m$ [kN]	0.493	0.143	1.773	1.712	1.603	1.7
Shear strength, $\tau$ [kPa]	<b>47.0</b>	<b>13.6</b>	<b>168.9</b>	<b>163.0</b>	<b>152.7</b>	<b>161.5</b>
Shear strength modulus, $G$ [kPa]	---	---	<b>2660</b>	<b>2071</b>	<b>2669</b>	<b>2467</b>

<sup>(1)</sup> Perforated panel.

<sup>(2)</sup> Average value without perforated panels.



## 4.5.2. Encapsulated VIP

Five specimens of encapsulated panels were tested. Figure B.18 shows some test specimens during the test, while Figure B.19 shows the rupture of the EPS layer. Three test specimens lost their vacuum during shear strength testing.

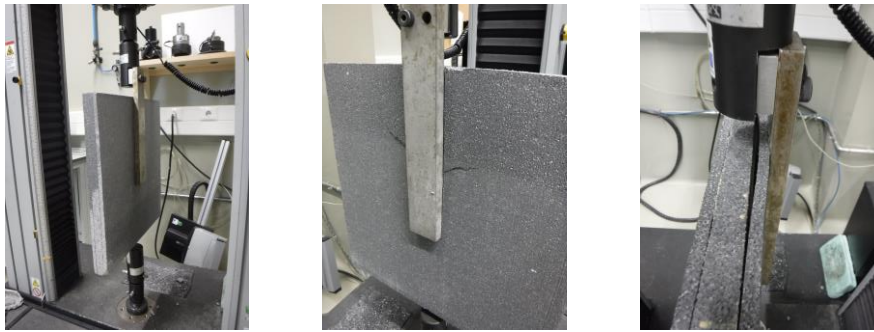


Figure B.18: Specimens during shear strength tests.



Figure B.19: Specimens after shear strength tests.

Table B.9 shows the dimensional characteristics of the test specimens used in the shear behaviour tests, as well as the test results. All tests showed a rupture of the EPS cover layer. The average shear strength obtained for encapsulated VIPs was 103 kPa (1.3kN).

Table B.9: Shear strength test results – VIP ETICS panels.

Specimen	Specimen 1	Specimen 2	Specimen 3	Specimen 4	Specimen 5	Average
Length [mm]	438	438	436	437	438	437
Width [mm]	437	437	437	437	437	437
Mass [g]	1059.1	1022.4	1033.9	1050.3	1040.4	1041.2
Thickness [mm]	41.4	38.2	40.1	39.1	38.4	39.5
Maximum force applied, $F_m$ [kN]	1.311	0.957	1.452	1.589	1.141	1.3
Shear strength, $\tau$ [kPa]	<b>104.9</b>	<b>76.6</b>	<b>116.2</b>	<b>127.1</b>	<b>91.3</b>	<b>103.2</b>
Location of rupture	EPS	EPS	EPS	EPS	EPS	EPS
Shear strength modulus, $G$ [kPa]	<b>3157</b>	<b>1532</b>	<b>3365</b>	<b>2932</b>	<b>3099</b>	<b>2817</b>



## 4.6. Resistance to perforation

### 4.6.1. VIP panel

Two VIP panels were tested concerning their resistance to perforation. One of them was a perforated panel. The results are presented in Table B.10. The results show that VIP have a puncture resistance of 25 mm. With a 20 mm indenter, the envelope barrier film was punctured.

**Table B.10:** Results of puncture resistance test of VIP panels.

Test specimen	Specimen 1			Specimen 2 <sup>(1)</sup>		
Length [mm]	400			400		
Width [mm]	400			400		
Thickness [mm]	25			28		
Mass after conditioning [g]	870.7			864.8		
Apparent density [kg/m <sup>3</sup> ]	219.5			196.0		
<b>Indenter diameter [mm]:</b>	Impact 1	Impact 2	Impact 3	Impact 1	Impact 2	Impact 3
30	Ok	Ok	Ok	Ok	Ok	Ok
25	Ok	Ok	Ok	Ok	Ok	Ok
20	Ok	Ok	<b>Punctured</b>	Ok	Ok	Ok
15	Punctured	Punctured	Punctured	<b>Punctured</b>	<b>Punctured</b>	<b>Punctured</b>

<sup>(1)</sup> Perforated panel.

### 4.6.2. Encapsulated VIP

An encapsulated panel was also tested. The results are presented in Table B.11.

**Table B.11:** Results of puncture resistance test of encapsulated VIP.

Test specimen	Specimen 1		
Length [mm]	436		
Width [mm]	435		
Thickness [mm]	40		
Mass after conditioning [g]	1045.5		
Apparent density [kg/m <sup>3</sup> ]	137.8		
<b>Indenter diameter [mm]:</b>	Impact 1	Impact 2	Impact 3
30	Ok	Ok	Ok
25	Ok	Ok	Ok
20	Ok	Ok	Ok
15	<b>Punctured</b>	<b>Punctured</b>	<b>Punctured</b>
12	Punctured	Punctured	Punctured

Regarding the encapsulated VIP, the results show that panels have a puncture resistance 20 mm. The EPS cover layer was damaged with indentors of 30 to 20 mm. However, the panel was only punctured (loss of vacuum) with an indenter of 15 mm as it is show in Figure B.20.

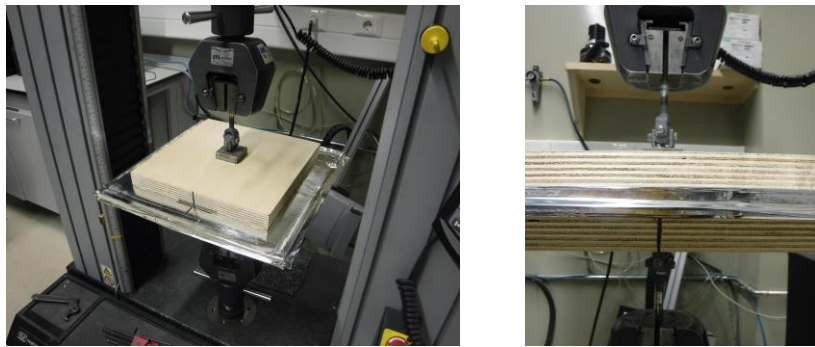


**Figure B.20:** VIP ETICS test specimen after perforation impacts.

## 4.7. Tensile strength perpendicular to faces

### 4.7.1. VIP panel

Five specimens of VIPs were tested, including one perforated panel (specimen 3). Figure B.21 shows some test specimens during the tensile strength tests.



**Figure B.21:** Test specimens during tensile strength test.

The results of tensile strength testing perpendicular to faces of VIP panels are presented in Table B.12. Excluding the previously perforated panels, the average shear strength obtained was 32 kPa (2.9 kN) – TR30 according EN 17140. All tests ended with the rupture of the glue layer between wood plate and specimen, which means that VIP panels have a shear strength resistance higher than 32 kPa. All the panels apparently maintained the vacuum.

**Table B.12:** Results of tensile strength tests of VIP panels.

Test specimen	Specimen 1	Specimen 2	Specimen 3 <sup>(1)</sup>	Specimen 4	Specimen 5	Average <sup>(2)</sup>
<b>Length [mm]</b>	401	400	400	398	399	399.6
<b>Width [mm]</b>	400	401	399	401	399	400.0
<b>Thickness [mm]</b>	23.6	25.3	27.0	22.2	22.2	23.3
<b>Maximum force, F<sub>m</sub> [kN]</b>	3.35	2.25	0.53	3.0	2.81	2.85
<b>Tensile strength perpendicular to faces, <math>\sigma_{mt}</math> [kPa]</b>	24.97	37.2	5.83	33.41	31.21	31.7
<b>Location of the rupture</b>	Wood	Glue	Glue	Wood	Glue	---

<sup>(1)</sup> Perforated panel.

<sup>(2)</sup> Average value without perforated panel.

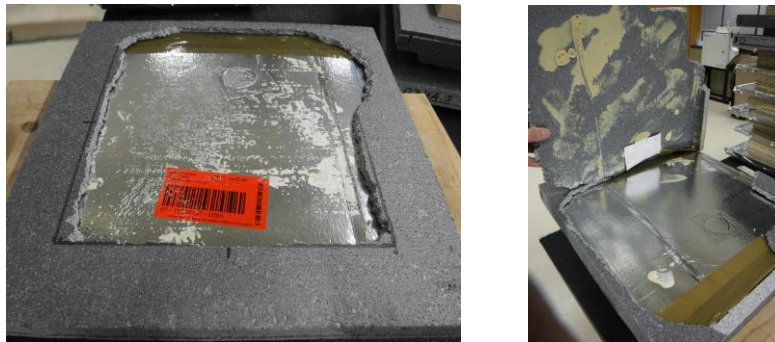
## 4.7.2. Encapsulated VIP

Regarding the encapsulated VIP, five specimens were tested. Figure B.22 shows some specimens during tensile strength test.



**Figure B.22:** Test specimens during tensile strength test.

Some specimens have failure in the EPS layer, while two of them the first failure was in the PU glue (connection between EPS cover layer and VIP panel). These specimens showed reduced tensile strength values (around 4.5 kPa). Figure B.23 shows some specimens after tests.



**Figure B.23:** Test specimens after tensile strength tests.

The results of tensile strength testing perpendicular to faces of encapsulated VIPs are presented in Table B.13. The average tensile strength obtained was 11.6 kPa (1.0 kN). All the panels apparently maintained the vacuum, with exception of specimen 3 which lost its vacuum during the test.

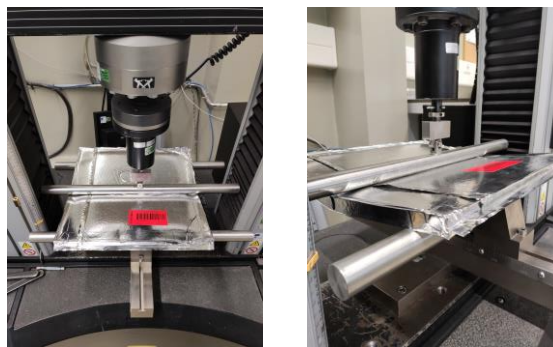
**Table B.13:** Results of tensile strength tests of encapsulated panels.

Test specimen	Specimen 1	Specimen 2	Specimen 3	Specimen 4	Specimen 5	Average
Length [mm]	435	435	429	436	437	434.4
Width [mm]	431	438	438	438	437	436.4
Thickness [mm]	39	39	38	39	39	39
Mass [g]	1011.3	1035.1	1023.4	1049.3	995.8	1023.0
Maximum force, $F_m$ [kN]	1.396	1.824	0.382	0.421	1.187	1.042
Tensile strength perpendicular to faces, $\sigma_{mt}$ [kPa]	<b>15.5</b>	<b>20.3</b>	<b>4.25</b>	<b>4.68</b>	<b>13.2</b>	<b>11.6</b>
Location of the rupture	EPS	EPS	PU glue	PU glue	EPS	---

## 4.8. Bending

### 4.8.1. VIP panel

Three VIP panels with dimensions of 400 mm x 400 mm were tested, including one perforated panel (specimen 1). Figure B.24 shows a test specimen during the bending test.

**Figure B.24:** Bending tests of VIP panels.

The test results are presented in Table B.14, which indicate an average maximum force of 538 N and a deflection of 9 mm. The failure pattern was verified as ductile. The perforated panel, as expected, has higher deflection and lower load values.

**Table B.14:** Bending results of VIP panels.

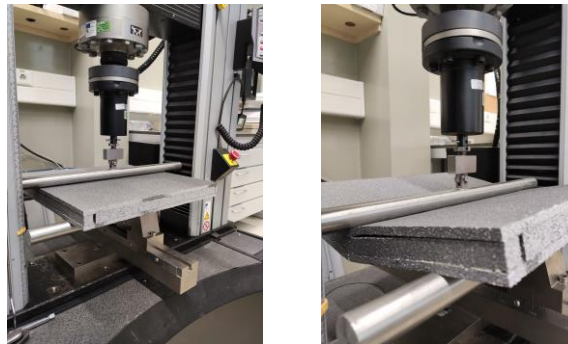
Test specimen	Specimen 1 <sup>(1)</sup>	Specimen 2	Specimen 3	Average <sup>(2)</sup>
Length [mm]	400	400	401	401
Width [mm]	401	401	401	401
Thickness [mm]	29	26	25	26
Mass after conditioning [g]	848.1	863.1	867.9	866
Apparent density [kg/m <sup>3</sup> ]	186.4	209.3	212.4	211
Span (L) [mm]	300	300	300	300
Maximum force (N)	<b>143.1</b>	<b>458.0</b>	<b>618.0</b>	<b>538</b>
Deflection at maximum force [mm]	<b>24.1</b>	<b>8.2</b>	<b>9.7</b>	<b>9.0</b>
Failure pattern	Ductile	Ductile	Ductile	Ductile

<sup>(1)</sup> Perforated panel.

<sup>(2)</sup> Average value without perforated panel.

## 4.8.2. Encapsulated VIP

Three encapsulated VIP panels were tested. Figure B.25 shows the test specimen during the bending test.



**Figure B.25:** Bending tests of VIP ETICS panels.

The test results are presented in Table B.15, which indicate an average maximum force of 811.1 N and a deflection of 13.3 mm. The failure pattern was verified as ductile. All the specimens have maintained their vacuum after testing.

**Table B.15:** Bending results of encapsulated VIP panels.

Test specimen	Specimen 1	Specimen 2	Specimen 3	Average <sup>(2)</sup>
Length [mm]	437	437	436	437
Width [mm]	437	435	438	437
Thickness [mm]	40	41	43	41
Mass after conditioning [g]	991.3	1046.0	1028.1	1022
Apparent density [kg/m <sup>3</sup> ]	130.2	133.5	125.8	130
Span (L) [mm]	300	300	300	300
Maximum force [N]	<b>692.4</b>	<b>782.3</b>	<b>958.7</b>	<b>811.1</b>
Deflection at maximum force [mm]	<b>12.8</b>	<b>12.8</b>	<b>14.3</b>	<b>13.3</b>
Failure pattern	Ductile	Ductile	Ductile	Ductile

## 4.9. Thermal conductivity

### 4.9.1. VIP panel

Five VIP panels with dimensions of 400 mm x 400 mm were tested in GHP apparatus, and other five test specimens were tested in HFM apparatus. Table B.16 shows the thermal conductivity results measured at centre of panel (CoP) at 10°C.

**Table B.16:** VIP thermal conductivity results measured at initial state.

Test method	Test specimen	Thickness [mm]	Apparent density at 23°C/50%RH [kg/m <sup>3</sup> ]	$\lambda_{10}$ , [W/(m.K)]	$\lambda_{10, \text{mean}}$ [W/(m.K)]	
<b>HFM</b>	Specimen 1	21.4	193.7	0.004459	<b>0.0043</b>	
	Specimen 2	21.1	196.1	0.004366		
	Specimen 3	20.8	191.6	<b>191.9</b>		0.004230
	Specimen 4	21.2	189.9	0.004159		
	Specimen 5	21.4	188.3	0.004375		
<b>GHP</b>	Specimen 6	21.3	185.6	0.004140	<b>0.0041</b>	
	Specimen 7	21.3	188.5	0.004190		
	Specimen 8	21.2	189.1	<b>187.8</b>		0.004123
	Specimen 9	21.2	189.5	0.004172		
	Specimen 10	21.3	186.1	0.004072		

After initial state thermal conductivity measurements, the test specimens were intentionally perforated (loss of vacuum) and the thermal conductivity was measured. Table B.17 shows the thermal conductivity results measured at centre of panel (CoP) at 10°C on perforated panels. The perforated panels showed a thermal conductivity around 5 times higher than in the initial state.

**Table B.17:** Thermal conductivity results on perforated panels.

Test method	Test specimen	Thickness [mm]	Apparent density at 23°C/50%RH [kg/m <sup>3</sup> ]	$\lambda_{10}$ [W/(m.K)]	$\lambda_{10, \text{mean}}$ [W/(m.K)]	
<b>HFM</b>	Specimen 1	22.3	186.9	0.021898	<b>0.0219</b>	
	Specimen 2	22.2	187.1	0.021621		
	Specimen 3	22.4	179.6	<b>183.2</b>		0.021950
	Specimen 4	22.4	181.3	0.022024		
	Specimen 5	22.4	181.2	0.021960		
	Specimen 6	21.6	182.8	0.021225		
<b>GHP</b>	Specimen 7	21.8	186.1	0.021223	<b>0.0212</b>	
	Specimen 8	21.5	186.9	<b>184.9</b>		0.021035
	Specimen 9	22.0	184.3	0.021477		
	Specimen 10	21.67	184.32	0.021080		

Regarding the effect of ageing<sup>2</sup> on the thermal conductivity of VIPs, an accelerated ageing was performed. The average thermal conductivity change at CoP estimated over the first 25 years in use (according the ageing test procedure) was 1.28 mW/(m.K) for 600 mm x 600 mm panels and 2.36 mW/(m.K) for 400 mm x 400 mm panels.

In addition, the linear thermal transmittance of VIP joints measured at an average temperature of 10°C was determined, resulting in linear thermal transmittance of 10.15 mW/(m.K) for VIP and 19.77 mW/(m.K) for encapsulated panels. However, these results can change as function of different kind of joints, as detailed in the chapter 3. Thus, the edge thermal bridging effects of VIP joints negatively affect the equivalent thermal conductivity of the VIP solution.

<sup>2</sup> The determination of the VIP thermal conductivity after ageing was performed at the LNE - *Laboratoire National de Métrologie et d'Essais* and FIW München - Research Institute for Thermal Insulation.



## 4.9.2. Encapsulated VIP

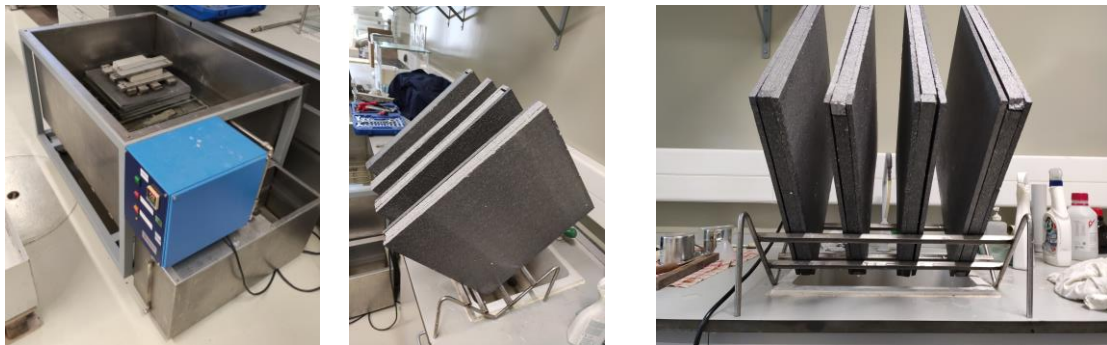
Four encapsulated VIP panels with dimensions of 440 mm x 440 mm were tested in a GHP apparatus. Table B.18 shows the thermal conductivity results measured at centre of panel (CoP) at 10°C, 25°C and 40°C.

**Table B.18:** Thermal conductivity results on encapsulated VIPs.

Test method	Test specimen	Thickness [mm]	$\lambda$ [W/(m.K)]			$\lambda_{10, \text{mean}}$ [W/(m.K)]
			10 °C	25 °C	40 °C	
GHP	Specimen 1	40.6	0.00744	0.00784	0.00831	<b>0.0075</b>
	Specimen 2	40.7	0.00751	0.00789	0.00838	
	Specimen 3	39.1	0.00739	0.00774	0.00829	
	Specimen 4	38.8	0.00750	0.00791	0.00840	

## 4.10. Water absorption

Four encapsulated VIP panels were tested. Figure B.26 shows the specimens during the water absorption test.



**Figure B.26:** Specimens during water absorption test: a) immersion during 28 days; b) drain during 10 min.

The test results are presented in Table B.19. The water absorption after 28 days of immersion (volume percentage),  $W_{lt}$  was 1.7%.

**Table B.19:** Results of water absorption test of encapsulated VIP panels.

Test specimen	Specimen 1	Specimen 2	Specimen 3	Specimen 4	Average
Length [mm]	437	437	437	437	437
Width [mm]	437	437	438	432	436
Thickness [mm]	42	41	41	40	41
Area [m <sup>2</sup> ]	0.19	0.19	0.19	0.19	0.19
Volume [m <sup>3</sup> ]	0.01	0.01	0.01	0.01	0.0
Mass before conditioning [g]	1077.0	1005.3	1012.7	987.1	1020.5
Mass after conditioning [g]	1077.0	1005.3	1012.7	987.1	1020.5
Mass after immersion, m <sub>28</sub> [g]	1223.7	1146.7	1147.0	1098.6	1154.0
W <sub>it</sub> [%]	<b>1.8</b>	<b>1.8</b>	<b>1.7</b>	<b>1.5</b>	<b>1.7</b>

## 5. Summary of experimental test results

Table B.20 summarizes the results obtained throughout laboratorial tests, for both: vacuum insulation panels and encapsulated VIPs, as well as for the intentionally perforated panels.

**Table B.20:** Summary of test results for VIP panels, VIP panels without vacuum and encapsulated VIPs.

Property		VIP panel	Perforated VIP panel	Encapsulated VIP
<b>Length x width, EN 822</b>	[mm]	401 x 401	401 x 401	437 x 437
<b>Thickness, EN 823</b>	[mm]	21	22	41
<b>Density, EN 1602</b>	[kg/m <sup>3</sup> ]	241	184	129
<b>Squareness, EN 824</b>	[mm/m]	---	---	<5
<b>Flatness, EN 825</b>	[mm/m]	---	---	<6
<b>Compressive stress at 10% compressibility, EN 826</b>	Compression force at 10%, F <sub>10</sub> [N]	9331	6575	10002
	Compressive stress at 10% strain, $\sigma_{10}$ [kPa]	134	94.2	143
<b>Point load, EN 12430</b>	Compression force at deformation of 5 mm [kN]	2.7	2.4	1.1
	Compression force at strain 20%, critical point [kN]	2.7	3.0	1.5
	Maximum force applied, F <sub>m</sub> [kN]	1.7	0.3	1.3
<b>Shear behaviour, EN 12090</b>	Shear strength, $\tau$ [kPa]	162	30.3	103
	Location of rupture	Barrier envelope/epoxy glue	Barrier envelope	EPS
	Shear strength modulus, G [kPa]	2467	---	2817
<b>Tensile strength perpendicular to faces, EN 1607</b>	Maximum force, F <sub>m</sub> [kN]	2.9	0.53	1.0
	Tensile strength perpendicular to faces, $\sigma_{mt}$ [kPa]	>32	5.8	12
	Maximum force [N]	538	143	811
<b>Bending, EN 12089</b>	Deflection at maximum force [mm]	9	24	13
	Failure pattern	Ductile	Ductile	Ductile
<b>Water absorption, EN 12087</b>	W <sub>lt</sub> [%]	---	---	1.7
<b>Dimensional stability under specifies temperature and humidity conditions, EN 1604</b>	Relative changes length, $\Delta\epsilon_l$ [%]	-0.1	---	-0.2
	Relative changes width, $\Delta\epsilon_b$ [%]	-0.3	---	-0.2
	Relative changes thickness, $\Delta\epsilon_d$ [%]	-0.8	---	-0.0
<b>Thermal resistance, ISO 8302, EN 12667, EN 17140</b>	Thermal conductivity [mW/(m.K)]	4.2 (5.3 <sup>(1)</sup> )	21.6	7.5 (11.3 <sup>(1)</sup> )
	Linear thermal transmittance [mW/(m.K)]	10.2	---	19.8
	Thermal resistance [(m <sup>2</sup> .K)/W]	5.02 (3.99 <sup>(1)</sup> )	1.019	5.34 (3.67 <sup>(1)</sup> )
<b>Resistance to perforation, ETAG004:2011</b>	---	Resistant at 25 mm	---	Resistant at 20 mm

<sup>(1)</sup> Including edge thermal bridging effect, considering a VIP panel with 400 mm x 400 mm.

According to EN 17140 [2] – VIP specification standard and EAD for VIP with cover layers [1], the encapsulated VIP fulfil the requirements to be used in buildings. Also, the ETICS EAD [20] requirements for ETICS bonded with supplementary mechanical fixings are accomplished by the encapsulated VIP, namely:

- A minimum value of shear strength according to EN 12090: 20 kPa;
- A minimum value of shear modulus according to EN 12090: 1000 kPa;
- All values of water absorption  $< 1 \text{ kg/m}^2$
- A maximum value  $\lambda_D$  (design value) according to EN 12667:  $0.065 \text{ W/(m.K)}$ .

For this reason, the VIP product designed for ETICS application could be used in ETICS with rendering. Nevertheless, the VIP ETICS kits must be studied following the ETICS EAD [20] test procedures, in order to validate the complete system behaviour, namely the response of a thin rendering system over the vacuum insulation panels, particularly since this insulation product is not presented on the indicative list of materials to be used in ETICS solutions. In addition, the use of super-insulating materials deserves particular attention, since higher thermal/mechanical stresses and hygrothermal heterogeneity in the VIP edges is to be expected (comparing with conventional insulation materials). As expected, panels without vacuum showed lower mechanical resistance, particularly in the shear behaviour and tensile strength tests.

## **6. Performance comparison with conventional insulation materials**

Table B.21 compares the VIP results with conventional insulation materials often used in ETICS solutions, namely expanded polystyrene (EPS), extruded polystyrene (XPS), expanded cork agglomerate (ICB) and mineral wool (MW). All the results were achieved at Itecons following the relevant specification standard for each insulation material.

**Table B.21:** VIP results comparison with conventional insulation materials.

	Property	Encapsulated VIP	EPS	XPS	ICB	MW
<b>Thickness, EN 823</b>	[mm]	41	60	61	61	60
<b>Density, EN 1602</b>	[kg/m <sup>3</sup> ]	129	19	32	101	130
<b>Flatness, EN 824</b>	[mm/m]	<5	---	---	---	---
<b>Squareness, EN 825</b>	[mm/m]	<6	---	---	---	---
<b>Compressive stress at 10% compressibility, EN 826</b>	Compressive stress at 10% strain, $\sigma_{10}$ [kPa]	143	108	489	128	48
<b>Point load, EN 12430</b>	Compressive force at strain 20%, critical point [kN]	1.5	N.A	N.A	0.93	N.A
<b>Shear behaviour, EN 12090</b>	Shear strength, $\tau$ [kPa]	103	110	270	55	8
	Shear strength modulus, $G$ [kPa]	2817	2600	---	4600	---
<b>Tensile strength perpendicular to faces, EN 1607</b>	Tensile strength perpendicular to faces, $\sigma_{mt}$ [kPa]	12	194	951	45	13
<b>Bending, EN 12089</b>	Maximum force [N]	811	197	--	--	---
	Deflection at maximum force [mm]	13	8	--	--	---
<b>Water absorption, EN 12087</b>	$W_{lt}$ [%]	1.7	3.4	0.2	7.2	---
<b>Dimensional stability under specific temperature and humidity conditions, EN 1604</b>	Relative changes length, $\Delta\epsilon_l$ [%]	-0.2	-0.1	0.2	---	< 1
	Relative changes width, $\Delta\epsilon_b$ [%]	-0.2	-0.1	-0.2	---	< 1
	Relative changes thickness, $\Delta\epsilon_d$ [%]	-0.0	-0.1	0.0	---	< 1
<b>Thermal resistance</b>	Thermal conductivity [mW/(m.K)]	7.5 (11.3 <sup>(1)</sup> )	35.0	33.9	39.0	36.8
	Thermal resistance [(m <sup>2</sup> .K)/W]	5.34 (3.67 <sup>(1)</sup> )	1.71	1.79	1.57	1.63

<sup>(1)</sup> thermal conductivity measured at 10°C including edge thermal bridging effect, considering an encapsulated VIP with 440 mm x 440 mm.

The results comparison shows that encapsulated VIP mechanical behaviour is generally close to (or better than) the other insulation materials. The VIP test results showed lower tensile strength. However, these results are similar to the MW panels behaviour. For the VIP solution, water absorption is lower than for EPS and higher than for XPS, which is assumed to result from the water absorption of the EPS protective cover layer (since VIP barrier envelope is theoretically water-tight). Dimensional stability under specific temperature and humidity conditions showed values close to those for polystyrene panels. Thermal conductivity of VIPs showed values around 5 times lower than traditional insulation materials. However, the equivalent thermal conductivity of the VIP considering edge thermal bridging effect reduces the thermal resistance of the solution by around 31%.

## 7. Final statements

In this document, the physical, hygrothermal and mechanical capabilities of a novel VIP product designed for ETICS solutions were evaluated in order to ensure the feasibility when exposed to weathering and other external agents. For this purpose, a laboratory campaign was carried out, which included tests on fumed silica VIP panels with and without EPS encapsulation (designed for ETICS application). The test results showed that the VIP solution under study is suitable for use in super-insulating ETICS. A comparison with conventional insulation materials test results was performed and discussed, revealing values within the range of the most used insulation materials in ETICS. Additional tests were performed in panels without vacuum (perforated panels), revealing lower mechanical resistances and a thermal conductivity 5 times higher than that of the VIP in its initial state.

## References

- [1] *European Assessment Document: Vacuum Insulation Panels (VIP) with factory applied protection layers*, EAD 040011-00-1201, European Organisation for Technical Approvals, 2017.
- [2] *Thermal insulation products for buildings - Factory-made vacuum insulation panels (VIP) - Specification*, EN 17140, European Committee for Standardization, 2020.
- [3] C. Santos, L. Matias, “ITE 50 - Coeficientes de Transmissão Térmica de Elementos da Envolvente dos Edifícios” (in portuguese), LNEC, Lisboa, 2006.
- [4] *Thermal insulating products for building applications - Determination of thickness* EN 823 European Committee for Standardization, 2013.
- [5] *Thermal insulating products for building applications - Determination of the apparent density*, EN 1602, European Committee for Standardization, 2013.
- [6] *Thermal insulating products for building applications - Determination of squareness*, EN 824, European Committee for Standardization, 2013.
- [7] *Thermal insulating products for building applications - Determination of flatness*, EN 825, European Committee for Standardization, 2013.
- [8] *Thermal insulating products for building applications - Determination of dimensional stability under specified temperature and humidity conditions*, EN 1604, European Committee for Standardization, 2013.
- [9] European Committee for Standardization, EN 12085 - Thermal insulating products for buildings applications - Determination of linear dimensions of test specimens, (2013).

- [10] *Thermal insulating products for building applications - Determination of compression behaviour*, EN 826, European Committee for Standardization, 2013.
- [11] *Thermal insulating products for building applications - Determination of behaviour under point load*, EN 12430, European Committee for Standardization, 2013.
- [12] *Thermal insulating products for building applications - Determination of shear behaviour*, EN 12090, European Committee for Standardization, 2013.
- [13] *Guideline for European Technical Approval of External Thermal Insulation Composite Systems (ETICS) with Rendering*, ETAG 004, European Organisation for Technical Approvals, Edition 2011.
- [14] *Thermal insulating products for building applications - Determination of tensile strength perpendicular to faces*, EN 1607, European Committee for Standardization, 2013.
- [15] *Thermal insulating products for building applications - Determination of bending behaviour*, EN 12089, European Committee for Standardization, 2013.
- [16] *Thermal insulation - Determination of steady-state thermal resistance and related properties - Guarded hot plate apparatus*, ISO 8302, International Organization for Standardization, 1991.
- [17] *Thermal performance of building materials and products - Determination of thermal resistance by means of guarded hot plate and heat flow meter methods - Products of high and medium thermal resistance*, EN 12667, European Committee for Standardization, 2001.
- [18] *Thermal insulating products for building applications - Determination of long term water absorption by immersion*, EN 12087, European Committee for Standardization, 2013.
- [19] *Thermal insulation products for buildings - Factory made wood fibre (WF) products - Specification*, EN 13171, European Committee for Standardization, 2015.
- [20] *European Assessment Document: External Thermal Insulation Composite Systems with rendering*, EAD 040083-00-0404, European Organisation for Technical Approvals, 2019.

